University of Venda

Multi-Scale Modelling of Vector-Borne Diseases

By

DEPHNEY MATHEBULA

A Thesis Submitted to the

UNIVERSITY OF VENDA

In Fulfilment of the Requirements for the Degree

of

Doctor of Philosophy (Mathematics)

in the

Department of Mathematics and Applied Mathematics

at

School of Mathematical and Natural Sciences

Promoter: Prof. W. Garira

Co-Promoter: Dr. S. Moyo

September 2018

Declaration of Authorship

I, DEPHNEY MATHEBULA, declare that this thesis has been composed entirely by myself and that it has not been submitted, in whole or in part, in any previous application for a degree. Except where stated otherwise by reference or acknowledgment, the work presented is entirely my own.

Signed: _____

Date: _____

Abstract

In this study, we developed multiscale models of vector-borne diseases. In general, the transmission of vector-borne diseases can be considered as falling into two categories, i.e. direct transmission and environmental transmission. Two representative vector-borne diseases, namely; malaria which represents all directly transmitted vector-borne diseases and schistosomiasis which represents all environmentally transmitted vector-borne diseases were studied. Based on existing mathematical modelling science base, we established a new multiscale modelling framework that can be used to evaluate the effectiveness of vector-borne diseases treatment and preventive interventions. The multiscale models consisted of systems of nonlinear ordinary differential equations which were studied for the provision of solutions to the underlying problem of the disease transmission dynamics. Relying on the fact that there is still serious lack of knowledge pertaining to mathematical techniques for the representation and construction of multiscale models of vector-bone diseases, we have developed some grand ideas to placate this gap. The central idea in multiscale modelling is to divide a modelling problem such as a vector-bone disease system into a family of sub-models that exist at different scales and then attempt to study the problem at these scales while simultaneously linking the sub-models across these scales. For malaria, we formulated the multiscale models by integrating four submodels which are: (i) a sub-model for the mosquito-to-human transmission of malaria parasite, (ii) a sub-model for the human-to-mosquito transmission of malaria parasite, (iii) a within-mosquito malaria parasite population dynamics sub-model and (iv) a within-human malaria parasite population dynamics sub-model. For schistosomiasis, we integrated the two subsystems (within-host and between-host sub-models) by identifying the within-host and between-host variables and parameters associated with the environmental dynamics of the pathogen and then designed a feedback of the variables and parameters across the within-host and between-host sub-models. Using a combination of analytical and computational tools we adequately accounted for the influence of the sub-models in the different multiscale models. The multiscale models were then used to evaluate the effectiveness of the control and prevention interventions that operate at different scales of a vector-bone disease system. Although the results obtained in this study are specific to malaria and schistosomiasis, the multiscale modelling frameworks developed are robust enough to be applicable to other vector-borne diseases.

Dr. D. Mathebula

Acknowledgements

I am grateful to Almighty God for His loving kindness, for saving and preserving my life through out my research. Moreso, for His continuous protection till this moment and always. Furthermore, I reverence God for granting me the strength and good health. For without Him this PhD work would not have come to completion and success.

I would like to express my special appreciation and thanks to my able, hard working, ever dynamic promoter and energetic promoter, Prof Winston Garira whose assistance, guidance, instruction, supervision and constructive criticism have brought about the originality of this work. May God Almighty continue to strengthen him in wisdom, knowledge and in all his endeavors. Thus, to my co-promoter, Dr. Simiso Moyo for his brilliant comments and suggestions which incented me to widen my research from various perspectives. I could not have imagined having a better promoter and co-promoter for my PhD study. I also want to appreciate the impact and contributions of my fellow Modelling Health and Environmental Linkages Research Group members.

A big thank you to my parents; Mr Daniel Mathebula and Mrs Dainah Mathebula for training me and making all the enabling environment conducive for my education and for all their financial support in the time past and now. For without God through them my study to this level would not have been possible. From deep down bottom of my heart I say Xikwembu a xi mi katekisi. May God in His benevolence and infinite kindness enable them live long to reap and enjoy the fruits of their labour. My sincere gratitude goes to my sisters; Constance, Precious, Winny, Doris, Sagwati and Nyiko. Also to my nephews, nieces; Tiyiselani, Blessing, Kamokgelo, Alucia, Hlonipho, Rithabile, Lwandle, Dzunisiwa, Shongile and Mhani Pfumelani. May the joy of the Lord flourish in their lives.

Again, I am using this opportunity to appreciate all of my friends and colleagues for their availability whenever I needed their assistance. I also appreciate my mentor, Dr Rejoyce Gavhi-Molefo for always supporting me personally and career-wise.

I gratefully acknowledge the funding received towards my PhD from the National Research Foundation (NRF) and the University of Venda. I am also thankful to the funding received from the Teaching Development Grand National Collaborative Project (TDG) to take leave to complete my study as well as to go for an international conference.

Lastly, I once again give praise and thanks to God for His abundance provisions, favours, mercies and kindness for starting a good work in me and for His ever faithfulness in completing this study.

To God Be The Glory!

Dedications

I dedicate this work to my parents.
"Leswinene swa tirheliwa n'wananga" Papa

Contents

Declaration of Authorship i

Abstract ii

Acknowledgements iv

Contents vii

List of Figures x

List of Tables xiii

1 Overview of vector-borne diseases 1
- 1.1 Introduction . . . 1
- 1.2 Vector-borne diseases transmission mechanisms . . . 4
- 1.3 Overview of multi-scale models categories for vector-borne disease systems . . . 6
- 1.4 Mathematical models of vector-borne diseases . . . 7
- 1.5 Problem statement . . . 10
- 1.6 Overall aim of the study . . . 11
- 1.7 Objectives of the study . . . 11
- 1.8 Structure of the study . . . 11

2 Multi-scale Modelling Of Directly Transmitted Vector-Borne Diseases 13
- 2.1 Introduction . . . 13
- 2.2 Derivation of the multi-scale Model for Malaria Elimination . . . 17
  - 2.2.1 The Four Sub-models of Malaria Transmission Dynamics . . . 17
  - 2.2.2 Integration of the Four Separate Sub-models of Malaria Transmission Dynamics into a Single multi-scale Model . . . 23
  - 2.2.3 Simplifying the Complete multi-scale Model for Malaria . . . 32
- 2.3 Mathematical Analysis Of The Baseline multi-scale Model Of Malaria Dynamics 41
  - 2.3.1 Positivity and boundedness of solutions of the malaria multi-scale model 41
  - 2.3.2 The Malaria Elimination State and Its Stability . . . 43
  - 2.3.3 Local Stability of the Malaria Elimination state . . . 49
  - 2.3.4 Global Stability of the Malaria Elimination state . . . 49

2.3.5 Estimating the Malaria Baseline Burden . . . 50
2.3.6 The Existence of the Endemic state . . . 52
2.3.7 The Local Stability of Malaria Baseline Endemic state . . . 54
2.3.8 Sensitivity Analysis of the Transmission Metrics of Baseline multi-scale Model . . . 61
2.3.9 The Influence of Within-host sub-models on between-host sub-models . . . 67
2.4 Summary . . . 72

3 Using multi-scale Modelling To Guide Malaria Control and Elimination 73
3.1 Introduction . . . 73
3.2 Evaluation of the comparative effectiveness of malaria health interventions using the basic reproductive number as the indicator of intervention effectiveness . . . 79
3.3 Evaluation of the comparative effectiveness of malaria health interventions using community gametocyte load as the indicator of intervention effectiveness . . . 82
3.4 Evaluation of the comparative effectiveness of malaria preventive and treatment interventions using community sporozoite load as the indicator of intervention effectiveness . . . 85
3.5 Summary . . . 88

4 Basic Schistosomiasis mathematical model with interventions 90
4.1 Introduction . . . 90
4.2 Basic Schistosomiasis mathematical model formulation . . . 95
4.2.1 Feasible Region of Equilibria of the Model . . . 100
4.2.2 Disease free equilibrium (DFE) . . . 102
4.2.3 Reproductive number . . . 102
4.2.4 Local Stability of DFE . . . 104
4.2.5 The Endemic Equilibrium State and Its Existence . . . 105
4.2.5.1 The Endemic Equilibrium State . . . 105
4.2.5.2 Existence of endemic equilibrium . . . 106
4.2.6 Sensitivity Analysis . . . 109
4.3 Basic Schistosomiasis Mathematical Model with control measures . . . 111
4.3.1 Properties of the model . . . 114
4.3.2 Reproductive Number . . . 114
4.3.3 Endemic equilibrium state . . . 116
4.3.4 Numerical simulations . . . 118
4.4 Summary . . . 128

5 Multi-scale Modelling of Environmentally Transmitted Vector-Borne Diseases 130
5.1 Introduction . . . 130
5.2 Transmission of Infectious Diseases That Are Environmentally Trasmitted . . . 133
5.3 Multi-scale Model of schistosomiasis . . . 137
5.3.1 Feasible Region of the Equilibria of the Model . . . 144
5.3.2 Determination of DFE and its Stability . . . 146
5.3.3 Reproductive Number . . . 146
5.3.4 Local Stability of DFE . . . 151

5.3.5 Global Stability of DFE 151
5.3.6 The Endemic Equilibrium State and its Stability 153
5.3.7 The Endemic Equilibrium 153
5.3.8 The Existence of the Endemic Equilibrium State 157
5.3.9 Local Stability of the Endemic Equilibrium 160
5.4 The Effect of Environment on Schistosomiasis transmission dynamics 168
5.5 Numerical Simulations 169
5.5.1 Methods 170
5.5.2 Results 172
5.6 Summary 181

6 Conclusions and Future Research Directions **182**
6.1 Conclusions 182
6.2 Future Research Directions 186

List of Figures

1.1 Deaths from vector-borne disease [15]. 3
1.2 A conceptual diagram illustrating the three different groups of transmission cycles for infections that are environmentally transmitted. 5

2.1 A conceptual diagram of the complete integrated multi-scale model of malaria baseline transmission dynamics where $\lambda_h = \beta_h M_h$. In this Figure δ_V stands for $\widehat{\delta_V}(P_v)$, δ_H stands for $\widehat{\delta_H}(M_h)$ and γ_H stands for $\widehat{\gamma_H}(M_h)$. 31
2.2 Graphs showing changes in (a) community gametocyte load (G_H), (b) population of infected mosquitoes I_V, (c) population of infected humans I_H, and (d): community sporozoite load P_V for different values of death rate of within-human gametocyte load μ_h: $\mu_h = 0.0625$, $\mu_h = 0.05938$, $\mu_h = 0.05625$, and $\mu_h = 0.05$. . 68
2.3 Graphs showing changes in (a) community gametocyte load (G_H), (b) population of infected mosquitoes I_V, (c) population of infected humans I_H, and (d): community sporozoite load P_V for different values of death rate of merozoites μ_m: $\mu_m = 0.0006$, $\mu_m = 0.006$, and $\mu_m = 0.06$. 69
2.4 Graphs showing changes in (a) community gametocyte load (G_H), (b) population of infected mosquitoes I_V, (c) population of infected humans I_H, and (d): community sporozoite load P_V for different values of merozoites produced per bursting infected red blood cell N_m: $N_m = 100$, $N_m = 200$, $N_m = 300$ and $N_m = 400$. 70
2.5 Graphs showing changes in (a) community gametocyte load (G_H), (b) population of infected mosquitoes I_V, (c) population of infected humans I_H, and (d): community sporozoite load P_V for different values of infection rate of erythrocytes by free merozoites in the blood stream β_h: $\beta_h = 0.0083$, $\beta_h = 0.0625$, and $\beta_h = 0.76$. 71

4.1 A conceptual diagram of the mathematical model of schistosomiasis in human and snail populations. 100
4.2 Numerical simulations showing dynamics of infected humans (I_H), infected snails (I_V), miracidia (M) and cercariae in water (P_W) over time in days for different values of efficacy of improved sanitation in reducing matured worms $g:\ g = 0.1,\ g = 0.4,\ g = 0.6$ and $g = 0.9$ 119
4.3 Numerical simulations showing dynamics of eggs on the land (E_L), eggs in the water (E_W), miracidia (M) and cercariae in water (P_W) over time in days for different values of efficacy of improved sanitation in reducing matured worms $g:\ g = 0.1,\ g = 0.4,\ g = 0.6$ and $g = 0.9$. 120

4.4 Numerical simulations showing dynamics of infected humans (I_H), infected snails (I_V), miracidia (M) and cercariae in water (P_W) over time in days for different values of efficacy of HEC in reducing human contact with unsafe water bodies a : $a = 0.9,\ a = 0.5,\ a = 0.3$ and $a = 0.1$. 121
4.5 Numerical simulations showing the dynamics of eggs on the land (E_L), eggs in the water (E_W), miracidia (M) and cercariae in water (P_W) over time in days for different values of efficacy of HEC in reducing human contact with unsafe water bodies a : $a = 0.9,\ a = 0.5,\ a = 0.3$ and $a = 0.1$, ... 122
4.6 Numerical simulations of the dynamics of infected humans (I_H), infected snails (I_V), miracidia (M) and cercariae in water (P_W) over time in days for different values of efficacy mollucicides in killing snails e : $e = 0.1,\ e = 0.4,\ e = 0.6$ and $e = 0.9$. 123
4.7 Numerical simulations showing dynamics of infected humans (I_H), infected snails (I_V), miracidia (M) and cercariae in water (P_W) over time in days for different values of efficacy mollucicides in killing snails e : $e = 0.1,\ e = 0.4,\ e = 0.6$ and $e = 0.9$, (model system 5.3.9). 124
4.8 Numerical simulations showing dynamics of eggs on the land (E_L), eggs in the water (E_W), miracidia (M) and cercariae in water (P_W) over time in days for different values of efficacy of treatment in reducing schistosome eggs f : $f = 0.1,\ f = 0.4,\ f = 0.6$ and $f = 0.9$. 125
4.9 Numerical simulations showing dynamics of infected humans (I_H), infected snails (I_V), miracidia (M) and cercariae in water (P_W) over time in days for different values of efficacy of climate change in reducing cercariae production by each infected snail n : $n = 0.1,\ n = 0.4,\ n = 0.6$ and $n = 0.9$. 126
4.10 Numerical simulations showing dynamics of infected humans (I_H), infected snails (I_V), miracidia (M) and cercariae in water (P_W), over time in days for different values of efficacy of extreme weather changes in reducing snail production capacity c : $c = 0.1,\ c = 0.4,\ c = 0.6$ and $c = 0.9$. 127

5.1 A conceptual diagram showing the four different groups of transmission cycles for infections that are environmentally trasmitted. 135
5.2 A conceptual diagram of the mathematical model of linked with-host and between-host dynamics of human schistosomiasis. 143
5.3 Simulations of model system (5.3.9) showing the evolution with time of (a) *top left*: infected humans, (b) *top right*: infected snails, (c) *bottom left*: miracidia in the physical water environment, and (d) *bottom right*: cercariae in the physical water environment for different values of rate of excretion of worm eggs by an infected human, α_E: $\alpha_E = 0.005$, $\alpha_E = 0.0039$ and $\alpha_E = 0.3$. 173
5.4 Simulations of model system (5.3.9) showing the evolution with time of (a) *top left*: infected humans, (b) *top right*: infected snails, (c) *bottom left*: miracidia in the physical water environment, and (d) *bottom right*: cercariae in the physical water environment for different values of natural death rate of worm eggs, μ_E: $\mu_E = 0.000685$, $\mu_E = 0.0025$ and $\mu_E = 0.005$. 174

5.5 Graphs of numerical solutions showing propagation of (a) *top left*: infected humans, (b) *top right*: infected snails, (c) *bottom left*: miracidia in the physical water environment, and (d) *bottom right*: cercariae in the physical water environment for different values of natural death rate of immature worms, μ_I: $\mu_I = 0.000685$, $\mu_I = 0.0005$ and $\mu_I = 0.5$. 175
5.6 Graphs of numerical solutions showing propagation of (a) *top left*: infected humans I_H, (b) *top right*: infected snail hosts I_V, (c) *bottom left*: miracidia in the physical water environment, and (d) *bottom right*: cercariae in physical water environment for different values of the rate of mature worm fecundity within an infected human, N_P: $N_P = 300$, $N_P = 600$, $N_P = 1200$ and $N_P = 2000$. 176
5.7 Graphs of numerical solutions showing propagation of (a) *top left*: immature worms within an infected human (W_I), (b) *top right*: mature worms within an infected human (W_P), (c) *bottom left*: worm eggs within an infected human (E_H), and (d) *bottom right*: cercariae within an infected human (P_H), for different values of the infection rate of humans by cercariae, β_H: $\beta_H = 0.028$, $\beta_H = 0.075$ and $\beta_H = 0.122$ 177
5.8 Graphs of numerical solutions showing propagation of (a) *top left*: immature worms within an infected human (W_I), (b) *top right*: mature worms within an infected human (W_P), (c) *bottom left*: worm eggs within an infected human (E_H), and (d) *bottom right*: cercariae within an infected human (P_H), for different values of the infection rate of snails by miracidia, β_V: $\beta_V = 0.000127$, $\beta_V = 0.000664$ and $\beta_V = 0.0012$ 178
5.9 Graphs of numerical solutions showing propagation of (a) *top left*: immature worms within an infected human (W_I), (b) *top right*: mature worms within an infected human (W_P), (c) *bottom left*: worm eggs within an infected human (E_H), and (d) *bottom right*: cercariae within an infected human (P_H), for different values of natural death rate of snails, μ_V: $\mu_V = 0.000596$, $\mu_V = 0.0014$, $\mu_V = 0.8$ and $\mu_V = 0.9$ 179
5.10 Graphs of numerical solutions showing propagation of (a) *top left*: immature worms within an infected human (W_I), (b) *top right*: mature worms within an infected human (W_P), (c) *bottom left*: worm eggs within an infected human (E_H), and (d) *bottom right*: cercariae within an infected human (P_H), within a single infected human, for different values of recruitment rate of new susceptible humans, Λ_H: $\Lambda_H = 800$, $\Lambda_H = 1000$ and $\Lambda_H = 1600$. 180

List of Tables

1.1 Examples of vectors and diseases they carry with their respective pathogens[10]. 3

2.1 A summary of the variables of the malaria multi-scale model given by (2.2.9). . . 37
2.2 Between-host (human and mosquito) parameter values and their description. . . . 39
2.3 Within-Mosquito and within-human parameter values and their description. . . . 40
2.4 Sensitivity indices of N_h, N_v and $\Re_0$. 63
2.5 Sensitivity indices of $\widetilde{G_H}$, $\widetilde{P_V}$, and $\mathcal{R}_0$ with respect to 34 parameters of the malaria disease system. 66

3.1 Summary of the actions of the components of the two malaria health interventions on disease dynamics. 75
3.2 Results of the assessment of comparative effectiveness of malaria interventions using the %age reduction of basic reproductive number ($\mathcal{R}_0$) as the indicator intervention effectiveness when each of the five interventions is assumed to have: (a) low efficacy of 0.30, (b) medium efficacy of 0.60, and (c) high efficacy of 0.90. 80
3.3 Results of the assessment of comparative effectiveness of malaria interventions using the %age reduction of endemic value of the community gametocyte load ($\widetilde{G_H}$) as the indicator intervention effectiveness when each of the five interventions is assumed to have: (a) low efficacy of 0.30, (b) medium efficacy of 0.60, and (c) high efficacy of 0.90. 83
3.4 Results of the assessment of comparative effectiveness of malaria interventions using %age reduction of the endemic value of the community sporozoite load ($\widetilde{P_V}$) as the indicator intervention effectiveness when each of the five interventions is assumed to have: (a) low efficacy of 0.30, (b) medium efficacy of 0.60, and (c) high efficacy of 0.90. 86

4.1 Description of parameters 101
4.2 Between-host and within-host schistosomiasis transmission dynamics Parameter values 109
4.3 Sensitivity Indices of R_0 111
4.4 Summary of control mechanisms of schistosomiasis 113

5.1 Summary of variables used in the model 138
5.2 Between-host parameter values for model system (3.9). 170
5.3 Within-host parameter values for model system (3.9). 171
5.4 Environmentally transmitted pathogens and their associated environmental parameter values for model system (3.9). 172

Chapter 1

Overview of vector-borne diseases

1.1 Introduction

Vector-borne diseases are illnesses caused by parasites, viruses and bacteria that are transmitted by organisms/vectors such as mosquitoes, sandflies, triatomine bugs, blackflies, ticks, tsetse flies, mites, snails and lice [8]. Vector-borne diseases transmission depends on three different factors, namely pathologic agent, arthropod vector, and human host [8]. Vector-borne diseases are commonly found in regions where access to safe drinking-water and sanitation systems are problematic [166].

Vectors are facilitators of many dangerous disease-causing organisms, the prevention and treatment of which cannot be effective for long without addressing the vector directly [11]. The characteristics of vector-borne diseases include high disease transmissibility, explosive, unpredicted spread of disease, resilience to control and prevention because of the vector's small size and sheer numbers as well as large range visas diseases that require direct contact [11].

The vector receives the pathogen from an infected host and transmits it either to an intermediary host or directly to the human host. The different stages of the pathogen's life cycle occur during this process and are intimately dependent upon the availability of suitable vectors and hosts [9]. Key components that determine the occurrence of vector-borne diseases include: (a) The abundance of vectors and intermediate and reservoir hosts;(b) The prevalence of the disease-causing pathogens suitably adapted to the vectors and human or animal host;(c) The local environmental

conditions, especially temperature and humidity and (d) The resilience behavior and immune status of the human population [9].

Each year there are more than 700 000 deaths from vector-borne diseases such as malaria, dengue, schistosomiasis, human African trypanosomiasis, leishmaniasis, Chagas disease, yellow fever, Japanese encephalitis and onchocerciasis, globally [162]. Since 2014, major outbreaks of dengue, malaria, chikungunya yellow fever and Zika have afflicted populations, claimed lives and overwhelmed health systems in many countries [162].

Schistosomiasis and malaria are the world's most prevalent vector-borne diseases [166]. Out of a world population of approximately 5300 million people in 1990, some 2200 million people were considered as being at high risk of contracting malaria, and some 60 million as being vulnerable to schistosomiasis [166]. Roughly 270 million people are actually infected with the malaria parasite and the current prevalence of schistosomiasis is about 200 million [166].

Dengue is the fastest spreading vector-borne disease of the twenty-first century [161]. More than 1.3 billion people in Africa are at risk of malaria, as over 75% of the population live in malaria-prone areas [161]. In 2002, Africa had more deaths from vector-borne diseases than any other continent (see figure 1.1) [15]. Because there is a high health risk for the vector-borne diseases and a large number of deaths associated with vector-borne diseases, it is important to increase our understanding of their transmission dynamics and be ready for any emerging vector-borne disease [11]. Table 1.1 represents the list of some of the important vector-borne diseases [10].

Main risk factors of vector borne diseases include climate variations, certain human activities, as well as movements of animals, people or goods. Human life is dependent on the earth's climate system. The interactions of the atmosphere, ocean, terrestrial and marine biospheres, chromosphere and land surface determine the earth's surface climate [12].

Climate change plays an important role in the seasonal pattern or temporal distribution of diseases that are carried and transmitted through vectors because the vector animals often thrive in particular climate conditions. For instance, warm and wet environments are excellent places for mosquitoes to breed. If the mosquitoes happen to be a species that can transmit the disease and if there is an infected population in the region, then the disease is more likely to spread in that area. Because they are sensitive to climate, the distribution and number of vectors is affected by climate change [13]. Adaptive strategies to climate change like irrigation can result in the increase of the risk of schistosomiaisis transmission [12].

The greatest effect of climate change on the transmission of vector-borne diseases is likely to be observed at the extremes of the range of temperatures at which transmission occurs. It is estimated that on average, global temperatures will have risen by $1.0 - 3.5^0C$ by 2100, thus increasing the likelihood of many vector-borne diseases [12]. The temporal and spatial changes

in temperature, precipitation and humidity that are expected to occur under different climate change scenarios will affect the biology and ecology of vectors as well as intermediate hosts [12]. Consequently, the risk of disease transmission is increased. The risk increases because, although arthropods can regulate their internal temperature by changing their behavior, they cannot do so physiologically, and are thus critically dependent on climate for their survival and development [12].

Disease and Host	**Pathogen**	**Vector**
Schistosomiasis in humans	Flatworm	Snails
Malaria in vertebrates	Plasmodium protozoan	Moisquitoes
Sleeping sickness in humans	Trypanosome protozoan	Tsetse flies
Lyme disease in humans	Bacterial spirochete	Ticks
Yellow fever in humans	Arbovirus	Mosquitoes
Bubonic plague in humans	Yersinia bacteria	Fleas on rodents
Typhus in humans	Rickettsial bacteria	Body lice
Strawberry crinkle virus disease	Rhabdovirus	Aphid
African cassava mosaic virus disease	Geminivirus	Whitefly
Pierce's disease in grapes	Xylella bacteria	Sharpshooter bugs

Table 1.1: Examples of vectors and diseases they carry with their respective pathogens[10].

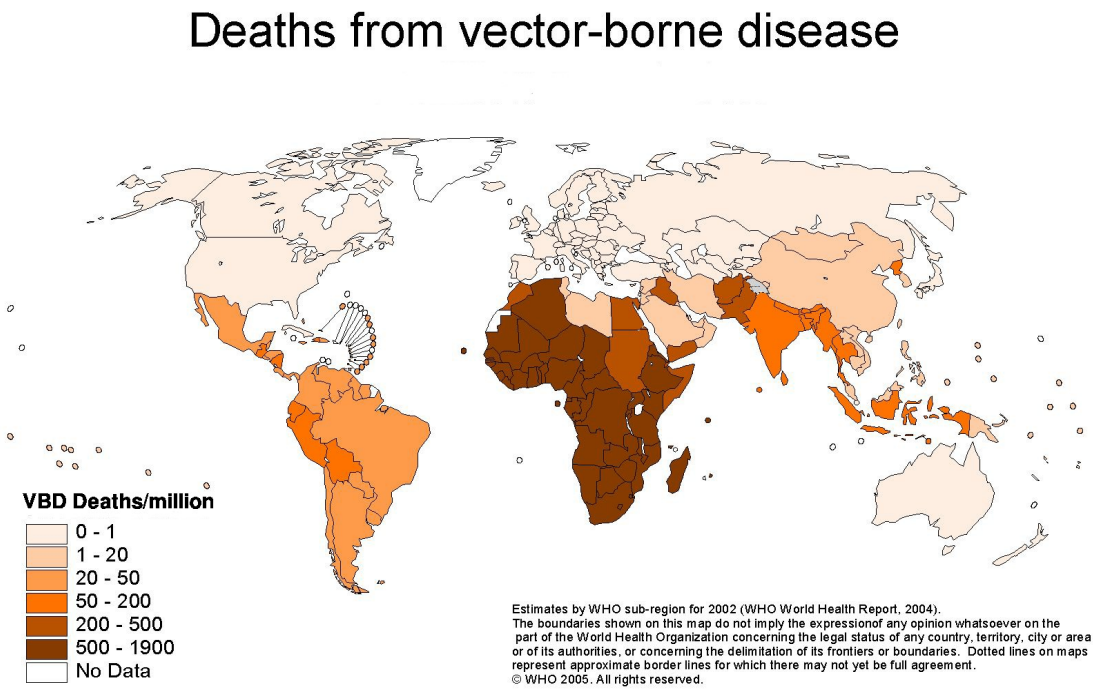

Figure 1.1: Deaths from vector-borne disease [15].

Significant progress has been made against vector-borne diseases control through a combination of poverty alleviation and socio-economic development, increased access to health services, large scale and more coordinated control programmes, and development of more effective control measures. As a result of these successes, the proportional attribution of vector-borne diseases to global mortality has declined in recent years [7]. However, not all vector-borne diseases are declining in incidence globally, and some diseases like malaria, which are decreasing at the global scale, are stable or increasing in specific locations. More efforts in controlling these diseases are therefore important attribution to global health, security and development. Moreover, policy markers engaged in control of vector-borne diseases need to take into account the following factors:(i) Climate change factors; (ii) Environmental factors; (iii) Within-host and between-host dynamics, that is, what happens at the population level and within infected individual and (iv) Cost involved in designing and implementing disease control measures.

Vector control relies on integrated vector management, that is, whenever possible, biological, environmental and use of insecticides control mechanisms complement each other. The early 20^{th} century discovery that mosquitoes transmitted diseases like malaria, yellow fever and dengue led quickly to draining bred and eventually to the use of pesticides, which reduced populations of these disease vectors. Access to water and sanitation is a very important factor in disease control and elimination [165].

1.2 Vector-borne diseases transmission mechanisms

In this section, we outline some of the vector-borne diseases transmission cycles by describing their transmission pathways and also give examples of each transmission cycle.

Transmission Cycle	Transmission Pathway	Examples
(a) 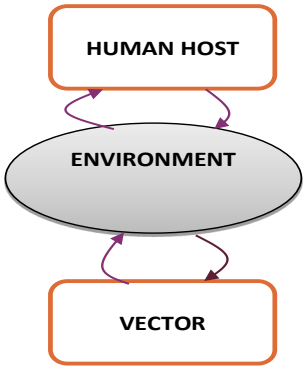	Vector-borne disease transmission is through ingestion/contact. Environmental contamination is through human and/or vector shedding the pathogen.	Schistosomiasis Guinea Worm
(b) 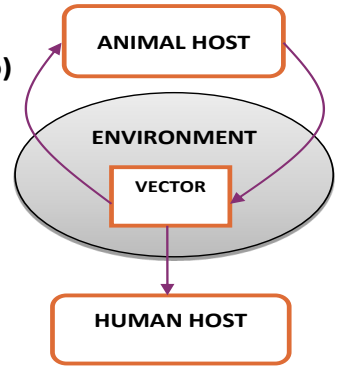	Host infection is through a bite by/or contact with an infected vector. Vector infection is through a bite by/or contact with an infected animal host.	Lyme Disease West Nile Virus
(c) 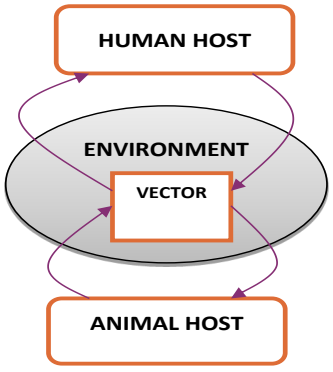	Host infection is through a bite by/or contact with an infected vector. Vector infection is through a bite by/or contact with an infected human orimal host.	Lymphatic Filariasis Dengue Malaria Onchocerciasis Trypanosomiasis

Figure 1.2: A conceptual diagram illustrating the three different groups of transmission cycles for infections that are environmentally transmitted.

Disease transmission cycle (a) in Figure 1.2 includes within-host and between-host infections that are environmentally transmitted. During the disease transmission, human and vector do not interact with each other directly, except through the shared parasites. For instance, for *schistosomiasis* and *guinea worm*, the environment contamination is through human and/or vector shedding the pathogen. In this transmission cycle, the transmission occurs either between the human-host and environment or between the vector and environment. There is no human and vector interaction in this cycle.

Disease transmission cycle (b) in Figure 1.2 includes the host infections through a bite by/or contact with an infected vector. Vector infection is through a bite or/by contact with an infected animal host. Vector-borne diseases that fall under this cycle are *yellow fever*, *lyme disease* and *west nile virus*. In this cycle, the human-host transmission occurs after the interaction between animal-host and vector in the environment. That is, the transmission occurs either from vector to human-host or from animal-host to vector.

Disease transmission cycle (c) in Figure 1.2 includes vector-borne infections that are through a bite by/or contact with an infected vector. The vector infection is through a bite by/or contact with an infected human or animal-host. For example, *Lymphatic*, *filarias*, *dengue*, *malaria*, *onchocerciasis* and *trypanosomiasis*. The transmission of host infection occurs after direct contact between human-host and vector in the environment or between animal-host and vector in the environment. In this cycle, the transmission does not occur from human to human or from vector to vector. In general, this is an indirect contact transmission, whereby transmission occurs when there is no direct contact from human-to-human. Contact occurs from a reservoir to contaminated surfaces or objects, or to vectors such as mosquitoes, flies, mites, ticks, rodents or dogs.

In our case, we follow the disease transmission pathways where environmental contamination is through human and/or vector shedding the pathogen (schistosomiasis) and where vector infection is through a bite by or direct contact with an infected human or animal host (malaria).

1.3 Overview of multi-scale models categories for vector-borne disease systems

In this section, we give a brief overview of multi-scale models categories for vector-borne disease systems, whereby the micro-scale and macro-scale of vector-borne disease systems are the within-host and between-host scales, respectively.

There are five categories of multi-scale models of infectious disease systems that integrate the within-host and between-host scale of disease systems, namely: (i) Individual-based multi-scale

models (IMSMs); (ii) Nested multi-scale models (NMSMs); (iii) Embedded multi-scale models (EMSMs); (iv) Hybrid multi-scale models (HMSMs) and coupled multi-scale models (CMSMs) for more details see [149]. However, in our study we develop coupled multi-scale and embedded models since they are relevant to vector-borne diseases systems whereby the disease transmission is either through environmental contamination or direct contact, respectively.

Coupled multi-scale models (CMSMs) are host-level immune-epidemiological models which take into account the diversity of pathogen and host species composition. CMSMs use parallel integration framework. Host-level immune-epidemiological models are either described homogeneously or in hybrid way. CMSMs take into account the host and pathogen species diversity. CMSMs category is either top-down or bottom-up multi-scale type or both [149].

Embedded multi-scale models (EMSMs) are host level immune-epidemiological models whereby within-host scale and between-host scale interact with each other resulting in reciprocal feedback. EMSMs category use embedded integration framework. It is a top-down and bottom-up modelling approach. There is a bidirectional flow of information between the within-host submodel and between-host sub-model in EMSMs category whereas there is only uni-directional flow of information in nested multi-scale models [149].

1.4 Mathematical models of vector-borne diseases

The model first developed by Ross [3] and subsequently modified by Macdonald [4] has influenced both the modeling and the application of control strategies to vector-borne diseases. Recently, mathematical models concerning the emergence and re-emergence of the vector-host infectious disease have been proposed and analyzed. For example, an ordinary differential equation compartmental model for the spread of dengue fever has been presented in [5]. Some mathematical work about the transmission dynamics of vector-borne diseases have been published recently [6].

In [181], a coupled multi-scale model was developed. The model combined within-host and between-host modelling framework for the evolution of antimalarial drugs resistance using a stochastic modelling approach. Each submodel for the between-host and for the within-host was first presented as a deterministic set of ODEs. The final, stochastic model was then obtained by translating each deterministic component into the corresponding stochastic model, using Gillespie tau-leap algorithms [180]. The authors established that the spread of drug resistance is generally less likely in areas of intense transmission, and therefore of increased competition between strains, an effect exacerbated when costs of drug resistance are higher. Further, they also used the

(Single-host multi-pathogen coupled multi-scale model) SHMP-CMSM to illustrate how treatment influences the spread of drug resistance, with a trade-off between slowing resistance and curbing disease incidence. The authors established that treatment coverage has a stronger impact on disease prevalence, whereas treatment efficacy primarily affects drug resistance spread, suggesting that coverage should constitute the primary focus of control efforts. For further examples of this multi-scale modelling approach refer to [178, 179, 182, 183, 185].

In [192], a typical example of Embedded multi-scale model arising from modelling the host level immuno-epidemiology of environmentally transmitted infectious disease systems is provided in the context of schistosomiasis infectious disease system. Using results from the analysis of the endemic equilibrium expression, the disease reproductive number R_0 , and numerical simulations of the full model, the authors were able to adequately account for the reciprocal influence of the linked within-host and between-host sub-models. In particular, the authors illustrated that for human schistosomiasis, the outcome of infection at the individual level determines if, when and how much the individual host will further transmit the infectious agent into the environment, eventually affecting the spread of the infection in the host population [192].

The most commonly modelled vector-borne diseases are malaria and dengue, but many others also cause notable burden to humans and other animals [163]. In [167], a model that explicitly coupled the between-host and within-host was developed. It was established that when the two sub-systems are explicitly coupled, the full system exhibits a backward bifurcation. Most models have focused on between-host and within-host processes separately. Previously, some attempts have been made to study models that coupled these two processes (between-host and within-host) [168, 169]. A multi-scale of malaria model inter-comparison that considered the impact of climate change on the disease transmission at global scale is presented in [164]. However the model failed to account for within-host and the complete life cycle of malaria.

In [175], a typical example of a single-host multi-pathogen coupled multi-scale model (SHMP-CMSM) for studying the immuno-epidemiology of infectious disease systems is presented in the context of a multi-group HIV/AIDS infection model. A multi-group coupled multi-scale model composed of within-host model of ODEs and between-host model of ODEs and first-order PDEs was formulated together with an optimal control problem subject to fusion inhibitors and protease inhibitors. This multi-scale model is further classified as a SHMP-CMSM of hybrid type. The optimality system was solved numerically. The numerical simulations obtained suggest that the combination of fusion and PIs reduces viral load at the within-host level and the disease-induced mortality at the population level. However, the results lead to an increase in the number of infectious individuals at the population level since infectious individuals live longer in the presence of drugs. For more examples of coupled multi-scale modelling approach refer to [170,

173, 179, 185] in the case of modelling multi-strain infections and [185] in the case of modelling multi-group infections.

The main challenges faced in modelling vector-borne diseases are as follows: exploring the effects of combinations of control measures and whether there are epidemiological and evolutionary synergies for using multiple control measures; understanding the roles of different hosts; how to measure control and infection patterns and heterogeneities in contact rates [164]. Despite the early seminal work by Ronald Ross, the increasing availability of big data still constitutes additional challenges concerning their coherent use by expanding the modeler's views into new macro and micro model structures [191].

Several BIDI-EMSMs for Toxoplasma gondii were developed and analyzed using distinct modifications where the within-host submodel and the between-host submodel are coupled through the pathogen load in the environment in [186, 188, 189]. The main findings from these studies is that infection may persist at population level even if the isolated between-host reproduction number is less than one. In [190] there is another good example of a BIDI-EMSM in the context of cholera transmission with both environmental and direct transmission.

In [177], a model of vector-host disease with both direct transmission and the vector-mediated transmission was investigated. The model incorporated some important epidemiological features, such as density-dependent birth rate in both host and vector populations and time dependent control functions. The model also took into account three types of control functions associated with personal protection, blood donor screening and vector reduction strategies. Their control plots indicated that the number of exposed and infected human decreased and the total number of vector population also decreased in the optimality system. By following Pontryagin's Maximum Principle, the control system was analyzed to determine the necessary conditions for the existence of an optimal control. Moreover, the number of exposed, infected hosts and the total number of vector population were minimized by using three control variables. The disease dynamics were investigated using a numerical method based on optimal control to identify the best strategy of a vector-borne disease in order to reduce infection and prevent vector host as well as direct contacts by using three controls. It was established through numerical results that preventive practices are very effective in reducing the incidence of infectious hosts and vectors [177]. Another example of direct transmission mode is presented in [176].

To the best of our knowledge only one BIDI-EMSM for directly transmitted infectious disease systems has been developed to date [187] in the context of a general viral infectious disease system. The model allows the two dynamic processes at both the within-host scale and the between-host scale to explicitly depend on each other. From the analysis of this BIDI-EMSM it is shown that new properties can emerge from the coupled system such as multiple endemic

equilibria and stability.

In this study, we are mainly interested in developing coupled and embedded multi-scale models of vector-borne diseases. Two representative examples of vector-borne diseases are used to illustrate ideas, namely malaria (a directly transmitted vector-borne disease) and schistosomiasis (a indirectly transmitted vector-borne disease). This will assist us in developing new mathematical modelling frameworks and their applications in control of vector-borne diseases. We take into account both between-host and within-host disease transmission dynamics following multi-scale modelling approach in [149].

1.5 Problem statement

Due to high rate of deaths from vector-borne diseases, it is imperative for us to come up with effective control measures that can be implemented in order to significantly control and reduce the spread of vector-borne diseases in Africa. It is estimated that in 2015 malaria caused 212 million clinical episodes and 429,000 deaths [148]. It is also estimated that more than 200,000 deaths annually are due to *schistosomiasis* [17]. Mathematical models have been a useful tool to gain insights into various aspects of vector-borne diseases transmission dynamics. In particular, the transmission dynamics of malaria and schistosomiasis. These insights can potentially assist us to assess comparative effectiveness and implications of various preventive and control measures. Current modelling frameworks based on compartmentalizing humans and mosquitoes into SIRS and SI or SEIRS and SEI are based on addressing a complicated question about which mosquito infects which human and which human infects which mosquito in a particular community. In this study, we present a new modelling framework based on addressing a more simpler question which is about how often are humans and mosquitoes get infected in a particular community. Since the data on which mosquito infects which human and which human infects which mosquito are difficult to obtain. Further, there is still no generalized framework for linking the within-host and between-host dynamics of infectious diseases. Furthermore, for linking the within-host and between-host dynamics of vector-borne diseases that are indirectly/environmentally trasmitted, there is a stumbling block in that there is a gap in knowledge on how environmental factors (through water, air, soil, food, fomites, etc.) alter many aspects of such infections including susceptibility to infective dose, persistence of infection, pathogen shedding and severity of the disease. In this study, we fill the gab by establishing new mathematical frameworks that will address a broader spectrum of both directly and indirectly transmitted vector-borne diseases.

1.6 Overall aim of the study

To develop multi-scale models for vector-borne diseases and use them to illustrate the comparative effectiveness of treatment and preventive measures for vector-borne diseases.

1.7 Objectives of the study

The objectives of the study are as follows.

- To develop a multi-scale model for directly transmitted vector-borne diseases with a special reference to malaria where the within-human and within-mosquito sub-models are uni-directionally coupled to human-to-mosquito and mosquito-to-human sub-models.
- To extend the multi-scale model for directly transmitted vector-borne diseases by incorporating treatment and preventive interventions (artemisinin-based combination therapy and long-lasting insecticide treated nets) for vector-borne diseases.
- To develop a multi-scale model for environmentally transmitted vector-borne diseases with a special reference to schistosomiasis. The model is based on the linkage of between-host scale and within-host scale sub-models.

1.8 Structure of the study

- **Chapter 2** deals with development of a baseline uni-directional coupled multi-scale model with a special reference to malaria where the within-human and within-mosquito sub-models are unidirectionally coupled to human-to-mosquito and mosquito-to-human sub-models.
- In **Chapter 3** extend, the baseline uni-directional coupled multi-scale model in **Chapter 2** by incorporating treatment and preventive interventions (artemisinin-based combination therapy and long-lasting insecticide treated nets).
- **Chapter 4** deals with the development of a basic transmission dynamics single-scale model for vector-borne diseases with a special reference to schistosomiasis.
- Whereas in **Chapter 5** we concern ourselves with the development of an embedded multi-scale model for environmentally/directly transmitted vector-borne diseases with a special reference to schistosomiasis.

- **Chapter 6** gives conclusions and future research directions.

Chapter 2

Multi-scale Modelling Of Directly Transmitted Vector-Borne Diseases

2.1 Introduction

Among the most important innovations in disease modelling in recent years is the development of multi-scale models of infectious diseases -the all-encompassing quantitative representation of an infectious disease system that can lay bare its mechanisms of transmission. This innovation requires a paradigm shift towards a sharper focus on understanding the disease dynamics and the mechanism of how it spreads among humans and animals.

Improving human and animal health can be achieved through integrating knowledge from epidemiology and immunology research with that from a broad spectrum of health research such as environmental health, molecular biology, population biology and microbiology. Efforts to develop multi-scale models of infectious diseases have been underpinned by a recent categorization framework that helps to categorize the different multi-scale models at different levels of organization of an infectious disease system [192]. This framework acknowledges that different pathogens interact with their hosts (humans, animals, vectors) in very different ways resulting in different types of multi-scale models of infectious disease systems that can be developed at the various levels of organization of an infectious disease system which include the cell level, the tissue level and the host level. Such models allow progressively greater spatial, temporal, or causal detail of infectious disease systems to be considered as the scales become finer. The development

of multi-scale models of infectious diseases in this way is even more possible now than ever before because infectious disease study has entered a new era dominated by the "omics" [193–196] as a result of the advent of high-throughput experimental technologies producing patient-specific data, establishing a complete cascade from genome, transcriptome, proteome, metabolome and physiome to health, forming a multi-scale, multi-science system that can assist in establishing the molecular basis of diseases.

In general, there is still widespread lack of knowledge on the mathematical techniques for the representation and construction of multi-scale models of infectious disease systems. The central idea in multi-scale modelling is to divide a modelling problem such as an infectious disease system into a family of sub-models that exist at different scales and then attempt to study the problem at these scales while simultaneously linking the sub-models across these scales. We therefore define multi-scale modelling as a modelling methodology in which a collection of partial models or sub-models from at least two different scales are integrated into a single model using a wide range of linking/coupling methods [200]. However, this divide-and-rule strategy poses new challenges in terms of strategies for problem decomposition and solution strategy, scale separation and coupling, integration and coupling of sub-models of different or same formalism and validation of multi-scale models. Some papers have proposed that multi-scale models of infectious disease systems can be developed through integrating a within-host sub-model and a between-host sub-model by making parameters of the between-host sub-model functions of the independent variable of the within-host sub-model [198–200]. The papers suggest that this can be achieved by, for example, making transmission parameters of the between-host sub-model functions of within-host pathogen load variables and immune response. But to date, this approach has not been successfully demonstrated for a specific infectious disease system. This chapter represents a first attempt to develop a multi-scale model of a specific infectious disease system - malaria using such an approach. The resulting multi-scale is a suitable candidate for guiding malaria control and reduction.

The explicit aim of this chapter is to develop a new coupled multi-scale model of malaria disease dynamics that integrate the within-host scale and between-host scale (human host and mosquito host) and demonstrate the utility and process by which this multi-scale model can be used to guide malaria control and elimination using two malaria interventions (artemisinin-based combination therapy and long-lasting insecticide treated nets). Malaria is the world's most prevalent vector-born disease. Three organisms are implicated in the transmission of this disease. These are the human host, the female Anopheles mosquito vector and the malaria parasite of the Plasmodium family which is made up of five different species (P. falciparum, P. vivax, P. malariae,

P. ovale and P. knowlesi). The most prevalent of these five species are P. falciparum and P. vivax with P. falciparum being the most pathogenic. Therefore, malaria transmission events take place in a dynamic, interconnected system composed of these three organisms (human, mosquito, plasmodium parasite) together with the environment with all its various domains (physical, biological, geographical, economic, social etc.) making malaria disease system a complex system. This complex nature of malaria as an infectious disease system makes the aggregate dynamics of this complex system non-linear and being characterized by the following properties [228]: (i) Openness - so that it may be difficult to determine malaria disease system boundaries, e.g. due to importation of malaria. (ii) A history - so that the past helps to shape the present behaviour of malaria disease system e.g. due to development of partial immunity due to prior exposure to malaria infection [202] or development of herd immunity due to prior exposure to malaria vaccination. (iii) Emergence - so that patterns emerge from the interaction of malaria disease system components (human host, mosquito vector, plasmodium parasite, environment), e.g. colonization of host and vector by the plasmodium parasite, establishment of plasmodium parasite within the host while evading immune responses, transmission of the parasite to new hosts and vectors, altered host and vector behaviour, use of host and vector as both transport and reservoir of malaria parasite, infection induced death of host, etc. (iv) Co-evolution - so that each of the three organisms implicated in transmission of malaria (human, mosquito and plasmodium) imposes selection on the other in a dynamic process of ongoing reciprocal change where the plasmodium parasite population imposes a selective influence on its hosts (human and mosquito) populations which respond to the selection, in turn imposing a selective influence on the plasmodium parasite population, with this cycle potentially repeated over and over with this process potentially involving traits like parasite infectivity, host resistance and parasite host-finding ability. (v) Self-organization - so that some overall order which is spontaneous (i.e not requiring control from an external agent) and robust (e.g. implementing control measures will result in a reduction in malaria burden from its intrinsic levels, but stopping implementing those control measures will result in malaria burden returning to intrinsic levels) arises from the local interactions between the components of malaria disease system (human host, mosquito vector, plasmodium parasite, environment) which result in malaria disease system being organized into a hierarchical multi-level (e.g. cell level, tissue level, host level) and multi-scale structure with scales ranging from molecular scale to ecosystem scale.

Malaria is a disease that has a long history of being targeted as a suitable candidate for global eradication. The process of global malaria eradication is expected to take place in the form of a series national malaria eliminations [208]. Therefore, the global effort to eradicate malaria is expected to take place in phases with malaria control and malaria elimination being respectively

the first and intermediate phases towards the ultimate goal of worldwide eradication of malaria. Control, elimination and eradication levels of an infectious disease system are defined by the World Health Organization (WHO) as follows [197]. (i) Malaria control means reducing the disease burden to a level at which it is no longer a public health problem. (ii) Malaria elimination means interrupting local mosquito-borne malaria transmission in a defined geographical area, i.e. zero incidence of locally contracted cases, although imported cases will continue to occur. Continued intervention measures are required. (iii) Malaria eradication means permanent reduction to zero of the worldwide incidence of malaria infection. However, while this understanding of control, elimination and eradication of an infectious disease system based on incidence and prevalence is useful for some practical purposes, it does not take into account the multi-scale nature of an infectious disease system. Since the most sure way to eliminate malaria in a defined geographical area is to eliminate the malaria parasite, we develop a multi-scale model of malaria disease dynamics based on plasmodium parasite population dynamics at both the within-host scale and the between-host scale. At the between-host scale the malaria parasite population dynamics is represented by some surrogate measurable quantity called community pathogen load. We first develop within-human and within-mosquito sub-models for malaria infection dynamics and then use these two sub-models to approximate malaria parasite population dynamics at the within-host (within-human and within-mosquito) scale and then up-scale these approximations to define community sporozoite load and community gametocyte load (collectively defined in this chapter as community pathogen load) which we use as public health measures of human-to-mosquito and mosquito-to-human malaria transmission dynamics.

This model contributes to already growing knowledge of multi-scale modelling of malaria [203–206]. Based on the categorization of multi-scale models of infectious diseases given in [192], these multi-scale models for mularia disease dynamics that have been developed at host level (that is, those integrating the within-host scale and the between-host scale) are either individual-based multi-scale models (IMSMs) such as [203] or they are hybrid multi-scale models (HMSMs) [204–206]. For general information on IMSMs of infectious diseases see [192]. The IMSM in [203] cannot be easily implemented to evaluate the comparative effectiveness of health interventions using standard disease transmission metrics such as reproductive numbers and endemic equilibria because it is not easy to derive explicit expressions of such quantities from these IMSMs. Moreover, the HMSMs developed in [204–206], cannot also be easily applied to evaluate the comparative effectiveness of health interventions that operate at different scale domains such as within-host scale and between-host scale because they do not use common metrics of disease transmission across scales. At within-host scale pathogen load is used as the metric for disease transmission while at between-host scale, disease class (i.e. infected class or prevalence) is used

as the metric for disease transmission. In this study, we develop a new coupled multi-scale model for malaria disease dynamics using pathogen load as a common metric for (i) infectiousness and (ii) disease transmission potential and as (iii) an indicator of the effectiveness of health interventions across scales. Although we use malaria disease system as a case study, the multi-scale modelling approach presented in this study is general enough and is in principle applicable to many other directly transmitted vector-borne diseases.

2.2 Derivation of the multi-scale Model for Malaria Elimination

To estimate the malaria baseline transmission dynamics, we develop a multi-scale model which incorporates the dynamics of all the three populations of living organisms that are implicated in the transmission of malaria which are the human host, the vector and plasmodium falciparum parasite. To achieve this, we first of all develop four separate sub-models for malaria transmission dynamics which are: (i) the mosquito-to-human malaria transmission sub-model, (ii) the human-to-mosquito malaria transmission sub-model, (iii) the within-human plasmodium falciparum parasite population dynamics sub-model and (iv) the within-mosquito plasmodium falciparum parasite population dynamics sub-model. These four separate sub-models are then integrated into a single multi-scale model of malaria transmission dynamics. Details of the derivations are given in the following three subsections of this section.

2.2.1 The Four Sub-models of Malaria Transmission Dynamics

The Four separate sub-models of malaria disease dynamics are formulated as follows:

1. **Mosquito-to-human malaria transmission sub-model**: This sub-model is described by an SIS model. This sub-model is formulated based on monitoring the dynamics of two populations which are susceptible humans S_H, and infected humans I_H so that the total human population is given by $N_H = S_H + I_H$. We make the following assumptions for this sub-model.

    i. There is no herd immunity in the human population as a result of prior exposure to the malaria infection or vaccination.

    ii. The infected human population can recover naturally from malaria infection.

    iii. The transmission parameter $\widehat{\beta_V}$ is a function of the number of infected mosquitoes so that $\widehat{\beta_V} = \widehat{\beta_V}(I_V)$.

iv. The dynamics of S_H and I_H are assumed to occur at slow time scale t compared to the within-human and within-mosquito sub-models for malaria parasite population dynamics so that $S_H = S_H(t)$ and $I_H = I_H(t)$.

These assumptions lead to the following sub-model for the mosquito-to-human malaria transmission dynamics.

$$\text{Mosquito-to-human sub-model}: \begin{cases} 1.\ \dfrac{dS_H(t)}{dt} = \Lambda_H - \widehat{\beta_V}(I_V)S_H(t) - \mu_H S_H(t) + \widehat{\gamma_H} I_H, \\ 2.\ \dfrac{dI_H(t)}{dt} = \widehat{\beta_V}(I_V)S_H(t) - \left[\mu_H + \widehat{\delta_H} + \widehat{\gamma_H}\right] I_H(t). \end{cases} \tag{2.2.1}$$

The first equation in sub-model system (2.2.1) describes the dynamics of susceptible humans. The population of susceptible humans is assumed to increase at a constant rate Λ_H through birth. This population is depleted through infection of susceptible humans at a variable rate $\widehat{\beta_V}(I_V)$ and natural death at a constant rate μ_H. The population of susceptible humans also increases through natural recovery of infected individuals at a rate $\widehat{\gamma_H}$. The second equation in sub-model system (2.2.1) describes the dynamics of infected humans. This population increases through infection of susceptible humans and decreases through natural death at a rate μ_H, through disease induced death at a rate $\widehat{\delta_H}$ and through natural recovery at rate $\widehat{\gamma_H}$.

2. **Human-to-mosquito malaria transmission sub-model**: This sub-model is described by an SI model and describes the transmission of malaria parasite from infected humans to susceptible mosquitoes. We make the following assumptions for this sub-model.

   i. The infected mosquitoes do not recover naturally from malaria infection.

   ii. The transmission parameter $\widehat{\beta_H}$ is a function of the number of infected humans so that $\widehat{\beta_H} = \widehat{\beta_H}(I_H)$.

   iii. The dynamics of S_V and I_V are assumed to occur at slow time scale t compared to the within-human and within-mosquito sub-models so that $S_V = S_V(t)$ and $I_V = I_V(t)$.

Based on these assumptions the sub-model for the human-to-mosquito malaria transmission dynamics becomes

$$\text{Human-to-mosquito sub-model}: \begin{cases} 1.\ \dfrac{dS_V(t)}{dt} = \Lambda_V - \widehat{\beta_H}(I_H)S_V(t) - \mu_V S_V(t), \\ 2.\ \dfrac{dI_V(t)}{dt} = \widehat{\beta_H}(I_H)S_V(t) - \left[\mu_V + \widehat{\delta_V}\right] I_V(t). \end{cases} \tag{2.2.2}$$

The first equation in sub-model system (2.2.2) describes the dynamics of susceptible mosquitoes. The first term on the right-hand side of this equation models the increase of susceptible mosquitoes through birth. The susceptible population of mosquitoes decreases through natural death at a constant rate μ_V, and through infection by humans at a variable rate $\widehat{\beta_H}(I_H)$. The second equation in sub-model system (2.2.2) describes the dynamics of infected mosquitoes. The population of infected mosquitoes increases through infection of susceptible mosquitoes at a rate $\widehat{\beta_H}(I_H)$. The same population decreases through natural death at a constant rate μ_V and also through infection induced death at a constant rate $\widehat{\delta_V}$.

3. **The within-human malaria parasite population dynamics sub-model**:
The within-human malaria parasite population dynamics describe the time evolution of four populations within an infected human host which are the population of susceptible erythrocytes R_h, the population of merozoite infected erythrocytes R_m, the population of free merozoites in the blood stream M_h and the population of gametocyte infected erythrocytes G_h. We make the following assumptions for these four within-human populations.

   i. There is no super-infection of humans.

   ii. There is no immune response in the infected human.

   iii. We only explicitly consider the blood stage parasite population dynamics and the liver stage malaria parasite population dynamics is only captured through merozoite initial value in the blood stream, $M_h = M_h(0)$.

   iv. The dynamics of the four populations within an infected human occurs at slow time scale s compared to mosquito-to-human and human-to-mosquito parasite transmission dynamics so that $M_h = M_h(s)$, $R_h = R_h(s)$, $R_m = R_m(s)$ and $G_h = G_h(s)$.

   v. The within-human gametocyte population G_h is a proxy for individual human infectiousness to mosquitoes.

Taking into account these assumptions, the sub-model describing the dynamics of the four within-human populations is proposed to be

$$\text{Within-human sub-model}: \begin{cases} 1.\ \dfrac{dR_h(s)}{ds} = \Lambda_h - \beta_h R_h(s) M_h(s) - \mu_b R_h(s), \\ 2.\ \dfrac{dR_m(s)}{ds} = (1-\pi)\beta_h R_h(s) M_h(s) - \alpha_m R_m(s), \\ 3.\ \dfrac{dM_h(s)}{ds} = N_m \alpha_m R_m(s) - \mu_m M_h(s), \\ 4.\ \dfrac{dG_h(s)}{ds} = \pi \beta_h R_h(s) M_h(s) - \Big[\alpha_h + \mu_h\Big] G_h(s). \end{cases} \tag{2.2.3}$$

In the sub-model system (2.2.3) the first equation describes the dynamics of susceptible erythrocytes (red blood cells). The population of susceptible red blood cells (RBCs) or erythrocytes is assumed to increase through supply of RBCs from the bone marrow [219] at rate Λ_h and decrease through infection. $\beta_h R_h(s) M_h(s)$ models the rate at which free merozoites infect erythrocytes where β_h is the rate of infection. The susceptible erythrocytes are also reduced through natural death at a constant rate μ_b. The second equation in sub-model system (2.2.3) describes the dynamics of merozoite infected erythrocytes. A merozoite that infects an erythrocyte has one of two potential fates [243]: (i) it may either become a trophozoite and repeat the cycle of merozoite production, or (ii) it may transform into a trophozoite and then undergo gametocytogenesis, a process in which gametocytes are formed within host erythrocyte. In the second equation we therefore assume that merozoite infected erythrocytes $R_m(s)$ which upon bursting will produce merozoites increase through a proportion $(1-\pi)$ of the total population of merozoite infected erythrocytes. Therefore, the first term in the second equation of sub-model system (2.2.3) models the rate of this proportion of merozoite infected erythrocytes increase while the second term models the rate of reduction of this proportion of merozoite infected erythrocytes through bursting to produce merozoites. In the sub-model system (2.2.3) the third equation describes the dynamics of the population of merozoites in the human blood stream. We assume that each bursting infected erythrocyte which is merozoite producing releases an average of N_m merozoites upon bursting. Therefore, $N_m \alpha_m R_m(s)$ models the rate of increase of merozoites in the human blood stream through bursting of infected erythrocytes. The population of merozoites is assumed to decay through natural death due to each merozoite having an average life-span of $\dfrac{1}{\mu_m}$ days. The fourth equation in sub-model system (2.2.3) describes the dynamics of the remaining proportion, π, of the total population

of merozoite infected erythrocytes, $G_h(s)$. This population of merozoite infected erythrocytes will after the merozoite has infected the erythrocyte transform into a trophozoite and then undergo gametocytogenesis, a process in which gametocytes are formed within host erythrocyte (either a male or female gametocyte is generated within the host erythrocyte). The human-to-mosquito transmission of malaria is mediated through this population of gametocytes [243]. The first term in the fourth equation of sub-model system (2.2.3) models the rate of increase of this population of gametocye infected erythrocytes. In this equation α_h is the rate at which gametocytes within erythrocytes mature and become infectious to mosquitoes. The mature and infectious gametocytes are detectable in the bloodstream at days 7 to 15 after the initial wave of merozoites from which they are derived [241, 242]. These gametocyte infected erythrocytes are assume to decay at a rate μ_h through natural death. This population of gametocyte infected erythrocytes within an infected human remain in an arrested developmental state until they are ingested by a mosquito where they complete their development and become either male or female gametes [243]. The lack of malaria interventions that significantly target gametocytes, as the human infectious reservoir that should be targeted to reduce human-to-mosquito malaria transmission has hampered progress towards malaria elimination.

4. **The within-mosquito malaria parasite population dynamics sub-model**:
Mosquitoes are the definitive hosts for the malaria parasites, where the sexual phase of the parasite's life cycle occurs in a process involving morphologically distinct life-stages [232, 233] called sporogony and culminates in the development of infectious form of the parasite called sporozoites. In this study, the within-mosquito malaria parasite population dynamics during sporogony is modelled by following the time evolution of five parasite developmental stages in the infected mosquito which are the population of gametocyte infected erythrocytes, $G_v(s)$, the population of gametes, $G_m(s)$, the population of zygotes $Z_v(s)$, the population of oocysts, $O_v(s)$, and the population of sporozoites, $P_v(s)$. We make the following assumptions for the dynamics of the four malaria parasite stage populations.

   i. There is super-infection of mosquito at a constant rate Λ_v since the mosquito cannot clear the infection and yet it takes several blood meals at different stages of its life time which may be contaminated with gametocytes.

   ii. There is no immune response in the mosquito.

   iii. The within-mosquito sporozoite population P_v is a proxy for individual mosquito infectiousness to humans.

iv. The population dynamics of the different malaria parasites at different stages of development occurs at slow time scale s compared to mosquito-to-human and human-to-mosquito parasite transmission dynamics so that $G_v = G_v(s)$, $Z_v = Z_v(s)$, $O_v = O_v(s)$ and $P_v = P_v(s)$.

v. We assume that within an infected mosquito, male and female gametes only fuse as pairs to form zygotes and those gametes that fail to locate a gamete of opposite sex to fuse with will, with time, die a natural death and therefore will not participate in zygote formation, making their contribution to mosquito infectiousness irrelevant.

These assumptions lead to the following system of differential equations for the within-mosquito malaria parasite population dynamics.

$$\text{Within-mosquito sub-model}: \begin{cases} 1.\ \dfrac{dG_v(s)}{ds} = \Lambda_v - \Big[\alpha_g + \mu_g\Big]G_v(s), \\ 2.\ \dfrac{dG_m(s)}{ds} = N_g\alpha_g G_v(s) - \Big[\alpha_s + \mu_s\Big]G_m(s), \\ 3.\ \dfrac{dZ_v(s)}{ds} = \dfrac{1}{2}\alpha_s G_m(s) - \Big[\alpha_z + \mu_z\Big]Z_v(s), \\ 4.\ \dfrac{dO_v(s)}{ds} = \alpha_z Z_v(s) - \Big[\alpha_k + \mu_k\Big]O_v(s), \\ 5.\ \dfrac{dP_v(s)}{ds} = N_k\alpha_k O_v(s) - \Big[\alpha_v + \mu_v\Big]P_v(s). \end{cases} \quad (2.2.4)$$

In the sub-model system (2.2.4) the first equation describes the dynamics of gametocyte infected erythrocytes within an infected mosquito after a mosquito has ingested a blood-meal from an infected human host. The first term, Λ_v, models super-infection of the infected mosquito. This is expected because mosquitoes do not recover from malaria parasite infection, and yet may take several other blood meals contaminated with gametocyte infected erythrocytes after taking the first blood meal contaminated with gametocyte infected erythrocytes. As soon as the gametocyte infected erythrocytes are ingested by the mosquito, the gametocytes are activated to undergo another developmental process called gametogenesis, a process in which gametes are formed within host erythrocyte (either male or female gametes are generated within the host erythrocyte) resulting in the erythrocyte bursting releasing gametes. In the first equation of sub-model system (2.2.3), α_g is the rate at which gametocyte infected erythrocytes burst releasing sex cells called gametes and μ_g is the natural decay rate of gametocyte infected erythrocytes within an infected mosquito. The

second equation in sub-model system (2.2.4) describes the dynamics of the population of gametes within an infected mosquito. We assume that each bursting gametocyte infected erythrocyte releases an average of N_g gametes upon bursting. Therefore, $N_g\alpha_g G_v(s)$ models the rate of increase of gametes within an infected mosquito. These gametes are assumed to decay at a rate μ_s. Further, these gametes also get depleted through male and female gametes fusing to form zygotes at a constant rate α_s. In the sub-model system (2.2.4) the third equation describes the dynamics of zygotes. The mean population of zygotes $Z_v(s)$, within a single infected mosquito is generated following developmental processes undergone by gametes to mature and pair up and fuse to form zygotes at rate $\frac{\alpha_s}{2}$. The introduction of the fraction $\frac{1}{2}$ multiplying the parameter α_s models the pairing of male and female gametes and fusing to form zygotes. We assume that the zygotes either die naturally at a rate μ_z or undergo further developmental changes into ookinetes (population of ookinetes is not explicitly modelled in this chapter), which invade the mosquito mid-gut lining and eventually develop into oocysts. The fourth equation in sub-model system (2.2.4) describes the dynamics of the population of oocysts. The mean population of oocysts is formed following developmental changes undergone by zygotes into ookinetes first (which are not explicitly represented in the model) and then ookinetes becoming oocysts at a rate α_z. Therefore, the first term in the fourth equation of sub-model system (2.2.4) models the rate of increase of the population of oocysts through developmental changes undergone by ookinetes to become oocysts while the second term models the rate of reduction of this population through either natural decay at a rate μ_k or through bursting of oocysts to produce sporozoites at an assumed rate of α_k. In the sub-model system (2.2.4) the fifth equation describes the dynamics of sporozoites. The population of sporozoites is generated following the completion of the Plasmodium development within the mosquito vector. We assume that each oocyst bursts at a rate of α_k releasing an average of N_k sporozoites upon bursting. Therefore, $N_k\alpha_k O_v(s)$ models the rate of increase of sporozoites within an infected mosquito. In this last equation α_v is the rate at which sporozoites mature and become infectious to humans and migrate to the salivary glands of the infected mosquito forming the infectious reservoir of an individual mosquito. The population of sporozoites is assumed to decay through each sporozoite having an average life-span of $\frac{1}{\mu_v}$ days.

2.2.2 Integration of the Four Separate Sub-models of Malaria Transmission Dynamics into a Single multi-scale Model

Having presented the four sub-models that separately describe the transmission of malaria at different scales, we now show how to integrate them into a single multi-scale model. Based on

our previous experience of developing multi-scale models for environmentally transmitted infectious disease systems [200, 201], we know that in general individual infectiousness links the within-host scale to between-host scale while exposure links between-host scale to the within-host scale [200, 201]. We apply these ideas to the current problem where the within-mosquito and within-human sub-models are unidirectionally coupled to the mosquito-to-human and human-to-mosquito malaria transmission dynamics sub-models respectively. The integration of the four sub-models is achieved in two steps. The first step in the integration of the four sub-models (2.2.1), (2.2.2), (2.2.3), (2.2.4) is to make assumptions about the relationship between the independent variables of the within-human and within-mosquito malaria parasite population dynamics which are G_h, P_v, M_h and the parameters of the human-to-mosquito and mosquito-to-human malaria parasite transmission at epidemiological scale which are $\widehat{\beta_V}(I_V)$, $\widehat{\beta_H}(I_H)$, $\widehat{\delta_V}$, $\widehat{\gamma_H}$ and $\widehat{\delta_H}$. The second step involves applying ecosystems concepts to the within-mosquito and within-human malaria parasite population dynamics [210–212] to derive the appropriate equations. Details of the specific derivations and assumptions are as follows.

1. In the context of malaria infection, when the human host is considered as an ecosystem [210–212], then host survival or death and host recovery can be considered as suitable metrics of the emergent ecosystem properties owing to merozoites since the merozoite stage of the malaria parasite is responsible for morbidity and mortality. So we assume that the disease induced death rate of humans $\widehat{\delta_V}$ and the malaria infected humans recovery rate $\widehat{\gamma_H}$ in the mosquito-to-human sub-model (2.2.1) is a function of the within-human merozoite population dynamics so that $\widehat{\delta_H} = \widehat{\delta_H}(M_h)$ and $\widehat{\gamma_H} = \widehat{\gamma_H}(M_h(s))$.

2. Similarly, in the context of malaria infection, when the mosquito vector is considered as an ecosystem [210–212], then mosquito survival or death can be considered as a suitable metric of the emergent ecosystem property owing to sporozoites since the sporozoite stage of the malaria parasite is responsible for infection induced death of the mosquito [234]. So we assume that the infection induced death rate of mosquitoes $\widehat{\delta_V}$ in the human-to-mosquito sub-model (2.2.2) is a function of the within-mosquito sporozoite population dynamics so that $\widehat{\delta_V} = \widehat{\delta_V}(P_v)$.

3. Further, we assume that the transmission parameter in the mosquito-to-human malaria transmission sub-model, $\widehat{\beta_V}$ is not just a function of the vector population alone $I_V(t)$, but of both the vector population $I_V(t)$ and sporozoite population $P_v(s)$ so that $\widehat{\beta_V} = \widehat{\beta_V}(P_v(s)I_V(t))$. The net effect of this assumption is to up-scale individual mosquito infectiousness $P_v(s)$ to population level or community level infectiousness $P_v(s)I_V(t)$. In addition, we interpret the quantity $P_v(s)I_V(t)$ to be a new variable at epidemiological scale

which we now denote by $P_V(t)$ so that $P_V(t) = P_v(s)I_V(t)$, which is a product of the average individual infected mosquito's sporozoite load and the number of infected mosquitoes. Here $P_V(t)$ is the total infectious reservoir of mosquitoes in the community which we refer to in this study as community sporozoite load. In terms of community sporozoite load, the transmission parameter for mosquito-to-human malaria transmission sub-model becomes $\widehat{\beta_V} = \widehat{\beta_V}(P_V(t))$. We further assume a Holling type II functional form of the function $\widehat{\beta_V}(P_V)$ so that the force of infection, denoted here by $\lambda_V(t)$, associated with infectivity of the community to humans becomes

$$\lambda_V(t) = \widehat{\beta_V}(P_V(t)) = \frac{\beta_V P_V(t)}{P_0 + P_V(t)} \tag{2.2.1}$$

where β_V is the exposure rate to a community with a population P_V of sporozoites per unit time, P_0 is the community sporozoite load that yields 50 percent chance of getting a human host infected with malaria after a bite by a mosquito in a particular community and

$$\lambda_V[P_V(t)] = \frac{P_V(t)}{P_0 + P_V(t)}, \tag{2.2.2}$$

is probability that a random bite by a mosquito vector in a particular community with a community sporozoite load $P_V(t)$ will infect the individual with malaria in that community. However, $P_V(t)$, is a new variable at epidemiological scale which we have just introduced. In order to derive the differential equation governing $P_V(t)$, we again appeal to the ideas of an ecosystem approach to the within-mosquito parasite population dynamics [210–212]. The ecosystem approach to the within-mosquito parasite population dynamics will enable us to explicitly couple the new epidemiological variable $P_V(t)$, to the within-mosquito parasite population dynamics. In particular it enables us to couple the differential equation for $P_V(t)$ to the differential equation for $P_v(s)$ at the within-mosquito scale. From model system (2.2.4), we know that the differential equation for $P_v(s)$ is

$$\frac{dP_v(s)}{ds} = N_k\alpha_k O_v(s) - [\alpha_v + \mu_v]P_v(s). \tag{2.2.3}$$

Applying the ecosystem concepts in [210–212] to the within-mosquito population dynamics of sporozoites, we assume that mosquitoes in a particular geographical area or community are small and unevenly distributed habitats or environments in which sporozoites can multiply and grow until they are mature to become infectious to humans. So at any time s each of these habitats is contaminated at a rate α_v since this is the rate at which sporozoites grow and become infectious within each of the mosquitoes. Now since at any time t we have a total of $I_V(t)$ of these contaminated habitats/environments contaminated with an

average of $P_v(s)$ sporozoites, then the rate of change of community sporozoite load $P_V(t)$, in the entire community made of $I_V(t)$ unevenly distributed habitats/environments in the community becomes

$$\frac{dP_V(t)}{dt} = P_v(s)\alpha_v I_V(t) - \alpha_V P_V(t), \tag{2.2.4}$$

where α_V is the rate of sporozoite elimination in a particular geographical area/country/-community so that the process of sporozoite elimination of community sporozoite load in a particular geographical area/country/community takes an average of $\frac{1}{\alpha_V}$ days. Since $P_V(t)$ is the total infectious reservoir of mosquitoes in a particular community defined here as community sporozoite load, then $\frac{1}{\alpha_V}$ days is the average time to eliminate the total infectious reservoir of mosquitoes and render all mosquitoes in a particular community non-infectious. Taking into account these derivations and assumptions the mosquito-to-human malaria transmission sub-model which is now coupled to the within-mosquito parasite population dynamics becomes

$$\begin{cases} 1.\ \dfrac{dS_H(t)}{dt} = \Lambda_H - \dfrac{\beta_V P_V(t)}{P_0 + P_V(t)} S_H(t) - \mu_H S_H(t) + \widehat{\gamma_H}(M_h(s)) I_H(t), \\ 2.\ \dfrac{dI_H(t)}{dt} = \dfrac{\beta_V P_V(t)}{P_0 + P_V(t)} S_H(t) - \left[\mu_H + \widehat{\gamma_H}(M_h(s)) + \widehat{\delta_H}(M_h(s))\right] I_H(t), \\ 3.\ \dfrac{dP_V(t)}{dt} = P_v(s)\alpha_v I_V(t) - \alpha_V P_V(t). \end{cases} \tag{2.2.5}$$

Community sporozoite load (CSL) $P_V(t)$, which is also a measure of the total infectious reservoir of mosquitoes in the community, is defined in this study as an aggregate population-level biomarker of a community's sporozoite burden over a specific time period and is being proposed in this study as a useful metric for assessing the overall impact of malaria health interventions targeted at the mosquito vector or the uptake of malaria interventions targeted at the mosquito vector and quantifying their impact on transmission of malaria from mosquitoes to humans. In line with a similar metric for HIV/AIDS [213–216], we therefore propose that this new public health measure of malaria transmission should be operationalized in the assessment of the path from control to elimination for malaria transmission in a particular community as (a) an indicator of a community's level of infectiousness and transmission probability of malaria to humans, (b) a measure of the effectiveness of malaria interventions targeted at the mosquito vector, and (c) a proximal maker of malaria incidence among mosquitoes and their potential to propagate malaria to humans.

4. Finally, we assume that the transmission parameter in the human-to-mosquito malaria transmission sub-model, $\widehat{\beta_H}$ is not just a function of the human population alone $I_H(t)$, but of both the human population $I_H(t)$ and gametocyte population $G_h(s)$ so that $\widehat{\beta_H} = \widehat{\beta_H}(G_h(s)I_H(t))$. The net effect of this assumption is also to up-scale individual human infectiousness $G_h(s)$ to population level or community level infectiousness $G_h(s)I_H(t)$. In addition, the quantity $G_h(s)I_H(t)$ is also a new variable at epidemiological scale which we now denote by $G_H(t)$ so that $G_H(t) = G_h(s)I_H(t)$, which is a product of the average individual infected human's gametocyte load and the number of infected humans. Here $G_H(t)$ is the total infectious reservoir of humans in the community which we refer to in this study as community gametocyte load. In terms of community gametocyte load, the transmission parameter for human-to-mosquito malaria transmission sub-model becomes $\widehat{\beta_H} = \widehat{\beta_H}(G_H(t))$. We further also assume a Holling type II functional form of the function $\widehat{\beta_H}(G_H)$ so that the force of infection, denoted here by $\lambda_H(t)$, associated with infectivity of the community to mosquito becomes

$$\lambda_H(t) = \widehat{\beta_H}(G_H(t)) = \frac{\beta_H G_H(t)}{G_0 + G_H(t)}, \tag{2.2.6}$$

where β_H is the exposure rate to a community with a population G_H of gametocytes per unit time, G_0 is the community gametocyte load that yields 50 percent chance of getting a mosquito vector infected with malaria after a bite of a human host by a mosquito in a particular community and

$$\lambda_H[G_H(t)] = \frac{G_H(t)}{G_0 + G_H(t)}, \tag{2.2.7}$$

is the probability that a random bite of a human host by a mosquito vector in a particular community with a community gametocyte load $G_H(t)$ will infect the mosquito with malaria in that community. However, because $G_H(t)$, is also a new variable at epidemiological scale which we have just introduced. In order to derive the differential equation governing $G_H(t)$, we again appeal to the ideas of an ecosystem approach to the within-human parasite population dynamics [210–212]. The ecosystem approach to the within-human parasite population dynamics will enable us to couple the new epidemiological variable $G_H(t)$, to the within-human parasite population dynamics. In particular it enables us to couple the differential equation for $G_H(t)$ to the differential equation for gametocyte $G_h(s)$ at the within-human scale. From model system (2.2.3), we know that the differential equation for $G_h(s)$ is

$$\frac{dG_h(s)}{ds} = \pi\beta_h R_h(s)M_h(s) - [\alpha_h + \mu_h]G_h(s). \tag{2.2.8}$$

Applying the ecosystem concepts in [210–212] to the within-human population dynamics of gametocytes, we assume that humans in a particular geographical area or community are small homogeneous and unevenly distributed habitats or environments in which gametocytes can multiply and grow until they are mature to become infectious to mosquitoes. So at any time s each of these habitats is contaminated at a rate α_h since this is the rate at which gametocytes grow and mature to become infectious within each of the human hosts. Now, since at any time t we have a total of $I_H(t)$ of these contaminated habitats/environments contaminated with an average of $G_h(s)$ gametocytes, then the rate of change of community gametocyte load, $G_H(t)$ in the entire community made of $I_H(t)$ homogeneous and unevenly distributed habitats/environments in the community becomes

$$\frac{dG_H(t)}{dt} = G_h(s)\alpha_h I_H(t) - \alpha_H G_H(t), \tag{2.2.9}$$

where α_H is the rate of elimination of this total infectious reservoir of humans in the community so that the process of gametocyte elimination in a particular geographical area/-country/community takes an average of $\frac{1}{\alpha_H}$ days. Since $G_H(t)$ is the total infectious reservoir of humans in a particular community defined here as community gametocyte load, then $\frac{1}{\alpha_H}$ days is the average time to eliminate the total infectious reservoir of humans and render all humans in a particular community non-infectious to mosquitoes. Taking into account these derivations and assumptions the human-to-mosquito malaria transmission sub-model which is now coupled to the within-human parasite population dynamics becomes

$$\begin{cases} 1.\ \dfrac{dS_V(t)}{dt} = \Lambda_V - \dfrac{\beta_H G_H(t)}{G_0 + G_H(t)} S_V(t) - \mu_V S_V(t), \\ 2.\ \dfrac{dI_V(t)}{dt} = \dfrac{\beta_H G_H(t)}{G_0 + G_H(t)} S_V(t) - \left[\mu_V + \widehat{\delta_V}(P_v(s))\right] I_V(t), \\ 3.\ \dfrac{dG_H(t)}{dt} = G_h(s)\alpha_h I_h(t) - \alpha_H G_H(t). \end{cases} \tag{2.2.10}$$

Community gametocyte load (CGL) $G_H(t)$, which is also a measure of the total infectious reservoir of humans in the community [217], is defined in this study as an aggregate population-level biomarker of a community's gametocyte burden over a specific time period and is being proposed in this study as a useful public health measure of malaria transmission for assessing the overall impact of malaria health interventions targeted at the

human host or the uptake of malaria interventions targeted at the human host and quantifying their impact on transmission of malaria from humans to mosquitoes. In line with a similar metric for HIV/AIDS [213–216], we therefore propose that this new measure should be operationalized in the assessment of the path from control to elimination for malaria transmission in a particular community as (a) an indicator of a community's level of infectiousness and transmission probability of malaria to mosquitoes, (b) a measure of the effectiveness of malaria interventions targeted at the human host, and (c) a proximal maker of malaria incidence among humans and their potential to propagate malaria to mosquito vectors.

Putting together all the various derivations and assumptions the complete multi-scale model for malaria transmission dynamics from human-to-human or from mosquito-to-mosquito becomes

$$
\begin{cases}
1. \ \dfrac{dS_H(t)}{dt} = \Lambda_H - \dfrac{\beta_V P_V(t)}{P_0 + P_V(t)} S_H(t) - \mu_H S_H(t) + \widehat{\gamma_H}(M_h(s)) I_H(t), \\
2. \ \dfrac{dI_H(t)}{dt} = \dfrac{\beta_V P_V(t)}{P_0 + P_V(t)} S_H(t) - \Big[\mu_H + \widehat{\gamma_H}(M_h(s)) + \widehat{\delta_H}(M_h(s))\Big] I_H(t), \\
3. \ \dfrac{dP_V(t)}{dt} = P_v(s)\alpha_v I_V(t) - \alpha_V P_V(t), \\
4. \ \dfrac{dS_V(t)}{dt} = \Lambda_V - \dfrac{\beta_H G_H(t)}{G_0 + G_H(t)} S_V(t) - \mu_V S_V(t), \\
\\
5. \ \dfrac{dI_V(t)}{dt} = \dfrac{\beta_H G_H(t)}{G_0 + G_H(t)} S_V(t) - \Big[\mu_V + \widehat{\delta_V}(P_v(s))\Big] I_V(t), \\
6. \ \dfrac{dG_H(t)}{dt} = G_h(s)\alpha_h I_H(t) - \alpha_H G_H(t), \\
7. \ \dfrac{dG_v(s)}{ds} = \Lambda_v - \Big[\alpha_g + \mu_g\Big] G_v(s), \\
8. \ \dfrac{dG_m(s)}{ds} = N_g \alpha_g G_v(s) - \Big[\alpha_s + \mu_s\Big] G_m(s), \\
9. \ \dfrac{dZ_v(s)}{ds} = \dfrac{1}{2}\alpha_s G_m(s) - \Big[\alpha_z + \mu_z\Big] Z_v(s), \\
\\
10. \ \dfrac{dO_v(s)}{ds} = \alpha_z Z_v(s) - \Big[\alpha_k + \mu_k\Big] O_v(s), \\
11. \ \dfrac{dP_v(s)}{ds} = N_k \alpha_k O_v(s) - \Big[\alpha_v + \mu_v\Big] P_v(s), \\
12. \ \dfrac{dR_h(s)}{ds} = \Lambda_h - \beta_h R_h(s) M_h(s) - \mu_b R_h(s), \\
13. \ \dfrac{dR_m(s)}{ds} = (1-\pi)\beta_h R_h(s) M_h(s) - \alpha_m R_m(s), \\
14. \ \dfrac{dM_h(s)}{ds} = N_m \alpha_m R_m(s) - \mu_m M_h(s), \\
15. \ \dfrac{dG_h(s)}{ds} = \pi \beta_h R_h(s) M_h(s) - \Big[\alpha_h + \mu_h\Big] G_h(s).
\end{cases}
\tag{2.2.11}
$$

We derived the multi-scale model system (2.2.11) by making the assumption that mosquitoes and humans are small homogeneous and unevenly distributed habitats/environments in the community in which sporozoites and gametocytes multiply and grow to become infectious. This assumption has the importance of establishing a modelling science base for directly transmitted vector-borne diseases that is comparable to an existing modelling science base for environmentally transmitted vector-borne diseases where the community pathogen load in the environment is explicitly incorporated into the model [200]. However, we note that there are some differences between these mosquitoes and humans as environments and some geographical environments in that they die and can move. But if we consider other geographical environments such as those associated with water-borne infections, we note that water bodies in which infective pathogens can multiply and grow can also dry-up which is analogous to death of habitat. In addition, there is some movement associated with these water environments as habitats for infective pathogens as the water flows in that the movements associated with these water environments results in transportation of the infective pathogen. The relationship between the fifteen variables in the complete multi-scale model systems (2.2.11) is shown schematically in Figure 2.1.

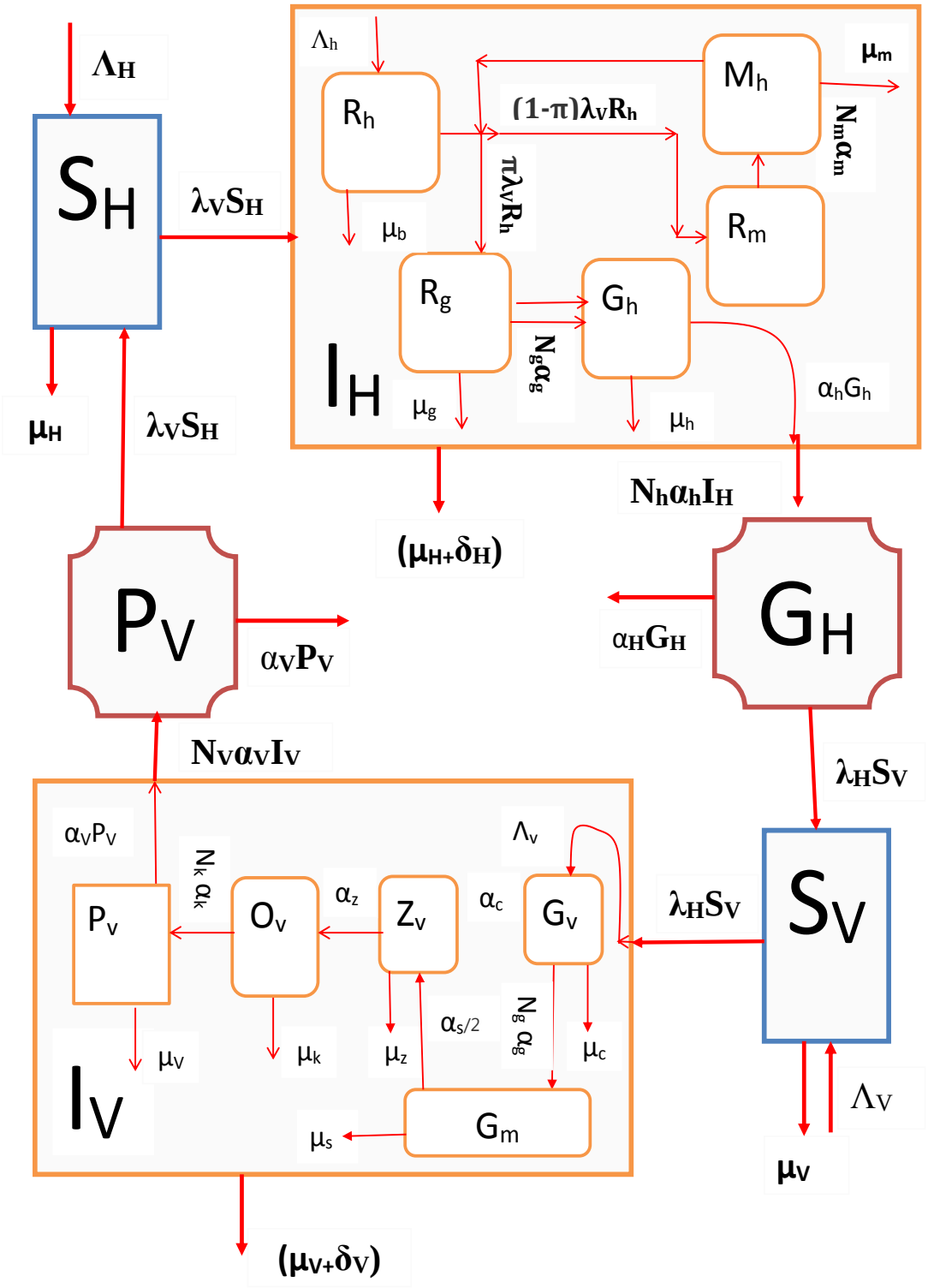

chch

Figure 2.1: A conceptual diagram of the complete integrated multi-scale model of malaria baseline transmission dynamics where $\lambda_h = \beta_h M_h$. In this Figure δ_V stands for $\widehat{\delta_V}(P_v)$, δ_H stands for $\widehat{\delta_H}(M_h)$ and γ_H stands for $\widehat{\gamma_H}(M_h)$.

This type of modelling framework enables us to develop the multi-scale model for malaria infectious disease system given by (2.2.11) without focusing on which mosquito infects which human and which human infects which mosquito in a particular community but only addressing the question about how often are individual humans and mosquitoes infected in a particular community. Data on which mosquito infects which individual and which human infects which mosquito are difficult to obtain. On the other hand, there is considerable data available on the effects of sporozoites, merozotes and gametocytes within infected humans and mosquitoes and the resulting responses of the human immune system [234–240, 242–249], and including data on the distribution of malaria within human and moquito populations (for example, the total number of infections and the rates of new infections) which are not being adequately applied to good effect in multi-scale modelling of malaria.

2.2.3 Simplifying the Complete multi-scale Model for Malaria

One of the difficulties in analyzing the multi-scale model system (2.2.11) is that two of the sub-models (within-mosquito and within-human sub-models) are in terms of a fast time scale s, while the other two sub-models (mosquito-to-human and human-to-mosquito sub-models) are in terms of a slow time scale t. We simplify this multi-scale model by making a slow and fast time scale analysis to the system. Consider the within-mosquito sub-model (2.2.4) and re-written here for quick reference as

$$\text{Within-mosquito sub-model}: \begin{cases} 1.\ \dfrac{dG_v(s)}{ds} = \Lambda_v - \Big[\alpha_g + \mu_g\Big]G_v(s), \\ 2.\ \dfrac{dG_m(s)}{ds} = N_g\alpha_g G_v(s) - \Big[\alpha_s + \mu_s\Big]G_m(s), \\ 3.\ \dfrac{dZ_v(s)}{ds} = \dfrac{1}{2}\alpha_s G_m(s) - \Big[\alpha_z + \mu_z\Big]Z_v(s), \\ 4.\ \dfrac{dO_v(s)}{ds} = \alpha_z Z_v(s) - \Big[\alpha_k + \mu_k\Big]O_v(s), \\ 5.\ \dfrac{dP_v(s)}{ds} = N_k\alpha_k O_v(s) - \Big[\alpha_v + \mu_v\Big]P_v(s). \end{cases} \tag{2.2.1}$$

We can write this system using the slow time scale t by assuming a relation between the fast and slow time-scales to be of the form $t = \epsilon s$, so that the within-mosquito malaria transmission dynamics sub-model can be written in terms of the slow time-scale as follows:

$$\begin{cases} 1.\ \epsilon\dfrac{dG_v(t)}{dt} &= \Lambda_v - \Big[\alpha_g + \mu_g\Big]G_v(t), \\ 2.\ \epsilon\dfrac{dG_m(t)}{dt} &= N_g\alpha_g G_v(t) - \Big[\alpha_s + \mu_s\Big]G_m(t), \\ 3.\ \epsilon\dfrac{dZ_v(t)}{dt} &= \dfrac{1}{2}\alpha_s G_m(t) - \Big[\alpha_z + \mu_z\Big]Z_v(t), \\ 4.\ \epsilon\dfrac{dO_v(t)}{dt} &= \alpha_z Z_v(t) - \Big[\alpha_k + \mu_k\Big]O_v(t), \\ 5.\ \epsilon\dfrac{dP_v(t)}{dt} &= N_k\alpha_k O_v(t) - \Big[\alpha_v + \mu_v\Big]P_v(t), \end{cases} \tag{2.2.2}$$

where ϵ is a constant highlighting the fast time scale of the within-mosquito sub-model compared to the slow time scale of the mosquito-to-human transmission sub-model. Since $0 < \epsilon << 1$, the within-mosquito malaria transmission dynamics sub-model can be assumed to be independent of time and we get:

$$\begin{cases} 1.\ \Lambda_v - \Big[\alpha_g + \mu_g\Big]\widetilde{G_v} &= 0, \\ 2.\ N_g\alpha_g\widehat{G_v} - \Big[\alpha_s + \mu_s\Big]\widetilde{G_m} &= 0, \\ 3.\ \dfrac{1}{2}\alpha_c\widetilde{G_m} - \Big[\alpha_z + \mu_z\Big]\widetilde{Z_v} &= 0, \\ 3.\ \alpha_z\widetilde{Z_v} - \Big[\alpha_k + \mu_k\Big]\widetilde{O_v} &= 0, \\ 4.\ N_k\alpha_k\widetilde{O_v} - \Big[\alpha_v + \mu_v\Big]\widetilde{P_v} &= 0. \end{cases} \tag{2.2.3}$$

From which we get

$$\begin{cases} 1.\ \widetilde{G_v} = \dfrac{\Lambda_v}{\alpha_g+\mu_g}, \\ 2.\ \widetilde{G_m} = \dfrac{\Lambda_v}{\alpha_s+\mu_s}.\dfrac{N_g\alpha_g}{\alpha_g+\mu_g}, \\ 3.\ \widetilde{Z_v} = \dfrac{\Lambda_v}{2}.\dfrac{1}{\alpha_z+\mu_z}.\dfrac{\alpha_s}{\alpha_s+\mu_s}, \\ 4.\ \widetilde{O_v} = \dfrac{\Lambda_v}{2}.\dfrac{1}{\alpha_k+\mu_k}.\dfrac{\alpha_z}{\alpha_z+\mu_z}.\dfrac{\alpha_c}{\alpha_s+\mu_s}.\dfrac{N_g\alpha_g}{\alpha_g+\mu_g}, \\ 5.\ \widetilde{P_v} = \dfrac{1}{2}.\dfrac{\Lambda_v}{\alpha_v+\mu_v}.\dfrac{N_k\alpha_k}{\alpha_k+\mu_k}.\dfrac{\alpha_z}{\alpha_z+\mu_z}.\dfrac{\alpha_s}{\alpha_s+\mu_s}.\dfrac{N_g\alpha_g}{\alpha_g+\mu_g}. \end{cases} \tag{2.2.4}$$

Consider also the within-human sub-model (2.2.3) and re-written here for quick reference as

$$\text{Within-human sub-model}: \begin{cases} 1.\ \dfrac{dR_h(s)}{ds} = \Lambda_h - \beta_h R_h(s) M_h(s) - \mu_b R_h(s), \\ 2.\ \dfrac{dR_m(s)}{ds} = (1-\pi)\beta_h R_h(s) M_h(s) - \alpha_m R_m(s), \\ 3.\ \dfrac{dM_h(s)}{ds} = N_m \alpha_m R_m(s) - \mu_m M_h(s), \\ 4.\ \dfrac{dG_h(s)}{ds} = \pi\beta_h R_h(s) M_h(s) - (\alpha_h+\mu_h) G_h(s). \end{cases} \tag{2.2.5}$$

We can also write this system in terms of the slow time scale t by assuming a relation between the fast and slow time-scales to be of the form $t = \epsilon s$, so that the within-human malaria transmission dynamics sub-model can be written in terms of the slow time-scale as follows:

$$\begin{cases} 1.\ \epsilon\dfrac{dR_h(t)}{dt} &= \Lambda_h - \beta_h R_h(t) M_h(t) - \mu_b R_h(t), \\ 2.\ \epsilon\dfrac{dR_m(t)}{dt} &= (1-\pi)\beta_h R_h(t) M_h(t) - \alpha_m R_m(t), \\ 3.\ \epsilon\dfrac{dM_h(t)}{dt} &= N_m \alpha_m R_m(t) - \mu_m M_h(t), \\ 4.\ \epsilon\dfrac{dG_h(t)}{dt} &= \pi\beta_h R_h(t) M_h(t) - (\alpha_h + \mu_h) G_h(t). \end{cases} \tag{2.2.6}$$

where ϵ is a constant highlighting the fast time scale of the within-human sub-model compared to the time scale of human-to-mosquito malaria transmission sub-model. Since $0 < \epsilon << 1$, the within-human malaria transmission dynamics sub-model can now be assumed to be independent of time and we get:

$$\begin{cases} 1.\ \Lambda_h - \beta_h \widetilde{R_h}\widetilde{M_h} - \mu_b \widetilde{R_h} &= 0, \\ 2.\ (1-\pi)\beta_h \widetilde{R_h}\widetilde{M_h} - \alpha_m \widetilde{R_m} &= 0, \\ 3.\ N_m \alpha_m \widetilde{R_m} - \mu_m \widetilde{M_h} &= 0, \\ 4.\ \pi\beta_h \widetilde{R_h}\widetilde{M_h} - (\alpha_h + \mu_h)\widetilde{G_h} &= 0. \end{cases} \tag{2.2.7}$$

From which we get

$$\begin{cases} 1.\ \widetilde{R_h} = \dfrac{\mu_m}{(1-\pi)N_m\beta_h} = \dfrac{\Lambda_h}{\mu_b\Re_0}, \\ 2.\ \widetilde{R_m} = \dfrac{(1-\pi)N_m\beta_h\Lambda_h - \mu_b\mu_m}{\mu_m\alpha_m\beta_h} = \dfrac{\mu_b\mu_m}{N_m\alpha_m\beta_h}\Big[\Re_0 - 1\Big], \\ 3.\ \widetilde{M_h} = \dfrac{(1-\pi)N_m\beta_h\Lambda_h - \mu_b\mu_m}{\mu_m\beta_h} = \dfrac{\mu_b}{\beta_h}\Big[\Re_0 - 1\Big], \\ 4.\ \widetilde{G_h} = \dfrac{\pi}{(1-\pi)}\Big[\dfrac{(1-\pi)N_m\beta_h\Lambda_h - \mu_b\mu_m}{N_m\beta_h(\alpha_h+\mu_h)}\Big] = \dfrac{\pi\Lambda_h}{(\alpha_h+\mu_h)\Re_0}\Big[\Re_0 - 1\Big], \\ 5.\ \Re_0 = \dfrac{(1-\pi)N_m\beta_h\Lambda_h}{\mu_b\mu_m}. \end{cases} \tag{2.2.8}$$

From the expressions (2.2.4) the total infectious reservoir of mosquitoes (community sporozoite load) $P_V(t)$ is now approximated by $\widetilde{P_v}I_V(t)$. Similarly, from the expressions (2.2.8) the total infectious reservoir of humans (community gametocyte load) $G_H(t)$ is now approximated by $\widetilde{G_h}I_H(t)$. Using the notation that $N_v = \widetilde{P_v}$ and $N_h = \widetilde{G_h}$, then the full multi-scale model (2.2.11) of malaria transmission dynamics is simplified to become

$$\begin{cases} 1.\ \dfrac{dS_H(t)}{dt} = \Lambda_H - \lambda_V(t)S_H(t) - \mu_H S_H(t) + \gamma_H I_H(t), \\ 2.\ \dfrac{dI_H(t)}{dt} = \lambda_V(t)S_H(t) - \Big[\mu_H + \delta_H + \gamma_H\Big]I_H(t), \\ 3.\ \dfrac{dP_V(t)}{dt} = N_v\alpha_v I_V(t) - \alpha_V P_V(t), \\ 4.\ \dfrac{dS_V(t)}{dt} = \Lambda_V - \lambda_H(t)S_V(t) - \mu_V S_V(t), \\ 5.\ \dfrac{dI_V(t)}{dt} = \lambda_H(t)S_V(t) - \Big[\mu_V + \delta_V\Big]I_V(t), \\ 6.\ \dfrac{dG_H(t)}{dt} = N_h\alpha_h I_H(t) - \alpha_H G_H(t), \end{cases} \tag{2.2.9}$$

where

$$\begin{cases} 1.\ \lambda_V(t) = \dfrac{\beta_V P_V(t)}{P_0 + P_V(t)}, \\ 2.\ \lambda_H(t) = \dfrac{\beta_H G_H(t)}{G_0 + G_H(t)}, \\ 3.\ N_v = \dfrac{1}{2}.\dfrac{\Lambda_v}{\alpha_v + \mu_v}.\dfrac{N_k\alpha_k}{\alpha_k + \mu_k}.\dfrac{\alpha_z}{\alpha_z + \mu_z}.\dfrac{\alpha_s}{\alpha_s + \mu_s}.\dfrac{N_g\alpha_g}{\alpha_g + \mu_g}, \\ 4.\ N_h = \dfrac{\pi}{(1-\pi)}\Big[\dfrac{(1-\pi)N_m\beta_h\Lambda_h - \mu_b\mu_m}{N_m\beta_h(\alpha_h + \mu_h)}\Big] = \dfrac{\pi\Lambda_h}{(\alpha_h + \mu_h)\Re_0}\Big[\Re_0 - 1\Big], \\ 5.\ \delta_H = \widehat{\delta_H}(\widetilde{M_h}),\ \text{a constant}, \\ 6.\ \delta_V = \widehat{\delta_V}(\widetilde{P_v}),\ \text{a constant}, \\ 7.\ \gamma_H = \widehat{\gamma_H}(\widetilde{M_h}),\ \text{a constant}. \end{cases} \tag{2.2.10}$$

Table 2.1 shows a summary of the variables of the multi-scale model (2.2.9).

Variable	Description
$S_H(t)$	Number of susceptible humans hosts at time t
$I_H(t)$	Number of infected human hosts at time t
$G_H(t)$	Community gametocyte load at time t
$S_V(t)$	Number of susceptible mosquito vectors at time t
$I_V(t)$	Number of infected mosquito vectors at time t
$P_V(t)$	Community sporozoite load at time t

Table 2.1: A summary of the variables of the malaria multi-scale model given by (2.2.9).

In the multi-scale model (2.2.9) the parameters G_0 and P_0 are the community gametocyte load and community sporozoite load that yield 50 percent chance of getting a human host and mosquito vector infected with malaria in a particular geographical area/community/country with community gametocyte load and community sporozoite load G_H and P_V respectively. In this study,

we interpret the quantities $\left(\frac{1}{G_0} \text{ and } \frac{1}{P_0}\right)$ as measures of a specific geographical area/community/country's susceptibility to malaria infection. We assume that every geographical area/community/country's malaria disease dynamics is characterized by a different set of susceptibility coefficients $\left(\frac{1}{G_0} \text{ and } \frac{1}{P_0}\right)$, to malaria infection which is intrinsic to that community and that these susceptibility coefficients are dependent on many factors which include [209]: (i) the mosquito vector species, their abundance and behaviour, (ii) the Plasmodium species, (iii) temperature and rainfall, (iv) geography and topography of the land, (v) amount and type of agriculture or land-cover in that area, (vi) strength of the health system, (vii) quality of housing in which people live, and (viii) how people spend their time in the places and times when vectors are feeding. Together, these characteristics will lead to particular malaria susceptibility coefficients $\left(\frac{1}{G_0} \text{ and } \frac{1}{P_0}\right)$ which determine the malaria baseline burden (the level of malaria burden that would exist in a given geographical area/community/country if no interventions are implemented to control it). This implies that certain reductions of malaria transmission observed in one geographical area/community/country following implementation of malaria health interventions may not be found in another geographical area/community/country where the same interventions are implemented. A summary of the parameters of the malaria multi-scale model given by (2.2.9) is presented in Table 2.2 and Table 2.3.

Parameter	Description	Initial Value	Range explored	Units	Source/ Rational
α_V	Rate of elimination of community sporozoite load	0.8	0.1-0.8	day^{-1}	[224]
Λ_V	Rate of supply of susceptible mosquitoes	200	200-400	day^{-1}	Estimated
β_V	Rate of infection of susceptible humans	0.2	0.2-0.4	day^{-1}	[225]
G_0	Saturation constant of community gametocyte load	100	10-500	day^{-1}	[220]
μ_V	Natural death rate of mosquitoes	0.12	-	day^{-1}	[220]
δ_V	Infection induced death rate of mosquitoes	0.00000426	0.00000426-0.00000533	day^{-1}	Estimated
Λ_H	Rate of supply of susceptible humans	0.037	0.033-0.05	day^{-1}	[225]
β_H	Rate of infection of susceptible mosquitoes	0.5	0.025-0.5	day^{-1}	[225]
α_H	Rate of elimination of community gametocyte load	0.002	0.002-0.005	day^{-1}	Estimated
μ_H	Natural death rate of humans	0.0000391	0.0000391	day^{-1}	[220]
γ_H	Natural recovery rate of humans	0.1667	0.1667	day^{-1}	Estimated
P_0	Saturation constant of community sporozoite load	100	10-500	day^{-1}	[220]
δ_H	Disease induced death rate of humans	0.0027	0.0001-0.5	day^{-1}	[225]

Table 2.2: Between-host (human and mosquito) parameter values and their description.

Parameter	Description	Initial Value	Range explored	Units	Source/ Rational
α_g	Rate at which gametocyte infected enrythocytes burst	96	-	day^{-1}	[220]
Λ_v	Rate of uptake of gametocytes through super infection of mosquito	3000	100-3000	day^{-1}	[220]
μ_g	Death rate of gametocytes	0.0625	0.0625	day^{-1}	[220]
N_g	Number of gametes produced per gametocyte infected enrythocyte	8	4-8	day^{-1}	[220]
α_s	Fertilization rate of gametes	0.08	0-0.15	$no.^{-1}day^{-1}$	[220]
μ_s	Natural decay rate of gametes	129	129	day^{-1}	[220]
α_z	Rate at which zygotes develop into oocysts	1.26	0.91-1.26	day^{-1}	[220]
μ_z	Natural decay rate of zygotes	1	-	day^{-1}	[220]
α_k	Bursting rate of oocysts to produce sporozoites	1	-	day^{-1}	[220]
μ_k	Natural decay rate of oocysts	0.00005	-	day^{-1}	[220]
N_k	Number of sporozoites produced per bursting oocyst	3000	3000-4000	day^{-1}	[220]
α_v	Rate at which sporozoites become infectious to humans	0.0625	-	day^{-1}	[220]
μ_v	Natural decay rate of sporozoites	0.8	0.1 - 0.8	day^{-1}	[220]
Λ_h	Rate of supply of susceptible red blood cells (erythrocytes)	0.25	0.142857-0.5	day^{-1}	[203]
β_h	Infection rate of erythrocytes by free merozoites	0.02	0.02-0.1	day^{-1}	[203]
μ_b	Natural decay rate of susceptible erythrocytes	1/120	1/120	day^{-1}	[203]
π	Proportion of gametocyte infected enrythocytes	0.1	0.1	day^{-1}	[203]
μ_m	Natural decay rate of free merozoites	0.05	0.05-0.5	day^{-1}	[224]
α_m	Rate at which erythrocytes burst to produce merozoites	1.0	1.0	day^{-1}	[224]
N_m	Number of merozoites produced per bursting erythrocyte	16	16-30	day^{-1}	[221],[222],[223]
α_h	Rate at which gametocytes develop and become infectious	0.02	0.02-0.9	day^{-1}	[203]
μ_h	Natural decay rate of gametocyte infected erythrocytes within infected humans	0.0625	0.0625	day^{-1}	[203]

2.3 Mathematical Analysis Of The Baseline multi-scale Model Of Malaria Dynamics

In this section, we use the multi-scale model (2.2.9) to characterize a malaria baseline burden using parameters given in Tables 2.2 and 2.3. In the context of the multi-scale model given by (2.2.9), the malaria baseline burden is the community gametocyte load and community sporozoite load (collectively called community pathogen load) that would exist in a particular geographical area/country/community if no control measures were implemented to reduce the malaria community pathogen load.

2.3.1 Positivity and boundedness of solutions of the malaria multi-scale model

Since the multi-scale model given by (2.2.9) describes human, mosquito, and malaria parasite populations, all parameters in the multi-scale model are non- negative and it can also be shown that the solutions of the multi-scale model (2.2.9) are non-negative, given non-negative initial values. In order to analyze this multi-scale model, we split it into four parts, namely the human population, mosquito population, community gametocyte load and community sporozoite load. Consider the biologically feasible region consisting of

$$\Omega = \left\{\Omega_H \times \Omega_V \times \Omega_G \times \Omega_P \subset \mathbb{R}^2_+ \times \mathbb{R}^2_+ \times \mathbb{R}_+ \times \mathbb{R}_+\right\} \tag{2.3.1}$$

where

$$\begin{cases} \Omega_H &= \left\{(S_H, I_H) \in \mathbb{R}^2_+ : 0 \leq N_H \leq \dfrac{\Lambda_H}{\mu_H}\right\}, \\ \Omega_V &= \left\{(S_V, I_V) \in \mathbb{R}^2_+ : 0 \leq N_H \leq \dfrac{\Lambda_V}{\mu_V}\right\}, \\ \Omega_G &= \left\{G_H \in \mathbb{R} : 0 \leq N_H \leq \dfrac{N_h \alpha_h \Lambda_H}{\mu_H \mu_H}\right\}, \\ \Omega_P &= \left\{P_V \in \mathbb{R} : 0 \leq N_V \leq \dfrac{N_v \alpha_v \Lambda_V}{\mu_V \mu_V}\right\}. \end{cases} \tag{2.3.2}$$

We follow the following steps to establish the positive invariance of Ω. Adding equations (1), (2), (3) and (4) of model system (2.2.9) gives,

$$\begin{cases} 1. \ \dfrac{dN_H}{dt} = \Lambda_H - \mu_H N_H - \delta_H I_H, \\ 2. \ \dfrac{dN_V}{dt} = \Lambda_V - \mu_V N_V - \delta_V I_V, \\ 3. \ \dfrac{dP_V}{dt} = N_v \alpha_v I_V - \alpha_V P_V, \\ 4. \ \dfrac{dG_H}{dt} = N_h \alpha_h I_H - \alpha_H G_H. \end{cases} \tag{2.3.3}$$

It follows that,

$$\begin{cases} 1. \ \dfrac{dN_H}{dt} \leq \Lambda_H - \mu_H N_H, \\ 2. \ \dfrac{dN_V}{dt} \leq \Lambda_V - \mu_V N_V, \\ 3. \ \dfrac{dP_V}{dt} \leq N_v \alpha_v N_V - \alpha_V P_V, \\ 4. \ \dfrac{dG_H}{dt} \leq N_h \alpha_h N_H - \alpha_H G_H. \end{cases} \tag{2.3.4}$$

From which we get

$$\begin{cases} 1. \ N_H(t) \leq N_H(0) e^{-\mu_H t} + \dfrac{\Lambda_H}{\mu_H}\Big[1 - e^{-\mu_H t}\Big], \\ 2. \ N_V(t) \leq N_V(0) e^{-\mu_V t} + \dfrac{\Lambda_V}{\mu_V}\Big[1 - e^{-\mu_V t}\Big], \\ 3. \ P_V(t) \leq P_V(0) e^{-\alpha_V t} + \dfrac{N_v \alpha_v \Lambda_V}{\mu_V \alpha_V}\Big[1 - e^{-\alpha_V t}\Big], \\ 4. \ G_H(t) \leq G_H(0) e^{-\alpha_H t} + \dfrac{N_h \alpha_h \Lambda_H}{\mu_H \alpha_H}\Big[1 - e^{-\alpha_H t}\Big]. \end{cases} \tag{2.3.5}$$

where $N_H(0)$, $N_V(0)$, $P_V(0)$ and $G_H(0)$ represent the values of total human population, total mosquito population, community sporozoite load (total infectious reservoir of mosquitoes) and community gametocyte load (total infectious reservoir of humans) evaluated at the initial values of the respective variables. Taking the limit as time gets large, we get the following expressions.

$$\begin{cases} 1. \ \lim\limits_{t\to\infty} \sup(N_H(t)) \leq \dfrac{\Lambda_H}{\mu_H}, \\ 2. \ \lim\limits_{t\to\infty} \sup(N_V(t)) \leq \dfrac{\Lambda_V}{\mu_V}, \\ 3. \ \lim\limits_{t\to\infty} \sup(P_V(t)) \leq \dfrac{N_v\alpha_v\Lambda_V}{\mu_V\mu_V}, \\ 4. \ \lim\limits_{t\to\infty} \sup(G_H(t)) \leq \dfrac{N_h\alpha_h\Lambda_H}{\mu_H\mu_H}. \end{cases} \tag{2.3.6}$$

Thus, the region Ω is positively invariant. Therefore, it is sufficient to consider the dynamics of the flow generated by (2.2.9) in Ω . In this region, the multi-scale model (2.2.9) is epidemiologically and mathematically well-posed. Thus, every solution of the multi-scale model (2.2.9) with initial conditions in Ω remains in Ω for all $t > 0$. Therefore, the ω-limit sets of the multi-scale model (2.2.9) are contained in Ω. We summarize this result in Theorem 2.1 below.

Theorem 2.1. *The region* $\Omega = \left\{\Omega_H \times \Omega_V \times \Omega_G \times \Omega_P \subset \mathbb{R}^2_+ \times \mathbb{R}^2_+ \times \mathbb{R}_+ \times \mathbb{R}_+\right\}$ *is positively invariant for the multi-scale model system (2.2.9) with non-negative initial conditions in* $\mathbb{R}^6_+$.

2.3.2 The Malaria Elimination State and Its Stability

The malaria elimination state, which is mathematically described as the disease-free equilibrium point is steady state solution of the malaria multi-scale model (2.2.9). This is a state characterized by the absence of community gametocyte load and community sporozoite load (collectively called community pathogen load) in a particular geographical area/country/community except through importation. In the absence of community pathogen load, this implies that $(I^0_H = G^0_H = I_V 0^0 = P^0_V = 0)$. Therefore, the disease-free state of the multi-scale model for malaria (2.2.9) is given by

$$E^0 = \left(S^0_H, I^0_H, G^0_H, S^0_V, I^0_V, P^0_V\right) = \left(\frac{\Lambda_H}{\mu_H}, 0, 0, \frac{\Lambda_V}{\mu_V}, 0, 0, \right). \tag{2.3.1}$$

The basic reproduction number denoted as R_0 , is a threshold value that is often used in public health to measure the spread of a disease. It is defined as the number of new infectious hosts that arise as a result of a single infected host being introduced into a fully susceptible population. When $R_0 < 1$, it implies that on average an infectious host infects less than one host throughout his/her period of infectiousness and in this case it is feasible to eliminate the disease. On the other hand, when $R_0 > 1$, then on average every infectious host infects more than one host during his/her period of infectiousness and the disease persists in the population. We use the next generation operator approach [100] to calculate the basic reproductive number from the multi-scale model (2.2.9). Using this approach, the multi-scale model given by (2.2.9) can be re-written in the form

$$\begin{cases} \dfrac{dX}{dt} = f(X, Y, Z), \\ \dfrac{dY}{dt} = g(X, Y, Z), \\ \dfrac{dZ}{dt} = h(X, Y, Z), \end{cases} \tag{2.3.2}$$

where

$$\begin{cases} X = (S_H, S_V), \\ Y = (I_H, I_V), \\ Z = (G_H, P_V). \end{cases} \tag{2.3.3}$$

The components X denote the number of susceptibles, while the components Y represent the number of infected individuals that do not transmit the disease. Components Z represent the number of individuals capable of transmitting the disease. Following [100] we define $\tilde{g}(X, Z)$ by

$$\tilde{g}(X^*, Z) = (\tilde{g_1}(X^*, Z), \tilde{g_2}(X^*, Z)) \tag{2.3.4}$$

with

$$\begin{cases} \tilde{g_1}(X^*, Z) = \dfrac{\beta_V P_V \Lambda_H}{\mu_H(P_0 + P_V)(\mu_H + \alpha_H + \delta_H)}, \\ \tilde{g_2}(X^*, Z) = \dfrac{\beta_H G_H \Lambda_V}{\mu_V(G_0 + G_H)(\mu_V + \delta_V)}. \end{cases} \tag{2.3.5}$$

By substituting the value of I_V and I_H and letting $h_1 = \frac{dP_V}{dt}$, $h_2 = \frac{dG_H}{dt}$ we have that

$$\begin{cases} h_1 = \dfrac{N_h\alpha_h\beta_V P_V \Lambda_H}{\mu_H(P_0+P_V)(\mu_H+\alpha_H+\delta_V)} - \alpha_H G_H, \\ \\ h_2 = \dfrac{N_v\alpha_v\beta_H G_H \Lambda_V}{(G_0+G_H)(\mu_V+\delta_V)} - \alpha_V P_V. \end{cases} \tag{2.3.6}$$

Let $A = D_z h(X^*, \tilde{g}(X^*, 0), 0)$ and further assume that A can be written in the form $A = M - D$, where $M \geq 0$ and $D > 0$, a diagonal matrix.
Then A becomes

$$A = \begin{pmatrix} -\alpha_H & \dfrac{N_h\alpha_h\beta_V\Lambda_H}{\mu_H P_0(\mu_H+\alpha_H+\delta_H)} \\ \dfrac{N_v\alpha_v\beta_H\Lambda_V}{\mu_V G_0(\mu_V+\delta_V)} & -\alpha_V \end{pmatrix}. \tag{2.3.7}$$

Since $A = M - D$, we deduce matrices M and D to be

$$M = \begin{pmatrix} 0 & \dfrac{N_h\alpha_h\beta_V\Lambda_H}{\mu_H P_0(\mu_H+\gamma_H+\delta_H)} \\ \dfrac{N_v\alpha_v\beta_H\Lambda_V}{\mu_V G_0(\mu_V+\delta_V)} & 0, \end{pmatrix}, \tag{2.3.8}$$

and

$$D = \begin{pmatrix} \alpha_H & 0 \\ 0 & \alpha_V \end{pmatrix} \quad \Rightarrow D^{-1} = \begin{pmatrix} \dfrac{1}{\alpha_H} & 0 \\ 0 & \dfrac{1}{\alpha_V}. \end{pmatrix}. \tag{2.3.9}$$

The basic reproductive number is the spectral radius (dominant eigenvalues) which is given by

$$\begin{cases} \mathcal{R}_0 = \rho(MD^{-1}) &= \sqrt{\dfrac{N_h\alpha_h}{(\mu_H+\delta_H+\gamma_H)}.\dfrac{\Lambda_V\beta_H}{\mu_V\alpha_H G_0}.\dfrac{N_v\alpha_v}{(\mu_V+\delta_V)}.\dfrac{\Lambda_H\beta_V}{\mu_H\alpha_V P_0}}, \\ \\ &= \sqrt{R_{0HC}.R_{0CV}.R_{OVC}.R_{0CH}}. \end{cases} \tag{2.3.10}$$

Therefore, the basic reproductive number $\mathcal{R}_0$ is the human-to-human or mosquito-to-mosquito malaria transmission coefficient and is made up of the following partial reproductive numbers.

i. *The human-to-community partial reproductive number ($\mathcal{R}_{0HC}$)*: This partial reproductive number is given by

$$\mathcal{R}_{0HC} = \frac{N_h \alpha_h}{(\mu_H + \delta_H + \gamma_H)}. \tag{2.3.11}$$

This is the average amount of infectious reservoir contributed to the community gametocyte load by each infected human host during his or her entire period of infectiousness. This quantity depends on the average number of gametocytes N_h, in the blood stream of an infected human, which is available for ingestion by a mosquito during her uptake of blood meals from an infected human during his or her entire period of infectiousness and is a composite parameter which in this study is interpreted as the endemic value of the population of gametocytes $\widetilde{G_h}$ which we have already determined from the within-human malaria transmission sub-model as

$$N_h = \widetilde{G_h} = \frac{\pi}{1-\pi}\left[\frac{(1-\pi)N_m\beta_h\Lambda_h - \mu_b\mu_m}{N_m\beta_h(\alpha_h + \mu_h)}\right] = \frac{\pi\Lambda_h}{\Re_0(\alpha_h + \mu_h)}\Big[\Re_0 - 1\Big]. \tag{2.3.12}$$

In the expression for R_{0HC}, α_h is the rate at which gametocytes develop and mature to become infectious within an infected human host in the blood stream. Therefore, $N_h\alpha_h$ is the rate that describes how much an infected person contributes to the community gametocyte load (the total infectious reservoir of humans in the community) during his/her entire period of infectiousness while $\dfrac{1}{(\mu_H + \delta_H + \gamma_H)}$ is the average gametocyte carriage time by each infected person.

ii. *The community-to-vector partial reproductive number (R_{0CV})*: This partial reproductive number is given by

$$R_{0CV} = \frac{\Lambda_V\beta_H}{\mu_V\alpha_H G_0}. \tag{2.3.13}$$

It describes the average number of infected mosquitoes arising from each infectious dose of gametocytes ingested from the total infectious reservoir of humans in the community. This partial reproductive number depends on the supply rate of susceptible mosquitoes Λ_V, the average life span of each susceptible mosquito $\dfrac{1}{\mu_V}$, the rate of contact of the susceptible mosquitoes with the infectious reservoir of humans β_H, the average time it takes to eliminate the infectious reservoir of humans in the community $\dfrac{1}{\alpha_H}$ and the community gametocyte load that yields 50% chance of a mosquito becoming infected with the malaria parasite, G_0.

iii. *The vector-to-community partial reproductive number ($\mathcal{R}_{0VC}$)*: This partial reproductive number is given by

$$\mathcal{R}_{0VC} = \frac{N_v\alpha_v}{(\mu_V + \delta_V)}. \tag{2.3.14}$$

This is also the average amount of infectious reservoir contributed to the community sporozoite load by each infected mosquito vector during her entire period of infectiousness. This quantity depends on the average number of sporozoites in the salivary glands of each infected mosquito N_v, which is available for injection into a human host by a mosquito during uptake of blood meals from a human during her entire period of infectiousness and is a composite parameter which in this study is interpreted as the endemic value of the within-mosquito population of sporozoites $\widetilde{P_v}$ which we have already determined from the within-mosquito malaria transmission sub-model as

$$N_v = \widetilde{P_v} = \frac{1}{2}.\frac{\Lambda_v}{\alpha_v+\mu_v}.\frac{N_k\alpha_k}{\alpha_k+\mu_k}.\frac{\alpha_z}{\alpha_z+\mu_z}.\frac{\alpha_s}{\alpha_s+\mu_s}.\frac{N_g\alpha_g}{\alpha_g+\mu_g}. \tag{2.3.15}$$

In the expression for R_{0VC}, α_v is the rate at which sporozoites are excreted from the midgut within an infected mosquito vector into the salivary glands. Therefore, $N_v\alpha_v$ is the rate that describes how much an infected mosquito contributes to the community sporozoite load (the total infectious reservoir of mosquitoes in the community) during her entire period of infectiousness while $\frac{1}{(\mu_V+\delta_V)}$ is the average sporozoite carriage time by each infected mosquito.

iv. *The community-to-human partial reproductive number ($\mathcal{R}_{0CH}$)*: This reproductive number is given by

$$\mathcal{R}_{0CH} = \frac{\Lambda_H\beta_V}{\mu_H\alpha_V P_0}. \tag{2.3.16}$$

It describes the average number of infected humans arising from each infectious dose of sporozoites injected from the total infectious reservoir of mosquitoes in the community. This partial reproductive number depends on the supply rate of susceptible mosquitoes Λ_H, the average life span of each susceptible mosquito $\frac{1}{\mu_H}$, the rate of contact of the susceptible humans with the infectious reservoir of mosquitoes β_V, the average time it takes to eliminate the infectious reservoir of mosquitoes in the community $\frac{1}{\alpha_V}$ and the community sporozoite load that yields 50% chance of a human becoming infected with the malaria parasite, P_0.

Another informative way of interpreting $\mathcal{R}_0$ is to consider it as a product of two partial reproductive numbers which are the human-to-mosquito partial reproductive number $\mathcal{R}_{0HV}$ and the mosquito-to-human partial reproductive number $\mathcal{R}_{0VH}$ so that

$$\begin{cases} R_0 &= \sqrt{\left[\dfrac{N_h\alpha_h}{(\mu_H+\delta_H+\gamma_H)}\dfrac{\Lambda_V\beta_H}{\mu_V\alpha_H G_0}\right]\left[\dfrac{N_v\alpha_v}{(\mu_V+\delta_V)}.\dfrac{\Lambda_H\beta_V}{\mu_H\alpha_V P_0}\right]}, \\ &= \sqrt{R_{0HV}.R_{OVH}}. \end{cases} \tag{2.3.17}$$

In Eq. (2.3.17), the quantity R_{0HV} is interpreted as follows. Consider a single newly infected human host entering a disease-free population of mosquitoes at equilibrium. This individual is still present and infectious and the expected number of mosquitoes infected by this human is approximately

$$\begin{cases} R_{0HV} &= \dfrac{N_h\alpha_h}{(\mu_H+\delta_H+\gamma_H)}\dfrac{\Lambda_V\beta_H}{\mu_V\alpha_H G_0}, \\ &= \dfrac{\pi}{1-\pi}\left[\dfrac{(1-\pi)N_m\beta_h\Lambda_h-\mu_b\mu_m}{N_m\beta_h(\alpha_h+\mu_h)}\right].\dfrac{\alpha_h\Lambda_H\beta_V}{(\mu_H+\delta_H+\gamma_H)\mu_H\alpha_V P_0}, \\ &= \dfrac{\pi\Lambda_h}{\Re_0(\alpha_h+\mu_h)}\left[\Re_0-1\right].\dfrac{\alpha_h\Lambda_H\beta_V}{(\mu_H+\delta_H+\gamma_H)\mu_H\alpha_V P_0}. \end{cases} \tag{2.3.18}$$

Therefore, the human-to-mosquito transmission coefficient R_{0HV} is composed of between-host disease parameters and within-human parameters. Similarly, in Eq. (2.3.17) the quantity R_{0VH} is interpreted as follows. Consider a single newly infected mosquito vector entering a disease-free population of humans at equilibrium. This mosquito is still present and infectious and the expected number of humans infected by this mosquito is approximately

$$\begin{cases} R_{0VH} &= \dfrac{N_v\alpha_v}{(\mu_V+\delta_V)}.\dfrac{\Lambda_H\beta_V}{\mu_H\alpha_V P_0}, \\ &= \dfrac{\Lambda_v}{2}.\dfrac{N_k\alpha_k}{\alpha_k+\mu_k}.\dfrac{\alpha_z}{\alpha_z+\mu_z}.\dfrac{\alpha_s}{\alpha_s+\mu_s}.\dfrac{N_g\alpha_g}{\alpha_g+\mu_g}.\dfrac{\alpha_v}{\alpha_v+\mu_v}.\dfrac{\Lambda_H\beta_V}{(\mu_V+\delta_V)\mu_H\alpha_V P_0}. \end{cases} \tag{2.3.19}$$

From Eq. (2.3.19) we also deduce that the mosquito-to-human transmission coefficient R_{0CH} is composed of between-host disease parameters and within-mosquito parameters.

2.3.3 Local Stability of the Malaria Elimination state

From Theorem 4.2 of van den Driesche and Watmough [97], if $R_0 < 1$ then the disease free equilibrium is locally asymptotically stable and the disease cannot persist in the population. This result is summarized in the following theorem.

Theorem 2.2. *The disease free equilibrium point E^0, of the multi-scale model system (2.2.9) is locally asymptotically stable whenever $R_0 < 1$ and unstable otherwise.*

Proof. The proof is not necessary since local stability of the disease free equilibrium is a consequence of Theorem 4.2 in van den Driessche and Watmough [97]. □

2.3.4 Global Stability of the Malaria Elimination state

In this sub-section, we investigate the global stability of DFE by following Castillo-Chavez's approach [97]. We re-write the multi-scale model system (2.2.9) in the form

$$\begin{cases} \dfrac{dX}{dt} = F(X, Z), \\ \\ \dfrac{dZ}{dt} = G(X, Z), G(X, 0) = 0, \end{cases} \tag{2.3.1}$$

where $X = (S_H, S_V) \in \mathbb{R}^2_+$ comprises of the uninfected components and $Z = (I_H, P_V, I_V, G_H) \in \mathbb{R}^4_+$ comprises of infected and infectious components. The disease free equilibrium is given by $E^0 = \left(\dfrac{\Lambda_H}{\mu_H}, 0, 0, \dfrac{\Lambda_V}{\mu_V}, 0, 0\right)$. For E^0 to be global asymptotically stable, the conditions H_1 and H_2 below must hold:

H_1 : For $\dfrac{dX}{dt} = F(X, 0), X^*$ is globally asymptotically stable.

H_2 : $G(X, Z) = AZ - \tilde{G}(X, Z)$, $\tilde{G}(X, Z) \geq 0$ for $(X, Z) \in R$ where $A = D_Z[G(X^*, 0)]$ is an M-matrix (the off diagonal elements of A are non-negative) and $\mathbb{R}^6_+$ is the region where the model is meaningful biologically.

Theorem 2.3. *The fixed point E^0 is a globally asymptotically stable equilibrium point of system (2.2.9) provided $R_0 < 1$ and assumptions H_1 and H_2 hold.*

Proof. Using model system (2.2.9), we investigate if the conditions H_1 and H_2 hold. In our case, we observe that

$$F(X,0) = \begin{pmatrix} \Lambda_H - \mu_H S_H \\ \Lambda_V - \mu_V S_V \end{pmatrix} \tag{2.3.2}$$

and

$$A = \begin{pmatrix} -\mu_H & \gamma_H & \frac{-\beta_V \Lambda_H}{P_0 \mu_H} & 0 & 0 & 0 \\ 0 & -(\mu_H + \delta_H + \gamma_H) & \frac{\beta_V \Lambda_H}{P_0 \mu_H} & 0 & 0 & 0 \\ 0 & 0 & -\alpha_V & 0 & N_v \alpha_v & 0 \\ 0 & 0 & 0 & -\mu_V & 0 & -\frac{\beta_H \Lambda_V}{G_0 \mu_V} \\ 0 & 0 & 0 & 0 & -(\mu_V + \delta_V) & \frac{\beta_H \Lambda_V}{G_0 \mu_V} \\ 0 & N_h \alpha_h & 0 & 0 & 0 & -\alpha_H \end{pmatrix}, \tag{2.3.3}$$

$$\tilde{G}(X,Z) = \begin{pmatrix} (\frac{\Lambda_H}{P_0 \mu_H} - \frac{S_H}{P_0 + P_V})\beta_V P_V \\ 0 \\ (\frac{\Lambda_V}{G_0 \mu_V} - \frac{S_V}{G_0 + G_H})\beta_H G_H \\ 0. \end{pmatrix}. \tag{2.3.4}$$

Since $S_H^0 = \frac{\Lambda_H}{\mu_H}\frac{1}{P_0} \geq \frac{S_H}{P_0 + P_V}$ and $S_V^0 = \frac{\Lambda_V}{\mu_V}\frac{1}{G_0} \geq \frac{S_V}{G_0 + G_H}$,
it is clear that $\tilde{G}(X,Z) \geq 0$ for all $(X,Z) \in \mathbb{R}_+^6$ and A is an M-matrix because the off diagonal elements of A are non-negative. Hence, the disease free equilibrium is globally asymptotically stable. □

2.3.5 Estimating the Malaria Baseline Burden

The malaria baseline burden can be approximated using the multi-scale model (2.2.9). The endemic equilibrium of the multi-scale model (2.2.9) can used an approximation of the malaria baseline burden. At the endemic equilibrium both human and mosquitoes vector are infected by sporozoites and gametocytes respectively and the endemic equilibrium is denoted here by $\widetilde{E} = (\widetilde{S_H}, \widetilde{I_V}, \widetilde{G_H}, \widetilde{S_V}, \widetilde{I_V}, \widetilde{P_V})$. We now give expressions for the endemic equilibrium and their interpretation. The endemic value of infected humans is given by

$$\widetilde{I_H} = \frac{\widetilde{\lambda_V}\widetilde{S_H}}{(\mu_H + \gamma_H + \delta_H)}. \tag{2.3.1}$$

We deduce from above equation that the infected population is determined by three quantities: the average time of stay of humans in the infected compartment, the rate of infection of susceptibles and the number of susceptible hosts. Further, the endemic value of susceptible humans is given by

$$\widetilde{S_H} = \frac{\Lambda_H + \gamma_H \widetilde{I_H}}{(\mu_H + \widetilde{\lambda_V})}. \tag{2.3.2}$$

We deduce from (2.3.2) the endemic value of the susceptible humans is proportional to the average time of stay in the susceptible compartment and the rate of supply of few susceptible through birth. Individuals exit this compartment either through death or infection. The endemic value of the community gametocyte load human is given by

$$\widetilde{G_H} = \frac{N_h \alpha_h \widetilde{I_H}}{\alpha_H}. \tag{2.3.3}$$

The endemic value of the community gametocyte load shows that this quantity is dependent on the number of infected humans and average gametocyte load within each infected human as well as the rate of elimination of the community gametocyte load. The endemic value of infected mosquitoes is given as follows.

$$\widetilde{I_V} = \frac{\widetilde{\lambda_V}\widetilde{S_V}}{(\mu_V + \delta_V)}. \tag{2.3.4}$$

From the expression of the endemic value of mosquitoes (2.3.4) we deduce that this quantity is the product of the rate of infection of mosquitoes and the average life span of an infected mosquito. The endemic value of susceptible mosquitoes is given by

$$\widetilde{S_V} = \frac{\Lambda_V}{(\widetilde{\lambda_H} + \mu_V)}. \tag{2.3.5}$$

The quantity given by (2.3.5) is a product of the rate of supply new susceptible mosquitoes and the average time of stay in the susceptible class. The expression for the endemic value of the community sporozoite load is given by

$$\widetilde{P_V} = \frac{N_v \alpha_v \widetilde{I_V}}{\alpha_V}. \tag{2.3.6}$$

We note from the expression (2.3.6) that this quantity is determined by three quantities: the number of infected mosquitoes, the average sporozoite load within an infected mosquito and the rate of elimination of community sporozoite load. We have just discussed the endemic state of

a malaria disease which is quantitatively represented by the endemic values of the multi-scale model system (2.2.9) but have not discussed the conditions under which this state can exist in a community. We accomplish this in the subsection that follows.

2.3.6 The Existence of the Endemic state

We now present some results concerning the existence of an endemic malaria in a community as conditions on a solution for multi-scale model system (2.2.9). To do, this we shall make use of the reproductive number, R_0.

Theorem 2.4. *The multi-scale model (2.2.9) has at least one endemic equilibrium solution given by*

$$\widetilde{E} = (\widetilde{S_H}, \widetilde{I_H}, \widetilde{S_V}, \widetilde{I_V}, \widetilde{P_V}, \widetilde{G_H}), \tag{2.3.1}$$

with $\widetilde{S_H}, \widetilde{I_H}, \widetilde{S_V}, \widetilde{I_V}, \widetilde{P_V}, \widetilde{G_H}$ all non-negative, whose existence and properties are determined by the threshold parameter R_0 where

$$R_0 = \sqrt{\frac{N_h \alpha_h \Lambda_H \beta_V}{\alpha_V P_0 \mu_H (\mu_H + \delta_H + \gamma_H)} . \frac{N_v \alpha_v \Lambda_V \beta_H}{\alpha_H G_0 \mu_V (\mu_V + \delta_V)}}, \tag{2.3.2}$$

and N_h and N_v are composite parameters describing within-human and within-mosquito malaria parasite population dynamics.

Proof. Let $\widetilde{E} = \widetilde{S_H}, \widetilde{I_H}, \widetilde{S_V}, \widetilde{I_V}, \widetilde{P_V}, \widetilde{G_H}$ be a constant solution of the model system (2.2.9) . We can easily express $\widetilde{S_H}, \widetilde{G_H}, \widetilde{S_V}, \widetilde{I_V}, \widetilde{P_V}$ in terms of $\widetilde{I_H}$ in the form

$$\begin{cases} \widetilde{S_H}(\widetilde{I_H}) &= \dfrac{(\Lambda_H - \gamma_H\widetilde{I_H})[b + c\widetilde{I_H}]}{b\mu_H + (a + c\mu_H)\widetilde{I_H}}, \\ \widetilde{S_V}(\widetilde{I_H}) &= \dfrac{\Lambda_V[\alpha_H G_0 + N_h\alpha_h\widetilde{I_H}]}{\mu_V\alpha_H G_0 + d\widetilde{I_H}}, \\ \widetilde{I_V}(\widetilde{I_H}) &= \dfrac{\Lambda_V N_h\alpha_h\beta_H\widetilde{I_H}}{[\mu_V + \delta_V][\mu_V\alpha_H G_0 + d\widetilde{I_H}]}, \\ \widetilde{P_V}(\widetilde{I_H}) &= \dfrac{N_v\alpha_v\Lambda_V N_h\alpha_h\beta_H\widetilde{I_H}}{\mu_V[\mu_V + \delta_V] + d[\mu_V + \delta_V][\mu_V + \beta_H]\alpha_V\widetilde{I_H}}, \\ \widetilde{G_H}(\widetilde{I_H}) &= \dfrac{N_h\alpha_H\widetilde{I_H}}{\alpha_H}, \\ \widetilde{\lambda_V}(\widetilde{I_H}) &= \dfrac{a\widetilde{I_H}}{[b + c\widetilde{I_H}]}, \\ \widetilde{\lambda_H}(\widetilde{I_H}) &= \dfrac{N_h\alpha_h\beta_H\widetilde{I_H}}{\alpha_H G_0 + N_h\alpha_h\widetilde{I_H}}, \end{cases} \tag{2.3.3}$$

where

$$\begin{cases} 1.\ a = \beta_V N_v\alpha_v\Lambda_V.N_h\alpha_h\beta_H, \\ 2.\ b = \mu_V[\mu_V + \delta_V]\alpha_H G_0\alpha_V P_0, \\ 3.\ c = N_v\alpha_v\Lambda_V.N_h\alpha_h\beta_H + N_h\alpha_h\alpha_V P_0[\mu_V + \delta_V][\mu_V + \beta_H], \\ 4.\ d = N_h\alpha_h[\mu_V + \beta_H], \\ 5.\ N_v &= \dfrac{1}{2}.\dfrac{\Lambda_v}{\alpha_v + \mu_v}.\dfrac{N_k\alpha_k}{\alpha_k + \mu_k}.\dfrac{\alpha_z}{\alpha_z + \mu_z}.\dfrac{\alpha_s}{\alpha_s + \mu_s}.\dfrac{N_g\alpha_g}{\alpha_g + \mu_g}, \\ 6.\ N_h &= \dfrac{\pi}{(1-\pi)}\Big[\dfrac{(1-\pi)\beta_h\Lambda_h - \mu_b\mu_m}{N_m\beta_h(\alpha_h + \mu_h)}\Big] = \dfrac{\pi\Lambda_h}{(\alpha_h + \mu_h)\Re_0}\Big[\Re_0 - 1\Big]. \end{cases} \tag{2.3.4}$$

Substituting the expressions in (2.3.3) in the equation for I_H which is given by

$$\frac{dI_H}{dt} = \lambda_V S_H - \Big[\mu_H + \delta_H + \gamma_H\Big] I_H,$$

at the endemic equilibrium we get:

$$\widetilde{I_H} = \frac{\mu_H(\mu_H + \delta_H + \gamma_H)b[R_0^2 - 1]}{a\gamma_H + [a + c\mu_H][\mu_H + \delta_H + \gamma_H]}, \tag{2.3.5}$$

where a, b and c are as defined by the expressions (2.3.4).

We can easily deduce from expression (2.3.5) that there exists one unique endemic equilibrium for model system (2.2.9) whenever $\mathcal{R}_0 > 1$. □

Apart from the fact that the endemic equilibrium values represented by expressions (2.3.3) and (2.3.5) synthesize important elements of human malaria transmission processes, we also note that the between-host endemic expressions for

$$\widetilde{S_H}, \widetilde{G_H}, \widetilde{S_V}, \widetilde{I_V}, \widetilde{P_V}, \widetilde{I_H}, \tag{2.3.6}$$

are determined by both within-host (human host and malaria host) disease parameters and between-host (human host and malaria host) disease parameters while the within-host composite parameters N_h and N_v are only determined by both the within-host disease parameters and not the between-host disease parameters. This confirms the uni-directional coupling and influence of within-host sub-models on between-host sub-models in the multi-scale model (2.2.9).

2.3.7 The Local Stability of Malaria Baseline Endemic state

Center Manifold Theory has been used to determine the local stability of a non-hyperbolic equilibrium (linearized matrix has at least one eigenvalue with zero real part). We now employ the Center Manifold Theory [229] to establish the local asymptotic stability of the endemic equilibrium of multi-scale model system (2.2.9). In order to apply the Center Manifold Theory, we make the following simplifications and change of variables. Let $S_H = x_1$, $I_H = x_2$, $P_V = X_3$, $S_V = x_4$, $I_V = x_5$ and $G_H = x_6$ so that $N_H = x_1 + x_2$ and $N_V = x_4 + x_5$. Further, by using the vector notation $\mathbf{x} = (x_1, x_2, x_3, x_4, x_5, x_6)^T$, the multi-scale model system (2.2.9) can be written in the form $\dfrac{d\mathbf{x}}{dt} = F(\mathbf{x})$ with

$$F(\mathbf{x}) = (f_1, f_2, f_3, f_4, f_5, f_6),$$

such that

$$\begin{cases} \dfrac{dS_H(t)}{dt} = \Lambda_H - \lambda_V x_1 - \mu_H x_2 + \gamma_H x_2 \\ \dfrac{dI_H(t)}{dt} = \lambda_V x_1 - (\mu_H + \delta_H + \gamma_H) x_2 \\ \dfrac{dP_V(t)}{dt} = N_v \alpha_v x_5 - \alpha_v x_3 \\ \dfrac{dS_V(t)}{dt} = \Lambda_V - \lambda_H x_4 - \mu_V x_4 \\ \dfrac{dI_V(t)}{dt} = \lambda_H x_4 - (\mu_V + \delta_V) x_5 \\ \dfrac{dG_H(t)}{dt} = N_h \alpha_h x_2 - \alpha_H x_6 \end{cases} \tag{2.3.1}$$

where,

$$\lambda_H(t) = \frac{\beta_V x_3(t)}{P_0 + x_3(t)}, \qquad \lambda_V(t) = \frac{\beta_H x_6(t)}{G_0 + x_6(t)}. \tag{2.3.2}$$

The method involves evaluating the Jacobian matrix of the system (2.2.9) at the disease-free equilibrium E^0 denoted by $J(E^0)$. The Jacobian matrix associated with equation system (2.2.9) at E^0 is given by

$$J(E^0) = \begin{pmatrix} -\mu_H & \gamma_H & \frac{-\beta_V \Lambda_H}{P_0} & 0 & 0 & 0 \\ 0 & -(\mu_H + \delta_H + \gamma_H) & \frac{\beta_V \Lambda_H}{P_0} & 0 & 0 & 0 \\ 0 & 0 & -\alpha_V & 0 & N_v \alpha_v & 0 \\ 0 & 0 & 0 & -\mu_V & 0 & -\frac{\beta_H \Lambda_V}{G_0 \mu_V} \\ 0 & 0 & 0 & 0 & -(\mu_V + \delta_V) & \frac{\beta_H \Lambda_V}{G_0 \mu_V} \\ 0 & N_h \alpha_h & 0 & 0 & 0 & -\alpha_H \end{pmatrix} \tag{2.3.3}$$

The reproductive number of system (2.2.9) is

$$R_0 = \sqrt{\frac{N_h \alpha_h}{(\mu_H + \delta_H + \gamma_H)} . \frac{\Lambda_V \beta_H}{\mu_V \alpha_H G_0} . \frac{N_v \alpha_v}{(\mu_V + \delta_V)} . \frac{\Lambda_H \beta_V}{\mu_H \alpha_V P_0}}. \tag{2.3.4}$$

Now let us consider $\beta_V = k\beta_H$, regardless of whether $k \in (0, 1)$ or $k \geq 1$ and let $\beta_H = \beta^*$. Taking β^* as the bifurcation parameter and if we consider $R_0 = 1$, and solve for β^*, we obtain

$$\beta^* = \sqrt{\frac{(\mu_H + \delta_H + \gamma_H)(\mu_V \alpha_H G_0)(\mu_V + \delta_V)(\mu_H \alpha_V P_0)}{k N_h \gamma_S \Lambda_V . \Lambda_V . N_v \alpha_v . \Lambda_H}}. \tag{2.3.5}$$

Note that the linearized system of the transformed equations (2.3.1) with bifurcation point β^* has a simple zero eigenvalue. Hence, the Center Manifold Theory can be used to analyse the dynamics of (2.3.1)) near $\beta_H = \beta^*$.

In particular, Theorem 4.1 in Castillo-Chavez and Song [230] reproduced here as Theorem 2.5 for convenience, will be used to show the local asymptotic stability of the endemic equilibrium point of (2.3.1) (which is the same as the endemic equilibrium point of the original system (2.2.9), for $\beta_H = \beta^*$).

Theorem 2.5. *Consider the following general system of ordinary differential equations with parameter ϕ:*

$$\frac{dx}{dt} = f(x, \phi), f : \mathbb{R}^n \times \mathbb{R} \longrightarrow \mathbb{R}, f : C^2(\mathbb{R}^n_+ \times \mathbb{R}), \tag{2.3.6}$$

where 0 is an equilibrium of the system, that is $f(0,\phi)=0$ *for all* ϕ*, and assume that*

A1. $A=D_xf(0,0)=((\partial f_i/\partial x_j)(0,0))$ *is linearization of system (2.3.1) around the equilibrium 0 with* ϕ *evaluated at 0. Zero is a simple eigenvalue of* A*, and other eigenvalues of* A *have negative real parts,*

A2. matrix A *has a right eigenvector* u *and a left eigenvector* v *corresponding to the zero eigenvalue.*

Let f_k *be the* k^{th} *component of* f *and*

$$\begin{cases} a &= \displaystyle\sum_{k,i,j=1}^{n} u_k v_i v_j \frac{\partial^2 f_k}{\partial x_i \partial x_j}(0,0), \\ b &= \displaystyle\sum_{k,i=1}^{n} u_k v_i \frac{\partial^2 f_k}{\partial x_i \partial \phi}(0,0). \end{cases} \tag{2.3.7}$$

The local dynamics of (2.3.1) around 0 are totally governed by a *and* b*.*

i. $a>0$, $b>0$*. When* $\phi<0$ *with* $|\phi|\ll 1$*, 0 is locally asymptotically stable, and there exists a positive unstable equilibrium; when* $0<\phi\ll 1$*, 0 is unstable and there exists a negative and locally asymptotically stable equilibrium.*

ii. $a<0$, $b<0$*. When* $\phi<0$ *with* $|\phi|\ll 1$*, 0 is unstable; when* $0<\phi\ll 1$*, 0 is locally asymptotically stable, and there exists a positive unstable equilibrium;*

iii. $a>0$, $b<0$*. When* $\phi<0$ *with* $|\phi|\ll 1$*, 0 is unstable, and there exists a locally asymptotically stable negative equilibrium; when* $0<\phi\ll 1$*, 0 is stable and a positive unstable equilibrium appears;*

iv. $a<0$, $b>0$*. When* ϕ *changes from negative to positive, 0 changes its stability from stable to unstable. Correspondingly a negative unstable equilibrium becomes positive and locally asymptotically stable*

In order to apply the above theorem, the following computations are necessary (it should be noted that we are using β^* as the bifurcation parameter, in place of ϕ in Theorem 2.5.

Eigenvectors of J_{β^*}: For the case when $R_0=1$, it can be shown that the Jacobian of (2.3.3) at $\beta_H=\beta^*$ (denoted by J_{β^*}) has a right eigenvector associated with the zero eigenvalue given by $u=[u_1,u_2,u_3,u_4,u_5,u_6]^T$, where

$$\begin{cases} u_1 &= -\dfrac{k\beta^{*2}\Lambda_H N_v\alpha_v\Lambda_V\Lambda_V}{P_0^2\mu_H^2\alpha_V G_0\mu_V(\mu_V+\delta_V)}+\dfrac{\gamma_H\alpha_H}{N_h\alpha_h\mu_H}, \\ u_2 &= \dfrac{\alpha_H}{N_h\alpha_h}, \\ u_3 &= -\dfrac{N_v\alpha_v\beta^*\Lambda_V}{\alpha_V G_0\mu_V(\mu_V+\delta_V)}, \\ u_4 &= -\dfrac{\beta^*\Lambda_V}{G_0\mu_V^*}, \\ u_5 &= \dfrac{\beta^*\Lambda_V}{G_0\mu_V^*(\alpha_V+\mu_V)}, \\ u_6 &= 1 \end{cases} \tag{2.3.8}$$

Further, the left eigenvector of $J(E^0)$ associated with the zero eigenvalue at $\beta_H=\beta^*$ is given by $v=[v_1,v_2,v_3,v_4,v_5,v_6]^T$, where

$$\begin{cases} v_1 &= 0, \\ v_2 &= \dfrac{N_h\alpha_h}{\mu_H+\delta_H+\gamma_H}, \\ v_3 &= \dfrac{k\beta^*\Lambda_H N_h\alpha_h}{P_0\mu_H(\mu_H+\delta_H+\gamma_H)}, \\ v_4 &= 0, \\ v_5 &= \dfrac{N_v\alpha_v k\beta^*\Lambda_H N_h\alpha_h}{(\mu_V+\delta_V)(\mu_H+\delta_H+\gamma_H)P_0\mu_H}, \\ v_6 &= 1. \end{cases} \tag{2.3.9}$$

Computation of bifurcation parameters a and b:

The sign of a is associated with the following non-vanishing partial derivatives of F:

$$\begin{cases} \dfrac{\partial^2 f_1}{\partial x_1 \partial x_6} = \dfrac{\partial^2 f_1}{\partial x_6 \partial x_1} = \dfrac{-\beta^*}{G_0}, \\ \dfrac{\partial^2 f_1}{\partial x_6^2} = -\dfrac{2\beta^* \Lambda_H}{\mu_H G_0^2}, \\ \dfrac{\partial^2 f_2}{\partial x_1 \partial x_6} = \dfrac{\partial^2 f_2}{\partial x_6 \partial x_1} = \dfrac{\beta^*}{G_0}, \\ \dfrac{\partial^2 f_2}{\partial x_6^2} = -\dfrac{2\beta^* \Lambda_H}{G_0^2 \mu_H}, \\ \dfrac{\partial^2 f_5}{\partial x_3 \partial x_4} = \dfrac{\partial^2 f_5}{\partial x_4 \partial x_3} = \dfrac{k\beta^* \Lambda_V}{P_0 \mu_V}, \\ \dfrac{\partial^2 f_5}{\partial x_3^2} = -\dfrac{2k\beta^* \Lambda_V}{\mu_V P_0^2}. \end{cases} \tag{2.3.10}$$

Substituting equation (2.3.10) into equation (2.3.1), we get

$$\begin{cases} a = \displaystyle\sum_{k,i,j=1}^{n} u_k v_i v_j \frac{\partial^2 f_k}{\partial x_i \partial x_j}(0,0) \\ = u_1 v_6^2 \dfrac{\partial^2 f_1}{\partial x_6^2} + u_2 v_6^2 \dfrac{\partial^2 f_2}{\partial x_6^2} + u_5 v_3^2 \dfrac{\partial^2 f_5}{\partial x_3^2}, \\ = -\left[\dfrac{-\beta^* N_v \alpha_v \Lambda_V}{P_0^2 \mu_H^2 \alpha_V G_0 \mu_V (\mu_V + \delta_V)} + \dfrac{\delta_H \alpha_H}{N_h \alpha_h \mu_H}\right] .1^2 . \dfrac{2\beta^* \Lambda_H}{\mu_H G_0^2} - \dfrac{\alpha_H}{N_h \alpha_h} .1^2 . \dfrac{2\beta^* \Lambda_H}{\mu_H G_0^2} - \\ \dfrac{\beta^* \Lambda_V}{G_0 \mu_V (\mu_V - \delta_V)} . \left[\dfrac{\beta^* \Lambda_H N_h \alpha_h}{P_0 \mu_H (\mu_H + \delta_H + \gamma_H)}\right]^2 . \dfrac{2k\beta^* \Lambda_V}{\mu_V P_0^2}, \\ = \dfrac{2\beta^{*2} N_v \alpha_v \Lambda_V}{P_0^2 \mu_H^2 \alpha_V G_0 \mu_V (\mu_V + \delta_V)} . \dfrac{\Lambda_H}{\mu_H G_0^2} - \dfrac{2\delta_H \alpha_H}{N_h \alpha_h \mu_H} . \dfrac{\beta^* \Lambda_H}{\mu_H G_0^2} - \dfrac{2\alpha_H \beta^* \Lambda_H}{N_h \alpha_h \mu_H G_0^2} . \\ -\dfrac{2k\beta^{*2} \Lambda_V^2}{G_0 P_0^2 \mu_V^2 (\mu_V - \delta_V)} \left[\dfrac{\beta^* \Lambda_H N_h \alpha_h}{P_0 \mu_H (\mu_H + \delta_H + \gamma_H)}\right]^2 < 0. \end{cases} \tag{2.3.11}$$

For the sign of b, it is associated with the following non-vanishing partial derivatives of F,

$$\begin{cases} \dfrac{\partial^2 f_1}{\partial\beta^*\partial x_6} = -\dfrac{\Lambda_H}{G_0\mu_H}, \\ \dfrac{\partial^2 f_2}{\partial\beta^*\partial x_6} = \dfrac{\Lambda_H}{G_0\mu_H}, \\ \dfrac{\partial^2 f_4}{\partial\beta^*\partial x_3} = \dfrac{-k\Lambda_V}{P_0\mu_V}, \\ \dfrac{\partial^2 f_5}{\partial\beta^*\partial x_3} = \dfrac{\Lambda_V}{P_0\mu_V}. \end{cases} \tag{2.3.12}$$

It follows from the above expression that

$$\begin{cases} b = \sum_{k,i=1}^{12} u_k v_i \dfrac{\partial^2 f_k}{\partial x_i \partial\phi}(0,0) \\ = u_1 v_6 \dfrac{\partial^2 f_1}{\partial\beta^*\partial x_6} + u_2 v_6 \dfrac{\partial^2 f_2}{\partial\beta^*\partial x_6} + u_4 v_3 \dfrac{\partial^2 f_4}{\partial\beta^*\partial x_3} + u_5 v_3 \dfrac{\partial^2 f_5}{\partial\beta^*\partial x_3} \\ = \left[\dfrac{-k\beta^{*2}\Lambda_H N_v \alpha_v \Lambda_V}{P_0^2\mu_H^2\alpha_V G_0\mu_V(\mu_V+\delta_V)} + \dfrac{\gamma_H\alpha_H}{N_h\alpha_h\mu_H}\right].1.\dfrac{-\Lambda_H}{\mu_H G_0} + \dfrac{\alpha_H}{N_h\alpha_h}.1.\dfrac{\Lambda_H}{\mu_H G_0} \\ - \left[\dfrac{-k\beta^{*2}\Lambda_V^2}{G_0\mu_V^2}.\dfrac{\Lambda_H N_h\alpha_h}{P_0\mu_H(\mu_H+\delta_H+\gamma_H).P_0\mu_V}\right] + \dfrac{\beta^*\Lambda_V}{G_0\mu_V(\mu_V+\delta_V)}.\dfrac{\beta^*\Lambda_H N_h\alpha_h}{P_0\mu_H(\mu_H+\delta_H+\gamma_H)}.\dfrac{\Lambda_H}{\mu_H G_0} \\ = \dfrac{k\beta^{*2}\Lambda_H^2 N_v\alpha_v\Lambda_V}{P_0^2\mu_H^2\alpha_V G_0\mu_V(\mu_V+\delta_V)} + \dfrac{\alpha_H\Lambda_H}{N_h\alpha_h\mu_H G_0} + \left[\dfrac{k\beta^{2*}\Lambda_V^2}{G_0\mu_V^2}.\dfrac{\Lambda_H N_h\alpha_h}{P_0\mu_H(\mu_H+\delta_H+\gamma_H).P_0\mu_V}\right] + \\ \dfrac{\beta^*\Lambda_V\Lambda_H^2 N_h\alpha_h}{G_0^2P_0^2\mu_V\mu_H^2(\mu_V+\delta_V)(\mu_H+\delta_H+\gamma_H)} - \dfrac{\delta_H\alpha_H\Lambda_H}{N_h\alpha_h\mu_H^2 G_0} > 0. \end{cases} \tag{2.3.13}$$

Thus, $a < 0$ and $b > 0$. Using Theorem 2.5, item (iv), we have establish the following result which only holds for $\mathcal{R}_0 > 1$ but close to 1:

Theorem 2.6. *The unique endemic equilibrium of the multi-scale models system (2.2.9) guaranteed by Theorem 2.5 is locally asymptotically stable for $R_0 > 1$ near 1.*

2.3.8 Sensitivity Analysis of the Transmission Metrics of Baseline multi-scale Model

In this subsection, we present results of the sensitivity analysis of six malaria transmission metrics (three at within-host scale and the other three at between-host scale) which we derived from the multi-scale model (2.2.9), with respect to thirty-five parameters of the multi-scale model (2.2.9). At within-host scale (within-human and within-mosquito) the three malaria transmission metrics are: (i) N_h (which we use as a proxy for individual human infectiousness to mosquitoes), (ii) N_v (which we use as a proxy for individual mosquito infectiousness to humans), and (iii) $\Re_0$ (which we use to characterize within-human reproductive capacity of merozoites). At between-host scale (humans and mosquitoes), the three malaria transmission metrics are: (i) community sporozoite load, P_V (which we take an indicator of a community's level of infectiousness and transmission probability of malaria to humans), (ii) community gametocyte load, G_H (which we also take an indicator of a community's level of infectiousness and transmission probability of malaria to mosquitoes), and (iii) malaria basic reproductive number, $\mathcal{R}_0$ (which we take as characterizing transmission potential of malaria at the start of the epidemic). In general, parameters to which these six malaria transmission metrics (multi-scale model outputs) are sensitive provide critical points for control and elimination of malaria parasite along its life-cycle which should be monitored and controlled during malaria outbreak. Using the approach in [231], for the sensitivity analysis, we note that the normalized sensitivity index with respect to parameter P of the three within-host scale malaria disease transmission metrics $(N_h, N_v, \Re_0)$ is given by

$$S^P_{\Gamma_w} = \frac{\partial \Gamma_w}{\partial P} \times \frac{P}{\Gamma_w}, \quad \Gamma_w = N_h, N_v, \Re_0, \tag{2.3.1}$$

Where

$$\begin{cases} 1.\ N_v = \frac{1}{2}.\frac{\Lambda_v}{\alpha_v+\mu_v}.\frac{N_k\alpha_k}{\alpha_k+\mu_k}.\frac{\alpha_z}{\alpha_z+\mu_z}.\frac{\alpha_s}{\alpha_s+\mu_s}.\frac{N_g\alpha_g}{\alpha_g+\mu_g}, \\ 2.\ N_h = \frac{\pi}{(1-\pi)}\Big[\frac{(1-\pi)N_m\beta_h\Lambda_h - \mu_b\mu_m}{N_m\beta_h(\alpha_h+\mu_h)}\Big] = \frac{\pi\Lambda_h}{(\alpha_h+\mu_h)\Re_0}\Big[\Re_0 - 1\Big], \\ 3.\ \Re_0 = \frac{(1-\pi)N_m\beta_h\Lambda_h}{\mu_b\mu_m}. \end{cases} \tag{2.3.2}$$

Table 2.4 shows the results of the evaluation of the sensitivity of the three within-host scale malaria disease transmission metrics $(N_h, N_v, \Re_0)$ to the multi-scale model (2.2.9)'s parameters.

Considering the sensitivity of N_h, N_v and $\Re_0$ to within-human and within-mosquito parameters in Table 2.3 we note the following results.

i. For the within-human parameters, we note from Table 2.4 that both N_h and $\Re_0$ have high sensitivity to β_h, μ_b, μ_m, N_m and α_h. This implies that care must be taken to improve the accuracy of these parameters during data collection if the utility and validity of the within-human malaria transmission sub-model given by (2.2.3) is to be improved. On the other hand, this also means that at individual level, interventions that target these parameters are likely to have a higher impact.

ii. N_h has little sensitivity to μ_h and Λ_h while $\Re_0$ has little sensitivity to π. This means that the within-human sub-model is robust with respect to these parameters (μ_h and Λ_h) when used to characterize within-human malaria disease dynamics when infection is at endemic levels, while the same sub-model is robust with respect to π when used to characterize within-human malaria disease dynamics when infection is at the start of the infection. Since these parameters also determine gametocyte dynamics at individual human level, it means that malaria interventions that target gametocytes are likely to have little impact on disease dynamics at individual level.

iii. We also note that N_v has high sensitivity to all within-mosquito sub-model parameters except α_g and μ_g. This means that the within-mosquito sub-model is robust with respect to α_g and μ_g. On the other hand, it also means that care must be taken in improving the accuracy of all within-mosquito malaria disease dynamics parameters (except α_g and μ_g) if the utility and validity of this sub-model is to be improved. Further, this also means that malaria interventions that target these parameters (except α_g and μ_g) are likely to be effective in reducing malaria parasite population growth within an infected mosquito.

SL.No.	Parameter	Sensitivity index of N_h	Sensitivity index of N_v	Sensitivity index of $\Re_0$
1	Λ_v	-	1.000000	-
2	α_g	-	0.000163	-
3	μ_g	-	-0.000163	-
4	N_g	-	1.000000	-
5	α_s	-	0.999380	-
6	μ_s	-	-0.999380	-
7	α_z	-	0.442478	-
8	μ_z	-	-0.442478	-
9	α_k	-	0.666667	-
10	μ_k	-	-0.666667	-
11	N_k	-	1.000000	-
12	α_v	-	-0.757576	-
13	μ_v	-	-0.242424	-
14	β_h	-1.000002	-	1.000000
15	μ_b	1.000002	-	-1.000000
16	π	1.052632	-	-0.052632
17	μ_m	1.000002	-	-1.000000
18	N_m	-1.000002	-	1.000000
19	α_h	-0.961538	-	-
20	μ_h	-0.038462	-	-
21	Λ_h	-0.000002	-	1.000000

Table 2.4: Sensitivity indices of N_h, N_v and $\Re_0$.

Further, using the approach in [231], for the sensitivity analysis, we note that the normalized sensitivity index of the three between-host scale malaria disease transmission metrics $(\widetilde{G_H}, \widetilde{P_V}, \mathcal{R}_0)$ with respect to parameter P is given by

$$S^P_{\Gamma_b} = \frac{\partial \Gamma_b}{\partial P} \times \frac{P}{\Gamma_b}, \quad \Gamma_b = \widetilde{G_H}, \widetilde{P_V}, \mathcal{R}_0, \tag{2.3.3}$$

where

$$\begin{cases} 1.\ \widetilde{G_H} = \dfrac{(\mathcal{R}_0^2-1).\mu_V G_0 \Lambda_H \beta_V .(\mu_H+\delta_H+\gamma_H)}{\Lambda_V \beta_H \mathcal{R}_{VH}[\beta_V(\mu_H+\delta_H)+\mu_H(\mu_H+\delta_H+\gamma_H)]+\Lambda_H\beta_V(\mu_V+\beta_H)(\mu_H+\delta_H+\gamma_H)}, \\ 2.\ \widetilde{P_V} = \dfrac{(\mathcal{R}_0^2-1).\mu_H P_0 \Lambda_V \beta_H .(\mu_H+\delta_H+\gamma_H)}{\Lambda_H \beta_V \mathcal{R}_{HV}(\mu_V+\beta_H)(\mu_H+\delta_H+\gamma_H)+\Lambda_V\beta_H[\mu_H(\mu_H+\delta_H+\gamma_H)+\beta_V(\mu_H+\delta_H)]} \\ 3.\ \mathcal{R}_0 = \sqrt{\dfrac{N_h\alpha_h\Lambda_V\beta_H}{\mu_V(\mu_H+\delta_H+\gamma_H)\alpha_H G_0}.\dfrac{N_v\alpha_v\Lambda_H\beta_V}{\mu_H(\mu_V+\delta_V)\alpha_V P_0}}. \end{cases} \quad (2.3$$

Table 2.5 shows the results of the evaluation of the sensitivity of the three between-host scale malaria disease transmission metrics ($\widetilde{G_H}, \widetilde{P_V}, \mathcal{R}_0$) to the multi-scale model (2.2.9)'s parameters. Considering the sensitivity of $\widetilde{G_H}$ to all the human-to-mosquito malaria disease dynamics sub-model parameters, we note the following results.

i. The malaria transmission metric $\widetilde{G_H}$ is highly sensitive to four between-host malaria transmission parameters Λ_H, γ_H, α_H and β_V and five within-human malaria transmission parameters β_h, μ_b, π, μ_m and N_m. This means that care must be taken in improving the accuracy of these parameters during data collection if the utility and validity of the human-to-mosquito malaria transmission sub-model is to be improved.

ii. On the other hand, because $\widetilde{G_H}$ has high sensitivity to the nine parameters (Λ_H, γ_H, α_H, β_V, β_h, μ_b, π, μ_m, N_m), then this implies that interventions that are focused on the human host that target these parameters are likely to have high impact in reducing human-to-mosquito malaria transmission.

iii. The malaria transmission metric $\widetilde{G_H}$ has low sensitivity to the remaining twenty-five malaria transmission parameters. This means that the human-to-mosquito malaria transmission sub-model in the multi-scale model given by (2.2.9) is robust with respect to these twenty-five parameters.

Considering the sensitivity of $\widetilde{P_V}$ to all the mosquito-to- human malaria disease dynamics sub-model parameters, we note the following results.

i. The malaria transmission metric $\widetilde{P_V}$ has high sensitivity to four between-host malaria transmission parameters Λ_V, α_V, μ_V, and β_H and eleven within-mosquito malaria transmission parameters (Λ_v, N_g, α_s, μ_s, α_z, μ_z, α_k, μ_k, N_k, α_v, μ_v). This means also that care must be taken in improving the accuracy of these parameters during data collection if the utility and validity of the mosquito-to- human malaria transmission sub-model is to be improved.

ii. Furthermore, because $\widetilde{P_V}$ has high sensitivity to the fifteen parameters (Λ_V, α_V, μ_V, β_H, Λ_v, N_g, α_s, μ_s, α_z, μ_z, α_k, μ_k, N_k, α_v, μ_v), then this implies that interventions that are focused on the mosquito vector that target these fifteen parameters are likely to have high impact in reducing mosquito-to- human malaria transmission.

iii. However, the malaria transmission metric $\widetilde{P_V}$ has low sensitivity to the remaining nineteen malaria transmission parameters. This means that the mosquito-to- human malaria transmission sub-model in the multi-scale model given by (2.2.9) is robust with respect to these twenty-five parameters.

Considering the sensitivity of $\mathcal{R}_0$ to the full malaria disease dynamics multi-scale model parameters, we note the following results.

i. The malaria transmission metric, $\mathcal{R}_0$, derived from the multi-scale model given by (2.2.9), has very low sensitivity to six parameters (δ_V, α_g, μ_g, Λ_h, α_h, μ_h). This again means that the full malaria transmission multi-scale model given by (2.2.9) is robust with respect to these six parameters.

ii. In addition, the malaria transmission metric, $\mathcal{R}_0$, derived from the multi-scale model given by (2.2.9), has high sensitivity to the remaining twenty-eight malaria disease dynamics parameters. This means also that care must be taken in improving the accuracy of these twenty-eight malaria disease dynamics parameters during data collection if the utility and validity of the full malaria transmission multi-scale model given by (2.2.9) is to be improved.

iii. On the other hand, because $\mathcal{R}_0$ has high sensitivity to the twenty-eight remaining malaria disease dynamics parameters then this implies that interventions that are focused on the controlling malaria disease system that target these twenty-eight parameters are likely to have high impact in reducing malaria transmission in the community, especially at the start of the malaria epidemic.

SL.No.	Parameter	Sensitivity index of $\widetilde{G_H}$	Sensitivity index of $\widetilde{P_V}$	Sensitivity index of $\mathcal{R}_0$
1	Λ_H	1.000000000	-0.000000243	0.500000000
2	γ_H	-0.980663693	0.000000001	-0.491917155
3	P_0	-0.000001477	0.000000000	-0.500000000
4	α_H	-1.000000000	0.000000243	-0.500000000
5	δ_H	-0.019060285	0.000000239	-0.007967464
6	β_H	0.000000286	0.666666585	0.500000000
7	μ_H	-0.000277498	0.000000004	-0.500115381
8	Λ_V	0.000001477	1.000000000	0.500000000
9	β_V	0.996777286	-0.000000001	0.500000000
10	α_V	-0.000001477	-1.000000000	-0.500000000
11	Λ_v	0.000001477	1.000000000	0.500000000
12	μ_V	-0.000001763	-0.999964257	-0.999982251
13	δ_V	0.000000000	-0.000035499	-0.000017749
14	G_0	0.000000000	0.000000243	-0.500000000
15	α_g	0.000000000	0.000162734	0.000081367
16	μ_g	0.000000000	-0.000162734	-0.000081367
17	N_g	0.000001477	1.000000000	0.500000000
18	α_s	0.000001476	0.999380229	0.499690115
19	μ_s	-0.000001476	-0.999380229	-0.499690115
20	α_z	0.000000654	0.442477876	0.221238938
21	μ_z	-0.000000654	-0.442477876	-0.221238938
22	α_k	0.000000738	0.500000000	0.250000000
23	μ_k	-0.000000738	-0.500000000	-0.250000000
24	N_k	0.000001477	1.000000000	0.500000000
25	α_v	0.000000358	0.242424242	0.121212121
26	μ_v	-0.000000358	-0.242424242	-0.121212121
27	β_h	-1.000002464	0.000000243	-0.500001232
28	μ_b	1.000002464	-0.000000243	0.500001232
29	π	1.052631708	-0.000000256	0.526315854
30	μ_m	1.000002464	-0.000000243	0.500001232
31	N_m	-1.000002464	0.000000243	-0.500001232
32	α_h	0.038461538	-0.000000009	0.019230769
33	μ_h	-0.038461538	0.000000009	-0.019230769
34	Λ_h	-0.000002464	0.000000000	-0.000001232

Table 2.5: Sensitivity indices of $\widetilde{G_H}$, $\widetilde{P_V}$, and $\mathcal{R}_0$ with respect to 34 parameters of the malaria disease system.

2.3.9 The Influence of Within-host sub-models on between-host sub-models

In the multi-scale model (2.2.9), the within-host scale sub-models influence between-host malaria disease dynamics and not the other may round. We use numerical simulations to illustrate this uni-directional coupling of the multi-scale model (2.2.9) using four with-human selected parameters which are μ_h, μ_m, N_m and β_h. More specifically, we illustrate the influence of these four within-human malaria disease dynamics parameters (μ_h, μ_m, N_m, β_h) on four key between-host scale variables (I_H, I_V, G_H, P_V). Changes in the four within-human malaria disease dynamics parameters (μ_h, μ_m, N_m, β_h) are associated with the following medical interventions (drugs and vaccines) effects: (i) variation in the killing of gametocytes within an infected human host, μ_h, (ii) variations in the killing merozoites within an infected human host, μ_m, (iii) variation in the replication of merozoites at within-cell scale in an infected human host, N_m, and (iv) variation in the transmission rate of merozoites at between-cell scale within an infected human host, β_h. The numerical simulations, which are conducted using the baseline parameter values given in Tables 2.2 and 2.3 are shown in Figures 2.2, 2.3, 2.4 and 2.5.

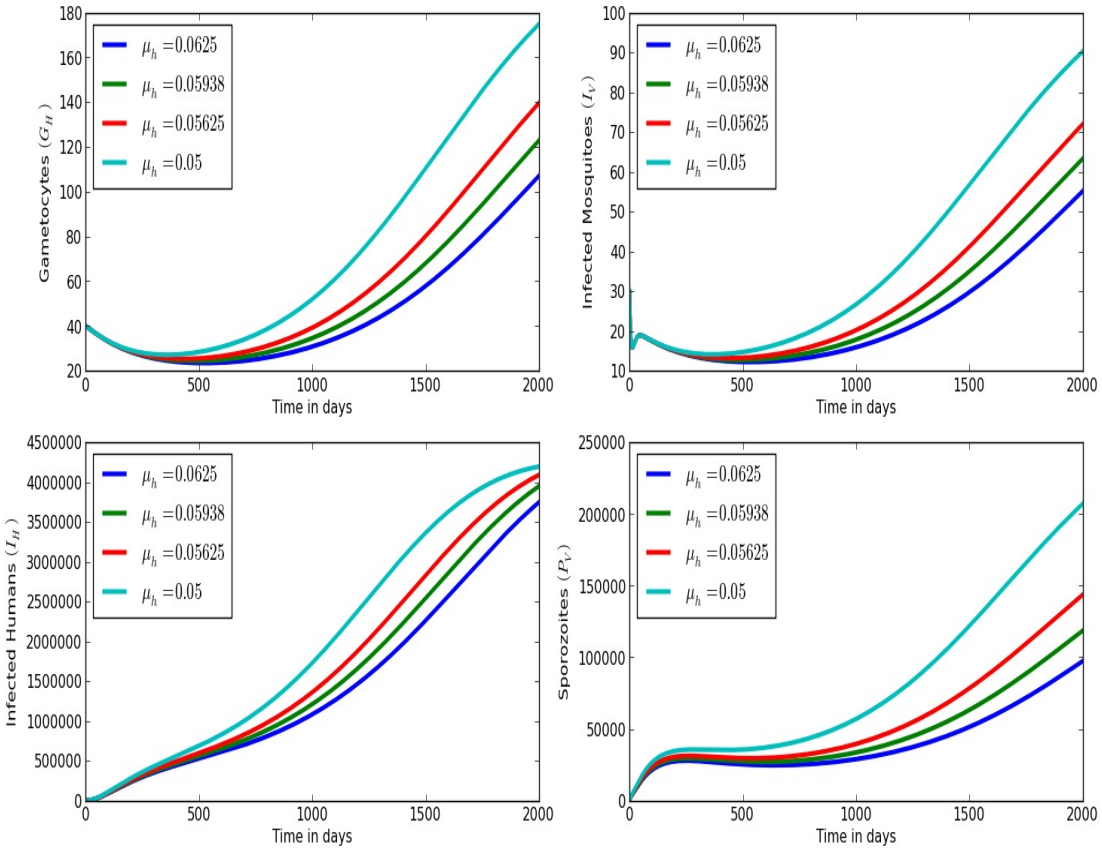

Figure 2.2: Graphs showing changes in (a) community gametocyte load (G_H), (b) population of infected mosquitoes I_V, (c) population of infected humans I_H, and (d): community sporozoite load P_V for different values of death rate of within-human gametocyte load μ_h: $\mu_h = 0.0625$, $\mu_h = 0.05938$, $\mu_h = 0.05625$, and $\mu_h = 0.05$.

Figure 2.2 shows variations in (a) community gametocyte load (G_H), (b) population of infected mosquitoes I_V, (c) population of infected humans I_H, and (d): community sporozoite load P_V for different values of death rate of within-human gametocyte load μ_h: $\mu_h = 0.0625$, $\mu_h = 0.05938$, $\mu_h = 0.05625$, and $\mu_h = 0.05$. The results show that as the death rate of gametocytes within infected humans increase, there is also a noticeable decrease in community gametocyte load (G_H), population of infected mosquitoes I_V, population of infected humans I_H and community sporozoite load (P_V) at between-host scale. The results imply that control measures aimed at giving treatments that kill gametocyte within infected individuals are good for the community in that they reduce transmission of malaria at population/community level.

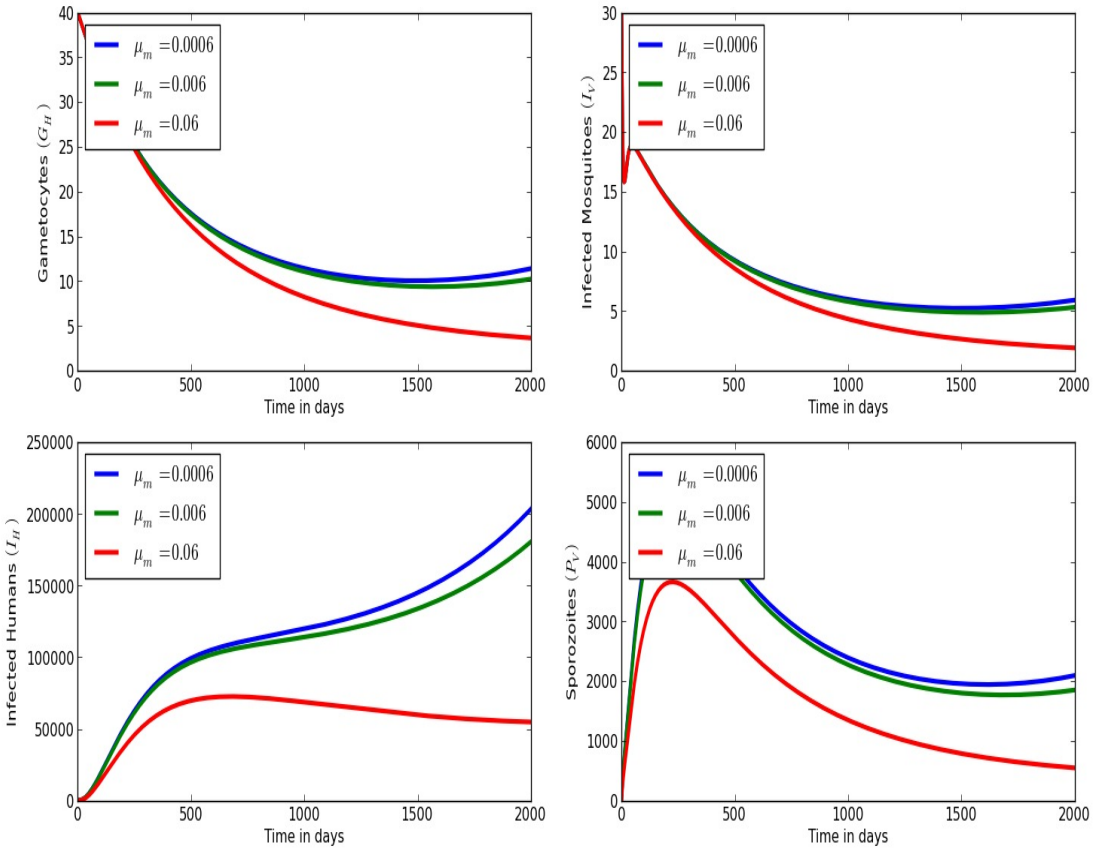

Figure 2.3: Graphs showing changes in (a) community gametocyte load (G_H), (b) population of infected mosquitoes I_V, (c) population of infected humans I_H, and (d): community sporozoite load P_V for different values of death rate of merozoites μ_m: $\mu_m = 0.0006$, $\mu_m = 0.006$, and $\mu_m = 0.06$.

Figure 2.3 shows changes in (a) community gametocyte load (G_H), (b) population of infected mosquitoes I_V, (c) population of infected humans I_H, and (d): community sporozoite load P_V for different values of death rate of merozoites μ_m: $\mu_m = 0.0006$, $\mu_m = 0.006$, and $\mu_m = 0.06$. From these results we notice that as the death rate of merozoites within infected humans increase, there is also a noticeable decrease in community gametocyte load, population of infected mosquitoes I_V, population of infected humans I_H and community sporozoite load at between-host scale. These results imply that treatments that cure an individual from malaria by increasing the killing rate of merozoites are equally good for both the individual and the community because the individual's transmission risk of malaria in the community is reduced.

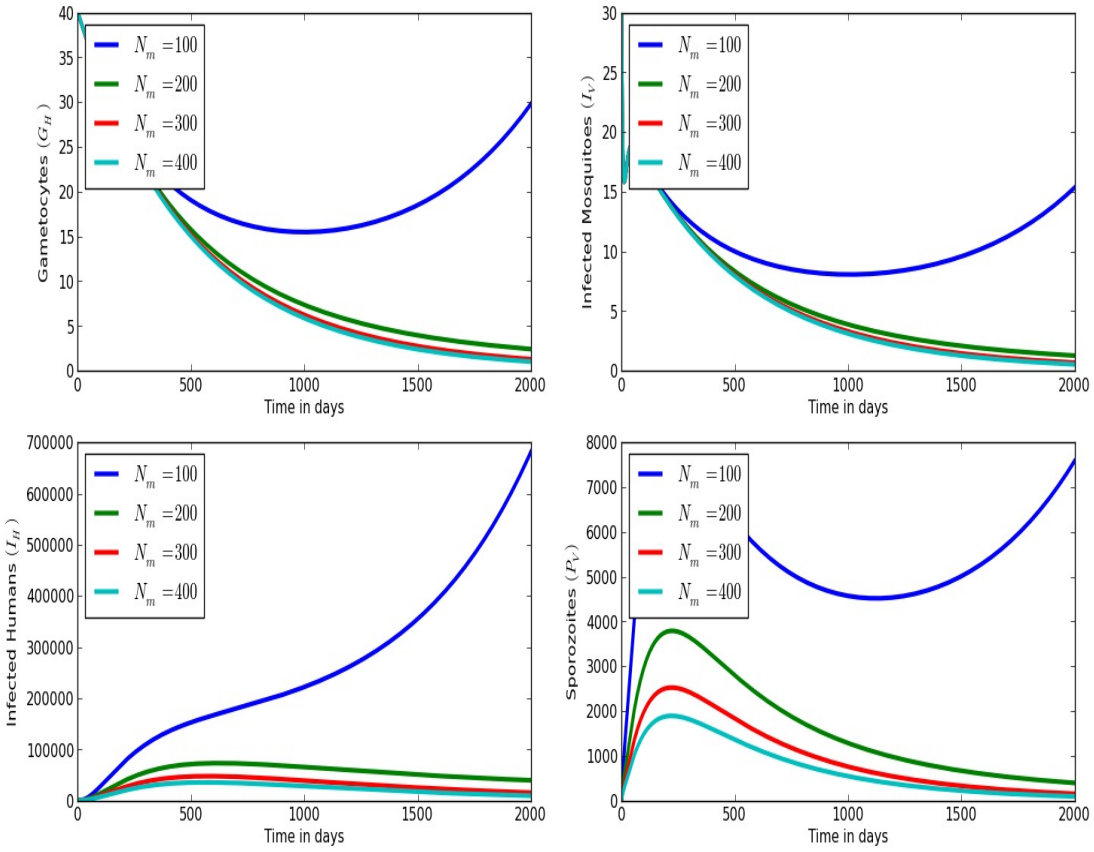

Figure 2.4: Graphs showing changes in (a) community gametocyte load (G_H), (b) population of infected mosquitoes I_V, (c) population of infected humans I_H, and (d): community sporozoite load P_V for different values of merozoites produced per bursting infected red blood cell N_m: $N_m = 100$, $N_m = 200$, $N_m = 300$ and $N_m = 400$.

Figure 2.4 shows variations in (a) community gametocyte load (G_H), (b) population of infected mosquitoes I_V, (c) population of infected humans I_H, and (d): community sporozoite load P_V for different values of merozoites produced per bursting infected red blood cell N_m: $N_m = 100$, $N_m = 200$, $N_m = 300$ and $N_m = 400$. These results show that as the average replication rate of merozoites at within-cell scale at individual level increases, transmission of malaria at community level also increases. Therefore, these results are proof-of-principle about the public health beneficial effects of treatments that reduce the replication rate of malaria parasite (merozoites) at individual level (within-human scale).

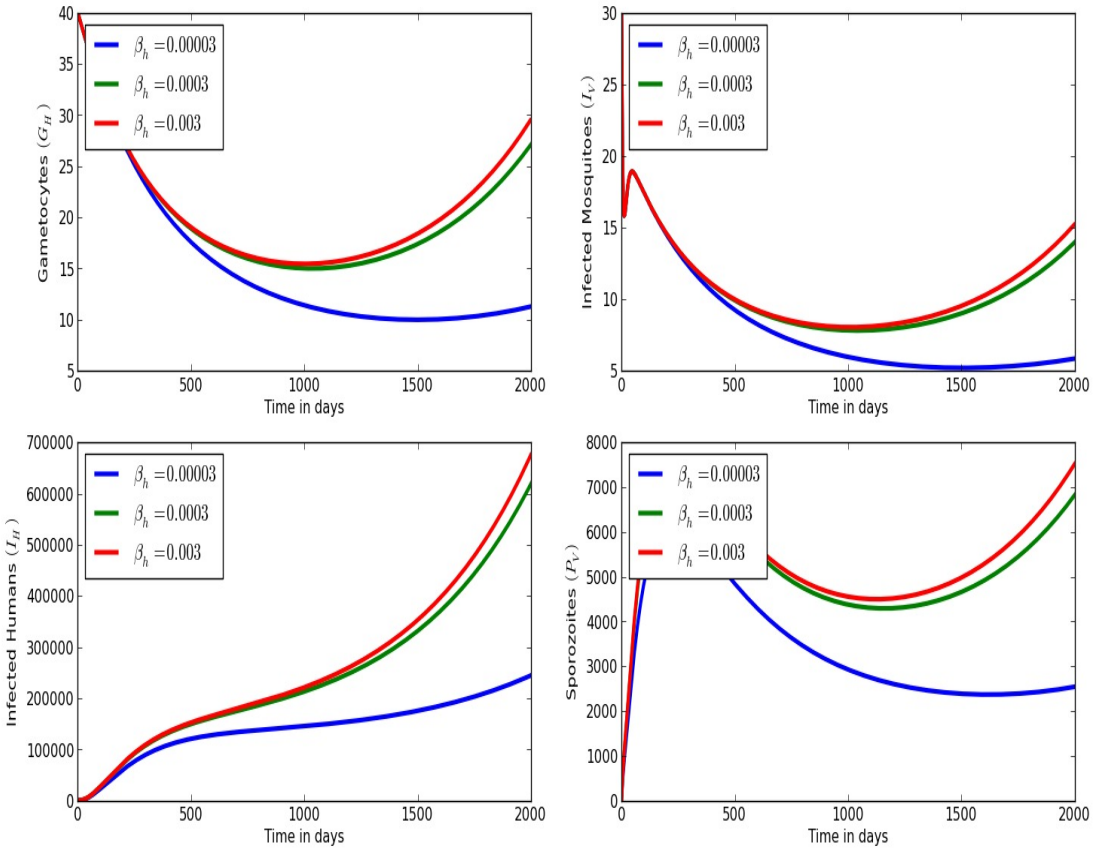

Figure 2.5: Graphs showing changes in (a) community gametocyte load (G_H), (b) population of infected mosquitoes I_V, (c) population of infected humans I_H, and (d): community sporozoite load P_V for different values of infection rate of erythrocytes by free merozoites in the blood stream β_h: $\beta_h = 0.0083$, $\beta_h = 0.0625$, and $\beta_h = 0.76$.

Figure 2.5 also shows variations in (a) community gametocyte load (G_H), (b) population of infected mosquitoes I_V, (c) population of infected humans I_H, and (d): community sporozoite load P_V for different values of infection rate of erythrocytes by free merozoites in the blood stream β_h: $\beta_h = 0.0083$, $\beta_h = 0.0625$, and $\beta_h = 0.76$. The results show that an increase in the average rate of infection rate of merozoites at individual level has important public health consequences at community level in that there is a proportional increase in the community gametocyte load, population of infected mosquitoes I_V, population of infected humans I_H and community sporozoite load at between-host scale.

Overall, the numerical results presented in this chapter are proof-of-principle about the public health benefits of treatment as prevention (TasP) as an important preventive health intervention

for malaria. In general, the use TasP as a preventive health intervention for any infectious disease is based on the fact that the transmission of an infectious disease system can be prevented by treating infected individuals so that they become less likely to transmit the infection to others. However, for malaria, since treatment operates at within-host scale while other malaria preventive interventions such as long-lasting insecticide treated nets operate at between-host scale, mathematical models that link the within-host scale and the between-host scale can be useful in evaluating the comparative effectiveness of malaria health interventions that operate at different scale domains of this infectious disease system. In the chapter that follows we use the multi-scale model system (2.2.9) to evaluate the comparative effectiveness of two malaria health interventions (artemisinin-based combination therapy and long-lasting insecticide treated nets).

2.4 Summary

The major innovation in this chapter is the establishment of an infectious disease modelling science base for directly transmitted vector-borne diseases which is comparable to an existing modelling science base for environmentally transmitted vector-borne diseases where pathogen load in the environment is explicitly incorporated into the model. We achieved this by assuming that individual mosquitoes and humans are small homogeneous and unevenly distributed habitats for malaria parasites in the community. Therefore, the multi-scale model presented in this chapter describes the mechanics of malaria transmission in a community in terms of the complete parasite life cycle. This modelling framework can be found useful as a global malaria control and elimination infrastructure and its future research. It more accurately describes the malaria transmission cycle including malaria infections in humans and mosquitoes. Current modelling frameworks based on compartmentalizing humans and mosquitoes into SIRS and SI or SEIRS and SEI are based on addressing a complicated question about which mosquito infects which human and which human infects which mosquito in a particular community but the new modelling framework presented in this study is based on addressing a more simpler question about how often are humans and mosquitoes infected in a particular community. Data on which mosquito infects which human and which human infects which mosquito are difficult to obtain. On the other hand, there is considerable data available on the effects of sporozoites, merozoites and gametocytes within infected humans and mosquitoes and the resulting responses of the human immune system [234–240, 242–249], and including data on the distribution of malaria within human and moquito populations (for example, the total number of infections and the rates of new infections).

Chapter 3

Using multi-scale Modelling To Guide Malaria Control and Elimination

3.1 Introduction

In this chapter, we extend the baseline multi-scale model (2.2.9) to incorporate two malaria health interventions: (i) artemisinin-based combination therapy (ACT) and (ii) long-lasting insecticide treated nets (LLTNs). ACT and its semi-synthetic derivatives are a group of drugs used against plasmodium falciparum malaria. Treatments containing an artemisinin derivative are now standard treatment worldwide for plasmodium falciparum malaria [1]. We then use the multi-scale model that incorporates the two malaria health interventions (ACT and LLTNs) to evaluate the comparative effectiveness of these two health interventions. However, ACT and LLTNs are complex malaria health interventions. We define complex health interventions as 'health interventions which are build up from a number of components, which may act independently and inter-dependently' [218]. This makes it hard to determine which component or combination of components has a higher comparative effectiveness. LLTNs have three components which are: (i) killing of mosquitoes effect of LLTNs, (ii) repelling of mosquitoes effect of LLTNs, and (iii) protection of host from mosquito bite effect of LLTNs. In this study ACT is assumed to have two components which are: (i) killing of gametocytes effect of ACT and (ii) killing of merozoites effect of ACT. In addition, these two malaria health interventions (ACT and LLTNs), operate at different scale domains of the malaria disease system with LLNTs operating at between-host

scale while ACT operates at within-host scale. This makes it difficult to use single scale models to evaluate the effectiveness of these interventions because this results in mismatch between the scale at which the interventions operate and the scale at which decisions on them are made. Assuming the use of the baseline multi-scale model system (2.2.9) to evaluate the effectiveness of the two malaria health interventions (ACT and LLTNs), then the parameters of the baseline multi-scale model system (2.2.9) are modified as follows.

i. *Long-lasting insecticide-treated nets (LLTN)*: Typically nets are assumed to have three effects [227]. Firstly, nets directly kill mosquitoes that lands on them. This has the net effect of increasing the natural death rate of mosquitoes so that that if nets have kill efficacy of k, then μ_V is modified so that $\mu_V \rightarrow (1+k)\mu_V$. Secondly, nets have a mosquito repellency effect which results in a longer gonotrophic cycle and possible diversion to a non-human blood host. The implication of this intervention is that if nets have repellency efficacy of r, then β_V and β_H are modified to become $\beta_V \rightarrow (1-r)\beta_V$ and $\beta_H \rightarrow (1-r)\beta_H$. Thirdly, nets have a direct protective effect for individuals sleeping under them. So if nets have an assumed protective efficacy on humans of p, then β_V and β_H are modified to become $\beta_V \rightarrow (1-p)\beta_V$ and $\beta_H \rightarrow (1-p)\beta_H$.

ii *Use ACT as first-line treatment*: If during the control phase effective treatment is given to all those identified with malaria infection and suppose that the killing efficacy on gametocyte is g and the kill efficacy on merozoite is m, then α_m is modified so that $\alpha_m \rightarrow (1+m)\alpha_m$, and μ_h is modified to become $\mu_h \rightarrow (1+g)\mu_h$.

A summary of the modifications of the multi-scale model given by (2.2.9) due to effects of the two malaria health interventions (Long-lasting insecticide-treated nets (LLTNs) and use ACT as first-line treatment) is given in Table 3.1.

SL.No.	Health Intervention	Mechanism of Intervention action	Modelling effect of intervention
1.	Killing of mosquitoes effect of LLTNs	Increases natural death rate of mosquitoes μ_V	$\mu_V \to \mu_V(1+k)$
2.	Repelling of mosquitoes effect of LLTNs	Decreases malaria transmission rates β_V and β_H	$\beta_V \to \beta_V(1-r)$ and $\beta_H \to \beta_H(1-r)$
3.	Protection of host from mosquito bite effect of LLTNs	Decreases malaria transmission rates β_V and β_H	$\beta_V \to \beta_V(1-p)$ and $\beta_H \to \beta_H(1-p)$
4.	Killing of merozoites effect of ACT	Increases death rate of merozoites μ_m	$\mu_m \to \mu_m(1+m)$
5.	Killing of gametocytes effect of ACT	Increases gametocytes death rate within infected humans μ_h	$\mu_h \to \mu_h(1+g)$
6.	Overall ACT emergent effect	Decreases disease induced death rate δ_H	$\delta_H \to \delta_H(1-\rho)$
7.	Overall ACT emergent effect	Increases patient's recovery rate γ_H	$\gamma_H \to \gamma_H(1+\phi)$

Table 3.1: Summary of the actions of the components of the two malaria health interventions on disease dynamics.

Taking into account all these modifications, the multi-scale model that incorporates the effects of the two malaria health interventions (ACT and LLTNs) becomes

$$
\begin{cases}
\dfrac{dS_H(t)}{dt} = \Lambda_H - \lambda_{VE}.S_H - \mu_H S_H + \gamma_H(1+\phi)I_H, \\
\dfrac{dI_H(t)}{dt} = \lambda_{VE}.S_H - \Big[\mu_H + \delta_H(1-\rho) + \gamma_H(1+\phi)\Big]I_H, \\
\dfrac{dP_V(t)}{dt} = N_v\alpha_v I_V - \alpha_V P_V, \\
\dfrac{dS_V(t)}{dt} = \Lambda_V - \lambda_{HE}.S_V - \mu_V(1+k)S_V, \\
\dfrac{dI_V(t)}{dt} = \lambda_{HE}.S_V - \Big[\mu_V(1+k) + \delta_V\Big]I_V, \\
\dfrac{dG_H(t)}{dt} = N_h\alpha_h I_H - \alpha_H G_H,
\end{cases} \tag{3.1.1}
$$

where

$$
\lambda_{HE} = \frac{\beta_V(1-r)(1-p)P_V(t)}{P_0 + P_V(t)} \text{ and } \lambda_{VE} = \frac{\beta_H(1-r)(1-p)G_H(t)}{G_0 + G_H(t)}. \tag{3.1.2}
$$

The multi-scale model given by (3.1.1) has a malaria control induced disease-free equilibrium given by

$$
E^1 = (S_H^1, I_H^1, G_H^1, S_V^1, I_V^1, P_V^1) = \Big(\frac{\Lambda_H}{\mu_H}, 0, 0, \frac{\Lambda_V}{\mu_V}, 0, 0, \Big). \tag{3.1.3}
$$

In addition, the multi-scale model given by (3.1.1) has a malaria control induced endemic equilibrium equilibrium given by

$$
\overline{E} = \Big(\overline{S_H}, \overline{I_H}, \overline{S_V}, \overline{I_V}, \overline{P_V}, \overline{G_H}\Big), \tag{3.1.4}
$$

where,

$$\overline{E} = \begin{cases} \overline{I_H} = \dfrac{\overline{\lambda_{VE}}.\overline{S_H}}{\left[\mu_H + \gamma_H(1+\phi) + \delta_H(1+\rho)\right]}, \\ \overline{S_H} = \dfrac{\Lambda_H + \gamma_H(1+\phi)\overline{I_H}}{(\mu_H + \overline{\lambda_{VE}})}, \\ \overline{G_H} = \dfrac{N_e\alpha_h\overline{I_H}}{\alpha_H}, \\ \overline{I_V} = \dfrac{\overline{\lambda_{VE}}.\overline{S_V}}{\left[\mu_V(1+k) + \delta_V\right]}, \\ \overline{S_V} = \dfrac{\Lambda_V}{\left[\overline{\lambda_{HE}} + \mu_V(1+k)\right]}, \\ \overline{P_V} = \dfrac{N_v\alpha_v\overline{I_V}}{\alpha_V}. \end{cases} \tag{3.1.5}$$

The stability and existence of the malaria induced elimination state E^1 and the malaria control induced endemic state $\overline{E}$ derived from the multi-scale model (3.1.1) can be established in the same way as for the baseline malaria multi-scale model (2.2.9). By modifying appropriate parameters from expressions derived from the baseline multi-scale model (2.2.9) it can be shown that the explicit values of the effective reproductive number $\mathcal{R}_E$, the malaria control induced endemic value of the community gametocyte load $\overline{G_H}$ and the malaria control induced endemic value of the community sporozoite load $\overline{P_V}$ derived from the multi-scale model (3.1.1) are given by

$$\begin{cases} \overline{G_H} = \dfrac{(\mathcal{R}_E^2 - 1)\mu_V(1+k)G_0\Lambda_H\beta_V(1-r)(1-p)Q_H}{\Lambda_V\beta_H(1-r)(1-p)\mathcal{R}_{HE}[Q_D + \mu_H Q_H] + \Lambda_H\beta_V(1-r)(1-p)Q_V Q_H}, \\ \overline{P_V} = \dfrac{(\mathcal{R}_E^2 - 1)\mu_H P_0\Lambda_V\beta_H(1-r)(1-p)Q_H}{\Lambda_H\beta_V(1-r)(1-p)\mathcal{R}_{VE}Q_V Q_H + \Lambda_V\beta_H(1-r)(1-p)[Q_D + \mu_H Q_H]}, \\ \mathcal{R}_E = \dfrac{N_e\alpha_h\Lambda_V\beta_H(1-r)(1-p)}{\mu_V(1+k)Q_H\alpha_H G_0}.\dfrac{N_v\alpha_v\Lambda_H\beta_V(1-r)(1-p)}{\mu_H[\mu_V(1+k)+\delta_V]\alpha_V P_0}. \end{cases} \tag{3.1.6}$$

where

$$\begin{cases} Q_H = \Big[\mu_H + \delta_H(1-\rho) + \gamma_H(1+\phi)\Big], \\ Q_D = \beta_V(1-r)(1-p)\Big[\mu_H + \delta_H(1-\rho)\Big], \\ Q_V = \Big[\mu_V(1+k) + \beta_H(1-r)(1-p)\Big], \\ N_e = \dfrac{\pi\Lambda_h}{[\alpha_h + \mu_h(1+g)]\Re_e}\Big[\Re_e - 1\Big], \\ N_v = \dfrac{\Lambda_v N_k \alpha_k \alpha_z \alpha_s N_g \alpha_g}{2(\alpha_v+\mu_v)(\alpha_k+\mu_k)(\alpha_z+\mu_z)(\alpha_s+\mu_s)(\alpha_g+\mu_g)}. \end{cases} \tag{3.1.7}$$

In the following three subsections, we evaluate the comparative effectiveness of the two malaria health interventions using the multi-scale model (3.1.1). We evaluate the comparative effectiveness of the two malaria health interventions using the proposed three public health measures of malaria disease dynamics which are (i) the basic reproductive number $\mathcal{R}_0$, (ii) the baseline endemic value of the community gametocyte load, $\widetilde{G_H}$ and (iii) the baseline endemic value of the community sporozoite load, $\widetilde{P_V}$. The determination of the comparative effectiveness of the two malaria health interventions is achieved by ranking the percentage (%age) reductions of the three public health public health measures ($\mathcal{R}_0$, $\widetilde{G_H}$, $\widetilde{P_V}$) for malaria transmission. The ranking of the %age reductions of the two public health measures of malaria disease dynamics is from 1 to 18 corresponding to the different combinations of the two malaria interventions and the combinations of their components. In the ranking, 1 corresponds to the lowest comparative effectiveness and 18 corresponds to the highest comparative effectiveness. The %age reductions of the three public health measures of malaria disease dynamics ($\mathcal{R}_0$, $\widetilde{G_H}$, $\widetilde{P_V}$) are calculated using the expressions given by (3.1.6) as follows.

$$\begin{cases} 1.\ \%age\ \text{reduction of}\ \mathcal{R}_0 = \Big[\dfrac{\mathcal{R}_0 - \mathcal{R}_E}{\mathcal{R}_0}\Big] \times 100, \\ 2.\ \%age\ \text{reduction of}\ \widetilde{G_H} = \Big[\dfrac{\widetilde{G_H} - \overline{G_H}}{\widetilde{G_H}}\Big] \times 100, \\ 3.\ \%age\ \text{reduction of}\ \widetilde{P_V} = \Big[\dfrac{\widetilde{P_V} - \overline{P_V}}{\widetilde{P_V}}\Big] \times 100, \end{cases} \tag{3.1.8}$$

where $\mathcal{R}_E$, $\overline{G_H}$ and $\overline{P_V}$ are the effective reproductive number, the malaria control induced endemic value of the community gametocyte load and the malaria control induced endemic value of the community sporozoite load respectively given by (3.1.6). The expressions in (3.1.8) are used to calculate the comparative effectiveness at low efficacy (CEL) which is taken to be 0.3, comparative effectiveness at medium efficacy (CEM) which is taken to be 0.6, and comparative effectiveness at high efficacy (CEH) which is taken to be 0.9 using each of the three public health measures of malaria disease dynamics ($\mathcal{R}_0$, $\widetilde{G_H}$, $\widetilde{P_V}$). The results of the comparative effectiveness of the two malaria health interventions and their respective components are given in the three sections that follow.

3.2 Evaluation of the comparative effectiveness of malaria health interventions using the basic reproductive number as the indicator of intervention effectiveness

In this section, we evaluate the comparative effectiveness of the two malaria health interventions (LLTNs and ACT) using the malaria basic reproductive number as the indicator of intervention effectiveness using efficacy data. Since a reproductive number characterizes disease transmission at the start of the epidemic as opposed to the situation when the disease has spread in the population and is at endemic levels, the effectiveness values obtained using the reproductive number characterize the performance of the interventions at the start of the epidemic. The effectiveness values of the two malaria interventions are obtained by calculating the percentage (%age) reduction of the basic reproductive number due to the use of the two malaria interventions. Table 3.2 shows the results of the evaluation of the comparative effectiveness of the two malaria health interventions and their associated components using the percentage reduction in the basic reproductive number as the indicator of intervention effectiveness.

No.	**Components of interventions used**	**%age reduction of $\mathcal{R}_0$ at low efficacy of 0.3**	**CEL**	**%age reduction of $\mathcal{R}_0$ at medium efficacy of 0.6**	**CEM**	**%age reduction of $\mathcal{R}_0$ at high efficacy of 0.9**	**CEH**
1	$\mathcal{R}_0$	0.00	1	0.00	1	0.00	1
2	$\mathcal{R}_{Ek}$	12.29	2	20.94	2	27.45	2
3	$\mathcal{R}_{Er}$	30.00	6	60.00	6	90.00	7
4	$\mathcal{R}_{Ep}$	30.00	6	60.00	6	90.00	7
5	$\mathcal{R}_{Em}$	16.74	3	37.65	3	69.40	3
6	$\mathcal{R}_{Eg}$	26.65	4	50.35	4	77.59	4
7	$\mathcal{R}_{Ekr}$	51.00	15	68.38	9	92.75	9
8	$\mathcal{R}_{Ekp}$	38.61	9	68.38	9	92.75	9
9	$\mathcal{R}_{Erp}$	51.00	15	84.00	16	99.00	16
10	$\mathcal{R}_{Emp}$	41.99	11	75.29	12	96.95	12
11	$\mathcal{R}_{Ekm}$	27.32	5	51.17	5	77.90	5
12	$\mathcal{R}_{Erm}$	41.99	11	75.29	12	96.95	12
13	$\mathcal{R}_{Ekg}$	35.97	8	61.11	8	83.82	6
14	$\mathcal{R}_{Erg}$	48.90	13	80.32	14	97.77	14
15	$\mathcal{R}_{Emg}$	38.92	10	68.89	11	92.95	11
16	$\mathcal{R}_{Epg}$	48.90	13	80.32	14	97.77	14
17	$\mathcal{R}_{Ekrp}$	57.02	17	87.35	17	99.2	17
18	$\mathcal{R}_{Ekrpmg}$	73.87	18	96.08	18	99.95	18

Table 3.2: Results of the assessment of comparative effectiveness of malaria interventions using the %age reduction of basic reproductive number ($\mathcal{R}_0$) as the indicator intervention effectiveness when each of the five interventions is assumed to have: (a) low efficacy of 0.30, (b) medium efficacy of 0.60, and (c) high efficacy of 0.90.

From Table 3.2, we deduce the following results:

a. Considering the use of LLTNs as the only malaria health intervention, we note that this intervention has three components which are (i) killing of mosquitoes effect, (ii) repelling of mosquitoes effect, and (iii) protection of host from mosquito bites effect. The results show that mosquito repellency effect and protection of host from mosquito bites effect have the highest but equal comparative effectiveness while the killing of mosquitoes effect has a much lower comparative effectiveness than these two components of LLTNs as a complex malaria health intervention.

b. Considering the use of ACT as the only malaria health intervention, we note that this intervention has two components which are (i) killing of merozoites effect, and (ii) killing of gametocytes effect. The results show that killing of gametocytes effect has a much higher comparative effectiveness than killing of merozoites effect. This is expected because gametocytes are associated with malaria transmission while merozoites (which infect red blood cells) are associated with malaria morbidity and mortality.

c. Comparing the effectiveness of two components at a time of the two malaria health interventions we note the following results.

   i. The combination of repelling of mosquitoes effect and protection of host from mosquito bites effect has the highest comparative effectiveness.

   ii. The combinations of repelling of mosquitoes effect and the killing of gametocytes effect on one side and that of protection of host from mosquito bites effect and the killing of gametocytes effect on the other side have the second highest but equal comparative effectiveness.

   iii. The combinations of repelling of mosquitoes effect and the killing of merozoites effect on one side and that of protection of host from mosquito bites effect and the killing of merozoites effect on the other side have the third highest but equal comparative effectiveness.

   iv. The combination of killing of merozoites effect and killing of gametocytes effect has the fourth comparative effectiveness.

   v. The combinations of repelling of mosquitoes effect and the killing of mosquitoes effect on one side and that of protection of host from mosquito bites effect and the killing of mosquitoes effect on the other side have the fifth highest but equal comparative effectiveness.

   vi. The combination of killing of mosquitoes effect and killing of gametocytes effect has the sixth comparative effectiveness.

   vii. The combination of killing of mosquitoes effect and killing of merozoites effect has the seventh comparative effectiveness.

d. Comparing the effectiveness of ACT and LLTNs, we note just like the case when using community sporozoite load as an indicator of intervention effectiveness, we note that in this case, LLTNs has a much higher comparative effectiveness than ACT.

e. We note that at 90% efficacy of each intervention, the two interventions can potentially eliminate malaria in a particular geographical area/community/country since they result in approximately 100% reduction of basic reproductive number when used in combination.

3.3 Evaluation of the comparative effectiveness of malaria health interventions using community gametocyte load as the indicator of intervention effectiveness

In this section, we again evaluate the comparative effectiveness of the two malaria health interventions (LLTNs and ACT) using the community gametocyte load as the indicator of intervention effectiveness using efficacy data. In the context of malaria control and elimination, community gametocyte load is a measure of the total infectious reservior of humans which we also propose in this chapter as a suitable public health measure for evaluating the overall performance of malaria health interventions targeted at the human host. It can therefore be used to guide malaria control and elimination in a particular geographical area/community/country as (i) an indicator of a community's level of infectiousness and transmission probability of malaria to mosquitoes, (ii) a measure of the effectiveness of malaria interventions targeted at the human host, and (iii) a proximal maker of malaria incidence among humans and their potential to propagate malaria to mosquitoes. Since the community gametocyte load characterizes transmission at epidemic levels as opposed to the situation when the epidemic is in its early stages, the effectiveness values obtained using the community gametocyte load characterize the performance of the interventions when malaria is at endemic levels. The effectiveness values of the two malaria interventions are obtained by calculating the percentage (%age) reduction of the community gametocyte load due to the use of the two malaria interventions. Table 3.3 shows the results of the evaluation of the comparative effectiveness of the two malaria health interventions and their associated components using the percentage reduction in the community gametocyte load as the indicator of intervention effectiveness.

No.	**Components of interventions used**	**%age reduction of $\widetilde{G_H}$ at low efficacy of 0.3**	**CEL**	**%age reduction of $\widetilde{G_H}$ at medium efficacy of 0.6**	**CEM**	**%age reduction of $\widetilde{G_H}$ at high efficacy of 0.9**	**CEH**
1	$\widetilde{G_H}$	0.0000	1	0.0000	1	0.0000	1
2	$\widetilde{G_{Hk}}$	0.0000	2	0.0000	2	0.0000	2
3	$\widetilde{G_{Hr}}$	0.1147	3	0.4004	3	2.3555	3
4	$\widetilde{G_{Hp}}$	0.1147	3	0.4004	3	2.3555	3
5	$\widetilde{G_{Hm}}$	29.3069	12	59.1999	12	89.2631	10
6	$\widetilde{G_{Hg}}$	45.1337	16	74.1268	16	94.2441	14
7	$\widetilde{G_{Hkr}}$	0.2782	6	0.4004	5	2.3556	5
8	$\widetilde{G_{Hkp}}$	0.1147	5	0.4004	5	2.3556	5
9	$\widetilde{G_{Hrp}}$	0.2782	6	1.3877	7	20.9763	7
10	$\widetilde{G_{Hpm}}$	28.6850	10	58.1236	10	89.4465	11
11	$\widetilde{G_{Hkm}}$	28.5999	9	57.9379	9	89.1488	9
12	$\widetilde{G_{Hrm}}$	28.6850	10	58.1236	10	89.4465	11
13	$\widetilde{G_{Hkg}}$	44.5850	13	73.3265	13	94.1829	13
14	$\widetilde{G_{Hrg}}$	44.6511	14	73.4442	14	94.3424	15
15	$\widetilde{G_{Hmg}}$	61.2095	18	89.3306	17	99.4183	17
16	$\widetilde{G_{Hpg}}$	44.6511	14	73.4442	14	94.3424	15
17	$\widetilde{G_{Hkrp}}$	0.2782	8	1.3877	8	20.9816	8
18	$\widetilde{G_{Hkrpmg}}$	60.9332	17	89.3874	18	99.5534	18

Table 3.3: Results of the assessment of comparative effectiveness of malaria interventions using the %age reduction of endemic value of the community gametocyte load ($\widetilde{G_H}$) as the indicator intervention effectiveness when each of the five interventions is assumed to have: (a) low efficacy of 0.30, (b) medium efficacy of 0.60, and (c) high efficacy of 0.90.

From Table 3.3, we deduce the following results.

a. Considering the use of LLTNs as the only malaria health intervention, we note that this intervention has three components which are (i) killing of mosquitoes effect, (ii) repelling of mosquitoes effect, and (iii) protection of host from mosquito bites effect. The results show that mosquito repellency effect and protection of host from mosquito bites effect, have the highest but equal comparative effectiveness while the killing of mosquitoes effect has a much lower comparative effectiveness than these two components of LLTNs as a malaria health intervention.

b. Considering the use of ACT as the only malaria health intervention, we note that this intervention has two components which are (i) killing of merozoites effect, and (ii) killing of gametocytes effect. The results show that killing of gametocytes effect has a much higher comparative effectiveness than killing of merozoites effect. This is expected because gametocytes are associated within malaria transmission while merozoites (which infect red blood cells) are associated with malaria morbidity and mortality.

c. Comparing the effectiveness of two components at a time of the two malaria health interventions we note the following results.

   i. The combination of killing of merozoites effect and killing of gametocytes effect has the highest comparative effectiveness.

   ii. The combinations of repelling of mosquitoes effect and the killing of gametocytes effect on one side and that of protection of host from mosquito bites effect and the killing of gametocytes effect on the other side have the second highest but equal comparative effectiveness.

   iii. The combination of killing of mosquitoes effect and killing of gametocytes effect has the third comparative effectiveness.

   iv. The combinations of repelling of mosquitoes effect and the killing of merozoites effect on one side and that of protection of host from mosquito bites effect and the killing of merozoites effect on the other side have the fourth highest but equal comparative effectiveness.

   v. The combination of killing of mosquitoes effect and killing of merozoites effect has the fifth comparative effectiveness.

   vi. The combination of repelling of mosquitoes effect and protection of host from mosquito bites effect has the sixth comparative effectiveness.

   vii. The combinations of repelling of mosquitoes effect and the killing of mosquitoes effect on one side and that of protection of host from mosquito bites effect and the killing of mosquitoes effect on the other side have the seventh highest but equal comparative effectiveness.

d. Comparing the effectiveness of ACT and LLTNs, we note that unlike the case when using community sporozoite load is used as an indicator of intervention effectiveness, we note that in this case, ACT has a much higher comparative effectiveness than LLTNs.

e. We also note that at 90% efficacy of each intervention, the two interventions can potentially eliminate malaria in a particular geographical area/community/country since they result

in approximately 100% reduction of community gametocyte load when implemented in combination.

3.4 Evaluation of the comparative effectiveness of malaria preventive and treatment interventions using community sporozoite load as the indicator of intervention effectiveness

In this section, we further evaluate the comparative effectiveness of the two malaria preventive and treatment interventions (LLTNs and ACT) using the community sporozoite load as the indicator of intervention effectiveness using efficacy data. Since the community sporozoite load also characterizes transmission at epidemic levels as opposed to the situation when the epidemic is at the initial stages, the effectiveness values obtained using the community sporozoite load also characterize the performance of the interventions when malaria is at endemic levels. The effectiveness values of the two malaria interventions are obtained by calculating the percentage (%age) reduction of the community sporozoite load due to the use of the two malaria interventions. In the context of malaria control and elimination, community sporozoite load is a measure of the total infectious reservoir of mosquitoes which we also propose in this chapter as a suitable public health measure for evaluating the overall performance of malaria preventive and treatment interventions targeted at the mosquito. It can therefore be used to guide malaria control and elimination in a particular geographical area/community/country as (i) an indicator of a community's level of infectiousness and transmission probability of malaria to humans, (ii) a measure of the effectiveness of malaria interventions targeted at the mosquito vector, and (iii) a proximal maker of malaria incidence among mosquitoes and their potential to propagate malaria to humans. Table 3.4 shows the results of the evaluation of the comparative effectiveness of the malaria preventive and treatment interventions and their associated components using the percentage reduction in the community sporozoite load as the indicator of intervention effectiveness.

No.	**Components of interventions used**	**%age reduction of $\widetilde{P_V}$ at low efficacy of 0.3**	**CEL**	**%age reduction of $\widetilde{P_V}$ at medium efficacy of 0.6**	**CEM**	**%age reduction of $\widetilde{P_V}$ at high efficacy of 0.9**	**CEH**
1	$\widetilde{P_V}$	0.0000	1	0.0000	1	0.0000	1
2	$\widetilde{P_{Vk}}$	7.1890	5	10.4095	5	14.8419	5
3	$\widetilde{P_{Vr}}$	11.4315	8	22.5051	8	63.5363	8
4	$\widetilde{P_{Vp}}$	11.4315	8	22.5051	8	63.5363	8
5	$\widetilde{P_{Vm}}$	0.0045	2	0.0097	2	0.0574	2
6	$\widetilde{P_{Vg}}$	0.0089	3	0.0193	3	0.1130	3
7	$\widetilde{P_{Vkr}}$	20.5188	14	36.7429	14	77.7038	14
8	$\widetilde{P_{Vkp}}$	20.5188	14	36.7429	14	77.7038	14
9	$\widetilde{P_{Vrp}}$	25.6055	16	50.4073	16	95.0418	16
10	$\widetilde{P_{Vpm}}$	11.4372	10	22.5194	10	63.6138	10
11	$\widetilde{P_{Vkm}}$	7.1943	6	10.4217	6	14.9200	6
12	$\widetilde{P_{Vrm}}$	11.4372	10	22.5194	10	63.6138	10
13	$\widetilde{P_{Vkg}}$	7.1995	7	10.4338	7	14.9957	7
14	$\widetilde{P_{Vrg}}$	11.4429	12	22.5337	12	63.6886	12
15	$\widetilde{P_{Vmg}}$	0.0191	4	0.0578	4	1.1672	4
16	$\widetilde{P_{Vpg}}$	11.4429	12	22.5337	12	63.6886	12
17	$\widetilde{P_{Vkrp}}$	35.8698	17	63.5371	17	97.3401	17
18	$\widetilde{P_{Vkrpmg}}$	35.9001	18	63.6142	18	97.5320	18

Table 3.4: Results of the assessment of comparative effectiveness of malaria interventions using %age reduction of the endemic value of the community sporozoite load ($\widetilde{P_V}$) as the indicator intervention effectiveness when each of the five interventions is assumed to have: (a) low efficacy of 0.30, (b) medium efficacy of 0.60, and (c) high efficacy of 0.90.

From Table 3.4, we deduce the following results:

a. Considering the use of LLTNs as the only malaria preventive and treatment intervention, we note, as previously indicated, that this intervention has three components which are (i) killing of mosquitoes effect, (ii) repelling of mosquitoes effect, and (iii) protection of host from mosquito bites effect. The results of evaluation of the comparative effectiveness of these three components of LLTNs are the same as those obtained when using community gametocyte load in that mosquito repellency effect and protection of host from mosquito bites effect, have the highest but equal comparative effectiveness while the killing

of mosquitoes effect has a much lower comparative effectiveness than these two components of LLTNs as a complex malaria preventive intervention. However, although ranking of the comparative effectiveness of these components using the two different indicators of effectiveness (community sporozoite load and community gametocyte load) is the same, the results show that the %age reductions of community sporozoite load at the different efficacy values are much higher than for community gametocyte load. This implies that these components of LLTNs as a complex malaria intervention are more effectiveness as interventions towards the mosquito vector than towards the human host.

b. Considering the use of ACT as the only malaria treatment intervention, we again note that this intervention has two components which are (i) killing of merozoites effect, and (ii) killing of gametocytes effect. The results of evaluation of the comparative effectiveness of these two components of ACT are also the same as those obtained when using community gametocyte load as the indicator of intervention effectiveness in that killing of gametocytes effect has a much higher comparative effectiveness than killing of merozoites effect. This is still expected because gametocytes are associated within malaria transmission while merozoites (which infect red blood cells) are associated with malaria morbidity and mortality. However, although ranking of the comparative effectiveness of these components ACT using the two different indicators of effectiveness (community sporozoite load and community gametocyte load) is the same, the results show that the %age reductions at the different efficacy values are much higher for community gametocyte load than for community sporozoite load. This also implies that ACT is more effective as an intervention towards the human host than towards the mosquito vector.

c. Comparing the effectiveness of two components at a time of the two malaria preventive and treatment interventions, we note the following results.

   i. Like in the case of using the basic reproductive number as the indicator of intervention effectiveness, the combination of repelling of mosquitoes effect and protection of host from mosquito bites effect has the highest comparative effectiveness.

   ii. The combinations of repelling of mosquitoes effect and the killing of mosquitoes effect on one side and that of protection of host from mosquito bites effect and the killing of mosquitoes effect on the other side have the second highest but equal comparative effectiveness.

   iii. The combinations of repelling of mosquitoes effect and the killing of gametocytes effect on one side and that of protection of host from mosquito bites effect and the killing of gametocytes effect on the other side have the third highest but equal comparative effectiveness.

iv. The combinations of repelling of mosquitoes effect and the killing of merozoites effect on one side and that of protection of host from mosquito bites effect and the killing of merozoites effect on the other side have the fourth highest but equal comparative effectiveness.

v. The combination of killing of mosquitoes effect and killing of gametocytes effect has the fifth comparative effectiveness.

vi. The combination of killing of mosquitoes effect and killing of merozoites effect has the sixth comparative effectiveness.

vii. The combination of killing of merozoites effect and killing of gametocytes effect has the lowest comparative effectiveness.

d. Comparing the effectiveness of ACT and LLTNs, we note unlike the case when using community gametocyte load as an indicator of intervention effectiveness, we note that in this case, LLTNs has a much higher comparative effectiveness than ACT.

e. We also note that at 90% efficacy of each intervention, the two interventions can potentially eliminate malaria in a particular geographical area/community/country since they result in approximately 100% reduction of community sporozoite load when implemented together as a combination.

3.5 Summary

The multi-scale model developed in this chapter enabled us to compare the effectiveness of malaria preventive and treatment interventions in terms of three different viewpoints: (i) in terms of the interventions targeted at the human host using community gametocyte as the indicator of intervention effectiveness, (ii) in terms of the interventions targeted at the mosquito vector using community sporozoite as the indicator of intervention effectiveness, and (iii) in terms of impact of interventions on overall disease dynamics using disease reproductive number as the indicator of intervention effectiveness. The results show that of the two components of ACT (killing of merozoites effect, and killing of gametocytes effect), treatments that kill gametocytes at individual level have a higher comparative effectiveness than those that kill merozoites at population/-community level. Furthermore, the results also show that among the three components of LLTNs which are targeted at the mosquito vector (killing of mosquitoes effect, repelling of mosquitoes effect, and protection of host from mosquito bites effect), repellency effect of LLTNs and protective effect of LLTNs have a higher comparative effectiveness than the killing of mosquito effect. This study also provided with proof-of-principle about the public health benefits of treatment as

prevention (TasP) as an important preventive intervention for malaria. In general, the use TasP as a preventive intervention for any infectious disease is based on the fact that the transmission of an infectious disease system can be prevented by treating infected individuals so that they become less likely to transmit the infection to others. However, for malaria, since treatment operates at within-host scale while other malaria interventions such as long-lasting insecticide treated nets operate at between-host scale, mathematical models that link the within-host scale and the between-host scale can be useful in evaluating the comparative effectiveness of malaria preventive and treatment interventions that operate at different scale domains of this infectious disease system. Although, the focus of this study was on one of the most important vector-borne disease - malaria, the framework is robust enough to be applicable to many other vector-borne diseases.

Chapter 4

Basic Schistosomiasis mathematical model with interventions

4.1 Introduction

Schistomiasis, which is well known as bilharzia, is a parasitic water-borne infection caused by digenetic trematodes that belong to the family schistosomatoidae. Five species of schistosomes are involved in human infection. The three principal agents are schistosoma mansoni and S. japonicum which are responsible for intestinal schistosomiasis and S. haematobium, the aetiologic agent of urinary schistosomiasis. The other two species responsible for intestinal disease though with low frequency are S.intercalatum and S. mekongi. It is transmitted through contact with contaminated bulk water sources such as lakes, ponds, rivers and dams. It is diagnosed through the detection of parasite eggs in stool or urine. Schistosomiasis is easily transmitted to those who are frequently in contact with contaminated freshwater, especially children who wade or play in water and women conducting domestic chores. It has been estimated that schistosomiasis and geohelmiths represent more than 40% of the global burden caused by all tropical diseases, excluding malaria [116]. There are more than 650 million people living in endemic areas, and about 200 million people infected worldwide [118]. Schistosomiasis transmission has been documented in 77 countries. The most severely affected countries in Africa are Angola, Central African Republic, Mozambique, Nigeria, Senegal, Sudan, the United Republic of Tanzania and Zambia [140]. However, those at risk of infection are in 52 countries. It is estimated that

at least 90% of those requiring treatment for schistosomiasis live in Africa. More than $200\ 000$ deaths annually are due to schistosomiasis [117].

The life cycle of the schistosome is complex and begins when schistosome eggs are released into freshwater through faeces and urine and consists of an obligatory alternation of sexual and asexual generations [120]. Schistosome eggs produced by the sexual stage leave people via urine or faeces, reach freshwater, shed their shells and hatch a ciliated free-swimming larva called a miracidium [130]. More than 50% of the eggs do not make it into the faecal or urinary stream but rather, they become entrapped in adjacent tissues or get carried away by the circulatory or lymphatic system and can become lodged in virtually any organ in the body [131]. A miracidium that locates an appropriate species and genotype snail, penetrates and infects it, multiplies asexually through two larval stages into thousands of cercariae that escape the snail and live in water. They swim until they encounter a skin of suitable warmth and smell, and infect humans by direct penetration of the skin. Once the cercariae penetrate the skin, they lose their tails and differentiate into larval forms called schistosomulae. A schistosomulum spends several days in the skin before exiting via blood vessels traversing to the lung, where it undergoes further developmental changes. It then migrates via the systematic circulation to the liver where it settles, reaches sexual maturity and pairs. Only those worm pairs that reach the portal system of the liver mature into adults. Subsequently, worm pairs migrate by the bloodstream to their definitive location; S. mansoni and S. japonicum to the small and large intestines and S. haematobium to the bladder and rectal veins [120].

Symptoms of schistosomiasis are caused by the body's reaction to the worm's eggs, not by the worms themselves. Intestinal schistosomiasis can result in abdominal pain, diarrhoea, and blood in the stool. Liver enlargement is common in advanced cases of infected individuals, and is frequently associated with an accumulation of fluid in the peritoneal cavity and hypertension of the abdominal blood vessels. In such cases, there may also be an enlargement of the spleen. Fibrosis of the bladder and ureter, and kidney damage are common findings in advanced cases [117].

Despite the success of control programmes, Schistosomiasis remains a serious public health problem in the world [132]. Over 230 million people require treatment for schistosomiasis every year. The number of people treated for schistosomiasis rose from 12.4 million in 2006 to 33.5 million in 2010 [140]. In this study, we take into account both man-made and natural control mechanisms. The natural control mechanisms include climate change and extreme weather changes such as heat waves, drought and floods of which we can not predict their occurrence. The man-made control measures include improved sanitation, chemotherapy, molluscicides and

health education campaigns. We take into account natural control mechanisms because it is possible that the disease vanish due to extreme weather changes. While man-made control measures are always intended to reduce schistosomiasis transmission, natural events may results in either on the desired effect of controlling schistosomiasis transmission (in which case we refer to these natural events as natural control measures) or the natural events may have the undesirable effect of amplifying transmission of schistosomiasis in the community. In this chapter, we focus on investigating the situation where natural events (herein referred to as natural control measures) are complementary to man-made control measures in curbing transmission of schistosomiasis. Natural control measures such as extreme heat result in drying of some natural water sources killing the snails which inhibit these environments. Equally other natural control measures such as extreme cold hinder the growth and reproductive capacity of snail population while land use change from agricultural activities to urban settlement will result in destruction of water sources where the snails habitat. Below we outline both man-made and natural control mechanisms.

1. *Climate change:* Climate change may alter geographical suitability of freshwater bodies for hosting parasite and snail populations. In [138], agent-based model of the temperature-sensitive stages of the schistosoma mansoni and intermediate host snail lifestyle is studied. Maps were produced showing predicted changes over the next 20 to 50 years. Temperatures are likely to become suitable for increased schistosomiasis transmission over much of Eastern Africa. This is likely to reduce the impact of control and elimination programmes.

2. *Land use:* The prevalence of infection in relation to land use and cover showed that, of 218 positive schools in the States, 140 schools were in regions with intensive small-scale agricultural practices, in a similar study by Okwori, he found fishermen and farmers mostly affected by schistosomiasis haematobium in Toto LGA of Nasarawa State, Nigeria [141]. This confirms that infection can only be transmitted where people engage in occupations that bring them in contact with snail populations.

3. *Extreme weather changes:* Extreme weather changes include heat waves, drought and floods. These changes have a great impact on schistosomiasis transmission though capturing these events within dynamical models will be challenging due to complexity in predicting their occurrence. Heat waves could potentially increase the transmission of schsitosomiasis and incidence of schistosomiasis especially in colder areas, resulting in outbreaks occurring in areas that normally experience little transmission [142]. Droughts of a sufficient length and severity may even lead to temporary or permanent elimination of a snail population from a site [142]. This is currently marginal for snail survival. Flooding may play a large role in determining the actual range of schistosomiasis, as opposed to its potential range, over coming decades [142]. Habitats can be made unsuitable for snails to

exist by alternate flooding and drying of water channels, covering and lining of canals and filling in of marshy areas [146].

4. *Treatment (Chemotherapy):* In [137], it was shown that chemotherapy plays an important role in the control of schistosomiasis, like in all other helminthic diseases. Reduction of morbidity after treatment has now been validated with metrofonare, oxamniquine and praziquantel [137]. In [143], it was found that when the average number of eggs before treatment was 3486, it dropped by 543 eggs per gram of tissue after treatment. Treating infected humans do not stop transmission of the parasite, which occurs when human sewage contaminates local water bodies and parasite eggs infect intermediate host snails. Treatment only reduces the worm burden as a result of reduction in the eggs production by infected individuals.

5. *Molluscicides:* In the past decades many schistosomiasis control programmes in Ghana, Madagascar, Zimbabwe, Brazil and elsewhere, have shown that vector-control by molluscicides, either on its own or in combination with other control strategies such as chemotherapy, environmental measures, health education etc. can be a rapid and efficient means of eradicating the spread of schistosomiasis. In 1965, the World Health Organisation supported the preparation and publication of screening and evaluation of molluscicides guidelines [136]. The efficacy of snail control can be enhanced if coupled with other control strategies [136]. Estimates from the aggregated studies indicate that vector-control alone typically reduced new infections by 64% and local prevalence declined over a period of years [144].

6. *Sanitation:* Sanitation is often considered as too expensive, but it is known what proportion it would make up compared with sums spent on classical measures for the control of schistosomiasis [145]. In [134], it was found that a $10-20\%$ reduction in the number of people with schistosomiasis might be achieved as a result of providing safe public water supplies. Nevertheless, improvement of the water supply continues to be neglected as a control measure. The construction and use of toilets should be encouraged to improve the standard of hygiene and to reduce the incidence of other faecal-borne diseases as well [135]. In [145], it was established that the decline in the rates of hospitalization for diarrhoea in infants was associated with improved sanitation and income.

7. *Health education:*Since all control strategies require the knowledge, attitudes and practices of a community, health education remains a high priority in control strategies programmes [133]. Health education approach can be established in all endemic areas drawing to attention personal hygiene and individual's role in controlling the spread of schistosomiasis as a result the will be reduction of human contact with unsafe water bodies.

Due to high risk for schistosomiasis pandemic and large number of deaths associated with schistosomiasis, it is important to increase our understanding of schistosomiasis transmission dynamics. Mathematical models have provided a useful tool to gain insights into the transmission and control of the vector-borne diseases. These insights can potentially guide us to assess the implications and effectiveness of different control mechanisms.

Several recent studies on schistosomiasis modeling have been published since 1965 [123]. Most of those have had little impact on field studies or on the design of disease control because of the little interaction between field workers and mathematicians [119]. MacDonald developed the first mathematical model for the study of schistosomiasis transmission dynamics [123]. The model has shown some potential for understanding the transmission dynamics and control of the disease. However, the model is based on the oversimplified biological assumptions that fail to account for all man-made and natural control mechanisms. The man-made control mechanisms such as chemotherapy, vector-control using mulluscicides, providing endemic communities with proper sanitation such as promoting the use of toilets and health education campaigns.

In [129], the basic schistosomiasis model which is an IS model was developed to represent the interaction between the miracidia and the susceptible snail and interaction between the cercariae and human beings. The model can be extended to account for man-made and natural control mechanisms. Our models will be of this kind. These models can be analysed numerically and mathematically.

In [124], the evolution outcomes result from interactions between schistosoma mansoni and its snail and human hosts are investigated mathematically. The model includes two types of snail hosts representing resident and mutant types. It has been found that the evolutionary trajectories of host-parasite interactions can be varied, and at times, counter-intuitive, based on parasite virulence, host resistance, and drug treatment. This model fails to account both human and snail populations. In [121], control problems of a mathematical model for schistosomiasis transmission dynamics were studied. They classified the humans and snails populations as uninfected and infected, and also considered cercariae and miracidia populations. Their model put forward the view that killing snails is the most effective way to control the transmission of schistosomiasis compared to drug treatment, cercariae control and health education. Their model did not include the eggs on the land and in the water and natural control mechanisms.

In [122], age-structured model with multiple strains of schistosome was studied in order to explore the role of drug treatment in the maintenance of a polymorphism of parasite strains that differ in their resistance levels. Moreover, in [18], a deterministic mathematical model was developed in order to study the transmission dynamics of schistosomiasis where cercariae and miracidia dynamics were incorporated. The results in [122] and [129] demonstrated that control

mechanisms that target the transmission of schistosomiasis from snail to human will be more effective in eradicating the spread of the disease than those that block the transmission from human to snail.

In [125], the potential impact of climate change on schistosomiasis transmission is studied in China. It was found that a temperature threshold of 15.40^c for the development of schistoma Japonium within the intermediate host snail and a temperature of 5.80^c at which half the snail sample investigated was in hibernation. Anderson and May introduced models for macroparasite-host interactions when the parasites had direct life-cycles involving only a single host population and one stage of parasites [126]. In [127], a free-living stage of the parasite was considered in the model. Interactions between schistosome infection and molluscan intermediate hosts (snails) were studied [128]. However, these models do not explicitly include snail and human transmission dynamics.

Based on the review, to date there are no mathematical models that take into account both snail and human populations together with man-made and natural control mechanisms. In this study, we investigate the most sensitive epidemiological parameters that have high impact in the spread of schistosomiasis. Furthermore, we introduce men-made and natural control measures based on the most sensitive parameters.

4.2 Basic Schistosomiasis mathematical model formulation

The mathematical model developed in this section is based on monitoring the dynamics of the eight populations at any time t which are susceptible humans $(S_H(t))$ and infected humans $(I_H(t))$ in the behavioural human environment, susceptible snails $(S_V(t))$ and infected snails $(I_V(t))$ in the physical water environment, cercariae $(P_W(t))$, miracidia $(M(t))$, worm eggs $(E_L(t))$, on the physical land environment and eggs on the physical water environment $(E_W(t))$.

The compartmental model in figure (4.1) describes the flow of eight different population classes. For simplicity we let $N_H = S_H + I_H$ be the total human population and $N_V = S_V + I_V$ be the total snail population where S_H denotes the susceptible humans, I_H denotes the infected humans. Similarly, S_V denotes the susceptible snails and I_V denotes the infected snails. The eggs on the land are denoted by E_L and the eggs in the physical water environment are denoted by E_W. The parasites, namely miracidia and cercariae are denoted by M and P_W respectively.

We make the following assumptions for the model:

i. There is no vertical transmission of the disease.

ii. The transmission of the disease in the snail and human populations is only through contact with infective free-living pathogens (miracidia and cercariae) in the physical water environment.

iii. There is no immigration of infectious humans.

iv. Seasonal and weather variations do not affect snail populations and contact patterns.

v. Infected snails do not reproduce due to castration by the miracidia.

vi. The within-host processes of schistosomiasis transmission are represented phenomenologically by parameters N_h (the number of eggs released by each infected human to environment) and N_S (the number of cercariae released into water environment by infected snail).

vii. The human host is assumed to be healthy, has not been previously exposed to the disease and has no immunity to infection.

viii. Infected snails and humans do not recover naturally from the infection or disease.

At any time t, new recruits enter the human and snail populations through birth at constant rates Λ_H and Λ_V respectively. There is a constant natural death rate μ_H and μ_V in the human and snail populations respectively. Infected human hosts have an additional mortality of δ_H. Similarly, infected snails have an additional mortality δ_V. $N_H(t)$ is the total human population and is given by

$$N_H(t) = S_H(t) + I_H(t). \tag{4.2.1}$$

Susceptible individuals acquire schistosomiasis through infection by cercariae in water at rate $\lambda_H(t)$ where

$$\lambda_H(t) = \frac{\beta_H P_W(t)}{P_0 + P_W(t)}, \tag{4.2.2}$$

with β_H being the maximum rate of exposure; P_0 is the half saturation constant of cercariae. From the functional response, we notice that at low parasite densities, contacts are directly proportional to host densities.

$N_V(t)$ is the total snail population and is given by

$$N_V(t) = S_V(t) + I_V(t). \tag{4.2.3}$$

Similarly, susceptible snails acquire schistosomiasis through infection by miracidia in water at rate $\lambda_V(t)$ where

$$\lambda_V(t) = \frac{\beta_V M(t)}{M_0 + M(t)}, \tag{4.2.4}$$

with β_V being the maximum rate of exposure and M_0 is the half saturation constant of miracidia. As in the case of humans, we notice that at low parasite densities, contacts are directly proportional to host densities.

Susceptible human population, S_H gains from the recruitment of individuals at the rate Λ_H through immigration. Susceptible individuals either die due to natural causes at the rate μ_H or acquire schistosomiasis through infection by cercariae in water at the rate λ_H.

The rate of change over time in days of susceptible human population is given by

$$\frac{dS_H}{dt} = \Lambda_H - \lambda_H S_H - \mu_H S_H. \tag{4.2.5}$$

Infected humans population is generated from susceptible individuals who have acquired schistosomiasis through infection by cercairae in water at the rate λ_H. They either die naturally or due the disease at the rates, μ_H and δ_H respectively. Infected individuals exit this compartment through production of eggs per infected individual, N_h and rate at which infected individual becomes eggs producing, γ_h. The total number of eggs produced at the population level is modelled then by $N_h\gamma_h I_H$. The change in the infected human population over time in days is given by

$$\frac{dI_H}{dt} = \lambda_H S_H - (\mu_H + \delta_H) I_H. \tag{4.2.6}$$

Schistosome eggs population on the land environment , E_L is generated from the total number of eggs produced at the population level on the land are modelled by $N_h\gamma_h I_H$. They either get washed away by running water environment into water physical water environment at the rate α_L or die naturally at the rate μ_L. The rate of change of schistosome eggs population on the land environment over time in days is given by

$$\frac{dE_L}{dt} = N_h\gamma_h I_H - (\mu_L + \alpha_L) E_L. \tag{4.2.7}$$

The population of schistoma eggs, $E_W(t)$, in the physical water environment is generated following inflow of schistoma eggs in running water from the contaminated physical land environment into the physical water environment at a rate α_L. We assume that these eggs die naturally in the physical water environment at a rate μ_W and hatch at a rate α_W releasing miracidia into the physical water environment. The rate of change of schistosome eggs population in the physical water environment over time in days is given by

$$\frac{dE_W}{dt} = \alpha_L E_L - (\mu_W + \alpha_W)E_W. \tag{4.2.8}$$

The population of miracidia, $M(t)$, in the physical water environment is generated through each egg hatching an average of N_W miracidia with eggs hatching at an average rate of α_W so that the total miracidia population in the physical water environment is modelled by $N_W\alpha_W E_W$. We assume that miracidia in the physical water environment die naturally at a rate μ_M. The rate of change of miracidia population over time in days is given by

$$\frac{dM}{dt} = N_W\alpha_W E_W - \mu_M M. \tag{4.2.9}$$

The cercariae population $P_W(t)$, in the physical water environment, is generated through shedding of cercariae by infected snails at an assumed rate of $N_S\gamma_S$ where N_S is the number of cercariae shed by each snail per day and γ_S is the rate at which infected snails become cercariae shedding. The total number of cercariae population in the physical water environment is given by $N_S\gamma_S I_V$. These cercariae are further assumed to have an average life span of $\frac{1}{\mu_S}$. The rate of change of cercariae population is given by

$$\frac{dP_W}{dt} = N_S\gamma_S I_V - \mu_S P_W. \tag{4.2.10}$$

Susceptible snails population gains from new recruits through birth at constant rate Λ_V. There is a constant natural death rate μ_V in the snail population. They acquire schistosomiasis through infection by miracidia in water at the rate $\lambda_V(t)$. The rate of change of susceptible snails over time in days is given by

$$\frac{dS_V}{dt} = \Lambda_V - \lambda_V S_V - \mu_V S_V. \tag{4.2.11}$$

Infected snails population is generated from snails that have acquired schistosomiasis through infection by miracidia in water at the rate $\lambda_V(t)$. They either die naturally or due to the disease at the rates, μ_V and δ_V respectively. The rate of change of infected snails over time in days is given by

$$\frac{dI_V}{dt} = \lambda_V S_V - (\mu_V + \delta_V) I_V. \tag{4.2.12}$$

Putting together the above formulations and assumptions gives the following system of differential equations:

$$\begin{cases} \frac{dS_H}{dt} = \Lambda_H - \lambda_H S_H - \mu_H S_H, \\ \frac{dI_H}{dt} = \lambda_H S_H - (\mu_H + \delta_H) I_H, \\ \frac{dS_V}{dt} = \Lambda_V - \lambda_V S_V - \mu_V S_V, \\ \frac{dI_V}{dt} = \lambda_V S_V - (\mu_V + \delta_V) I_V, \\ \frac{dE_L}{dt} = N_h \gamma_h I_H - (\mu_L + \alpha_L) E_L, \\ \frac{dE_W}{dt} = \alpha_L E_L - (\mu_W + \alpha_W) E_W, \\ \frac{dM}{dt} = N_W \alpha_W E_W - \mu_M M, \\ \frac{dP_W}{dt} = N_S \gamma_S I_V - \mu_S P_W. \end{cases} \tag{4.2.13}$$

The model flow diagram is depicted in Figure (4.1), and the associated parameters are further defined in Table (4.2).

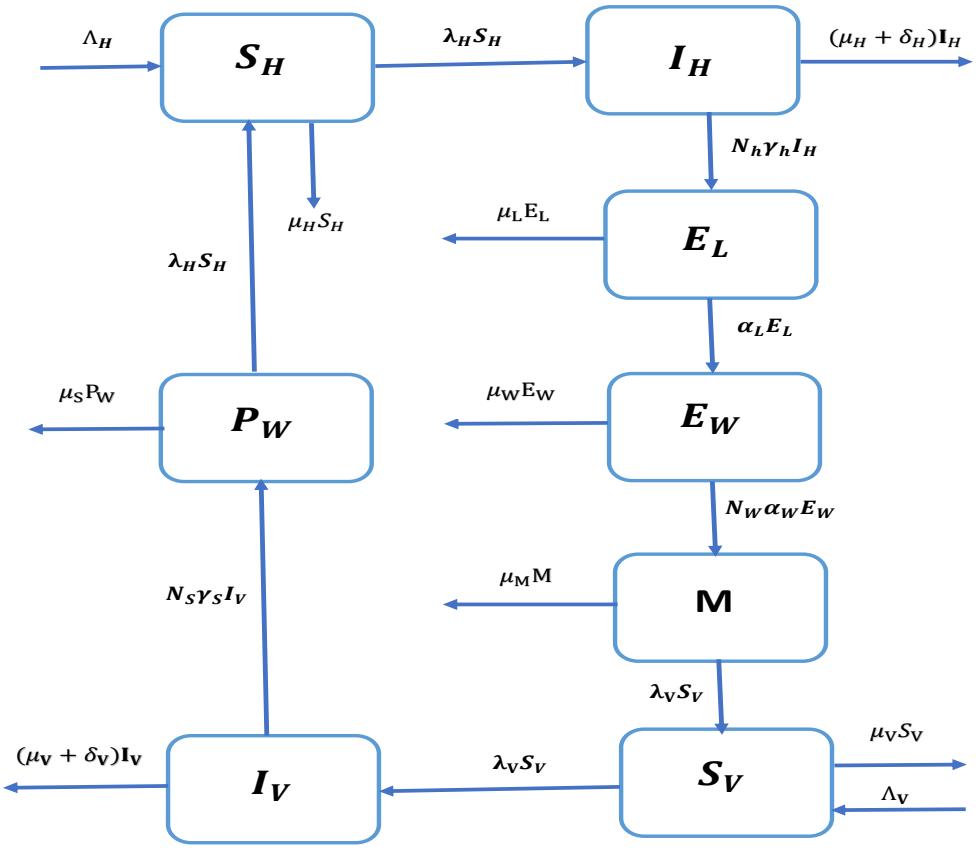

Figure 4.1: A conceptual diagram of the mathematical model of schistosomiasis in human and snail populations.

4.2.1 Feasible Region of Equilibria of the Model

Since the model system (4.2.13) monitors the dynamics of the human and snail populations, it is empirical that all the model variables stay positive at all times. We introduce a region of feasibility, Ω.

$$\begin{aligned}\Omega \;=\; & \{(S_H, I_H, S_V, I_V, E_L, E_W, M, P_W) \in R_+^8 : 0 \leq S_H + I_H \leq M_1, \\ & 0 \leq S_V + I_V \leq M_2,\ 0 \leq E_L \leq M_3,\ 0 \leq E_W \leq M_4,\ 0 \leq M \leq M_5, 0 \leq P_W \leq M_6\}.\end{aligned}$$

Letting $N_H = S_H + I_H$ and adding the first and second equations in system (4.2.13) gives

$$\frac{dN_H}{dt} \leq \Lambda_H - \mu_H N_H. \tag{4.2.1}$$

Parameter	Parameter description
Λ_H	Recruitment rate of susceptible human population.
Λ_V	Recruitment rate of susceptible snail population.
β_H	Human maximum exposure rate.
β_V	Snail maximum exposure rate.
μ_H	Natural death rate in the human population.
μ_V	Natural death rate in the snail population.
μ_L	Natural death rate of eggs worms in the physical land.
μ_W	Natural death rate of eggs worms in the water.
μ_M	Natural death rate of miracidia.
μ_S	Rate at which cercariea die.
δ_H	Additional mortality rate of infected humans.
δ_V	Additional mortality rate of infected snails.
α_L	Rate which schistoma eggs are washed away by running water into the physical water environment.
α_W	Rate at which miracidia is released into the physical water environment.
γ_h	Rate at which infected individual becomes eggs producing.
N_h	Number of eggs produced per infected host.
γ_S	Rate at which infected snails become cercariae shedding.
N_S	Number of cercariae produced by each snail per day.
N_W	Number of miracidia produced from each worm egg
M_0	Saturation constant of miracidia
P_0	Saturation constant of cercariae

Table 4.1: Description of parameters

Then we have

$$\lim_{t\to\infty} \sup(N_H(t)) \leq \frac{\Lambda_H}{\mu_H}. \tag{4.2.2}$$

Similarly, letting $N_V = S_V + I_V$ and adding the third and fourth equations in system (4.2.13) gives

$$\frac{dN_V}{dt} \leq \Lambda_V - \mu_V N_V. \tag{4.2.3}$$

This implies that

$$\lim_{t\to\infty} \sup(N_V(t)) \leq \frac{\Lambda_V}{\mu_V}. \tag{4.2.4}$$

Hence, all feasible solutions of model system (4.2.13) enter the region Ω, where

$$\begin{cases} M_1 = \dfrac{\Lambda_H}{\mu_H}, \\ M_2 = \dfrac{\Lambda_V}{\mu_V}, \\ M_3 = \dfrac{N_h\gamma_h\Lambda_H}{\mu_H(\alpha_L+\mu_L)}, \\ M_4 = \dfrac{\alpha_L N_h\gamma_h\Lambda_H}{(\alpha_L+\mu_L)(\alpha_W+\mu_W)\mu_H}, \\ M_5 = \dfrac{N_W\alpha_W\alpha_L N_h\gamma_h\Lambda_H}{\mu_M\mu_H(\alpha_L+\mu_L)(\alpha_W+\mu_W)}, \\ M_6 = \dfrac{N_S\gamma_S\Lambda_V}{\mu_S\mu_V}. \end{cases} \tag{4.2.5}$$

Thus, Ω is positively invariant and attracting. It is therefore sufficient to search for the solutions of the model system (4.2.13) in Ω.

4.2.2 Disease free equilibrium (DFE)

At the disease-free equilibrium, there is no cercariae, miracidia, worms and eggs and hence no infection in the human and snail populations. By simple calculations, the disease-free equilibrium of the model system (4.2.13) is given as

$$U_0 = \left(\frac{\Lambda_H}{\mu_H}, 0, \frac{\Lambda_V}{\mu_V}, 0, 0, 0, 0, 0\right). \tag{4.2.1}$$

4.2.3 Reproductive number

The basic reproductive number, denoted by R_0, is the average number of secondary cases produced by a typical infected individual during her/his entire life as infectious when introduced in a population of susceptibles [97]. We follow the next generation operator approach to derive the basic reproductive number [97]. The model system (4.2.13) can be written in the form

$$\begin{cases} \dfrac{dX}{dt} = f(X,Y,Z), \\ \dfrac{dY}{dt} = g(X,Y,Z), \\ \dfrac{dZ}{dt} = h(X,Y,Z). \end{cases} \tag{4.2.1}$$

where

$$\begin{cases} X = (S_H, S_V), \\ Y = (I_H, I_V, E_L, E_W), \\ Z = (M, P_W). \end{cases} \tag{4.2.2}$$

Components of X are ordered pair representing, respectively, susceptible human and snail, while components of Y represent the number of infected individuals that do not transmit the disease. Components of Z represent the number of individuals capable of transmitting the disease. Let

$$U_0 = \left(\frac{\Lambda_H}{\mu_H}, 0, \frac{\Lambda_V}{\mu_V}, 0, 0, 0, 0, 0\right) \tag{4.2.3}$$

denote the disease free equilibrium state and let

$$\tilde{g}(X^*, Z) = (\tilde{g}_1(X^*, Z), \tilde{g}_2(X^*, Z), \tilde{g}_3(X^*, Z), \tilde{g}_4(X^*, Z)) \tag{4.2.4}$$

with

$$\begin{cases} \tilde{g}_1(X^*, Z) &= \dfrac{\beta_H \Lambda_H P_W}{\mu_H(\mu_H + \delta_H)(P_0 + P_W)}, \\ \tilde{g}_2(X^*, Z) &= \dfrac{\beta_V \Lambda_V M}{\mu_V(\mu_V + \delta_V)(M_0 + M)}, \\ \tilde{g}_3(X^*, Z) &= \dfrac{N_h \gamma_h \beta_H P_W \Lambda_H}{\mu_H(\mu_H + \delta_H)(P_0 + P_W)(\alpha_L + \mu_L)}, \\ \tilde{g}_4(X^*, Z) &= \dfrac{\alpha_L N_h \gamma_h \beta_H \Lambda_H P_W}{\mu_H(\mu_H + \delta_H)(P_0 + P_W)(\alpha_L + \mu_L)(\alpha_W + \mu_W)}. \end{cases} \tag{4.2.5}$$

Let $A = D_z h(X^*, \tilde{g}(X^*, 0), 0)$ and further assume that A can be written in the form $A = M - D$, where $M \leq 0$ and $D > 0$, a diagonal matrix.

Then A becomes

$$A = \begin{bmatrix} -\mu_W & \dfrac{N_W \alpha_W \alpha_L N_h \gamma_h \beta_H \Lambda_H}{\mu_H(\mu_H + \delta_H)(\alpha_L + \mu_L)(\alpha_W + \mu_W)P_0} \\ \dfrac{N_S \gamma_S \beta_V \Lambda_V}{\mu_V(\mu_V + \delta_V)M_0} & -\mu_S \end{bmatrix}. \tag{4.2.6}$$

Since $A = M - D$, we define matrices M and D as follows

$$M = \begin{bmatrix} 0 & \dfrac{N_W \alpha_W \alpha_L N_h \gamma_h \beta_H \Lambda_H}{\mu_H(\mu_H + \delta_H)(\alpha_L + \mu_L)(\alpha_W + \mu_W)P_0} \\ \dfrac{N_S \gamma_S \beta_V \Lambda_V}{\mu_V(\mu_V + \delta_V)M_0} & 0 \end{bmatrix}, \qquad D = \begin{bmatrix} \mu_M & 0 \\ 0 & \mu_S \end{bmatrix}.$$

The basic reproductive number is the spectral radius (dominant eigenvalue) of the matrix MD^{-1}, that is,

$$R_0 = \sqrt{R_{0H}R_{0V}} \tag{4.2.7}$$

where

$$R_{0H} = \frac{N_W\alpha_W\alpha_L N_h\gamma_h\beta_H\Lambda_H}{\mu_S\mu_H(\mu_H+\delta_H)(\alpha_L+\mu_L)(\alpha_W+\mu_W)P_0}, \tag{4.2.8}$$

and

$$R_{0V} = \frac{N_S\gamma_S\beta_V\Lambda_V}{\mu_V(\mu_V+\delta_V)\mu_M M_0}. \tag{4.2.9}$$

The quantity R_{0H} represents the expected number of snails infected by a single newly infected human host entering a completely susceptible snail population at the equilibrium. This individual is still present and infectious. That is, the average number of new infections through environment-to-host transmission caused by one infected individual in a susceptible snail population. Note that R_{0H} comprises of human population epidemiological parameters.

The quantity R_{0V} represents the expected number of humans infected by a single newly infected snail entering a completely susceptible population at the equilibrium. This snail is still present and infectious. That is, the average number of new infections through host-to-host transmission caused by one infected snail in its infectious lifetime. Note that R_{0V} comprises of snail population epidemiological parameters.

4.2.4 Local Stability of DFE

From Theorem 4.2 of van den Driesche and Watmough [97], if the basic reproduction number R_0 is less than one, then the disease free equilibrium is locally asymptotically stable and the disease cannot invade the population. This is summarized in the following theorem.

Theorem 4.1. *The disease free equilibrium point E^0, of model system (4.2.13) is locally asymptotically stable whenever $R_0 < 1$ and unstable otherwise.*

Proof. The proof is not needed since local stability of the disease free equilibrium is a consequence of Theorem 4.2 of van den Driessche and Watmough [97].

4.2.5 The Endemic Equilibrium State and Its Existence

4.2.5.1 The Endemic Equilibrium State

At the endemic equilibrium point both humans and snails are infected by cercariae and miracidia, respectively and the endemic equilibrium of the model system (4.2.13) is given by

$$E^* = (S_H^*, I_H^*, S_V^*, I_V^*, E_L^*, E_W^*, M^*, P_W^*)$$

where

$$\begin{cases} S_H^* &= \dfrac{\Lambda_H}{\mu_H + \lambda_H^*}, \\ I_H^* &= \dfrac{\lambda_H^* \Lambda_H}{(\mu_H + \delta_H)(\mu_H + \lambda_H^*)}, \\ S_V^* &= \dfrac{\Lambda_V}{\mu_V + \lambda_V^*}, \\ I_V^* &= \dfrac{\lambda_V^* \Lambda_V}{(\mu_V + \lambda_V^*)(\delta_V + \mu_V)}, \\ E_L^* &= \dfrac{N_h \gamma_h \Lambda_H \lambda_H^*}{(\mu_H + \lambda_H^*)(\delta_H + \mu_H)(\alpha_L + \mu_L)}, \\ E_W^* &= \dfrac{\alpha_L N_h \gamma_h \Lambda_H \lambda_H^*}{(\mu_H + \lambda_H^*)(\delta_H + \mu_H)(\alpha_L + \mu_L)(\alpha_W + \mu_W)}, \\ M^* &= \dfrac{N_W \alpha_W \alpha_L N_h \gamma_h \Lambda_H \lambda_H^*}{(\mu_H + \lambda_H^*)(\delta_H + \mu_H)(\alpha_L + \mu_L)(\alpha_W + \mu_W)\mu_M}, \\ P_W^* &= \dfrac{N_S \gamma_S \Lambda_V \lambda_V^*}{(\mu_V + \lambda_V^*)(\delta_V + \mu_V)\mu_S}. \end{cases} \tag{4.2.1}$$

At the endemic equilibrium state, the susceptible human population given by the expression S_H^* is proportional to the average time of stay of individuals in the susceptible compartment and the supply rate of new susceptible individuals through birth. Susceptible individuals exit this compartment either through death or infection.

The infected human population at the endemic equilibrium given by I_H^* is directly proportional to a product of three quantities: the average time of stay in the infected compartment, the rate of

infection of susceptible individuals and the number of susceptible hosts.

The susceptible snail population at the endemic equilibrium given by S_V^* equals the product of the average time of stay in this compartment and the rate of supply of new susceptible snails through birth.

The infected snail population endemic equilibrium given by I_V^* is influenced by the average life span of infected snails, the rate of infection of snails and the number/density of susceptible snails.

The egg population on the physical land environment endemic equilibrium given by E_L^* is influenced by the life span of eggs, the rate at which infected human hosts excrete schistosome eggs and the total number of humans infected with schistosomiasis.

The egg population in the water environment endemic equilibrium given by E_W^* is influenced by the average life span of the eggs and the rate at which the eggs are transported into the physical water environment by flowing water.

The endemic equilibrium associated with miracidia population in the physical water environment given by M^* is influenced by the life span of miracidia and worm fecundity.

The endemic equilibrium associated with cercariae population in the physical water environment given by P_W^* is influenced by the the reduction in the life span of cercariae in the physical water environment and the rate at which infected snails shed cercariae in the physical water environment. Thus, control measures intended to kill snails reduce schistosomiasis transmission.

4.2.5.2 Existence of endemic equilibrium

In this section, we make use of the reproductive number denoted by R_0 to show the existence of the endemic equilibrium (4.3.1) for the model system (4.2.13).

We start by stating the following theorem:

Theorem 4.2. *The model formulated in terms of propositions has at least one endemic equilibrium solution given by* $E^* = (S_H^*, I_H^*, S_V^*, I_V^*, E_L^*, E_W^*, M^*, P_W^*)$, *with all components of* E^* *being non-negative, whose existence and properties are determined by the threshold parameter* R_0, *where*

$$R_0 = \sqrt{\frac{N_W \alpha_W \alpha_L N_h \gamma_h \beta_H \Lambda_H}{\mu_H \mu_M (\mu_H + \delta_H)(\alpha_L + \mu_L)(\alpha_W + \mu_W) P_0} \cdot \frac{N_S \gamma_S \beta_V \Lambda_V}{\mu_S \mu_V (\mu_V + \delta_V) M_0}}.$$

Proof. Let $S_H^*, I_H^*, S_V^*, I_V^*, E_L^*, E_W^*, M^*, P_W^*$ be a constant solution of the model system (4.2.13). We can easily express $S_H^*, I_H^*, S_V^*, E_L^*, E_W^*, M^*, P_W^*$ in terms of I_V^* as follows:

$$\begin{cases} S_H^*(I_V^*) = \dfrac{\Lambda_H(P_0\mu_S + N_S\gamma_S I_V^*)}{\mu_H(P_0\mu_S + N_S\gamma_S I_V^*) + \beta_H N_S\gamma_S I_V^*}, \\ I_H^*(I_V^*) = \dfrac{\Lambda_H\beta_H N_S\gamma_S I_V^*}{[\mu_H(P_0\mu_S + N_S\gamma_S I_V^*) + \beta_H N_S\gamma_S I_V^*](\mu_H + \delta_H)}, \\ S_V^*(I_V^*) = \dfrac{a_0[\mu_H(P_0\mu_S + N_S\gamma_S I_V^*) + \beta_H N_S\gamma_S I_V^*] + a_1\Lambda_V}{a_0[\mu_H(P_0\mu_S + N_S\gamma_S I_V^*) + \beta_H N_S\gamma_S I_V^*] + a_1 + \beta_V a_1}, \\ E_L^*(I_V^*) = \dfrac{N_h\gamma_h N_S\gamma_S\beta_H I_V^*}{[\mu_H(P_0\mu_S + N_S\gamma_S I_V^*) + \beta_H N_S\gamma_S I_V^*](\mu_L + \alpha_L)(\mu_H + \delta_H)}, \\ E_W^*(I_V^*) = \dfrac{\alpha_L N_h\gamma_h\Lambda_H\beta_H N_S\gamma_S I_V^*}{\mu_M(\mu_W + \alpha_W)(\mu_L + \alpha_L)(\mu_H + \delta_H)[\mu_H(P_0\mu_S + N_S\gamma_S I_V^*) + \beta_H N_S\gamma_S I_V^*]}, \\ M^*(I_V^*) = \dfrac{a_1}{\mu_M(\mu_W + \alpha_W)(\mu_L + \alpha_L)(\mu_H + \delta_H)[\mu_H(P_0\mu_S + N_S\gamma_S I_V^*) + \beta_H N_S\gamma_S I_V^*]}, \\ P_W^*(I_V^*) = \dfrac{N_S\gamma_S I_V^*}{\mu_S}. \end{cases} \tag{4.2.2}$$

where

$$a_0 = M_0\mu_M(\mu_W + \alpha_W)(\mu_L + \alpha_L)(\mu_H + \delta_H) \text{ and } a_1 = N_W\alpha_W\alpha_L N_S\gamma_S\Lambda_H\beta_H I_V^*.$$

Substituting the expressions in (4.2.2) in the equation of I_V which is given by $\dfrac{dI_V}{dt} = \lambda_V S_V - (\mu_V + \delta_V)I_V$, at the endemic equilibrium state, we get the following polynomial:

$$b_0 + b_1 I_V^* + b_2 I_V^{*2} = 0$$

where

$$\begin{cases} b_0 = \beta_H N_S \gamma_S a_0 \mu_H \mu_S - a_0 \mu_H \mu_S (\mu_V + \delta_V), \\ b_1 = \beta_H N_S \gamma_S + N_W \alpha_W \alpha_L N_S \gamma_S^2 \Lambda_H \beta_H^2 - (\mu_H + \delta_H)[P_0 \mu_S (a_0 \mu_H N_S \gamma_S + a_0 \beta_H N_S \gamma_S) + N_W \alpha_W N_S \gamma_S], \\ b_2 = -(\mu_V + \delta_V)[a_0^2 \mu_H + a_0 \beta_H N_S \gamma_S + N_S \gamma_S N_W \alpha_W \alpha_L N_S \gamma_S \Lambda_H \beta_H + N_W \alpha_W \alpha_L N_S \gamma_S \Lambda_H \beta_H N_S \gamma_S \beta_V]. \end{cases} \tag{4.2.3}$$

Solving for I_V^*, we get

$I_V^* = \dfrac{-b_1 \pm \sqrt{b_1^2 - 4b_2 b_0}}{2b_2} > 0.$

We only consider $I_V^* = \dfrac{-b_1 + \sqrt{b_1^2 - 4b_2 b_0}}{2b_2} > 0$ since $I_V^* = \dfrac{-b_1 - \sqrt{b_1^2 - 4b_2 b_0}}{2b_2}$ is negative and hence, it is biological meaningless.

The existence of the endemic equilibrium states will hold provided the following conditions are positive.

$$\begin{cases} -b_1 + \sqrt{b_1^2 - 4b_2 b_0} > 0, \\ b_1^2 < b_1^2 + 4b_2(A - BR_0^2), \\ 0 < 4b_2(A - BR_0^2). \end{cases} \tag{4.2.4}$$

where $A = \beta_H N_S \gamma_S M_0 \mu_W (\mu_W + \alpha_W)(\mu_L + \alpha_L)(\mu_H + \delta_H)$ and

$B = \dfrac{M_0 \mu_M \mu_H^2 \mu_S^2 \mu_W^2 (\mu_V + \delta_V) P_0 (\mu_W + \alpha_W)^2 (\mu_L + \alpha_L)^2 (\mu_H + \delta_H)^2}{\alpha_L \gamma_H \beta_H \Lambda_H N_S \gamma_S \beta_V \Lambda_V}.$

From equation (4.2.4) we have the following conditions:

- If $B < 0$ and $A > 0$, then $R_0 > 1$, that is, there exists an endemic point.
- If $B > 0$, $A > 0$, and $A < B$ then $R_0 > 1$, that is, there exists an endemic point.

□

4.2.6 Sensitivity Analysis

Sensitivity analysis is used to determine how sensitive a model is, to changes in the values of the parameters of the model. It provides information on factors that most contribute to the output variability. In this section, we perform sensitivity analysis by calculating the sensitivity indices of the basic reproduction number R_0, because they determine whether schistosomiasis spreads in the human and snail populations or not. These indices tell us how crucial each parameter is to the spread of schistosomiasis and which parameters should be targeted for intervention strategies [226]. We apply the method presented in [160] to investigate which parameters in our model have a high impact on R_0. These parameters have to be taken into consideration in control measures. According to [160], the normalized forward sensitivity index of a variable to a parameter, is a ratio of the relative change in the variable to the relative change in parameter. When the variable is a differentiable function of the parameter, the sensitivity index may alternatively be defined using partial derivatives. To determine the sensitivity indices we use the following definition and the parameter values in Table 2.

Parameter	**Value**	**Range**	**Units**	**Source**
Λ_H	800	800-1600	$Humans\ day^{-1}$	*Assumed*
Λ_V	2500	2500-5000	$Snails\ day^{-1}$	*Assumed*
μ_H	0.0000384	0.0000384-0.14	day^{-1}	[200]
μ_V	0.0014	0.000569-0.9	day^{-1}	[200]
μ_L	0.2	0.142857-0.5	day^{-1}	[200]
μ_W	0.11	0.11-0.833	day^{-1}	[200]
μ_M	2.2	2-2.66	day^{-1}	[200]
μ_S	0.4	0.33-0.5	day^{-1}	[200]
γ_S	0.02	0.0119-0.04	day^{-1}	[200]
δ_H	0.0013699	0.0039-0.039	day^{-1}	[200]
δ_V	0.002	0.002-0.05	day^{-1}	[200]
α_L	0.0004	0.0004-0.4	day^{-1}	*Assumed*
α_W	0.05	0.05-0.0625	day^{-1}	[200]
β_H	0.023	0.028-0.122	day^{-1}	[200]
β_V	0.000127	0.000127-0.0012	day^{-1}	[200]
γ_h	0.1	0.1-0.9	day^{-1}	*Assumed*
N_h	110	110-1000	day^{-1}	*Assumed*
N_S	110	110-500	day^{-1}	[200]
N_W	110	110-500	day^{-1}	[200]
M_0	10^8	$10^4 - 10^{10}$	-	*Assumed*
P_0	10^{10}	$10^4 - 10^{10}$	-	*Assumed*
α_V	-	0.1-0.7	-	*Assumed*

Table 4.2: Between-host and within-host schistosomiasis transmission dynamics Parameter values

Definition 4.3. The normalized forward sensitivity index of a variable, ν, that depends on a differentiable parameter ξ is defined as:

$$S_{\xi}^{\nu} = \frac{\partial \nu}{\partial \xi} \times \frac{\xi}{\nu}.$$

By definition (6.1), we determined the partial derivatives of R_0 with respect to each parameter of the model system (2.13) multiplied by respective parameter divided by R_0. The sensitivity indices are summarized in Table 3 which are ordered from most sensitive to the least. The sensitivity analysis results are categorised into five groups, namely A, B, C, and D, where category A represents snail mortality parameter, category B represents the parameters associated with the recruitment and transmission of both snail and human populations, eggs on the land and in the water and parasites within infected hosts. Category C is associated with additional snail mortality, category D represents miracidia released into water environment and category E represents parameters associated with natural death rates and saturation of parasites. The most sensitive parameter on the basic reproductive number is the natural death rate of infected snails. Since $S_{\mu_V}^{R_0} = -0.7$, it implies that increasing μ_V by 10%, decreases R_0 by 7%. That is, killing infected snails is the most effective way of eliminating schistosomiasis. We recall that $\Lambda_V, \Lambda_H, \beta_H, \beta_V, N_W, N_h, \gamma_h, N_S$ and γ_S, are recruitment rate of susceptible snail population, recruitment rate of susceptible human population, maximum exposure rate, snail maximum exposure rate, number of miracidia produced by each snail per day, rate at which infected individual becomes eggs producing, rate at which infected snails become cercariae shedding, additional mortality rate of infected snails, and the rate at which miracidia is released into the physical water environment, respectively. The sensitivity index of these parameters is $+0.5$ implying that increasing these parameters by 10% will lead to an increase in R_0 by 5%. These parameters have a direct proportional relation to R_0, that is, an increase in each of these parameters will bring about the same proportion in R_0, likewise, a decrease in each of these parameters will bring about an equivalent decrease in R_0. Recall that $\mu_L, \mu_S, \mu_M, \mu_W, \delta_H, M_0$ andP_0 are natural death rate of eggs worms on the land, natural death rate of cercariae, natural death rate of miracidia, natural death rate of eggs worms in the water, additional mortality rate of infected humans, saturation constant of miracidia and saturation constant of cercariae, respectively. Their sensitive index is -0.5 meaning that increasing each of these rates by 10% will lead to a decrease in R_0 by 5%. We also observe that an increase in additional mortality rate of infected snails ; δ_V by 10% will lead to a decrease in R_0 by 3%. It is clear that an increase in either of these rates is neither ethical nor practical. Therefore, the natural control mechanisms will be the option in reducing the transmission of the disease if we are to focus on these parameters, though we cannot rely much on them since we can not predict their occurrence. Lastly, increasing a rate at which miracidia

is released into the water environment, α_W by 10% will lead to an increase in R_0 by 2%. When designing and planning intervention programmes more efforts must be focused on the reduction of the following parameters: $\mu_V, \Lambda_V, \Lambda_H, \beta_H, \beta_V, N_W, N_h, \gamma_h, N_S, \gamma_S,$ and δ_V. The man-made control mechanisms will be applicable in this case.

Parameter	**Sensitivity index**	**10% Increase in**
A:μ_V	-0.7	**A** leads to 7% decrease in R_0
B:$\mu_L, \mu_S, \mu_W, \delta_H, M_0, P_0$	-0.5	**B** leads to 5% decrease in R_0
C:δ_V	-0.3	**C** leads to 3% decrease in R_0
D:α_W	$+0.2$	**D** leads to 2% increase in R_0
E:$\Lambda_H, \Lambda_V, \beta_H, \beta_V, N_W, N_h, N_S, \gamma_S$	$+0.5$	**E** leads to 5% increase in R_0

Table 4.3: Sensitivity Indices of R_0

In the next section, we extend the basic model in order to incorporate control measures. The control measures are going to focus more on the most sensitive parameters.

4.3 Basic Schistosomiasis Mathematical Model with control measures

Despite the success of control programmes in the world, schistosomiasis remains a serious public health problem [132]. In this section, we extend the model in the previous section in order to incorporate the man-made and natural schistosomiasis control measures. The parameters described in Table 1 remain the same, except that we have control measures parameters incorporated into the previous model. The description of new parameters is as follows:

The effect of health education campaigns (HEC) is modelled by $\beta_H(1-a)$ where a is the efficacy of HEC. When $a = 0$, it implies that the HEC alone is not effective in reducing human contact with contaminated water bodies, whereas $a = 1$ implies that the HEC is 100% effective in reducing human contact with contaminated water bodies.

The effect of climate change in reducing cercariae production by each snail is modelled by $N_S(1-n)$ where n is the efficacy of climate change. When $n = 0$, it implies that climate change alone is not reliable in reducing cercariae production by each snail whereas $n = 1$ implies that climate change is 100% effective in reducing cercariae production by each snail.

The effect of extreme weather changes in reducing snail production capacity is modelled by $\Lambda_V(1-c)$ where c is the efficacy of extreme weather changes. When $c = 0$, extreme whether

changes are not reliable in reducing snail production capacity whereas $n = 1$ implies that extreme weather changes are 100% effective in reducing snail production capacity.

The effect of improved sanitation and treatment in reducing matured worms and schistosome eggs, respectively, is modelled by $N_h(1-g)(1-f)$ where g is the efficacy of improved sanitation and f is the efficacy of treatment. When $g = 0$, it implies that good environmental sanitation associated with construction and use of toilets by individuals in schistosomiasis endemic areas alone is not effective in reducing the environmental contamination. This implies that there might be other factors which contribute in contamination of the environment other than good sanitation associated with construction and use of toilets in endemic areas. When $g = 1$, it implies that good environmental sanitation associated with construction and use of toilets by individuals in schistosomiasis endemic areas is 100% effective. When $f = 0$, it implies that treatment alone is not effective whereas when $f = 1$, it implies that treatment is 100% effective.

In [200], the effects of climatological environment change were not explicitly incorporated. Our model explicitly incorporates climate change in reducing water levels associated with free-living pathogens (cercariae and miracidia). The descriptions of both P_0 and M_0 are similar to the ones in [14]. The effect of climate change in reducing water levels associated with cercariae is modelled by $P_0(1 - b)$ where b is the efficacy of climate change in reducing water levels associated with cercariae. When $b = 0$, it means that climate change alone cannot lead to a reduction in water volumes that can lead to death of the snails and cercariae whereas $b = 1$ implies that climate change is 100% effective in reducing water volumes. Climate change may either lead to a reduction in the disease transmission since cercariae become more saturated when the water level is high or increase in the disease transmission when the water level is low since cercariae become less saturated when the water level is low, that is, force of infection associated with humans, λ_H, is inversely proportional to P_0. Thus λ_H is higher whenever water levels are low, than when they are high.

The effect of climate change in reducing water levels associated with miracidia is modelled by $M_0(1 - d)$, where d is the efficacy of climate change in reducing water levels associated with miracidia. When $d = 0$, it implies that climate change has no effect in the reduction of water levels whereas $d = 1$ implies that climate change has 100% effect in reducing the water levels. The force of infection associated with snails, λ_V, is inversely proportional to M_0. Thus λ_V is higher whenever water levels are low, compared to when they are high. Schistosomiasis epidemic areas close to rivers, streams and ponds are in constant tension between temperatures which stimulates the growth of cercariae and miracidia. Increased water levels also lead to moderate infections. The summary of control mechanisms is represented on table 4.4.

Parameter Modified	**Model representation**	**Mechanism of control**
β_H	$\beta_H(1-a)$	a: Efficacy of health education campaigns in reducing human contact with contaminated waters.
P_0	$P_0(1-b)$	b:Efficacy of climate change in reducing water levels that tend to stimulating cercariae growth in the water.
Λ_V	$\Lambda_V(1-c)$	c: Efficacy of extreme weather changes in reducing snail production capacity.
M_0	$M_0(1-d)$	d:Efficacy of climate change in reducing water levels that tend to stimulating miracidia growth in the water.
μ_v	$\mu_v(1-e)$	e: Efficacy of molluscicides in killing snails.
N_h	$N_h(1-g)(1-f)$	g,f: Efficacy of improved sanitation and treatment in reducing matured worms and schistosome eggs, respectively.
N_S	$N_S(1-n)$	n : Efficacy of climate change in reducing cercariae production by each snail.
μ_M	$\mu_M(1-m)$	m : Efficacy of extreme weather changes in reducing the rate at which miracidia die.
μ_S	$\mu_S(1-r)$	r : Efficacy of climate change in reducing the rate at which cercariae die.

Table 4.4: Summary of control mechanisms of schistosomiasis

The mathematical model of schistosomiasis in human and snail populations with control measures takes the form

$$\begin{cases} \frac{dS_H}{dt} &= \Lambda_H - \lambda_H S_H - \mu_H S_H, \\ \frac{dI_H}{dt} &= \lambda_H S_H - (\mu_H + \delta_H) I_H, \\ \frac{dS_V}{dt} &= \Lambda_V - \lambda_V S_V - \mu_V (1-e) S_V, \\ \frac{dI_V}{dt} &= \lambda_V S_V - (\mu_V (1-e) + \alpha_V) I_V, \\ \frac{dE_L}{dt} &= N_h \gamma_h (1-f)(1-g) I_H - (\mu_L + \alpha_L) E_L, \\ \frac{dE_W}{dt} &= \alpha_L E_L - (\mu_W + \alpha_W) E_W, \\ \frac{dM}{dt} &= N_W \alpha_W E_W - \mu_M (1-m) M, \\ \frac{dP_W}{dt} &= N_S (1-n) \gamma_S I_V - \mu_S (1-r) P_W. \end{cases} \tag{4.3.1}$$

where

$$\lambda_H = \frac{\beta_H (1-a) P_W}{P_0 (1-b) + P_W} \text{ and } \lambda_V = \frac{\beta_V M}{M_0 (1-d) + M}.$$

4.3.1 Properties of the model

The feasibility of the model solutions, equilibria and stability analysis can be established using the same techniques as in the previous sections. In the next section we determine the reproductive number and equilibrium states of the model system .

4.3.2 Reproductive Number

The feasibility of the model solutions, equilibria and stability analysis can be established using the same techniques as in the previous sections. In the next section we determine the reproductive number and equilibrium states of the model system .

In the absence of cercariae, miracidia, eggs and control measures we have no infections in the human and snail populations. Thus, the model system (5.3.9) has a disease-free equilibrium state

$$E_0 = \left(\frac{\Lambda_H}{\mu_H}, 0, \frac{\Lambda_V}{\mu_V}, 0, 0, 0, 0, 0\right). \tag{4.3.1}$$

Following the same approach for getting reproductive number as in the previous section we get basic reproductive number which is the spectral radius of the matrix MD^{-1}, that is,

$$R_{0C} = \sqrt{R_{0HC}R_{0VC}} \tag{4.3.2}$$

where

$$R_{0HC} = \frac{N_W\alpha_W\alpha_L N_h\gamma_h(1-f)(1-g)\beta_H(1-a)\Lambda_H}{\mu_H(\mu_H+\delta_H)(\alpha_L+\mu_L)(\alpha_W+\mu_W)P_0(1-b)\mu_S(1-r)}, \tag{4.3.3}$$

and

$$R_{0VC} = \frac{N_S\gamma_S(1-n)\beta_V\Lambda_V}{\mu_V(1-e)M_0(1-d)(\mu_V(1-e)+\delta_V)\mu_M(1-m)}. \tag{4.3.4}$$

The quantity R_{0C} measures the effectiveness of both man-made and natural control mechanisms in eradicating the spread of schistosomiasis in both human and snail populations. It is composed of the product of two distinct basic reproductive numbers, R_{0HC} and R_{0VC}. It is clear that R_{0HC} and R_{0VC} are positive.

The quantity R_{0HC} represents the number of secondary infected humans cases produced by a typical newly infected snail host during the period of infection in a completely susceptible population. R_{0HC} is inversely proportional to efficacy of improved sanitation, g; treatment, f and HEC, a. An increase in either of these man-made control mechanisms will lead to a decline in R_{0HC}. For instance, if efficacy of HEC is increased, it will decrease human maximum exposure to contaminated water bodies , β_H. This will eventually lead to a decline in R_{0HC}. It is also directly proportional to the efficacy of climate change in reducing water levels associated with cercariae and miracidia, although relying on climate change is neither practical nor ethical.

The quantity R_{0VC} represents the number of secondary infected snails cases produced by a typical newly infected human host during the period of infection in a completely susceptible population. R_{0VC} is inversely proportional to the efficacy of climate change in reducing cercariae production by each snail, n and the efficacy of extreme weather changes in reducing snail production capacity, c. An increase in either of these rates will eventually lead a decrease in R_{0VC}. This quantity is also directly proportional to the efficacy of snail elimination by mollucicide, e; efficacy of climate change in reducing water levels associated with miracidia, d; and efficacy

of extreme weather changes in reducing the rate at which miracidia die, m. We observe that mollucicide can be more reliable in eliminating the snails in order to reduce R_{0VC}, other than depending on extreme weather changes and climate change.

4.3.3 Endemic equilibrium state

The endemic equilibrium of the model system (5.3.9) is given by

$$\hat{E} = (\hat{S_H}, \hat{I_H}, \hat{S_V}, \hat{I_V}, \hat{E_L}, \hat{E_W}, \hat{M}, \hat{P_W})$$

where

$$\begin{cases} \hat{S_H} &= \dfrac{\Lambda_H}{\mu_H + \hat{\lambda_H}}, \\ \hat{I_H} &= \dfrac{\hat{\lambda_H}\Lambda_H}{(\mu_H + \delta_H)(\mu_H + \hat{\lambda_H})}, \\ \hat{S_V} &= \dfrac{\Lambda_V(1-c)}{\mu_V(1-e) + \hat{\lambda_V}}, \\ \hat{I_V} &= \dfrac{\hat{\lambda_V}\Lambda_V(1-c)}{(\mu_V(1-e) + \hat{\lambda_V})(\delta_V + \mu_V(1-e))}, \\ \hat{E_L} &= \dfrac{N_h\gamma_h(1-f)(1-g)\hat{\lambda_H}\Lambda_H}{(\mu_L + \alpha_L)(\mu_H + \delta_H)}, \\ \hat{E_W} &= \dfrac{\alpha_L N_h\gamma_h(1-f)(1-g)\hat{\lambda_H}\Lambda_H}{(\mu_L + \alpha_L)(\hat{\lambda_H} + \mu_H)(\alpha_W + \mu_W)(\mu_H + \delta_H)}, \\ \hat{M} &= \dfrac{N_W\alpha_W\alpha_L N_h\gamma_h(1-f)(1-g)\hat{\lambda_H}\Lambda_H}{(\mu_L + \alpha_L)(\mu_H + \hat{\lambda_H})(\mu_H + \delta_H)(\mu_W + \alpha_W)\mu_M(1-m)}, \\ \hat{P_W} &= \dfrac{N_S\gamma_S(1-n)\hat{\lambda_V}\Lambda_V(1-c)}{(\mu_V(1-e) + \delta_V)(\hat{\lambda_V} + \mu_V(1-e))\mu_S(1-r)}. \end{cases} \tag{4.3.1}$$

The susceptible human population at the endemic equilibrium state is similar to S_H, except that the force of infection is associated with the efficacy of health education campaigns, cercariae saturation constant rate , efficacy of climate change in controlling both natural death rate of

cercariae and production of cercariae, efficacy of extreme weather changes in reducing snail production and efficacy of mollucicides in killing snails. The number of susceptible human population is given by

$$\hat{S_H} = \frac{\Lambda_H}{\mu_H + \hat{\lambda_H}}, \tag{4.3.2}$$

with

$$\hat{\lambda_H} = \frac{\beta_H(1-a)\hat{P_W}}{P_0(1-b) + \hat{P_W}}. \tag{4.3.3}$$

At the endemic equilibrium state, the infected humans endemic equilibrium is similar to I_H^* except that the rate of infection of susceptible associated with control mechanisms in $\hat{S_H}$. The number of infected individuals is given by

$$\hat{I_H} = \frac{\hat{\lambda_H}\Lambda_H}{(\mu_H + \delta_H)(\mu_H + \hat{\lambda_H})}. \tag{4.3.4}$$

At the endemic equilibrium state the susceptible snail population is similar to S_V^* except that it is associated with efficacy of mollucicides in killing snails, efficacy of extreme weather changes in reducing snails production capacity, efficacy of improved sanitation and treatment in reducing matured worms and schistosome eggs, respectively. It is also associated with efficacy of extreme weather changes in controlling natural death rate of miracidia and saturation constant of cercariae. The number of susceptible snail population is given by

$$\hat{S_V} = \frac{\Lambda_V(1-c)}{\mu_V(1-e) + \hat{\lambda_V}}, \tag{4.3.5}$$

with

$$\hat{\lambda_V} = \frac{\beta_V \hat{M}}{M_0(1-d) + \hat{M}}. \tag{4.3.6}$$

The infected snail population at the endemic equilibrium is associated with the control mechanism that regulates the number susceptible snails. The number of infected snail population is given by

$$\hat{I_V} = \frac{\hat{\lambda_V}\Lambda_V(1-c)}{(\mu_V(1-e) + \hat{\lambda_V})(\delta_V + \mu_V(1-e))}. \tag{4.3.7}$$

The schistosome eggs population on the physical land environment at the endemic equilibrium

is the same as E_L^* , except that it is associated with the efficacy of improved sanitation and treatment in reducing matured worms and schistosome eggs, respectively. It is also associated with the efficacy of health education campaigns in reducing human contact with contaminated water bodies and efficacy of extreme weather changes in controlling saturation constant of cercariae. The number of schistosome eggs population on the physical land environment is given by

$$\hat{E_L} = \frac{N_h\gamma_h(1-f)(1-g)\hat{\lambda_H}\Lambda_H}{(\mu_L+\alpha_L)(\mu_H+\delta_H)}. \tag{4.3.8}$$

The schistosome eggs population in the physical water environment at the endemic equilibrium is similar to E_W^*, except that it is associated with the control mechanisms that control schistosome eggs on the land. The number of schisitosome eggs population in the physical water environment is given by

$$\hat{E_W} = \frac{\alpha_L N_h\gamma_h(1-f)(1-g)\hat{\lambda_H}\Lambda_H}{(\mu_L+\alpha_L)(\hat{\lambda_H}+\mu_H)(\alpha_W+\mu_W)(\mu_H+\delta_H)}. \tag{4.3.9}$$

The miracidia population, at the equilibrium state is similar to M^* except that it is influenced by the efficacy of extreme weather changes in controlling natural death rate of miracidia and efficacy of improved sanitation and treatment in reducing matured worms and schistosome eggs, respectively. The number of miracidia population is given by

$$\hat{M} = \frac{N_W\alpha_W\alpha_L N_h\gamma_h(1-f)(1-g)\hat{\lambda_H}\Lambda_H}{(\mu_L+\alpha_L)(\mu_H+\hat{\lambda_H})(\mu_H+\delta_H)(\mu_W+\alpha_W)\mu_M(1-m)}. \tag{4.3.10}$$

At the endemic equilibrium state the cercariae population is the same as P_W^* except that it is associated with the control mechanisms of infected snails and efficacy of climate change on reducing cercariae production by each snail and controlling the natural death rate of cercariae. The number of cercariae population is given by

$$\hat{P_W} = \frac{N_S\gamma_S(1-n)\hat{\lambda_V}\Lambda_V(1-c)}{(\mu_V(1-e)+\delta_V)(\hat{\lambda_V}+\mu_V(1-e))\mu_S(1-r)}. \tag{4.3.11}$$

4.3.4 Numerical simulations

In this subsection we present numerical simulation results of model system (4.2.13) and model system (5.3.9) which are simulated using Python version V2.6 on the Linux operating system. We used the odeint function in the Scipy.integrate package in Python. The parameter values used for numerical simulations are obtained from [129] (Table 4.2) and the initial conditions

are: $S_H(0) = 200000, I_H(0) = 200, S_V(0) = 40000, I_V(0) = 10, E_L(0) = 40, E_W(0) = 40, M(0) = 20, P_W(0) = 0$. The simulations carried out in this section show the dynamics of the change with time in days of miracidia, cercariae, infected humans, infected snails, susceptible humans, susceptible snails, eggs on the land and eggs in the water environment.

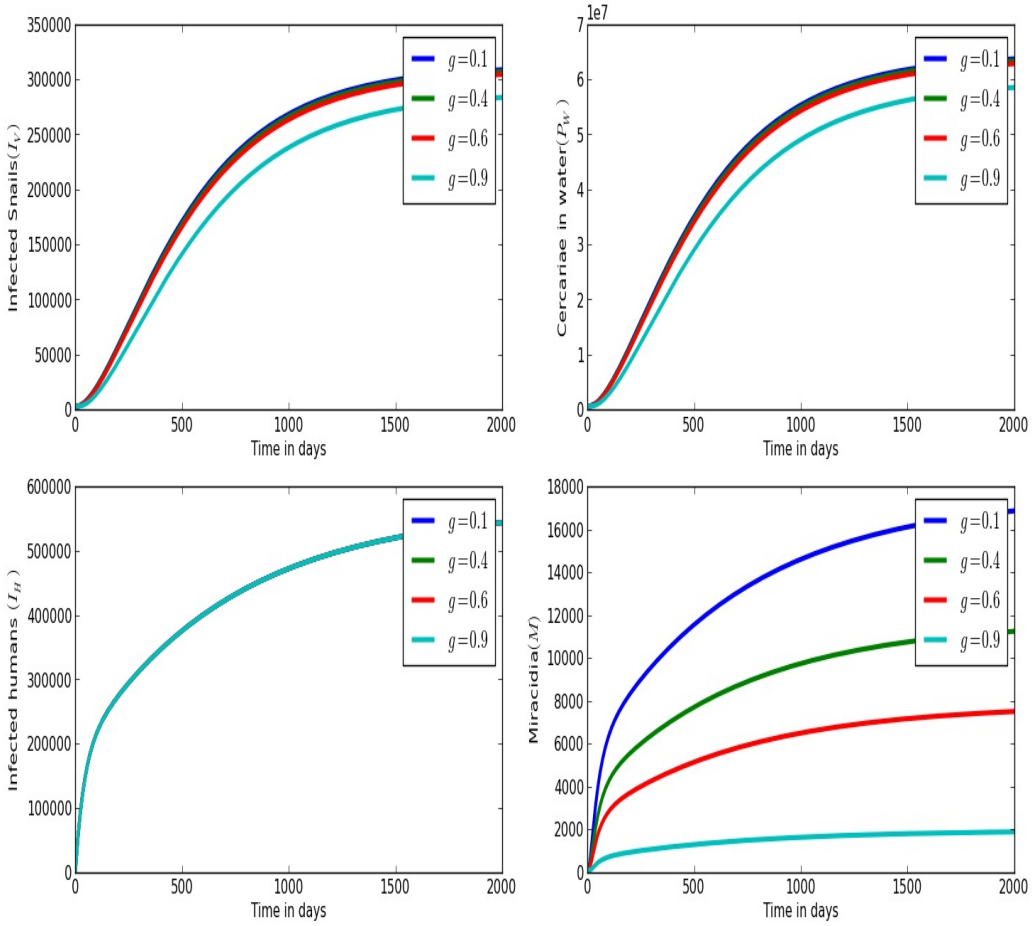

Figure 4.2: Numerical simulations showing dynamics of infected humans (I_H), infected snails (I_V), miracidia (M) and cercariae in water (P_W) over time in days for different values of efficacy of improved sanitation in reducing matured worms g : $g = 0.1,\ g = 0.4,\ g = 0.6$ and $g = 0.9$.

Figure 4.2 shows that the more environmental contamination is reduced, which is due to efficacy of good environmental sanitation practices associated with construction and use of toilets by individuals in schistosomiasis endemic areas is increased, the less the infected snails, cercariae in water, and miracidia but infected humans remain constant, which implies that reducing the number of infected humans and infected snails cannot be achieved unless infected humans also get treated simultaneously with killing of snails by molluccides.

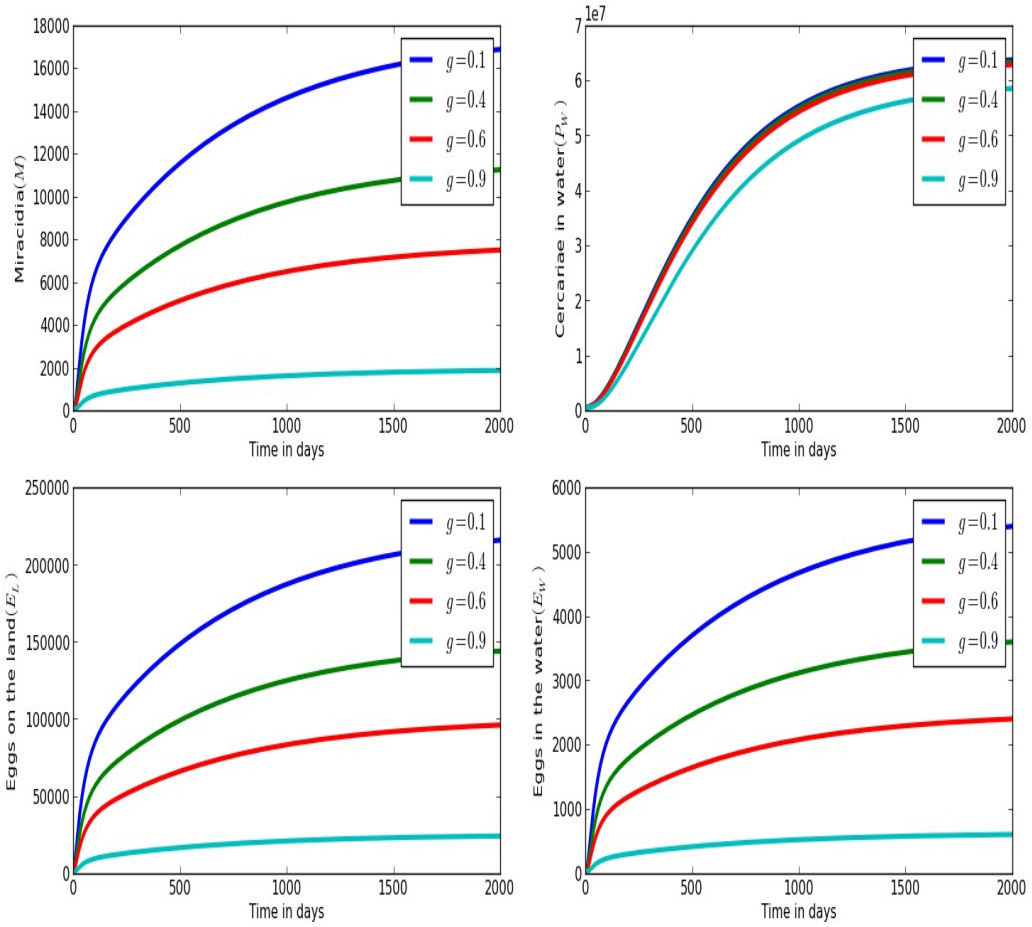

Figure 4.3: Numerical simulations showing dynamics of eggs on the land (E_L), eggs in the water (E_W), miracidia (M) and cercariae in water (P_W) over time in days for different values of efficacy of improved sanitation in reducing matured worms g : $g = 0.1,\ g = 0.4,\ g = 0.6$ and $g = 0.9$.

MacDonald [123] suggested that very high sanitation levels, that is, reducing the number of eggs reaching water has a negligible effect on mean worm load compared to the combined effects of treating infected humans and keeping them out of infected water. This is due to the water that the intermediate hosts (snails) live in is typically saturated with miracidia and almost all snails are infected. Figure 4.3 that when the efficacy of good environmental sanitation practices associated with construction and use of toilets by individuals in schistosomiasis endemic areas is increased, miracidia, cercariae in the water, eggs on the land and eggs in the water decrease and reach steady state at the same time, while cercariae in the water slowly decrease. This is a good indication that by reducing environmental contamination, the spread of schistosomiasis can be eradicated. This supports the results in [123].

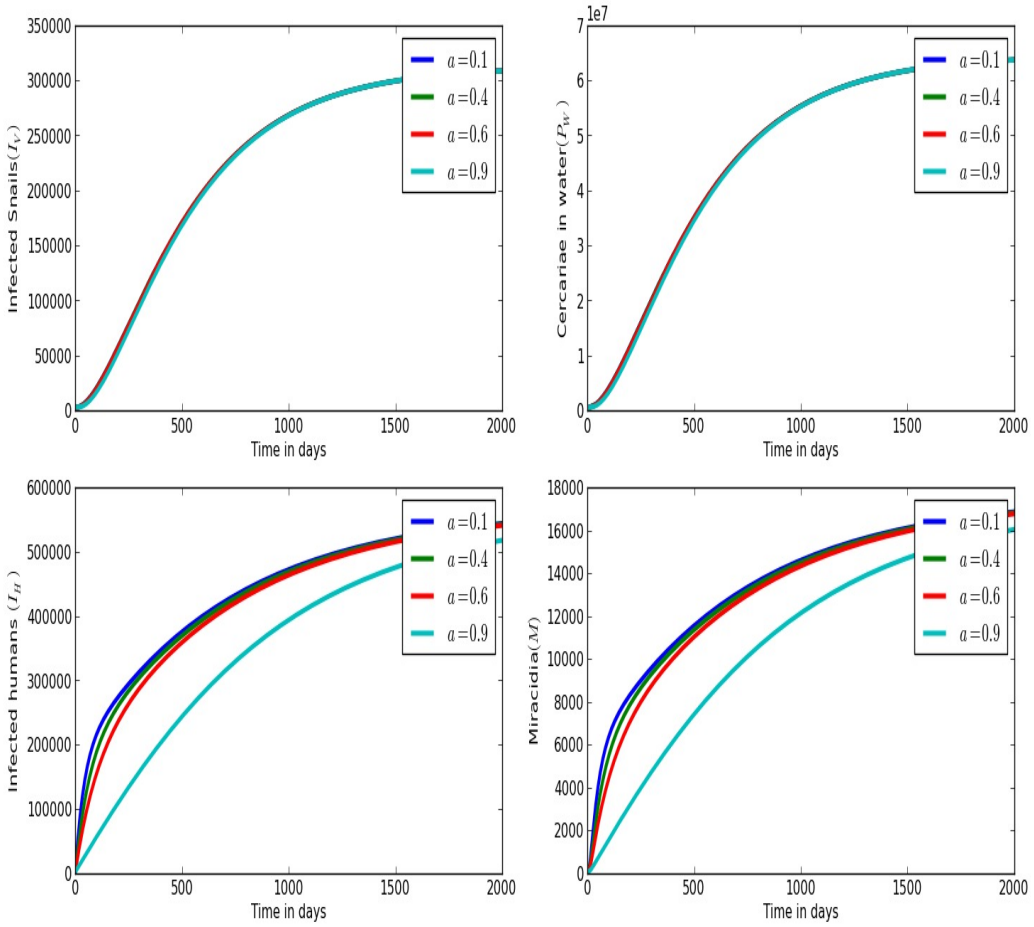

Figure 4.4: Numerical simulations showing dynamics of infected humans (I_H), infected snails (I_V), miracidia (M) and cercariae in water (P_W) over time in days for different values of efficacy of HEC in reducing human contact with unsafe water bodies a : $a = 0.9,\ a = 0.5,\ a = 0.3$ and $a = 0.1$.

Figure 4.4 shows that the more efficacy of HEC, the less the infected snails, infected humans, cercariae in water and meracidia, which is true because if people are not getting into contact with unsafe water bodies then they will not be infected, thus knowledge is crucial. HEC are effective in reducing the spread of schistosomiasis in both humans and snails populations.

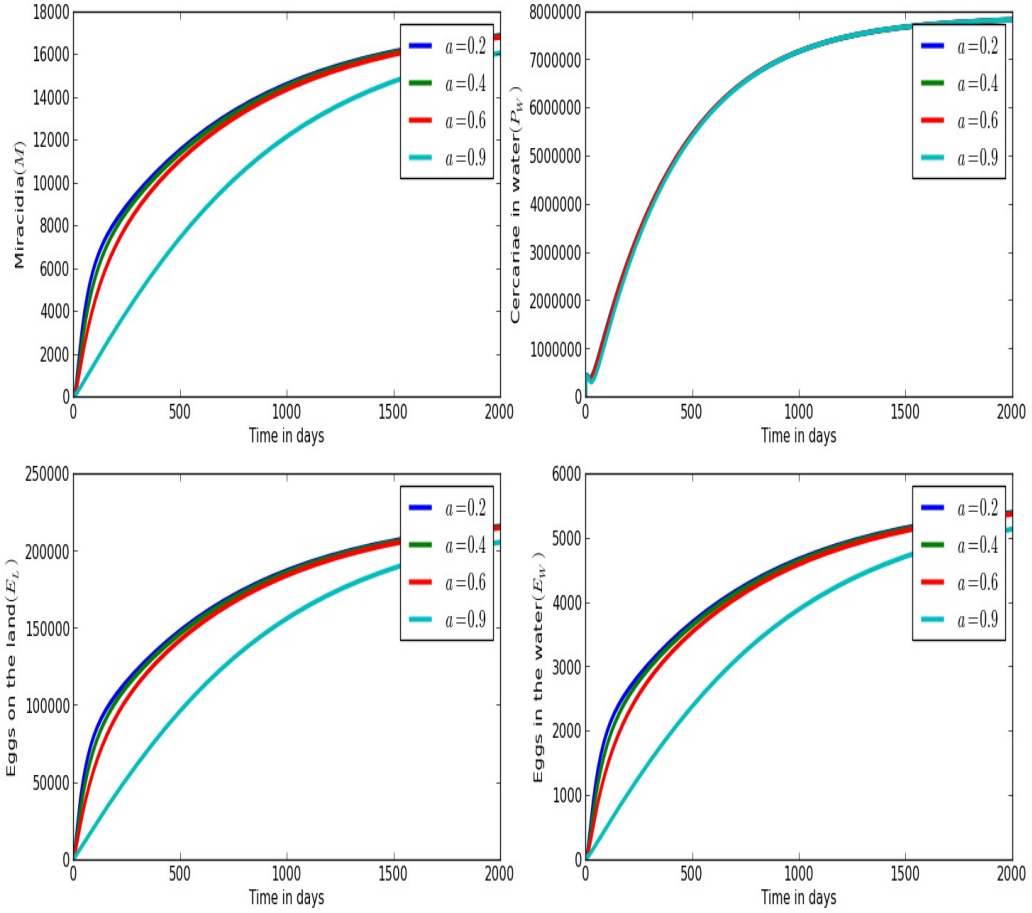

Figure 4.5: Numerical simulations showing the dynamics of eggs on the land (E_L), eggs in the water (E_W), miracidia (M) and cercariae in water (P_W) over time in days for different values of efficacy of HEC in reducing human contact with unsafe water bodies $a:\ a = 0.9,\ a = 0.5,\ a = 0.3$ and $a = 0.1$,

Figure 4.5 shows that a reduction in the number of miracidia, cercariae in water, eggs on the land and eggs in the water as the efficacy of health education campaigns increases. This simply implies that if humans are not exposed to unsafe water bodies then they cannot contaminate the water which results to reproduction of eggs on the land and eggs in the water which leads to reproduction of more meracidia and cercariae in the water.

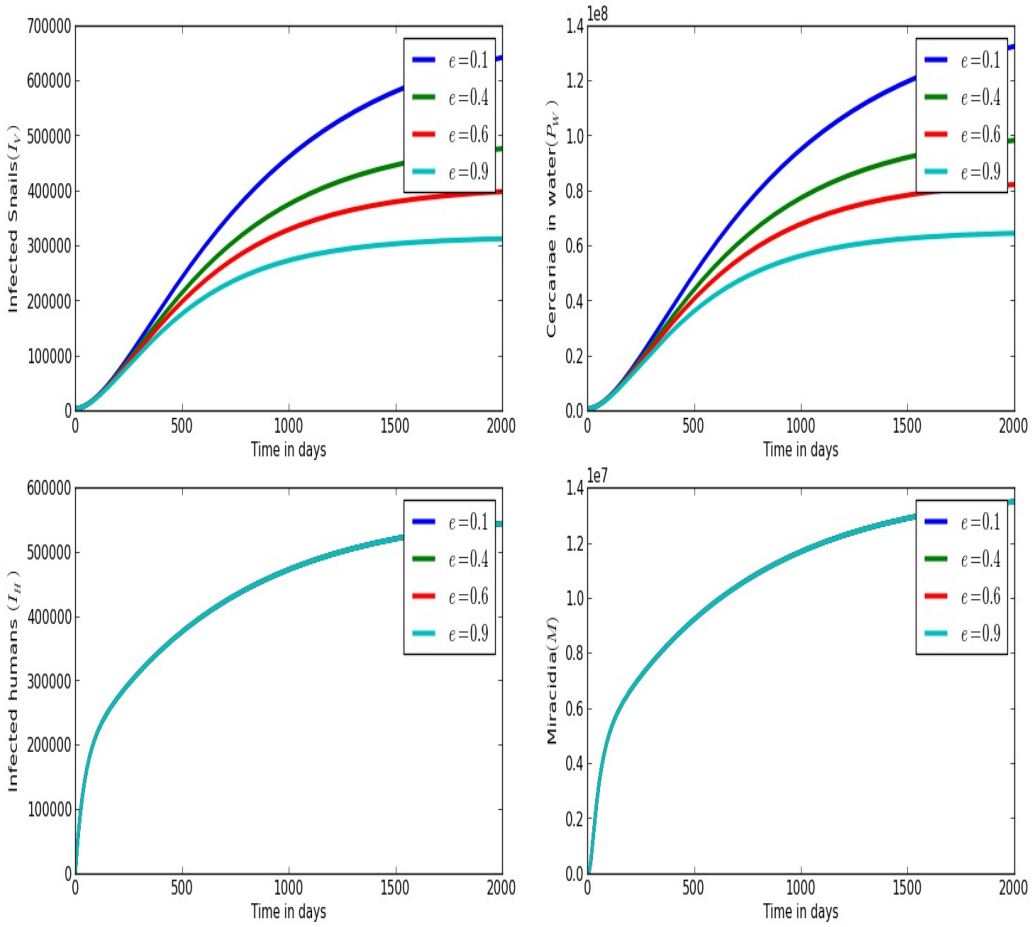

Figure 4.6: Numerical simulations of the dynamics of infected humans (I_H), infected snails (I_V), miracidia (M) and cercariae in water (P_W) over time in days for different values of efficacy mollucicides in killing snails e : $e = 0.1,\ e = 0.4,\ e = 0.6$ and $e = 0.9$.

Figure 4.6 shows a decrease in the number of new infections in snail population and cercariae population while infected humans population and miracidia populations remain constant.

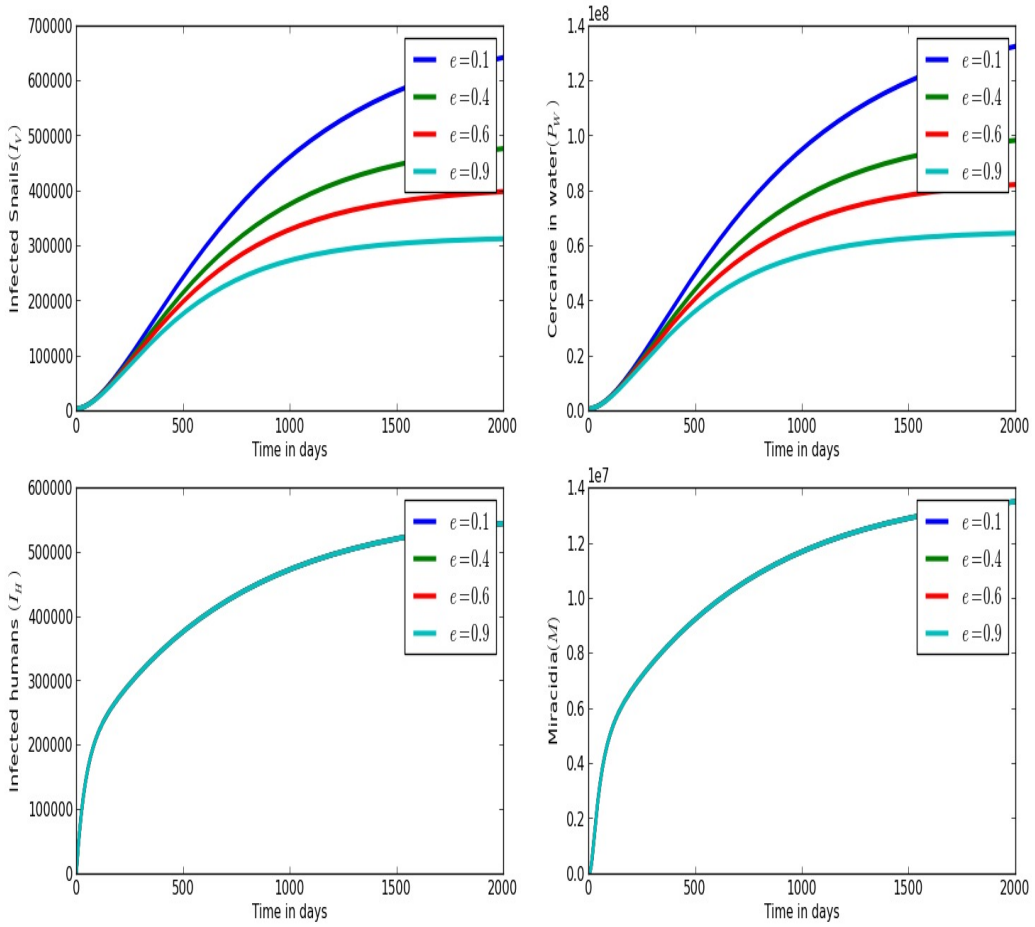

Figure 4.7: Numerical simulations showing dynamics of infected humans (I_H), infected snails (I_V), miracidia (M) and cercariae in water (P_W) over time in days for different values of efficacy mollucicides in killing snails $e:\ e = 0.1,\ e = 0.4,\ e = 0.6$ and $e = 0.9$, (model system 5.3.9).

Figure 4.7 shows that vector-control can be effective provided it is coupled with other control measures that can eliminate miracidia and reduce the number of infected humans with schistosomiasis.

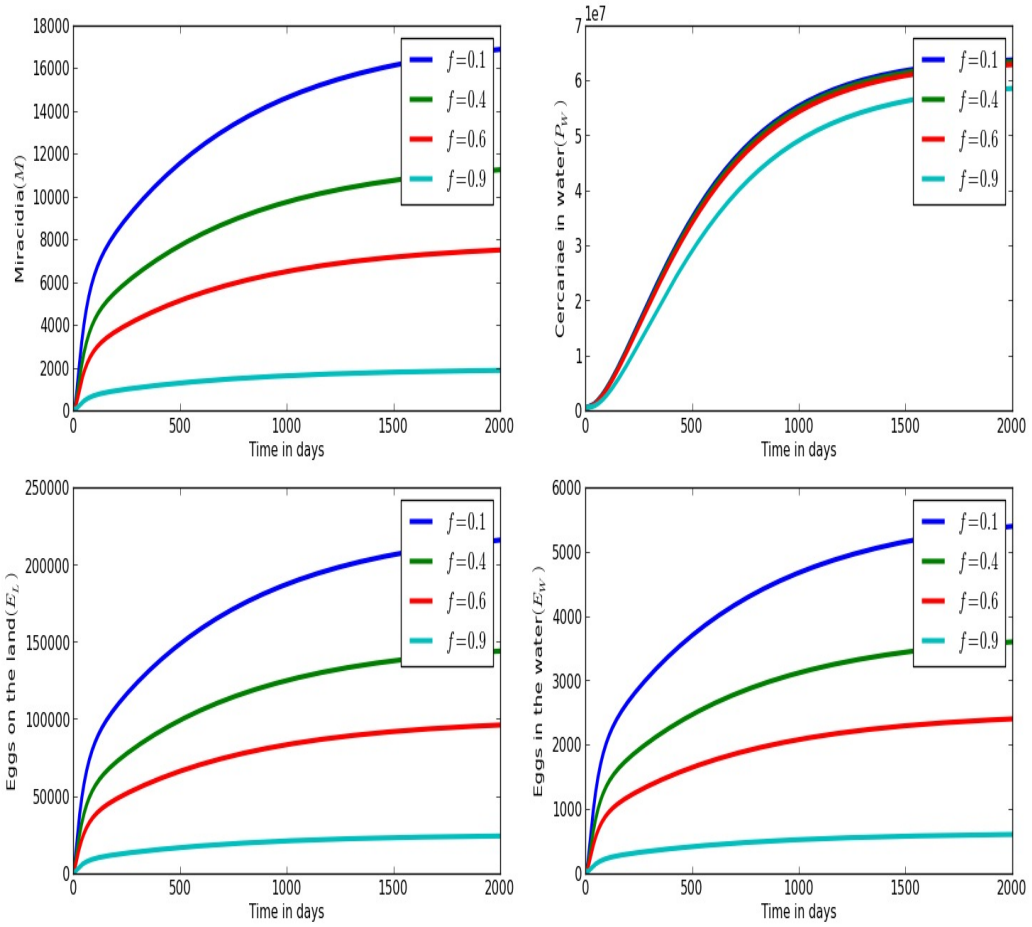

Figure 4.8: Numerical simulations showing dynamics of eggs on the land (E_L), eggs in the water (E_W), miracidia (M) and cercariae in water (P_W) over time in days for different values of efficacy of treatment in reducing schistosome eggs f : $f = 0.1$, $f = 0.4$, $f = 0.6$ and $f = 0.9$.

From Figure 4.8 we observe that miracidia, eggs on the land, eggs in the water reach stable steady state at the same time whereas cercariae in the water persists. This implies that treating infected individuals can only assist in reducing the number of miracidia, eggs on the land and eggs in the water. Control measure that can eliminate cercariae in the water should be implemented at the same time as treating infected individuals.

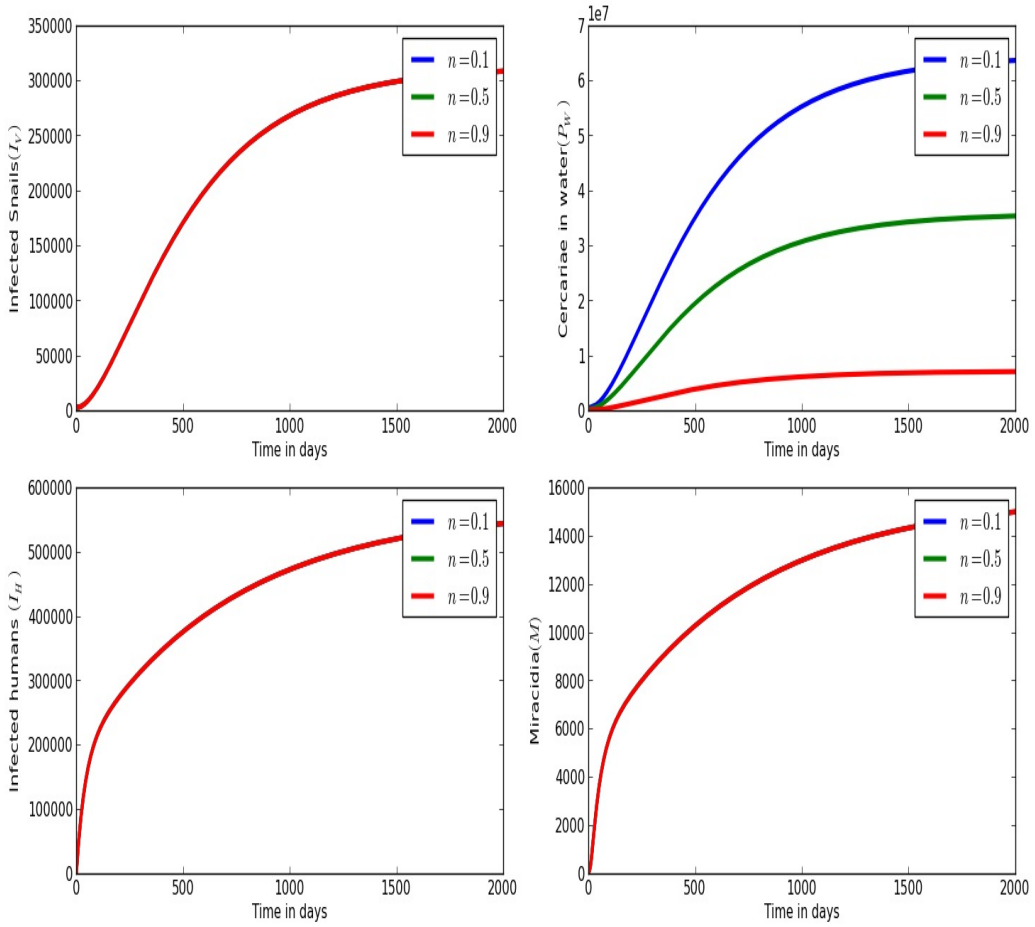

Figure 4.9: Numerical simulations showing dynamics of infected humans (I_H), infected snails (I_V), miracidia (M) and cercariae in water (P_W) over time in days for different values of efficacy of climate change in reducing cercariae production by each infected snail n : $n = 0.1,\ n = 0.4,\ n = 0.6$ and $n = 0.9$.

Figure 4.9 shows that increasing the efficacy of climate change in reduction of cercariae production by each infected snail will only reduce the cercariae population in the water but the infected snails, infected humans and miracidia populations remain constant. This implies that when implementing control measures all the sensitive epidemiological parameters must be taken into consideration.

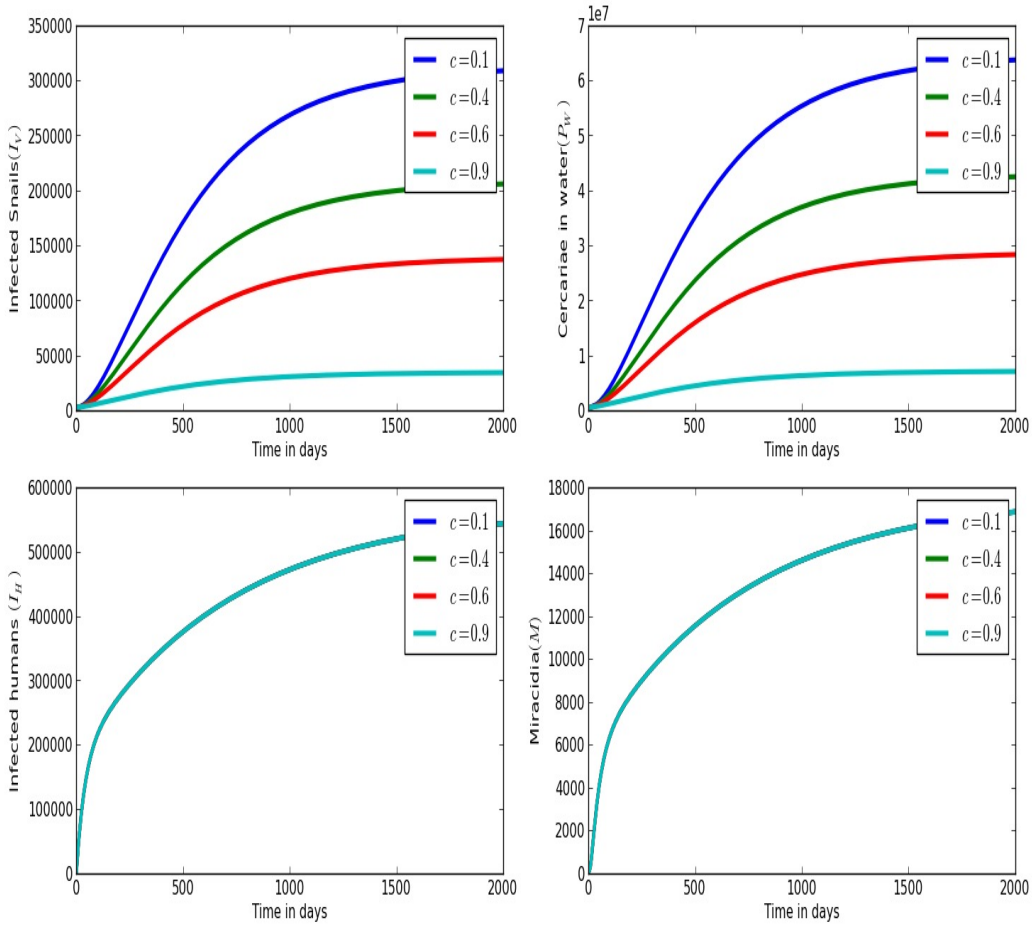

Figure 4.10: Numerical simulations showing dynamics of infected humans (I_H), infected snails (I_V), miracidia (M) and cercariae in water (P_W), over time in days for different values of efficacy of extreme weather changes in reducing snail production capacity c : $c = 0.1$, $c = 0.4$, $c = 0.6$ and $c = 0.9$.

From Figure 4.10 we observe that increasing the efficacy of extreme weather changes leads to a reducing in snail capacity. The reduction of snail production capacity by 90% can assist in reducing the cercariae production therefore the disease can be eradicated.

4.4 Summary

In this chapter, we first developed a mathematical model that monitors transmission dynamics of schistosome parasites in three different environments, namely, physical land environment, physical water environment and within-host environment for both human and snail populations. The compartmental model describes the dynamics of eight populations at any time t which are: susceptible humans, $S_H(t)$, and infected humans; $I_H(t)$, in the behavioural human environment; susceptible snails, $S_V(t)$; infected snails, $I_V(t)$ in the physical water environment; cercariae, $P_W(t)$; miracidia, $M(t)$; worm eggs on the physical land environment, $E_L(t)$; and worm eggs on the physical water environment, $E_W(t)$. This model is developed with a view of identifying the sensitive epidemiological parameters to be considered during control measures implementation. We investigated the mathematical properties of the model and established that the model is mathematically and epidemiologically well-posed. The sensitivity analysis results suggest that the reproductive number is more sensitive to snail mortality rate. Increasing snail mortality rate by 10% lead to a decline in the reproductive number, R_0, by 7%. The results suggest that more efforts have to focus on killing infected snails. We also obsevered that increasing the natural death rates and parasites saturations lead to a decline in R_0, though increasing either of these rates is neither practical nor ethical. In this case, natural control mechanisms can be the only option although their occurrence cannot be predicted. Other sensitive parameters include all the parameters associated with the disease transmission, recruitment rates, eggs on the land and in the water environments and parasites within infected hosts. Increasing either of theses rates by 10% lead to an increase in the reproductive number by 5%. Since there is a direct relationship between R_0 and these rates, it implies that decreasing these rates by 10% will eventually lead to a decrease in the R_0 by 5%. In this case, man-made control mechanisms can be applicable in reducing the transmission of schistosome parasites.

Lastly, we extended the basic model based on the most sensitive parameters. We also incorporated effectiveness of man-made and natural control mechanisms into the basic model. We determined the reproductive number and equilibrium points. Man-made control mechanisms include vector-control; treatment; improved sanitation associated with construction and toilets usage; good hygiene practices and proving endemic communities with human waste disposal systems; and conducting health education campaigns. The natural control mechanisms include extreme weather changes and climate change. We numerically confirmed that if man-made control mechanisms are simultaneously implemented, in particular, vector-control; treating infected individuals; conducting health education campaigns and improving sanitation; the disease can be controled and reduced. The same implies when health education campaigns and improved sanitation associated with construction and toilets usage are implemented. It is advisable to focus on

one category, especially the ones that are associated with the disease transmission, recruitment rates, eggs on the land and in the water environments and parasites within infected hosts and snail mortality when implementing control measures due to cost effectiveness. Implementing all the above man-made control mechanisms can cost a lot of money, as such, we can extend our model in order to include cost effectiveness and also base our study in a specific endemic area in order to make it more realistic. In the preceeding chapter, we extend this model in other to explicitly incorporate the within-host transmission dynamics that will result in embedded multi-scale model.

Chapter 5

Multi-scale Modelling of Environmentally Transmitted Vector-Borne Diseases

5.1 Introduction

The disciplinary separation of immunology, epidemiology of infectious diseases and environmental health have hampered progress on research of infectious diseases. Because of this disciplinary separation, traditional approaches to studying infectious diseases through mathematical modeling are largely based on the idea that diseases consist of dynamic processes across temporal, spatial and biological scales and that specific models can be developed to study a particular disease system at a particular scale. Two dominant disciplinary fields that address the modelling of subsystems relevant to the study of infectious diseases include mathematical modelling of between-host dynamics of infectious disease transmission (see [27]-[35] and references therein) (mathematical models of infectious disease transmission) and mathematical modelling of within-host dyanmics of infectious diseases (see [39]-[45] and references therein) (modelling pathogen-immune interactions). At the larger scale of mathematical modelling of between-host modelling of infectious diseases, models have been developed in the past to aid public health decision makers to make strategic decisions about control of infectious diseases (see for example [36]-[38] and references therein). The standard approach in these models is to classify the host population into compartments within which individuals behave homogeneously. These models have been used to aid understanding of the disease transmission dynamics and increase our capabilities for

control of infectious diseases with fewer resources. At the smaller scale (host-immune interactions level) of the within-host dynamics of infectious diseases, mathematical models have been developed to study the interaction of the pathogen and the immune system in order to elucidate the mechanisms and outcomes of infection within a single host (see for example [46] and references therein). These models are mainly based on ordinary differential equations describing the evolution in time of the number of immune cells, pathogens and target cells. However, we are still missing a general theory of how to link the within-host and between-host dynamics of infectious diseases. This situation has opened up gaps in knowledge and missed opportunities for understanding and predicting disease risks as well as designing interventions and preventive health programs. The general framework will greatly aid interpretation of data, and provide insight into a number of issues pertaining to infectious diseases such as persistence of infection, virulence and infectivity. From a theoretical point of view, the most appropriate way to facilitate the task of linking within-host and between-host dynamics of infectious diseases is to identify in each sub-system variables or parameters that affect the dynamics of the other sub-system, and then design a feedback of these variables or parameters across models in a consistent way. Therefore, capturing how the dynamics at a given scale affect and are affected by those at the other scale is the specific challenge at hand in the mathematical modelling of linked within-host and between-host dynamics of infectious diseases. Recent efforts to link the within-host and between-host dynamics of infectious diseases include [47]-[72]. In the context of deterministic mathematical modelling, we have, to date witnessed the development of four different coupling principles that organize and inform the research that lead to linked mathematical models of the within-host and between-host dynamics of infectious diseases which are as follows.

1. **Linked through nesting principles**: Here the linking of the within-host and between-host models is achieved through a nested modeling approach [53]-[62]. This is done in three stages. The first step in this approach is to develop a within-host model. The second step is to define an epidemiological model (between-host model). The third and final step is to nest the within-host model within an epidemiological model by linking the dynamics of the within-host model to the epidemiological model through either a structural variable or parameter of the epidemiological model. In the case of linking a within-host dynamics to an epidemiological model through a structural variable (of the epidemiological model), the epidemiological model must be structured through time-since-infection [60]. The time since-infection is then used as an independent variable in the immunological model, which is valid only in the infected epidemiological model compartment. In the case of linking within-host dynamics model to an epidemiological model through parameters, the parameters of the epidemiological model are expressed as functions of the dependent variables of the immunological model (within-host model). For example, transmission rate may be

assumed to be a function of the parasite load, or disease induced mortality may be assumed to be a function of the parasite load and the immune system [59].

2. **Linked through network modeling principles**: This modeling framework is achieved through developing a within-host model first and then modify this model by placing each individual in the population within a simple randomly distributed network of N people such that the pathogen load variable of a given individual is linked with the pathogen load variable of adjacent individuals within the network [61]-[63]. This is achieved by making an assumption that the rate at which a person's incoming flow of free pathogen particles is proportional to the pathogen load of their neighbours.

3. **Linked through developing a within-host inspired between-host model**: In this modeling framework, the link is based on developing a physiologically structured epidemiological model [65]-[71]. The physiological aspect normally considered here is cellular and their genetic variations (immune response) and how they modulate infection and disease progression. Very often, this task is accomplished through subdividing the entire population of the hosts into various sub-classes corresponding to different levels of immune protection: naive or completely susceptible, completely or partially immune, vaccinated, immune compromised (e.g. due to HIV co-infection) or protected from infection due to certain genetic factors. Modelling the dynamics of the distribution of humans with regard to their immune status in this way is a critical step in understanding the relationship between the dynamics of recurrent infections and the dynamic variability of the acquired immunity to these diseases within a host population [70].

4 **Linked through environmental contamination**: This is the case for infections with free-living pathogens growing in the environment [72]. In this case, the disease triad: host, pathogen and a contaminated environment (such as water, air, food, soil, objects or contact surfaces) must be present and interact appropriately for the infectious disease to occur. The linking here of within-host and between-host dynamics is based on the idea that disease process time-scales here can be separated into three distinct times scales. The first disease process time scale is at the within-host (individual host) level. It is related to the reproductive cycle of the pathogen within the host and its interaction with the host immune system. This disease process typically occurs on a fast time-scale. The second disease process time-scale is the one associated with infection between individuals, that is, the epidemiological time-scale (between-host time scale) that takes place according to contacts of susceptible hosts and the free-living pathogen in the environment. This disease process typically occurs at an intermediate time-scale. The third disease process time-scale is the environmental time-scale. For infections with free-living pathogens in the environment,

the environment is an important driver. For such infections, the pathogen may survive in the environment for some time, and further, the abundance of the pathogen in the environment is occasionally replenished by infectious hosts that excrete the pathogen into the environment. This disease process typically occurs at a slow time-scale. This third disease process time-scale is the key to providing a functional link for with-host and between-host models of infectious diseases. We show in this work that the linking of within-host model and between-host model which is structured by both pathogen load within an infected host and the density/number of infected/infectious hosts. This linking approach of within-host and between-host models has been previously proposed in [72] based on an arbitrary functional form. Using human schistosomiasis as an example, we demonstrate the approach here based on explicit consideration of the biology of the disease. The focus in this chqpter is on clarifying the determination of the functional form of the linkage between the within-host and between-host disease dynamics and how this encapsulates the underlying biology of the disease process.

The obvious distinction between models for other diseases and those infectious diseases with free-living pathogens in the environment is that the latter usually have at least one extra equation describing the dynamics of parasite in the environment. From a theoretical point of view, this chapter is about the role this extra equation plays in linking the within-host and between-host dynamics of infectious diseases with free living pathogens in the environment.

5.2 Transmission of Infectious Diseases That Are Environmentally Trasmitted

For infectious diseases that are environmentally transmitted, the environmental influences (biological, geophysical, economic and social) on disease transmission chains are fundamental to understanding these complex diseases. An estimated 24% of the global disease burden and 23% of death can be attributed to environmental factors [73]-[79]. Infectious diseases with the largest absolute burden attributable to modifiable environmental factors include diarrhea, lower respiratory infections and malaria [73]-[76]. To reflect on the idea that the environment serves as a reservoir of infectious free-living pathogens for infection of human, animals and plants [80]-[81], we hypothesize four different groups of transmission cycles that result in infections with the environment acting as a reservoir of infectious free-living pathogens. Figure 5.1 is a conceptual representation of the four different groups of transmission cycles for infections with free-living pathogens in the environment. The first group (see Figure 5.1(a)) includes infectious diseases

for which the environment (e.g. food, water, air, soil) play a significant role in the pathogen transmission cycle. Here transmission occurs between humans and the environment directly. No other host animal or vector are involved . The second group (see Figure 5.1(b)) still includes infectious diseases for which the environment (as in the first group) still plays a significant role in the pathogen's transmission cycle. The difference with the first group is that although the environment still remains an integral part of the transmission chain, an animal host mediates the transmission. The third group (see Figure 5.1(c)) still includes infectious diseases for which the environment (as in the second group) still plays a significant role in the transmission cycle. The difference with the second group is that although the environment still remains an integral part of the transmission chain, a vector (instead of an animal host) mediates the transmission. The fourth group (see Figure 5.1(d)) includes some pathogens that cause zoonotic diseases. Here humans are the dead end hosts and no person-to-person transmission is possible. The group includes non-vector-borne zoonotic diseases in which pathogens are transmitted indirectly through the environment or directly from a host to the human.

Human schistosomiasis was chosen in this study as a conceptual framework for the mathematical modelling of linked within-host and between-host dynamics of infections with free-living pathogens in the environment partly because of the simplicity of its transmission chain where the human and snail hosts do not interact with each other directly except through the shared schistosome parasites (see Figure 5.1(c)) in the physical water environment and also partly because of the availability of preliminary work on single scale modeling approaches [45, 84] of human schistosomiasis infection in an appropriate form for infections with free-living pathogens in the environment.

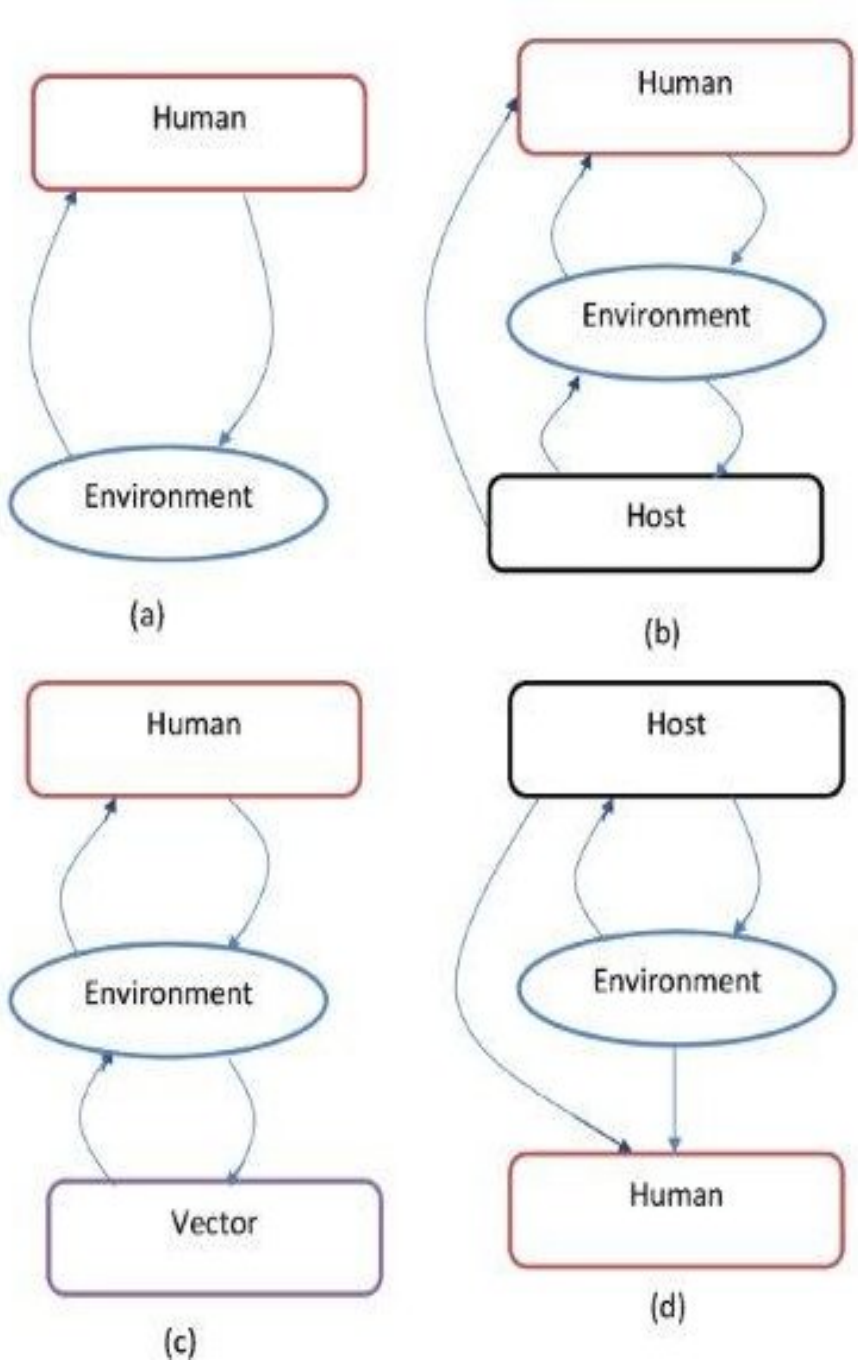

Figure 5.1: A conceptual diagram showing the four different groups of transmission cycles for infections that are environmentally trasmitted.

Human schistosomiasis, mediated by the water-borne schistosome parasite is a global health concern, being the third most devastating tropical disease in the world after malaria and intestinal helminthiasis [86]-[92]. Most schistosomiasis infections occur in resource-limited settings with

more than 200 million people being infected with schistosomiasis of which 85% live in Africa, while globally an estimated 200 000 deaths are attributable to schistosomiasis annually [89, 92]. The major forms of human schistosomiasis are caused by species of the water-borne flatworm or blood flukes called schistosomes, but the three most commonly found are *Schistosoma mansoni*, *Schistosoma japonicum*, and *Schistosoma haematobium*. *Schistosoma haematobium* affects the urinary tract and kidneys, as well as the reproductive systems and is concentrated in Africa and the Middle East. *Schistosoma mansoni* is the most widespread while *Schistosoma japonica* is primarily found in Asia and these two cause chronic hepatic and intestinal fibrosis [89]. The life cycle of the schistosome parasite is complex [86]-[92]. The complexity of the life cycle of the schistosome parasite includes three factors: (a) multiple interacting hosts (human and snail hosts), (b) multiple infective pathogenic species (miracidia and cercariae), and (c) structural complexity of the environmental domains (biological, geographical, economic, and social) in which transmission occurs. For more information about the complex life cycle of human schistosomiasis the published works [86]-[92] provide more details. Only a brief description is provided in this section.The reproductive cycle of schistosomiasis starts with parasitic worm eggs released into freshwater through faeces and urine. The schistosome eggs produced by the sexual stage leave people via urine or faeces, reach freshwater, shed their shells and hatch a ciliated free-swimming larva called a miracidium that seek out to infect certain species of snail that serve as intermediate host [92]. A miracidium that locates an appropriate species and genotype snail, penetrates and infects it, multiplies asexually through two larval stages into thousands of free-living cercariae that escape the snail and live in water. The infected snails release cercariae 4-6 weeks after infection [89]. The cercariae swim until they encounter a skin of suitable warmth and smell, and infect humans by direct penetration of the skin. Once the cercariae penetrate the skin, they lose their tails and differentiate into larval forms called schistosomulae.

A schistosomulum spends several days in the skin before exiting via blood vessels traversing to the lung, where it undergoes further developmental changes. It then migrates via the systematic circulation to the liver where it settles, reaches sexual maturity and pairs. Only those worm pairs that reach the portal system of the liver mature into adults [89]. Thereafter, worm pairs migrate by the bloodstream to their definitive location; S. mansoni and S. japonicum to the small and large intestines and S. haematobium to the bladder and rectal veins [89]. The worms lay thousands of eggs that cause damage as they work through tissues. The eggs, which are highly antigenic and can induce an intense granulomatous response, migrate through the bowel or bladder wall to be shed via faeces or urine. The eggs, released into the water in urine or faeces, restart the cycle.

5.3 Multi-scale Model of schistosomiasis

The model that we formulate traces explicitly the life-cycle of the schistosome parasite in three different environments which are the physical water environment (which is also affected by the physical climatological environment), the physical land environment, the human biological environment (within-host parasite dynamics). The full model is based on monitoring the dynamics of the twelve populations at any time t which are susceptible humans $S_H(t)$, and infected humans $I_H(t)$ in the behavioural human environment, susceptible snails $S_V(t)$ and infected snails $I_V(t)$ in the physical water environment, cercariae $P_W(t)$, miracidia $M(t)$ and worm eggs $E_W(t)$, in the physical water environment, cercariae $P_H(t)$, immature schistosome worms $W_I(t)$, mature schistosome worms $W_P(t)$ and worm eggs $E_H(t)$ in the biological human environment (within host parasite dynamics) and worm eggs $E_L(t)$, in the physical land environment. The model follows embedded multi-scale modelling approach, whereby within-host and between-host scales instigate each other. A summary of model variables is given in table 5.1 here, while a summary of parameter values is given in tables 5.2, 5.3 and 5.4 in section 5.5.

Variable	**Variable Description**	**Initial Value**	
$S_H(t)$:	The susceptible human population size in the behavioural human environment	200,000	
$I_H(t)$:	The infected human population size in the behavioural human environment	2000	
$S_V(t)$:	The susceptible snail population size in the physical water environment	40,000	
$I_V(t)$:	The infected snail population size in the physical water environment	3000	
$P_H(t)$:	The cercariae population size in the biological human environment	200	
$W_I(t)$:	The immature worm population size in the biological human environment	30	
$W_P(t)$:	The mature worm population size in the biological human environment	0	
$E_H(t)$:	The worm eggs population size in the biological human environment	0	
$E_L(t)$:	The worm eggs population size in the physical land environment	40	
$E_W(t)$:	The worm eggs population size in the physical water environment	40	
$M(t)$:	The miracidia population size in the physical water environment	20	
$P_W(t)$:	The cercariae population size in the physical water environment	50	

Table 5.1: Summary of variables used in the model

We make the following assumptions for the model:

i. There is no vertical transmission of the disease.

ii. The transmission of the disease in the snail and human populations is only through contact with infective free-living pathogens (miracidia, $M(t)$ and cercariae $P_W(t)$ respectively) in the physical water environment.

iii. There is no immigration of infectious humans.

iv. Seasonal and weather variations do not affect snail populations and contact patterns.

v. Infected snails do not reproduce due to castration by the miracidia.

vi. There is no immune response in both snail and human populations.

vii. The human host is assumed to be healthy, has not been previously exposed to the disease and has no immunity to infection.

viii. Infected snails and humans do not recover naturally from the infection/disease.

ix. Mature worms $W_P(t)$, migrate from the liver only as pairs and that those that fail to locate a partner will, with time, die a natural death and therefore will not participate in producing eggs, making their contribution to pathology irrelevant.

x. When a mature worm dies, its former partner does not re-mate, and the contribution of the pair to pathology is lost, so we assume a pair death for mature worms for simplicity.

At any time t, new recruits enter the human and snail populations through birth at constant rates Λ_H and Λ_V respectively. There is a constant natural death rate μ_H and μ_V in the human and snail populations respectively. Infected human hosts have an additional mortality of δ_H. Similarly, infected snails have an additional mortality δ_V. $N_H(t)$ is the total human population and is given by

$$N_H(t) = S_H(t) + I_H(t). \tag{5.3.1}$$

Susceptible humans acquire schistosomiasis through infection by cercariae in the physical water environment at rate $\lambda_H(t)$ where

$$\lambda_H(t) = \frac{\beta_H P_W(t)}{P_0 + \epsilon P_W(t)}, \tag{5.3.2}$$

with β_H being the maximum rate of exposure; ϵ is the limitation of growth velocity of cercariae with the increase of cases; P_0 is the half saturation constant. From the functional response, we notice that at low parasite densities, contacts are directly proportional to host densities.

$N_V(t)$ is the total snail population and is given by

$$N_V(t) = S_V(t) + I_V(t). \tag{5.3.3}$$

Similarly, susceptible snails acquire schistosomiasis through infection by miracidia in the physical water environment at rate $\lambda_V(t)$ where

$$\lambda_V(t) = \frac{\beta_V M(t)}{M_0 + \epsilon M(t)}, \tag{5.3.4}$$

with β_V being the maximum rate of exposure; ϵ is the limitation of growth velocity of miracidia with the increase of cases; M_0 is the half saturation constant. From the functional response, we also notice that at low parasite densities, contacts are directly proportional to host densities.

Considering the average cercariae population within a single infected human host $P_H(t)$, we note that this population is generated following uptake of cercariae through cercariae skin penetration of the human host. In the general population, this uptake of cercariae through skin penetration is actually the transmission of the cercariae pathogen from the physical water environment to susceptible humans at a rate of $\lambda_H(t)S_H(t)$ resulting in $I_H(t)$ infected humans. Therefore, in general, a single susceptible human host will uptake cercariae at an average rate of

$$\frac{\lambda_H(t)S_H(t)}{I_H(t)}, \tag{5.3.5}$$

where $\lambda_H(t)$, $S_H(t)$ and $I_H(t)$ are as defined previously. In our modelling of the mean cercariae population within a single infected human host $P_H(t)$, we further assume that the event of cercariae uptake through skin penetration of a single human host in a population with $S_H(t)$ susceptible humans, $I_H(t)$ infected humans and $P_W(t)$ cercariae load happens through a single transition defined by

$$(S_H(t), I_H(t), P_W(t)) \longrightarrow (S_H(t)-1, I_H(t)+1, P_W(t)) = (S_h(t), I_h(t), P_W(t)). \tag{5.3.6}$$

Therefore, the average rate of uptake of cercariae by a single susceptible human host through skin penetration is modelled by $\lambda_h(t)S_h(t)$ resulting in one infected human host where

$$\lambda_h(t) = \frac{\beta_H P_W(t)}{(P_0 + \epsilon P_W(t))I_h(t)}, \qquad S_h(t) = S_H(t) - 1, \quad I_h(t) = I_H(t) + 1. \tag{5.3.7}$$

where β_H, ϵ and P_0 remain as in the previous definitions.

This implies that the mean cercariae population within a single infected human host $P_H(t)$, increases at a variable mean rate given by

$$\frac{\lambda_H(t)S_h(t)}{I_h(t)} = \lambda_h(t)S_h(t). \tag{5.3.8}$$

Skin penetration by cercariae causes a local inflammatory response evidenced by a rash, called swimmer's itch, which is believed to involve immediate and delayed hypersensitivity reactions. The mean cercariae population within a single infected human host $P_H(t)$, is assumed to decay through natural death at a constant rate μ_C and to exit the skin to the lung via blood vessels at a rate α_C, where they undergo developmental changes to become immature worms.

The mean population of immature worms $W_I(t)$, within a single infected human host is generated following developmental changes undergone by cercariae to become immature worms at a rate α_C. These immature worms are assumed to die naturally at a rate μ_I and migrate to the liver at a rate α_I.

The mean population of mature worms $W_P(t)$, within a single infected human host is generated following developmental changes undergone by immature worms to become mature worms at a rate $\frac{\alpha_I}{2}$. These developmental changes result in immature worms reaching sexual maturity, pairing up and then migrating, through the blood stream to their definitive locations. The introduction of the fraction $\frac{1}{2}$ multiplying the parameter α_I models the pairing of immature worms on reaching sexual maturity. We assume that mature worms die naturally at a rate μ_P and migrate to their definitive locations at a rate α_P.

The mean population of schistoma eggs $E_H(t)$, within a single infected human host is generated through each worm pair laying an average of N_P eggs per day having migrated to its definitive location at a rate α_P. We model the rate at which these eggs die inside the human body by the parameter μ_E and the rate at which they are excreted by the human host into the physical land environment by α_E.

The population of schistoma eggs $E_L(t)$, contaminating the physical land environment is generated following excretion of schistoma eggs by the human host in either urine or faeces into the physical land environment. We note that each infected human host excretes these eggs at a rate $\alpha_E E_H(t)$ and for a total of $I_h(t)$ infected humans, the rate of contamination of the physical land environment by schistoma eggs becomes $I_h(t)\alpha_E E_H(t)$. These schistoma eggs are assumed to die naturally at a rate μ_L and to be washed away by running water into the physical water environment at a rate α_L.

The population of schistoma eggs $E_W(t)$, in the physical water environment is generated following inflow of schistoma eggs in running water from the contaminated physical land environment into the physical water environment at a rate α_L. We assume that these eggs die naturally in the physical water environment at a rate μ_W and hatch at a rate α_W releasing miracidia into the physical water environment.

The population of miracidia $M(t)$, in the physical water environment is generated through each egg hatching an average of N_W miracidia with eggs hatching at an average rate of α_W so that the total miracidia population in the physical water environment is modelled by $N_W \alpha_W E_W$. We assume that miracidia in the physical water environment die naturally at a rate μ_M.

The cercariae population $P_W(t)$, in the physical water environment, is generated through shedding of cercariae by infected snails at an assumed rate of $N_S \gamma_S$, where N_S is the number of

cercariae shed by each snail per day and γ_S is the rate at which infected snails become cercariae shedding. These cercariae are further assumed to have an average life span of $\frac{1}{\mu_S}$. Putting together the above formulations and assumptions gives the following system of differential equations:

$$\begin{cases} \frac{dS_H}{dt} = \Lambda_H - \lambda_H S_H - \mu_H S_H, \\ \frac{dI_H}{dt} = \lambda_H S_H - (\mu_H + \delta_H) I_H, \\ \frac{dS_V}{dt} = \Lambda_V - \lambda_V S_V - \mu_V S_V, \\ \frac{dI_V}{dt} = \lambda_V S_V - (\mu_V + \delta_V) I_V, \\ \frac{dP_H}{dt} = \lambda_h S_h - (\alpha_C + \mu_C) P_H, \\ \frac{dW_I}{dt} = \alpha_C P_H - (\alpha_I + \mu_I) W_I, \\ \frac{dW_P}{dt} = \frac{\alpha_I}{2} W_I - (\alpha_P + \mu_P) W_P, \\ \frac{dE_H}{dt} = N_P \alpha_P W_P - (\alpha_E + \mu_E) E_H, \\ \frac{dE_L}{dt} = I_h \alpha_E E_H - (\alpha_L + \mu_L) E_L, \\ \frac{dE_W}{dt} = \alpha_L E_L - (\alpha_W + \mu_W) E_W, \\ \frac{dM}{dt} = N_W \alpha_W E_W - \mu_M M, \\ \frac{dP_W}{dt} = N_S \gamma_S I_V - \mu_S P_W. \end{cases} \tag{5.3.9}$$

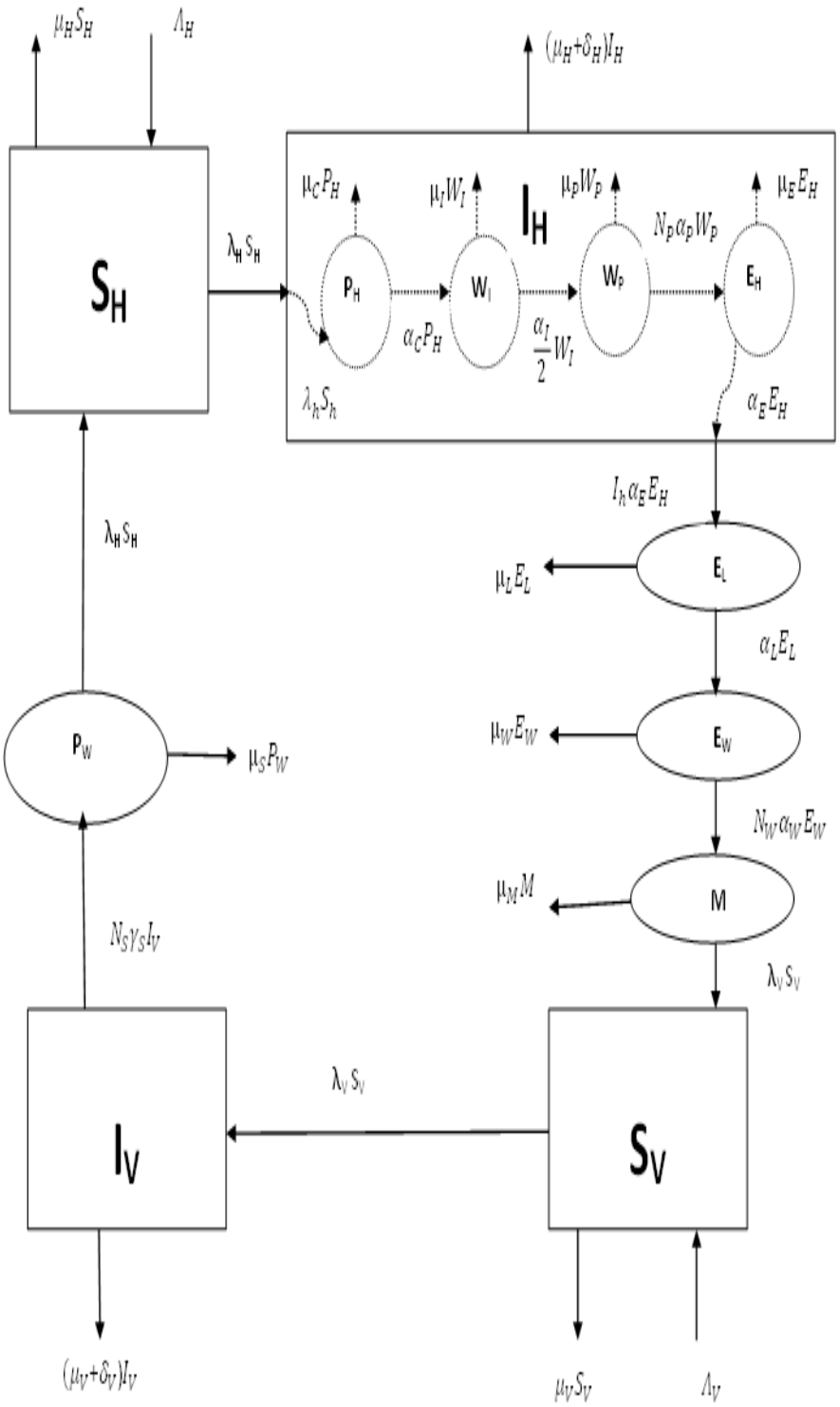

Figure 5.2: A conceptual diagram of the mathematical model of linked with-host and between-host dynamics of human schistosomiasis.

The model flow diagram is depicted in Figure 5.2, and the associated parameters are given in tables 5.2, 5.3 and 5.4 in 5.5.

5.3.1 Feasible Region of the Equilibria of the Model

All parameters and state variables for model system (5.3.9) are assumed to be non-negative to be consistent with human and animal populations. Further, it can be verified that for model system (5.3.9), all solutions with non-negative initial conditions remain bounded and non-negative.

Letting $N_H = S_H + I_H$ and adding equations (1) and (2) in system (5.3.9) gives

$$\frac{dN_H}{dt} \leq \Lambda_H - \mu_H N_H.$$

This implies that

$$\lim_{t\to\infty} \sup(N_H(t)) \leq \frac{\Lambda_H}{\mu_H}. \tag{5.3.1}$$

Similarly, letting $N_V = S_V + I_V$ and adding equations (3) and (4) in system (5.3.9) gives

$$\frac{dN_V}{dt} \leq \Lambda_V - \mu_V N_V. \tag{5.3.2}$$

This implies that

$$\lim_{t\to\infty} \sup(N_V(t)) \leq \frac{\Lambda_V}{\mu_V}. \tag{5.3.3}$$

Using equations (5.3.1) and (5.3.3) similar expressions can be derived for the remaining model variables. Hence, all feasible solutions of system (5.3.9) are positive and eventually enter the invariant attracting region

$$\begin{aligned}\Omega \;=\; & ((S_H, I_H, S_V, I_V, P_H, W_I, W_P, E_H, E_L, E_W, M, P_W) : 0 \leq S_H + I_H \leq M_1, \\ & 0 \leq S_V + I_V \leq M_2,\;\; 0 \leq P_H \leq M_3,\;\; 0 \leq W_I \leq M_4, \\ & 0 \leq W_P \leq M_5,\;\; 0 \leq E_H \leq M_6,\;\; 0 \leq E_L \leq M_7, \\ & 0 \leq E_W \leq M_8,\;\; 0 \leq M \leq M_9,\;\; 0 \leq P_W \leq M_{10}),\end{aligned} \tag{5.3.4}$$

where

$$
\begin{cases}
M_1 = \dfrac{\Lambda_H}{\mu_H}, \\
M_2 = \dfrac{\Lambda_V}{\mu_V}, \\
M_3 = \dfrac{1}{\alpha_C + \mu_C}.M_{11}, \\
M_4 = \dfrac{\alpha_C}{\alpha_I + \mu_I}.\dfrac{1}{\alpha_C + \mu_C}.M_{11}, \\
M_5 = \dfrac{1}{2}.\dfrac{\alpha_I}{\alpha_P + \mu_P}.\dfrac{\alpha_C}{\alpha_I + \mu_I}.\dfrac{1}{\alpha_C + \mu_C}.M_{11}, \\
M_6 = \dfrac{N_P\alpha_P}{\alpha_E + \mu_E}.\dfrac{1}{2}.\dfrac{\alpha_I}{\alpha_P + \mu_P}.\dfrac{\alpha_C}{\alpha_I + \mu_I}.\dfrac{1}{\alpha_C + \mu_C}.M_{11}, \\
M_7 = \dfrac{\alpha_E}{\alpha_L + \mu_L}.\dfrac{N_P\alpha_P}{\alpha_E + \mu_E}.\dfrac{1}{2}.\dfrac{\alpha_I}{\alpha_P + \mu_P}.\dfrac{\alpha_C}{\alpha_I + \mu_I}.\dfrac{1}{\alpha_C + \mu_C}.M_{11}, \\
M_8 = \dfrac{\alpha_L}{\alpha_W + \mu_W}.\dfrac{\alpha_E}{\alpha_L + \mu_L}.\dfrac{N_P\alpha_P}{\alpha_E + \mu_E}.\dfrac{1}{2}.\dfrac{\alpha_I}{\alpha_P + \mu_P}.\dfrac{\alpha_C}{\alpha_I + \mu_I}.\dfrac{1}{\alpha_C + \mu_C}.M_{11}, \\
M_9 = \dfrac{N_W\alpha_W}{\mu_M}.\dfrac{\alpha_L}{\alpha_W + \mu_W}.\dfrac{\alpha_E}{\alpha_L + \mu_L}.\dfrac{N_P\alpha_P}{\alpha_E + \mu_E}.\dfrac{1}{2}.\dfrac{\alpha_I}{\alpha_P + \mu_P}.\dfrac{\alpha_C}{\alpha_I + \mu_I}.\dfrac{1}{\alpha_C + \mu_C}.M_{11}, \\
M_{10} = \dfrac{N_S\gamma_S}{\mu_S}.\dfrac{\Lambda_V}{\mu_V} \\
M_{11} = \dfrac{\beta_H\gamma_S\Lambda_V(\Lambda_H - \mu_H)}{(P_0\mu_S\mu_V + \epsilon N_S\gamma_S\Lambda_V)(\Lambda_H + \mu_H)}, \quad \text{for} \quad \Lambda_H > \mu_H.
\end{cases}
\tag{5.3.5}
$$

Thus, whenever $\Lambda_H > \mu_H$, Ω is positively invariant and attracting and it is sufficient to consider solutions of model system (5.3.9) in Ω. Existence, uniqueness and continuation results for system (5.3.9) hold in this region and all solutions starting in Ω remain there for all $t \geq 0$. Hence, model system (5.3.9) is mathematically and epidemiologically well-posed and it is sufficient to consider the dynamics of the flow generated by model system (5.3.9) in Ω. We shall assume in all that follows (unless stated otherwise) that $\Lambda_H > \mu_H$.

5.3.2 Determination of DFE and its Stability

The equilibrium states of the model are obtained by setting the right-hand side of system (5.3.9) to zero. The system admits two equilibrium states which are the disease-free equilibrium and the endemic state. At the disease-free equilibrium, there is no cercariae, miracidia, worms and eggs and hence no infection in the human and snail populations. Thus, the model system (5.3.9) has a disease-free equilibrium given by

$$\begin{aligned} E^0 &= \left(S_H^0, I_H^0, S_V^0, I_V^0, P_H^0, W_I^0, W_P^0, E_H^0, E_L^0, E_W^0, M^0, P_W^0\right), \\ &= \left(\frac{\Lambda_H}{\mu_H}, 0, \frac{\Lambda_V}{\mu_V}, 0, 0, 0, 0, 0, 0, 0, 0, 0\right). \end{aligned} \tag{5.3.1}$$

The key parameter in many epidemic models which identifies the most important factors in the disease transmission cycle is the basic reproductive number, R_0, which we calculate in the next section.

5.3.3 Reproductive Number

The reproductive number R_0, defined as the average number of secondary infections produced by a single infectious host, introduced into a totally susceptible population [95]-[100] is one of the most important tools in the analysis of disease outbreak. For most disease outbreaks, if $R_0 < 1$, then the outbreak will disappear with time, whereas if $R_0 > 1$, then the outbreak will persist at endemic levels. In the context of human schistosomiasis infection, the quantity R_0 defines the expected number human/snail schistosomiasis infections generated by a single human/snail during the entire period of infectiousness of the human/snail introduced in a completely susceptible human/snail population. Therefore, in this case R_0 quantifies transmission of schistosomiasis from human to human or snail to snail. This is because of the fact that starting from a single infected human, schistosomiasis has to go through a snail before it can infect another human. Similarly, starting from a single infected snail, schistosomiasis has to go through a human being before it can infect another snail. We use the next generation operator approach to calculate the

basic reproduction number [100]. Model system (5.3.9) can be written in the form

$$\begin{cases} \dfrac{dX}{dt} &= f(X,Y,Z), \\ \dfrac{dY}{dt} &= g(X,Y,Z), \\ \dfrac{dZ}{dt} &= h(X,Y,Z), \end{cases} \tag{5.3.1}$$

where

$$\begin{cases} X &= (S_H, S_V), \\ Y &= (I_H, I_V, P_H, W_I, W_P, E_H, E_L, E_W), \\ Z &= (M, P_W). \end{cases} \tag{5.3.2}$$

Components of X denote the number of susceptibles, while components of Y represent the number of infected individuals that do not transmit the disease. Components of Z represent the number of individuals capable of transmitting the disease. Following [100] we define $\tilde{g}(X^*, Z)$ by

$$\tilde{g}(X^*,Z) = (\tilde{g}_1(X^*,Z), \tilde{g}_2(X^*,Z), \tilde{g}_3(X^*,Z), \tilde{g}_4(X^*,Z), \tilde{g}_5(X^*,Z), \tilde{g}_6(X^*,Z), \tilde{g}_7(X^*,Z), \tilde{g}_8(X^*,Z)), \tag{5.3.3}$$

with

$$\begin{cases} \tilde{g}_1(X^*, Z) &= \dfrac{\beta_H \Lambda_H P_W}{\mu_H(\mu_H + \delta_H)(P_0 + \epsilon P_W)}, \\ \tilde{g}_2(X^*, Z) &= \dfrac{\beta_V \Lambda_V M}{\mu_V(\mu_V + \delta_V)(M_0 + \epsilon M)}, \\ \tilde{g}_3(X^*, Z) &= \dfrac{1}{\alpha_C + \mu_C}.F_H, \\ \tilde{g}_4(X^*, Z) &= \dfrac{1}{\alpha_I + \mu_I}.\dfrac{\alpha_C}{\alpha_C + \mu_C}.F_H, \\ \tilde{g}_5(X^*, Z) &= (\dfrac{1}{2}.\dfrac{1}{\alpha_P + \mu_P}.\dfrac{\alpha_I}{\alpha_I + \mu_I}.\dfrac{\alpha_C}{\alpha_C + \mu_C}.F_H, \\ \tilde{g}_6(X^*, Z) &= \dfrac{1}{2}, \dfrac{1}{\alpha_E + \mu_E}.\dfrac{N_P \alpha_P}{\alpha_P + \mu_P}.\dfrac{\alpha_I}{\alpha_I + \mu_I}.\dfrac{\alpha_C}{\alpha_C + \mu_C}.F_H, \\ \tilde{g}_7(X^*, Z) &= \dfrac{1}{2}.\dfrac{1}{\alpha_L + \mu_L}.\dfrac{\alpha_E}{\alpha_E + \mu_E}.\dfrac{N_P \alpha_P}{\alpha_P + \mu_P}.\dfrac{\alpha_I}{\alpha_I + \mu_I}.\dfrac{\alpha_C}{\alpha_C + \mu_C}.F_W, \\ \tilde{g}_8(X^*, Z) &= \dfrac{1}{2}.\dfrac{1}{\alpha_W + \mu_W}.\dfrac{\alpha_L}{\alpha_L + \mu_L}.\dfrac{\alpha_E}{\alpha_E + \mu_E}.\dfrac{N_P \alpha_P}{\alpha_P + \mu_P}.\dfrac{\alpha_I}{\alpha_I + \mu_I}.\dfrac{\alpha_C}{\alpha_C + \mu_C}.F_W, \end{cases} \tag{5.3.4}$$

where

$$\begin{cases} F_H &= \dfrac{\beta_H(\Lambda_H - \mu_H)(\mu_H + \delta_H)P_W}{\mu_H(\mu_H + \delta_H)(P_0 + \epsilon P_W) + \beta_H \Lambda_H P_W}, \\ F_W &= \dfrac{\beta_H(\Lambda_H - \mu_H)P_W}{\mu_H(P_0 + \epsilon P_W)}. \end{cases} \tag{5.3.5}$$

Let $A = D_Z h(X^*, \tilde{g}(X^*, 0), 0)$ and further assume that A can be written in the form $A = M - D$, where $M \geq 0$ and $D > 0$, a diagonal matrix. Then A becomes

$$A = \begin{bmatrix} -\mu_M & \dfrac{C_H}{P_0} \\ \dfrac{C_V}{M_0} & -\mu_S \end{bmatrix}, \tag{5.3.6}$$

where

$$C_H = \frac{1}{2}.\frac{N_W\alpha_W}{\alpha_W+\mu_W}.\frac{\alpha_L}{\alpha_L+\mu_L}.\frac{\alpha_E}{\alpha_E+\mu_E}.\frac{N_P\alpha_P}{\alpha_P+\mu_P}.\frac{\alpha_I}{\alpha_I+\mu_I}.\frac{\alpha_C}{\alpha_C+\mu_C}.\frac{\beta_H(\Lambda_H-\mu_H)}{\mu_H} \text{ and} \tag{5.3.7}$$

$$C_V = \frac{\beta_V N_S\gamma_S\Lambda_V}{\mu_V(\mu_V+\delta_V)}. \tag{5.3.8}$$

Since $A = M - D$, we deduce matrices M and D to be

$$M = \begin{bmatrix} 0 & \frac{C_H}{P_0} \\ \frac{C_V}{M_0} & 0 \end{bmatrix}, \qquad D = \begin{bmatrix} \mu_M & 0 \\ 0 & \mu_S \end{bmatrix}. \tag{5.3.9}$$

The basic reproductive number is the spectral radius (dominant eigenvalue) of the matrix MD^{-1}, that is,

$$R_0 = \rho(MD^{-1}). \tag{5.3.10}$$

In this case,

$$R_0 = \sqrt{\frac{C_H}{P_0\mu_S}.\frac{C_V}{M_0\mu_M}} = \sqrt{R_{0H}R_{0HS}} = \sqrt{R_{0WH}R_{0SH}R_{0HS}} \tag{5.3.11}$$

In equation 5.3.11, the quantity R_{0HS} is interpreted as follows. Consider a single newly infected human host entering a disease-free population of snails at equilibrium. This individual is still present and infectious and the expected number of snails infected by this human is approximately

$$R_{0HS} = \frac{\beta_V N_S\gamma_S\Lambda_V}{M_0\mu_M\mu_V(\mu_V+\delta_V)}. \tag{5.3.12}$$

Therefore, the human to snail transmission coefficient R_{0HS} is composed of between-host disease parameters only. Similarly, in equation 5.3.11, the quantity R_{0H} is interpreted as follows. Consider a single newly infected snail host entering a disease-free population of humans at equilibrium. This snail is still present and infectious and the expected number of humans infected by this snail is approximately

$$\begin{aligned} R_{0H} &= \frac{N_W\alpha_W}{\alpha_W+\mu_W}.\frac{\alpha_L}{\alpha_L+\mu_L}.\frac{1}{2}.\frac{\alpha_E}{\alpha_E+\mu_E}.\frac{N_P\alpha_P}{\alpha_P+\mu_P}.\frac{\alpha_I}{\alpha_I+\mu_I}.\frac{\alpha_C}{\alpha_C+\mu_C}.\frac{\beta_H(\Lambda_H-\mu_H)}{P_0\mu_H\mu_S}, \\ &= R_{0WH}R_{0SH}. \end{aligned} \tag{5.3.13}$$

From equation (5.3.13) we deduce that the snail to human transmission coefficient R_{0H} is a product of two other transmission coefficients which are the between-host (snail to human) transmission coefficient R_{0SH} and the within-host (within-human) R_{0WH} which are given by

$$R_{0SH} = \frac{N_W \alpha_W}{\alpha_W + \mu_W} . \frac{\alpha_L}{\alpha_L + \mu_L} . \frac{\beta_H (\Lambda_H - \mu_H)}{P_0 \mu_H \mu_S}, \tag{5.3.14}$$

and

$$R_{0WH} = \frac{1}{2} . \frac{\alpha_E}{\alpha_E + \mu_E} . \frac{N_P \alpha_P}{\alpha_P + \mu_P} . \frac{\alpha_I}{\alpha_I + \mu_I}, \frac{\alpha_C}{\alpha_C + \mu_C}, \tag{5.3.15}$$

respectively.

Therefore, the basic reproductive number R_0, given by

$$R_0 = \sqrt{R_{0WH} R_{0SH} R_{0HS}}. \tag{5.3.16}$$

is composed of both within-host and between-host disease parameters, and R_{0HS}, R_{0SH} and R_{0WH} are given by equations (5.3.12), (5.3.14) and (5.3.15) respectively.

From the expression for R_0 in equation (5.3.16) we make the following deductions.

a. The between-host transmission parameters (snail to human and human to snail) such as supply of new susceptible snails $N_S \gamma_S$ and humans Λ_H, contact rate between hosts (snails and humans) and infected waters β_V and β_H, the rate at which schistosome eggs in water hatch to become miracidia $N_W \alpha_W$, the rate at which infected snails contaminate the physical water environment with cercariae γ_S all contribute to the transmission of human schistosomiasis. Therefore, control measures such as killing of snails by use of molluscicides and reducing contact between the human and snail hosts and infected waters through educating the public may help to reduce human schistosomiasis transmission.

b. The within-host transmission parameters (within the human host) such as the rates at which (a) cercariae within the human host become immature worms α_C, (b) immature worms become mature worms $\frac{\alpha_I}{2}$, (c) mature worms lay eggs $N_P \alpha_P$ and the rates at which the cercariae within the human host and the worms die all contribute to the transmission of human schistosomiasis. Therefore immune mechanisms that kill cercariae and worms and destroy eggs within the human host and also treatment intended to kill mature worms may help to reduce human schistosomiasis transmission.

Therefore, we conclude that both epidemiological (between-host) and immunological (within-host) factors affect the transmission of human schistosomiasis.

5.3.4 Local Stability of DFE

From Theorem 4.2 of van den Driesche and Watmough [97], if the basic reproduction number R_0 is less than one, then the disease free equilibrium is locally asymptotically stable and the disease cannot invade the population. This is summarized in the following theorem.

Theorem 5.1. *The disease free equilibrium point E^0, of model system (5.3.9) is locally asymptotically stable whenever $R_0 < 1$ and unstable otherwise.*

Proof. The proof is not needed since local stability of the disease free equilibrium is a consequence of Theorem 4.2 in van den Driessche and Watmough [97].

5.3.5 Global Stability of DFE

Theorem 2 in [97] establishes that the disease free equilibrium is locally asymptotically stable whenever $R_0 < 1$ and unstable when $R_0 > 1$. In this section, we list two conditions that if met, also guarantee the global asymptotic stability of the disease free state. We write system (5.3.9) in the form:

$$\begin{cases} \dfrac{dX}{dt} &= F(X,Z), \\ \dfrac{dZ}{dt} &= G(X,Z), \qquad G(X,0)=0, \end{cases} \tag{5.3.1}$$

where $X = (S_H, S_V)$ comprises of the uninfected components and

$$Z = (I_H, I_V, P_H, W_I, W_P, E_H, E_L, E_W, M, P_W)$$

comprises of infected and infectious components.

$$E^0 = (X^*, 0) = \left(\frac{\Lambda_H}{\mu_H}, 0, \frac{\Lambda_V}{\mu_V}, 0, 0, 0, 0, 0, 0, 0, 0, 0\right)$$

denotes the disease free equilibrium of the system. To guarantee global asymptotic stability, the conditions $(H1)$ and $(H2)$ below must be met [100].

H1. For $\dfrac{dX}{dt} = F(X,0)$, X^* is globally asymptotically stable (g.a.s),

H2. $G(X,Z) = AZ - \hat{G}(X,Z)$, $\hat{G}(X,Z) \geq 0$ for $(X,Z) \in \mathbb{R}^+_{12}$ where $A = D_Z G(X^*, 0)$ is an M-matrix and R^+_{12} is the region where the model makes biological sense.

In our case,

$$F(X,0) = \begin{bmatrix} \Lambda_H - \mu_H S_H \\ \Lambda_V - \mu_V S_V \end{bmatrix}, \tag{5.3.2}$$

and

$$A = \begin{pmatrix} a_1 & 0 & 0 & 0 & 0 & 0 & 0 & 0 & 0 & \frac{\beta_H \Lambda_H}{P_0 \mu_H} \\ 0 & a_2 & 0 & 0 & 0 & 0 & 0 & 0 & \frac{\beta_V \Lambda_V}{M_0 \mu_V} & 0 \\ 0 & 0 & a_3 & 0 & 0 & 0 & 0 & 0 & 0 & \frac{\beta_H(\Lambda_H - \mu_H)}{P_0 \mu_H} \\ 0 & 0 & \alpha_C & a_4 & 0 & 0 & 0 & 0 & 0 & 0 \\ 0 & 0 & 0 & \frac{\alpha_I}{2} & a_5 & 0 & 0 & 0 & 0 & 0 \\ 0 & 0 & 0 & 0 & N_P \alpha_P & a_6 & 0 & 0 & 0 & 0 \\ 0 & 0 & 0 & 0 & 0 & \alpha_E & a_7 & 0 & 0 & 0 \\ 0 & 0 & 0 & 0 & 0 & 0 & \alpha_L & a_8 & 0 & 0 \\ 0 & 0 & 0 & 0 & 0 & 0 & 0 & N_W \alpha_W & -\mu_M & 0 \\ 0 & N_S \gamma_S & 0 & 0 & 0 & 0 & 0 & 0 & 0 & -\mu_S \end{pmatrix}. \tag{5.3.3}$$

where,

$$\begin{cases} a_1 &= -(\mu_H + \delta_H), \\ a_2 &= -(\mu_V + \delta_V), \\ a_3 &= -(\alpha_C + \mu_C), \\ a_4 &= -(\alpha_I + \mu_I, \\ a_5 &= -(\alpha_P + \mu_P), \\ a_6 &= -(\alpha_E + \mu_E), \\ a_7 &= -(\alpha_L + \mu_L), \\ a_8 &= -(\alpha_W + \mu_W). \end{cases} \tag{5.3.4}$$

$$\hat{G}(X,Z) = \begin{bmatrix} \left(\frac{\Lambda_H}{P_0\mu_H} - \frac{S_H}{P_0+\epsilon P_W}\right)\beta_H P_W \\ \left(\frac{\Lambda_V}{M_0\mu_V} - \frac{S_V}{M_0+\epsilon M}\right)\beta_V M \\ 0 \\ 0 \\ 0 \\ 0 \\ 0 \\ 0 \\ 0 \\ 0 \end{bmatrix}. \tag{5.3.5}$$

Since $S_H^0\left(=\frac{\Lambda_H}{\mu_H}\right)\frac{1}{P_0} \geq \frac{S_H}{P_0+\epsilon P_W}$ and $S_V^0\left(=\frac{\Lambda_V}{\mu_V}\right)\frac{1}{M_0} \geq \frac{S_V}{M_0+\epsilon M}$, it is clear that $\hat{G}(X,Z) \geq 0$ for all $(X,Z) \in \mathbb{R}_{12}^+$. It is also clear that matrix A is an M-matrix since the off diagonal elements of A are non-negative.We state a theorem which summarizes the above result.

Theorem 5.2. *The fixed point* $E^0 = \left(\frac{\Lambda_H}{\mu_H}, 0, \frac{\Lambda_V}{\mu_V}, 0, 0, 0, 0, 0, 0, 0, 0, 0\right)$ *is a globally asymptotically stable (g.a.s) equilibrium of system (5.3.9) if* $R_0 < 1$ *and the assumptions* $(H1)$ *and* $(H2)$ *are satisfied.*

5.3.6 The Endemic Equilibrium State and its Stability

At the endemic equilibrium both humans and snails are infected by cercariae and miracidia respectively and the endemic equilibrium is given by

$$E^* = (S_H^*, I_H^*, S_V^*, I_V^*, P_H^*, W_I^*, W_P^*, E_H^*, E_L^*, E_W^*, M^*, P_W^*). \tag{5.3.1}$$

We give expressions for the endemic equilibrium and their interpretations in the following subsections and also prove its existence.

5.3.7 The Endemic Equilibrium

The endemic value of susceptible humans is given by

$$S_H^* = \frac{\Lambda_H}{\mu_H + \lambda_H^*}. \tag{5.3.1}$$

We deduce from equation (5.3.1) that the equilibrium state associated with susceptible humans is proportional to the average time of stay in the susceptible compartment and the rate of supply of new susceptibles through birth. Individuals exit this compartment either through death or infection. The endemic value of infected humans is given by

$$I_H^* = \frac{\lambda_H^* S_H^*}{\mu_H + \delta_H} = \frac{\Lambda_H \lambda_H^*}{(\mu_H + \delta_H)(\mu_H + \lambda_H^*)}. \tag{5.3.2}$$

We note from equation (5.3.2) that the infected population at the endemic equilibrium is directly proportional to three quantities: the average time of stay in the infected compartment, the rate of infection of susceptibles and the number/density of susceptible hosts. The quantity of infected snails at endemic equilibrium is given by

$$S_V^* = \frac{\Lambda_V}{\mu_V + \lambda_V^*}. \tag{5.3.3}$$

Equation (5.3.3) implies that at equilibrium, the susceptible snail population equals the product of the average time of stay in this compartment and the rate of supply of new susceptibles through birth. At endemic equilibrium, the population of infected snails is given by

$$I_V^* = \frac{\lambda_V^* S_V^*}{\mu_V + \delta_V} = \frac{\Lambda_V \lambda_V^*}{(\mu_V + \delta_V)(\mu_V + \lambda_V^*)}. \tag{5.3.4}$$

Therefore, infected snail population's endemic equilibrium is a product of three quantities: the average life span of infected snails, the rate of infection of snails and the number/density of susceptible snails.

By setting

$$Z_H^* = \Lambda_H - (\mu_H + \lambda_H^*) > 0,$$

the endemic equilibria for P_H^*, W_I^*, W_P^*, E_H^*, E_L^*, E_W^* and M^* can be expressed in terms of this quantity as follows. The average population of cercariae within a single infected human host at endemic equilibrium is given by

$$P_H^* = \frac{\lambda_h^* S_h^*}{\alpha_C + \mu_C} = \frac{1}{\alpha_C + \mu_C} \cdot \frac{(\mu_H + \delta_H)\lambda_H^* Z_H^*}{\Lambda_H \lambda_H^* + (\mu_H + \delta_H)(\mu_H + \lambda_H^*)}. \tag{5.3.5}$$

The endemic equilibrium of the average cercariae population inside a single human host is directly proportional to the life span of cercariae within a single infected human host and the rate of infection of a single susceptible to become an infected human host. Thus immune pressures that

destroy cercariae within an infected human host reduce cercariae endemic equilibrium. This expression implies a link between within-host cercariae dynamics and human population dynamics. The population of immature worms within a single infected human host at endemic equilibrium is given by

$$W_I^* = \frac{\alpha_C P_H^*}{\alpha_I + \mu_I} = \frac{1}{\alpha_I + \mu_I} \cdot \frac{\alpha_C}{\alpha_C + \mu_C} \cdot \frac{(\mu_H + \delta_H)\lambda_H^* Z_H^*}{\Lambda_H \lambda_H^* + (\mu_H + \delta_H)(\mu_H + \lambda_H^*)}. \tag{5.3.6}$$

Therefore, the population of immature worms at endemic equilibrium increases with an increase in the average life-span of immature worms and the rate at which cercariae become mature worms. Therefore, treatment and immune responses focused on killing cercariae and immature worms reduce the endemic equilibrium associated with immature worms within a human host. The population of mature worms within a single infected human host at endemic equilibrium is given by

$$\begin{aligned} W_P^* &= \frac{1}{2} \cdot \frac{\alpha_I W_I^*}{\alpha_P + \mu_P}, \\ &= \frac{1}{2} \cdot \frac{1}{\alpha_P + \mu_P} \cdot \frac{\alpha_I}{\alpha_I + \mu_I} \cdot \frac{\alpha_C}{\alpha_C + \mu_C} \cdot \frac{(\mu_H + \delta_H)\lambda_H^* Z_H^*}{\Lambda_H \lambda_H^* + (\mu_H + \delta_H)(\mu_H + \lambda_H^*)}. \end{aligned} \tag{5.3.7}$$

We conclude from equation (5.3.7) that the rate at which paired immature worms become mature worms and the life-span of mature worms determine the level of endemic equilibrium associated with mature worms within a human host. There immune responses and treatment aimed at killing mature worms reduce the endemic equilibrium. The average schistosome egg population within a single infected human host at endemic equilibrium is given by

$$\begin{aligned} E_H^* &= \frac{N_P \alpha_P W_P^*}{\alpha_E + \mu_E}, \\ &= \frac{1}{2} \cdot \frac{1}{\alpha_E + \mu_E} \cdot \frac{N_P \alpha_P}{\alpha_P + \mu_P} \cdot \frac{\alpha_I}{\alpha_I + \mu_I} \cdot \frac{\alpha_C}{\alpha_C + \mu_C} \cdot \frac{(\mu_H + \delta_H)\lambda_H^* Z_H^*}{\Lambda_H \lambda_H^* + (\mu_H + \delta_H)(\mu_H + \lambda_H^*)} \end{aligned} \tag{5.3.8}$$

Equation (5.3.8) implies that at equilibrium the average schistosome egg population within an infected human host is directly proportional to the average egg life span and worm fecundity. Thus, immune responses which reduce worm fecundity and those that destroy eggs within an infected human host reduce the endemic equilibrium associated with worm eggs. The population of schistosome eggs on the physical land environment at the endemic equilibrium is given by

$$\begin{aligned} E_L^* &= \frac{\alpha_E E_H^*(I_H^*+1)}{\alpha_L+\mu_L}, \\ &= \frac{1}{2}.\frac{1}{\alpha_L+\mu_L}.\frac{\alpha_E}{\alpha_E+\mu_E}.\frac{N_P\alpha_P}{\alpha_P+\mu_P}.\frac{\alpha_I}{\alpha_I+\mu_I}.\frac{\alpha_C}{\alpha_C+\mu_C}.\frac{\lambda_H^* Z_H^*}{(\mu_H+\lambda_H^*)}. \end{aligned} \tag{5.3.9}$$

We deduce from equation (5.3.9) that the life span of eggs, the rate which each infected human host excrete schistosome eggs and the total number of humans infected by schistosomiasis all influence the endemic equilibrium associated with schistosome eggs in the physical land environment. Therefore, atopy aspects [64] reduce the endemic equilibrium of schistosome eggs in the physical land environment. The endemic equilibrium of schistosome eggs in the physical water environment at is given by

$$\begin{aligned} E_W^* &= \frac{\alpha_L E_L^*}{\alpha_W+\mu_W}, \\ &= \frac{1}{2}.\frac{1}{\alpha_W+\mu_W}.\frac{\alpha_L}{\alpha_L+\mu_L}.\frac{\alpha_E}{\alpha_E+\mu_E}.\frac{N_P\alpha_P}{\alpha_P+\mu_P}.\frac{\alpha_I}{\alpha_I+\mu_I}.\frac{\alpha_C}{\alpha_C+\mu_C}.\frac{\lambda_H^* Z_H^*}{(\mu_H+\lambda_H^*)} \end{aligned} \tag{5.3.10}$$

Equation (5.3.10) indicates that the endemic schistosome egg population in the physical water environment is influenced by the average life span of the eggs and the rate at which the eggs are transported into physical water environment by flowing water. Therefore, rainfall conditions which wash away the schistosome eggs into the physical water environment affect the transmission of human schistosomiasis. The endemic equilibrium value associated asociated with miracidia in the physical water environment is given by

$$\begin{aligned} M^* &= \frac{N_W\alpha_W E_W^*}{\mu_M}, \\ &= \frac{1}{2}.\frac{N_W\alpha_W}{\mu_M}.\frac{\alpha_L}{\alpha_L+\mu_L}.\frac{\alpha_E}{\alpha_E+\mu_E}.\frac{N_P\alpha_P}{\alpha_P+\mu_P}.\frac{\alpha_I}{\alpha_I+\mu_I}.\frac{\alpha_C}{\alpha_C+\mu_C}.\frac{\lambda_H^* Z_H^*}{(\mu_H+\lambda_H^*)} \end{aligned} \tag{5.3.11}$$

We note from equation (5.3.11) that the life span of miracidia and worm fecundity all directly influence the endemic levels of miracidia in the physical water environment. The circariae population in the physical water environment at endemic equilibrium is given by

$$P_W^* = \frac{N_S\gamma_S I_V^*}{\mu_S} = \frac{\Lambda_V N_S\gamma_S\lambda_V^*}{\mu_S\left(\mu_V+\delta_V\right)\left(\mu_V+\lambda_V^*\right)}. \tag{5.3.12}$$

From equation (5.3.12), we conclude that the life span of cerccariae in the physical water environment and the rate at which infected snails shed cercariae in the physical water environment

reduce the endemic equilibrium. Thus, interventions intended to kill snails, particularly infected snails reduce schistosomiasis transmission.

5.3.8 The Existence of the Endemic Equilibrium State

In this section we present some results concerning the existence of an endemic equilibrium or constant solution for model system (5.3.9). To do this we shall make use of a threshold parameter, which we have already denoted by R_0.

Theorem 5.3. *The model (5.3.9) formulated in terms of proportions has at least one endemic equilibrium solution given by*

$$E^* = (S_H^*, I_H^*, S_V^*, I_V^*, P_H^*, W_I^*, W_P^*, E_H^*, E_L^*, E_W^*, M^*, P_W^*)$$

with $S_H^*, I_H^*, S_V^*, I_V^*, P_H^*, W_I^*, W_P^*, E_H^*, E_L^*, E_W^*, M^*, P_W^*$ all non-negative, whose existence and properties are determined by the threshold parameter R_0 where

$$R_0 = \sqrt{\frac{N_S\gamma_S\beta_V\Lambda_V}{\mu_V\mu_M M_0(\mu_V+\delta_V)}.\frac{\alpha_C}{\alpha_C+\mu_C}.\frac{\alpha_I}{\alpha_I+\mu_I}.\frac{N_P\alpha_P}{\alpha_P+\mu_P}.\frac{\alpha_E}{\alpha_E+\mu_E}.\frac{\alpha_L}{\alpha_L+\mu_L}.\frac{N_W\alpha_W}{\alpha_W+\mu_W}.\frac{\beta_H(\Lambda_H-\mu_H)}{2P_0\mu_H\mu_S}}. \tag{5.3.1}$$

Proof. Let $E^* = S_H^*, I_H^*, S_V^*, I_V^*, P_H^*, W_I^*, W_P^*, E_H^*, E_L^*, E_W^*, M^*, P_W^*$ be a constant solution of the model system (5.3.9) . We can easily express $S_H^*, I_H^*, S_V^*, P_H^*, W_I^*, W_P^*, E_H^*, E_L^*, E_W^*, M^*, P_W^*$ in terms of I_V^* in the form

$$
\begin{cases}
S_H^*(I_V^*) &= \dfrac{\Lambda_H\left(P_0\mu_S+\epsilon N_S\gamma_S I_V^*\right)}{\mu_H\left(P_0\mu_S+\epsilon N_S\gamma_S I_V^*\right)+\beta_H N_S\gamma_S I_V^*},\\[2ex]
I_H^*(I_V^*) &= \dfrac{1}{\mu_H+\delta_H}.\dfrac{\beta_H\Lambda_H N_S\gamma_S I_V^*}{\mu_H\left(P_0\mu_S+\epsilon N_S\gamma_S I_V^*\right)+\beta_H N_S\gamma_S I_V^*},\\[2ex]
S_V^*(I_V^*) &= \dfrac{\Lambda_V(M_0+\epsilon Q_V Z_V^*)}{\mu_V(M_0+\epsilon Q_V Z_V^*)+\beta_V Q_V Z_V^*},\\[2ex]
P_H^*(I_V^*) &= \dfrac{1}{\alpha_C+\mu_C}.\dfrac{Z_V^*}{I_H^*+1},\\[2ex]
W_I^*(I_V^*) &= \dfrac{1}{\alpha_I+\mu_I}.\dfrac{\alpha_C}{\alpha_C+\mu_C}.\dfrac{Z_V^*}{I_H^*+1},\\[2ex]
W_P^*(I_V^*) &= \dfrac{1}{2}.\dfrac{1}{\alpha_P+\mu_P}.\dfrac{\alpha_I}{\alpha_I+\mu_I}.\dfrac{\alpha_C}{\alpha_C+\mu_C}.\dfrac{Z_V^*}{I_H^*+1},\\[2ex]
E_H^*(I_V^*) &= \dfrac{1}{2}.\dfrac{1}{\alpha_E+\mu_E}.\dfrac{N_P\alpha_P}{\alpha_P+\mu_P}.\dfrac{\alpha_I}{\alpha_I+\mu_I}.\dfrac{\alpha_C}{\alpha_C+\mu_C}.\dfrac{Z_V^*}{I_H^*+1},\\[2ex]
E_L^*(I_V^*) &= \dfrac{1}{2}.\dfrac{1}{\alpha_L+\mu_L}.\dfrac{\alpha_E}{\alpha_E+\mu_E}.\dfrac{N_P\alpha_P}{\alpha_P+\mu_P}.\dfrac{\alpha_I}{\alpha_I+\mu_I}.\dfrac{\alpha_C}{\alpha_C+\mu_C}.Z_V^*,\\[2ex]
E_W^*(I_V^*) &= \dfrac{1}{2}.\dfrac{1}{\alpha_W+\mu_W}.\dfrac{\alpha_L}{\alpha_L+\mu_L}.\dfrac{\alpha_E}{\alpha_E+\mu_E}.\dfrac{N_P\alpha_P}{\alpha_P+\mu_P}.\dfrac{\alpha_I}{\alpha_I+\mu_I}.\dfrac{\alpha_C}{\alpha_C+\mu_C}.Z_V^*,\\[2ex]
M^*(I_V^*) &= \dfrac{1}{2}.\dfrac{1}{\mu_M}.\dfrac{N_W\alpha_W}{\alpha_W+\mu_W}.\dfrac{\alpha_L}{\alpha_L+\mu_L}.\dfrac{\alpha_E}{\alpha_E+\mu_E}.\dfrac{N_P\alpha_P}{\alpha_P+\mu_P}.\dfrac{\alpha_I}{\alpha_I+\mu_I}.\dfrac{\alpha_C}{\alpha_C+\mu_C}.Z_V^*,\\[2ex]
P_W^*(I_V^*) &= \dfrac{N_S\gamma_S I_V^*}{\mu_S}\\[2ex]
\lambda_H^*(I_V^*) &= \dfrac{\beta_H N_S\gamma_S I_V^*}{P_0\mu_S+\epsilon N_S\gamma_S I_V^*},\\[2ex]
\lambda_V^*(I_V^*) &= \dfrac{\beta_V Q_V Z_V^*}{M_0+\epsilon Q_V Z_V^*},
\end{cases}
\tag{5.3.2}
$$

where

$$Z_V^* = \frac{\beta_H N_S \gamma_S I_V^*}{P_0\mu_S + \epsilon N_S\gamma_S I_V^*}.\frac{(\Lambda_H - \mu_H)(P_0\mu_S + \epsilon N_S\gamma_S I_V^*) - \beta_H N_S\gamma_S I_V^*}{\mu_H(P_0\mu_S + \epsilon N_S\gamma_S I_V^*) + \beta_H N_S\gamma_S I_V^*} \text{ and}$$

$$Q_V = \frac{1}{2}.\frac{1}{\mu_M}.\frac{N_W\alpha_W}{\alpha_W + \mu_W}.\frac{\alpha_L}{\alpha_L + \mu_L}.\frac{\alpha_E}{\alpha_E + \mu_E}.\frac{N_P\alpha_P}{\alpha_P + \mu_P}.\frac{\alpha_I}{\alpha_I + \mu_I}.\frac{\alpha_C}{\alpha_C + \mu_C}.$$

Substituting the expressions in (5.3.2) in the equation for I_V which is given by

$$\frac{dI_V}{dt} = \lambda_V S_V - (\mu_V + \delta_V)I_V,$$

at the endemic equilibrium we get:

$$I_V^*\left[A{I_V^*}^2 + BI_V^* + C\right] = 0, \tag{5.3.3}$$

where

$$\begin{aligned} A &= (N_S\gamma_S)^2(\beta_V + \epsilon\mu_V)(\mu_V + \delta_V)Q_V\left[\beta_V^2 + \epsilon\beta_H(\Lambda_H - \mu_H)\right] \\ &+ \epsilon(N_S\gamma_S)^2(\beta_V + \epsilon\mu_H)(\beta_V + \epsilon\mu_V)(\mu_V + \delta_V), \end{aligned} \tag{5.3.4}$$

$$\begin{aligned} B &= (1 - R_0^2)P_0^2\mu_S^2 + \beta_H(\Lambda_H - \mu_H)N_S\gamma_S(\beta_V + \epsilon\mu_V)(\mu_V + \delta_V)Q_V P_0\mu_S \\ &+ P_0\mu_S(\mu_V + \delta_V)M_0\mu_V N_S\gamma_S(\beta_V + \epsilon\mu_H) + \beta_V^3(N_S\gamma_S)^2\Lambda_V Q_V, \end{aligned} \tag{5.3.5}$$

and

$$C = (1 - R_0^2)P_0^2\mu_S^2(\mu_V + \delta_V)M_0\mu_V N_S\gamma_S\epsilon\mu_H. \tag{5.3.6}$$

Equation (5.3.3) can be written in the form

$$A.I_V^*\left[{I_V^*}^2 + E_V I_V^* + F_V\right] = 0, \tag{5.3.7}$$

where $E_V = \dfrac{B}{A}$ and $F_V = \dfrac{C}{A}$. Note that $A > 0$ for all values of R_0 and $C < 0$ for $R_0 > 1$ while B can be positive or negative for $R_0 > 1$.

Equation (5.3.7) gives $I_V^* = 0$, which corresponds to the disease-free equilibrium point and

$$I_V^* = \frac{1}{2}\left[-E_V \pm \sqrt{E_V^2 - 4F_V}\right] > 0, \tag{5.3.8}$$

for the endemic equilibrium. Since $F_V < 0$ for $R_0 > 1$, we can easily deduce from expression (5.3.8) that only one positive endemic equilibrium exists for $R_0 > 1$. Consequently, there exists one unique endemic equilibrium for model system (5.3.9) whenever $R_0 > 1$. □

Apart from the fact that the endemic equilibrium values represented by expressions (5.3.2) as well as expressions (5.3.1)-(5.3.12) synthesize important elements of human schistosomiasis transmission processes, we note that the between-host endemic expressions for

$$S_H^*, I_H^*, S_V^*, I_V^*, E_L^*, E_W^*, M^*, P_W^* \tag{5.3.9}$$

are determined by both within-host disease parameters and between-host disease parameters and in turn, the within-host endemic expressions for

$$P_H^*, W_I^*, W_P^*, E_H^* \tag{5.3.10}$$

are also determined by both the within-host disease parameters and between-host disease parameters. This confirms the reciprocal influence of within-host and between-host transmission dynamics of human schistosomiasis.

5.3.9 Local Stability of the Endemic Equilibrium

Theorem 5.3 has established the existence of a unique endemic equilibrium for model system (5.3.9) without providing any information about its stability. We make use of a bifurcation approach to address this concern [97]-[102]. Center Manifold Theory has been used to determine the local stability of a non-hyperbolic equilibrium (linearization matrix has at least one eigenvalue with zero real part) [97]-[102]. We now employ the Center Manifold Theory [101] to establish the local asymptotic stability of the endemic equilibrium of model system (5.3.9).

In order to apply the Center Manifold Theory, we make the following simplifications and change of variables. Let $S_H = x_1$, $I_H = x_2$, $S_V = X_3$, $I_V = x_4$, $P_H = x_5$, $W_I = x_6$, $W_P = x_7$, $E_H = x_8$, $E_L = x_9$, $E_W = x_{10}$, $M = x_{11}$ and $P_W = x_{12}$ so that $N_H = x_1 + x_2$ and $N_V = x_3 + x_4$. Further, by using the vector notation $\mathbf{x} = (x_1, x_2, x_3, x_4, x_5, x_6, x_7, x_8, x_9, x_{10}, x_{11}, x_{12})^T$, model system (5.3.9) can be written in the form $\frac{d\mathbf{x}}{dt} = F(\mathbf{x})$ with

$$F(\mathbf{x}) = (f_1, f_2, f_3, f_4, f_5, f_6, f_7, f_8, f_9, f_{10}, f_{11}, f_{12}),$$

such that

$$
\begin{cases}
\dfrac{dx_1}{dt} &= \Lambda_H - \lambda_H x_1 - \mu_H x_1, \\
\dfrac{dx_2}{dt} &= \lambda_H x_1 - (\mu_H + \delta_H) x_2, \\
\dfrac{dx_3}{dt} &= \Lambda_V - \lambda_V x_3 - \mu_V x_3, \\
\dfrac{dx_4}{dt} &= \lambda_V x_3 - (\mu_V + \delta_V) x_4, \\
\dfrac{dx_5}{dt} &= \lambda_h S_h - (\alpha_C + \mu_C) x_5, \\
\dfrac{dx_6}{dt} &= \alpha_C x_5 - (\alpha_I + \mu_I) x_6, \\
\dfrac{dx_7}{dt} &= \dfrac{\alpha_I}{2} x_6 - (\alpha_P + \mu_P) x_7, \\
\dfrac{dx_8}{dt} &= N_P \alpha_P x_7 - (\alpha_E + \mu_E) x_8, \\
\dfrac{dx_9}{dt} &= I_h \alpha_E x_8 - (\alpha_L + \mu_L) x_9, \\
\dfrac{dx_{10}}{dt} &= \alpha_L x_9 - (\alpha_W + \mu_W) x_{10}, \\
\dfrac{dx_{11}}{dt} &= N_W \alpha_W x_{10} - \mu_M x_{11}, \\
\dfrac{dx_{12}}{dt} &= N_S \gamma_S x_3 - \mu_S x_{12},
\end{cases}
\tag{5.3.1}
$$

where,

$$
\lambda_H(t) = \frac{\beta_H x_{12}(t)}{P_0 + \epsilon x_{12}(t)}, \qquad \lambda_V(t) = \frac{\beta_V x_{11}(t)}{M_0 + \epsilon x_{11}(t)}. \tag{5.3.2}
$$

The method involves evaluating the Jacobian matrix of the system (5.3.1) at the disease-free equilibrium E^0 denoted by $J(E^0)$. The Jacobian matrix associated with equation system (5.3.1)

at E^0 is given by

$$J(E^0) = \begin{pmatrix} -\mu_H & 0 & 0 & 0 & 0 & 0 & 0 & 0 & 0 & 0 & 0 & -\frac{\beta_H \Lambda_H}{P_0 \mu_H} \\ 0 & b_1 & 0 & 0 & 0 & 0 & 0 & 0 & 0 & 0 & 0 & \frac{\beta_H \Lambda_H}{P_0 \mu_H} \\ 0 & 0 & -\mu_V & 0 & 0 & 0 & 0 & 0 & 0 & 0 & -\frac{\beta_V \Lambda_V}{M_0 \mu_V} & 0 \\ 0 & 0 & 0 & b_2 & 0 & 0 & 0 & 0 & 0 & 0 & \frac{\beta_V \Lambda_V}{M_0 \mu_V} & 0 \\ 0 & 0 & 0 & 0 & b_3 & 0 & 0 & 0 & 0 & 0 & 0 & \frac{\beta_H(\Lambda_H - \mu_H)}{P_0 \mu_H} \\ 0 & 0 & 0 & 0 & \alpha_C & b_4 & 0 & 0 & 0 & 0 & 0 & 0 \\ 0 & 0 & 0 & 0 & 0 & \frac{\alpha_I}{2} & b_5 & 0 & 0 & 0 & 0 & 0 \\ 0 & 0 & 0 & 0 & 0 & 0 & N_P \alpha_P & b_6 & 0 & 0 & 0 & 0 \\ 0 & 0 & 0 & 0 & 0 & 0 & 0 & \alpha_E & b_7 & 0 & 0 & 0 \\ 0 & 0 & 0 & 0 & 0 & 0 & 0 & 0 & \alpha_L & b_8 & 0 & 0 \\ 0 & 0 & 0 & 0 & 0 & 0 & 0 & 0 & 0 & N_W \alpha_W & -\mu_M & 0 \\ 0 & 0 & 0 & N_S \gamma_S & 0 & 0 & 0 & 0 & 0 & 0 & 0 & -\mu_S \end{pmatrix}, \tag{5.3.3}$$

where,

$$\begin{cases} b_1 &= -(\mu_H + \delta_H), \\ b_2 &= -(\mu_V + \delta_V,) \\ b_3 &= -(\alpha_C + \mu_C), \\ b_4 &= -(\alpha_I + \mu_I), \\ b_5 &= -(\alpha_P + \mu_P), \\ b_6 &= -(\alpha_E + \mu_E), \\ b_7 &= -(\alpha_L + \mu_L), \\ b_8 &= -(\alpha_W + \mu_W). \end{cases} \tag{5.3.4}$$

From expression (5.3.16) the reproductive number of system (5.3.1) is

$$R_0 = \sqrt{\frac{N_S \gamma_S \beta_V \Lambda_V}{\mu_V \mu_M M_0 (\mu_V + \delta_V)} . \frac{\alpha_C}{\alpha_C + \mu_C} . \frac{\alpha_I}{\alpha_I + \mu_I} . \frac{N_P \alpha_P}{\alpha_P + \mu_P} . \frac{\alpha_E}{\alpha_E + \mu_E} . \frac{\alpha_L}{\alpha_L + \mu_L} . \frac{N_W \alpha_W}{\alpha_W + \mu_W} . \frac{\beta_H(\Lambda_H - \mu_H)}{2 P_0 \mu_H \mu_S}}. \tag{5.3.5}$$

Now let us consider $\beta_V = k\beta_H$, regardless of whether $k \in (0,1)$ or $k \geq 1$ and let $\beta_H = \beta^*$. Taking β^* as the bifurcation parameter and if we consider $R_0 = 1$, and solve for β^*, we obtain

$$\beta^* = \sqrt{\frac{\mu_V \mu_M M_0(\mu_V + \delta_V)}{kN_S\gamma_S\Lambda_V}.\frac{\alpha_C + \mu_C}{\alpha_C}.\frac{\alpha_I + \mu_I}{\alpha_I}.\frac{\alpha_P + \mu_P}{N_P\alpha_P}.\frac{\alpha_E + \mu_E}{\alpha_E}.\frac{\alpha_L + \mu_L}{\alpha_L}.\frac{\alpha_W + \mu_W}{N_W\alpha_W}.\frac{2P_0\mu_H\mu_S}{(\Lambda_H - \mu_H)}}. \tag{5.3.6}$$

Note that the linearized system of the transformed equations (5.3.1) with bifurcation point β^* has a simple zero eigenvalue. Hence, the Center Manifold Theory [101] can be used to analyze the dynamics of (5.3.1) near $\beta_H = \beta^*$.

In particular, Theorem 4.1 in Castillo-Chavez and Song [230], reproduced below as Theorem 5.4 for convenience, will be used to show the local asymptotic stability of the endemic equilibrium point of (5.3.1) (which is the same as the endemic equilibrium point of the original system (5.3.9), for $\beta_H = \beta^*$).

Theorem 5.4. *Consider the following general system of ordinary differential equations with parameter ϕ:*

$$\frac{dx}{dt} = f(x,\phi), f : \mathbb{R}^n \times \mathbb{R} \longrightarrow \mathbb{R}, f : C^2(\mathbb{R}^2 \times \mathbb{R}), \tag{5.3.7}$$

where 0 is an equilibrium of the system, that is $f(0,\phi) = 0$ for all ϕ, and assume that

A1. $A = D_x f(0,0) = ((\partial f_i/\partial x_j)(0,0))$ is linearization of system (5.3.1) around the equilibrium 0 with ϕ evaluated at 0. Zero is a simple eigenvalue of A, and other eigenvalues of A have negative real parts,

A2. matrix A has a right eigenvector u and a left eigenvector v corresponding to the zero eigenvalue.

Let f_k be the k^{th} component of f and

$$\begin{cases} a = \sum_{k,i,j=1}^{n} v_k v_i v_j \frac{\partial^2 f_k}{\partial x_i \partial x_j}(0,0), \\ b = \sum_{k,i=1}^{12} v_k v_i v_j \frac{\partial^2 f_k}{\partial x_i \partial \phi}(0,0). \end{cases}$$

The local dynamics of (5.3.1) around 0 are totally governed by a and b.

i. $a > 0$, $b > 0$. *When* $\phi < 0$ *with* $|\phi| \ll 1$, *0 is locally asymptotically stable, and there exists a positive unstable equilibrium; when* $0 < \phi \ll 1$, *0 is unstable and there exists a negative and locally asymptotically stable equilibrium.*

ii. $a < 0$, $b < 0$. *When* $\phi < 0$ *with* $|\phi| \ll 1$, *0 is unstable; when* $0 < \phi \ll 1$, *0 is locally asymptotically stable, and there exists a positive unstable equilibrium;*

iii. $a > 0$, $b < 0$. *When* $\phi < 0$ *with* $|\phi| \ll 1$, *0 is unstable, and there exists a locally asymptotically stable negative equilibrium; when* $0 < \phi \ll 1$, *0 is stable and a positive unstable equilibrium appears;*

iv. $a < 0$, $b > 0$. *When* ϕ *changes from negative to positive, 0 changes its stability from stable to unstable. Correspondingly a negative unstable equilibrium becomes positive and locally asymptotically stable*

In order to apply the above theorem, the following computations are necessary (it should be noted that we are using β^* as the bifurcation parameter, in place of ϕ in Theorem 5.4).

Eigenvectors of J_{β^*}: For the case when $R_0 = 1$, it can be shown that the Jacobian of (5.3.1) at $\beta_H = \beta^*$ (denoted by J_{β^*}) has a right eigenvector associated with the zero eigenvalue given by $u = [u_1, u_2, u_3, u_4, u_5, u_6, u_7, u_8, u_9, u_{10}, u_{11}, u_{12}]^T$, where

$$
\begin{cases}
u_1 = -\dfrac{\beta^*}{P_0\mu_H}.\dfrac{\Lambda_H}{\mu_H}, \\
u_2 = \dfrac{\beta^*}{P_0\mu_H}.\dfrac{\Lambda_H}{\mu_H+\delta_H}, \\
u_3 = -\dfrac{\mu_S(\mu_V+\delta_V)}{N_S\gamma_S\mu_V}, \\
u_4 = \dfrac{\mu_S}{N_S\gamma_S}, \\
u_5 = \dfrac{1}{\alpha_C+\mu_C}.\dfrac{\beta^*(\Lambda_H-\mu_H)}{P_0\mu_H}, \\
u_6 = \dfrac{1}{\alpha_I+\mu_I}.\dfrac{\alpha_C}{\alpha_C+\mu_C}.\dfrac{\beta^*(\Lambda_H-\mu_H)}{P_0\mu_H}, \\
u_7 = \dfrac{1}{2}.\dfrac{1}{\alpha_P+\mu_P}.\dfrac{\alpha_I}{\alpha_I+\mu_I}.\dfrac{\alpha_C}{\alpha_C+\mu_C}.\dfrac{\beta^*(\Lambda_H-\mu_H)}{P_0\mu_H}, \\
u_8 = \dfrac{1}{2}.\dfrac{1}{\alpha_E+\mu_E}.\dfrac{\alpha_P}{\alpha_P+\mu_P}.\dfrac{\alpha_I}{\alpha_I+\mu_I}.\dfrac{\alpha_C}{\alpha_C+\mu_C}.\dfrac{\beta^*(\Lambda_H-\mu_H)}{P_0\mu_H}, \\
u_9 = \dfrac{1}{2}.\dfrac{1}{\alpha_L+\mu_L}.\dfrac{N_P\alpha_P}{\alpha_E+\mu_E}.\dfrac{\alpha_P}{\alpha_P+\mu_P}.\dfrac{\alpha_I}{\alpha_I+\mu_I}.\dfrac{\alpha_C}{\alpha_C+\mu_C}.\dfrac{\beta^*(\Lambda_H-\mu_H)}{P_0\mu_H}, \\
u_{10} = \dfrac{1}{2}.\dfrac{1}{\alpha_W+\mu_W}.\dfrac{\alpha_L}{\alpha_L+\mu_L}.\dfrac{N_P\alpha_P}{\alpha_E+\mu_E}.\dfrac{\alpha_P}{\alpha_P+\mu_P}.\dfrac{\alpha_I}{\alpha_I+\mu_I}.\dfrac{\alpha_C}{\alpha_C+\mu_C}.\dfrac{\beta^*(\Lambda_H-\mu_H)}{P_0\mu_H}, \\
u_{11} = \dfrac{1}{2}.\dfrac{N_W\alpha_W}{\alpha_W+\mu_W}.\dfrac{\alpha_L}{\alpha_L+\mu_L}.\dfrac{N_P\alpha_P}{\alpha_E+\mu_E}.\dfrac{\alpha_P}{\alpha_P+\mu_P}.\dfrac{\alpha_I}{\alpha_I+\mu_I}.\dfrac{\alpha_C}{\alpha_C+\mu_C}.\dfrac{\beta^*(\Lambda_H-\mu_H)}{P_0\mu_H\mu_M} = \dfrac{R_{0H}\mu_S}{\mu_M}, \\
u_{12} = 1.
\end{cases}
\tag{5.3.8}
$$

Further, the left eigenvector of $J(E^0)$ associated with the zero eigenvalue at $\beta_H = \beta^*$ is given by $v = [v_1, v_2, v_3, v_4, v_5, v_6, v_7, v_8, v_9, v_{10}, v_{11}, v_{12}]^T$, where

$$
\begin{cases}
v_1 &= 0, \\
v_2 &= 0, \\
v_3 &= 0, \\
v_4 &= \dfrac{M_0\mu_V\mu_M}{\beta_V N_S\gamma_S}, \\
v_5 &= \dfrac{1}{2}.\dfrac{\alpha_C}{\alpha_C+\mu_C}.\dfrac{\alpha_I}{\alpha_I+\mu_I}.\dfrac{N_P\alpha_P}{\alpha_P+\mu_P}.\dfrac{\alpha_E}{\alpha_E+\mu_E}.\dfrac{\alpha_L}{\alpha_L+\mu_L}.\dfrac{N_W\alpha_W}{\alpha_W+\mu_W}, \\
v_6 &= \dfrac{1}{2}.\dfrac{\alpha_I}{\alpha_I+\mu_I}.\dfrac{N_P\alpha_P}{\alpha_P+\mu_P}.\dfrac{\alpha_E}{\alpha_E+\mu_E}.\dfrac{\alpha_L}{\alpha_L+\mu_L}.\dfrac{N_W\alpha_W}{\alpha_W+\mu_W}, \\
v_7 &= \dfrac{N_P\alpha_P}{\alpha_P+\mu_P}.\dfrac{\alpha_E}{\alpha_E+\mu_E}.\dfrac{\alpha_L}{\alpha_L+\mu_L}.\dfrac{N_W\alpha_W}{\alpha_W+\mu_W}, \\
v_8 &= \dfrac{\alpha_E}{\alpha_E+\mu_E}.\dfrac{\alpha_L}{\alpha_L+\mu_L}.\dfrac{N_W\alpha_W}{\alpha_W+\mu_W}, \\
v_9 &= \dfrac{\alpha_L}{\alpha_L+\mu_L}.\dfrac{N_W\alpha_W}{\alpha_W+\mu_W}, \\
v_{10} &= \dfrac{N_W\alpha_W}{\alpha_W+\mu_W}, \\
v_{11} &= 1, \\
v_{12} &= \dfrac{M_0\mu_V\mu_M(\mu_V+\delta_V)}{k\beta^*\Lambda_V N_S\gamma_S} = \dfrac{1}{R_{0HS}}.
\end{cases}
\tag{5.3.9}
$$

Computation of bifurcation parameters a and b:

The sign of a is associated with the following non-vanishing partial derivatives of F:

$$\begin{cases} \dfrac{\partial^2 f_4}{\partial x_3 \partial x_{11}} = \dfrac{\partial^2 f_4}{\partial x_{11} \partial x_3} = \dfrac{\beta_V}{M_0}, \\ \dfrac{\partial^2 f_4}{\partial x_{11}^2} = -\dfrac{2\epsilon\beta_V}{M_0^2} \\ \dfrac{\partial^2 f_5}{\partial x_1 \partial x_{12}} = \dfrac{\partial^2 f_5}{\partial x_{12} \partial x_1} = \dfrac{\beta_H}{P_0}, \\ \dfrac{\partial^2 f_5}{\partial x_{12}^2} = -\dfrac{2\beta_H \epsilon(\Lambda_H - \mu_H)}{P_0^2 \mu_H}. \\ \dfrac{\partial^2 f_5}{\partial x_2 \partial x_{12}} = \dfrac{\partial^2 f_5}{\partial x_{12} \partial x_2} = -\dfrac{\beta_H \epsilon(\Lambda_H - \mu_H)}{P_0 \mu_H}, \\ \dfrac{\partial^2 f_9}{\partial x_2 \partial x_8} = \dfrac{\partial^2 f_9}{\partial x_8 \partial x_2} = \alpha_E. \end{cases} \tag{5.3.10}$$

Substituting equatin (5.3.10) into equation (5.3.8), we get

$$\begin{aligned} a &= -\frac{2R_{0H}\mu_S^2}{M_0\mu_M}\left[\frac{k\beta^*\Lambda_V + \epsilon R_0^2\mu_V^2}{R_{0HS}\Lambda_V\mu_V}\right] - \frac{2R_{0H}\mu_S^2}{P_0}\left[\frac{\beta^*\Lambda_H}{\mu_H(\Lambda_H - \mu_H)} + \epsilon\right], \\ &= -2R_{0H}\mu_S^2\left[\frac{k\beta^*\Lambda_V + \epsilon R_0\mu_V^2}{M_0\mu_V\mu_M\Lambda_V R_{0HS}} + \frac{\beta^*\Lambda_H + \epsilon\mu_H(\Lambda_H - \mu_H)}{P_0\mu_H\mu_S(\Lambda_H - \mu_H)}\right] < 0. \end{aligned} \tag{5.3.11}$$

For the sign of b, it is associated with the following non-vanishing partial derivatives of F,

$$\begin{cases} \dfrac{\partial^2 f_4}{\partial \beta^* \partial x_{11}} = \dfrac{k\Lambda_V}{M_0\mu_V}, \\ \dfrac{\partial^2 f_5}{\partial \beta^* \partial x_{12}} = \dfrac{\Lambda_H - \mu_H}{P_0\mu_H}. \end{cases} \tag{5.3.12}$$

It follows from the above expression that

$$b = \frac{2R_{0H}}{\beta^*} > 0. \tag{5.3.13}$$

Thus, $a < 0$ and $b > 0$. Using Theorem 5.4, item (iv), we have established the following result which only holds for $R_0 > 1$ but close to 1:

Theorem 5.5. *The unique endemic equilibrium guaranteed by Theorem 5.4 is locally asymptotically stable for* $R_0 > 1$ *near 1.*

5.4 The Effect of Environment on Schistosomiasis transmission dynamics

The model system (5.3.9) presented in this work does not explicitly incorporate environmental factors such as the effect of climatological environment. But with minor modifications, the model can incorporate climate change. First consider the two forces of infection which appear in model system (5.3.9) which are

$$\lambda_H(t) = \frac{\beta_H P_W(t)}{P_0 + \epsilon P_W(t)}, \tag{5.4.1}$$

and

$$\lambda_V(t) = \frac{\beta_V M(t)}{M_0 + \epsilon M(t)}. \tag{5.4.2}$$

Then consider the water level in which cercariae, miracidia and snails live and where infections of both humans and snails take place. Assume that the water volume can be described by the following ordinary differential equation:

$$\frac{dW}{dt} = P + S - DW. \tag{5.4.3}$$

where P is precipitation, S is water flow rate upstream into the site of infection and D is drainage rate of water downstream from the site of infection per volume of water W. Using the volume of water, W, we can modify the two previous forces of infection to become:

$$\lambda_H(t) = \frac{\beta_H P_W(t)}{K_H W + \epsilon P_W(t)}, \tag{5.4.4}$$

and

$$\lambda_V(t) = \frac{\beta_V M(t)}{K_V W + \epsilon M(t)}. \tag{5.4.5}$$

where K_A and K_V are constants that re-scale water volume so that transmission of infection from the water to humans and snails occurs at 50% of the maximum rate of $K_H W$ and $K_V W$ respectively. In the absence of seasonal variations in water flow or precipitation, the equilibrium water level becomes:

$$W^* = \frac{P+S}{D}. \tag{5.4.6}$$

Thus, in the absence of seasonal variations in water flow and precipitation, the two forces of infection become:

$$\lambda_H(t) = \frac{\beta_H P_W(t)}{K_H W^* + \epsilon P_W(t)}. \tag{5.4.7}$$

$$\lambda_V(t) = \frac{\beta_V M(t)}{K_V W^* + \epsilon M(t)}. \tag{5.4.8}$$

and if we define

$$K_H W^* = P_0, \qquad K_V W^* = M_0, \tag{5.4.9}$$

then, we are back to original model equations (5.3.9), and all the results we have obtained so far and in particular equilibrium solutions and the reproductive number remain the same except that P_0 and M_0 are now given a new interpretation in those results of re-scaled water volume in which infection of both humans and snails occur. With this new interpretation of P_0 and M_0 and the results obtained from the analysis of the model, we make the following deductions:

a. The forces of infection λ_H and λ_V, are inversely proportional to P_0 and M_0 respectively. Therefore, the force of infection experienced by humans and snails is higher when water levels are low, than when they are high.

b. The reproductive number R_0, is inversely proportional to P_0 and M_0. Therefore, schistosomiasis outbreaks in regions close to rivers, streams and ponds are in constant tension between temperatures, which tend to stimulate growth of the free-living infective pathogens in the physical water environment (cercariae and miracidia), and increased water volumes, which tend to buffer infections.

5.5 Numerical Simulations

In this section, we present numerical simulations of model system (5.3.9) in order to illustrate some of the analytical results obtained in this chapter.

5.5.1 Methods

The numerical simulations were done using a set of within-host and between-host parameters in tables 5.2, 5.3 and 5.4 and initial values given in table 5.1 . The values of the model parameters are either from published literature or from estimations as values of some parameters are generally not reported in literature. For those parameters which are not reported in literature, their values were only indirectly approximated from inferences reported in the published literature. The model system (5.3.9) is simulated using Python version V2.6 on the Linux operating systems. We used the odeint function in the scipy.integrate package in python.

Parameter	**Meaning**	**Initial Value**	**Range explored**	**Units**	**Source/ Rational**
Λ_H	Supply of susceptible humans	800	800-1600	$humans\ day^{-1}$	Assumed
Λ_V	Supply of susceptible snails	2500	2500-5000	$snails\ day^{-1}$	Assumed
μ_H	Natural death rate of humans	0.0000384	0.0000384-0.14	day^{-1}	[93]
μ_V	Natural death rate of snails	0.0014	0.000569-0.9	day^{-1}	[85]
δ_H	Disease induced death rate of humans	0.0013699	0.0039-0.039	day^{-1}	[90]
δ_V	Disease induced death rate of snails	0.002	0.002-0.05	day^{-1}	[82]
β_H	Maximum exposure rate of Humans	0.028	0.028-0.122	day^{-1}	[82]
β_V	Maximum exposure rate of Snails	0.000127	0.000127-0.0012	day^{-1}	[82]

Table 5.2: Between-host parameter values for model system (3.9).

Parameter	**Description**	**Initial Value**	**Range explored**	**Units**	**Source/ Rational**
α_C	Migration rate of cercariae from skin to lung	0.33	0.33-0.997	day^{-1}	Assumed
μ_C	Natural death rate of cercariae	0.003	0.003-0.004	day^{-1}	Assumed
α_I	Migration rate of immature worms from skin to lungs	0.0004	0.0004-0.4	day^{-1}	Assumed
μ_I	Natural death rate of immature worms	0.000685	0.0005-0.5	day^{-1}	[91]
α_P	Migration rate of mature worms from skin to lungs	0.0004	0.0004-0.4	day^{-1}	Assumed
μ_P	Natural death rate of mature worms	0.000183	$0.000183-0.0003$	day^{-1}	[88]
N_P	Numbers of eggs produced	300	300 - 2000	$worm^{-1}$ day^{-1}	[84]
α_E	Excretion rate of eggs into environment	0.0004	0.0004-0.4	day^{-1}	Assumed
μ_E	Natural death rate of eggs worms	0.0025	0.000685-0.005	day^{-1}	[92]

Table 5.3: Within-host parameter values for model system (3.9).

Parameter	Description	Value	Range explored	Units	Source/ Rational
μ_L	Death rate of eggs on land	0.2	$0.142857-0.5$	day^{-1}	[45]
α_W	Rate at which eggs hatch in water	0.05	0.05-0.0625	day^{-1}	[83]
μ_W	Death rate of eggs in water	0.11	0.11-0.833	day^{-1}	[83]
N_W	Number of miracidia produced from each worm egg	110	110-500	day^{-1}	[83]
μ_M	Death rate of miracidia	2.2	2-2.66	day^{-1}	[83]
γ_S	Rate at which infected snails become cercariae shedding	0.02	$0.0119-0.04$	day^{-1}	[82]
μ_S	Rate at which cercariae die	0.4	0.33 - 0.5	day^{-1}	[91], [82]
N_S	Number of cercariae produced	4128	2476-8400	$snail^{-1}$ day^{-1}	[82]
M_0	Saturation constant of miracidia	10^8	10^4-10^{10}	–	Assumed
P_0	Saturation constant of cercariae	10^10	10^4-10^{10}	–	Assumed
ϵ	Limitation of growth velocity of cercariae with the increase of cases	1	–	–	[87]

Table 5.4: Environmentally transmitted pathogens and their associated environmental parameter values for model system (3.9).

5.5.2 Results

In the following, we present the results of the simulations for model system (5.3.9 in graphical form.

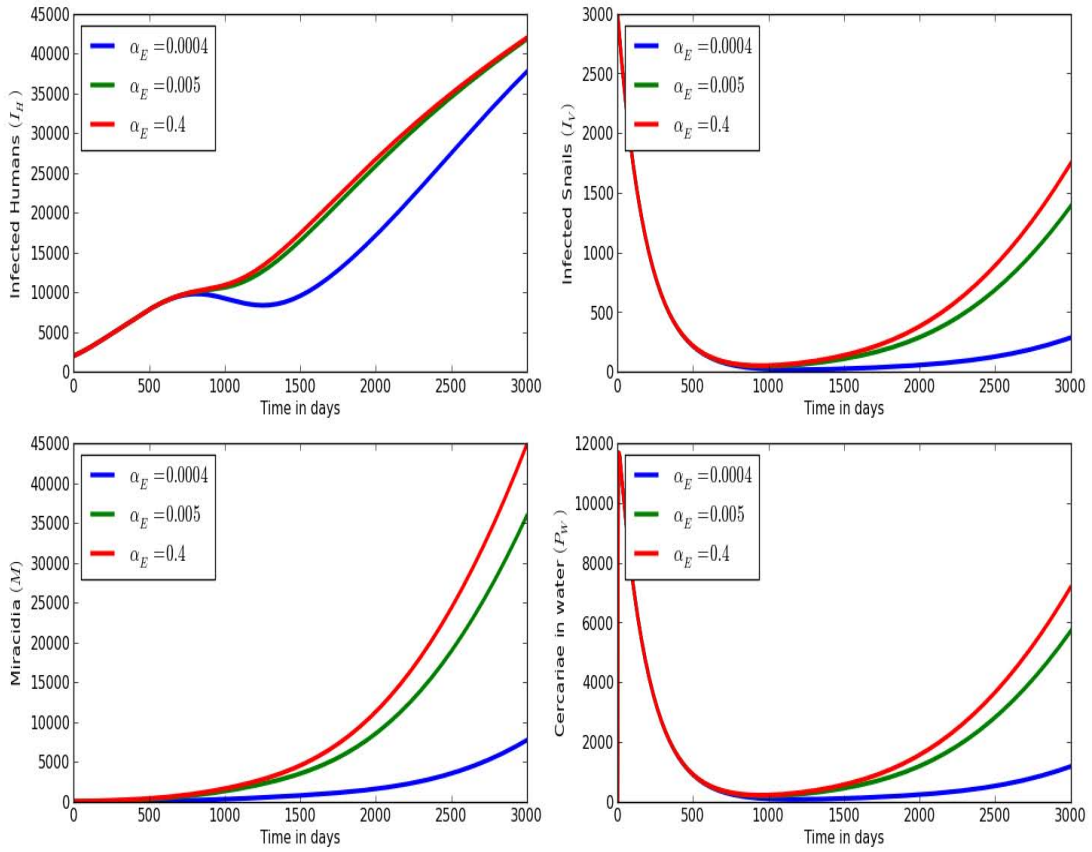

Figure 5.3: Simulations of model system (5.3.9) showing the evolution with time of (a) *top left*: infected humans, (b) *top right*: infected snails, (c) *bottom left*: miracidia in the physical water environment, and (d) *bottom right*: cercariae in the physical water environment for different values of rate of excretion of worm eggs by an infected human, α_E: $\alpha_E = 0.005$, $\alpha_E = 0.0039$ and $\alpha_E = 0.3$.

Figure 5.3 illustrates the solution profiles of the population of (a) Top left: Infected humans (I_H), (b) Top right: Infected snails (I_V) (c) bottom left: Miracidia (M) in the physical water environment, and (d): bottom right: cercariae (P_W) in the physical water environment for different values of excretion rate of worm eggs into physical land environment α_E: $\alpha_E = 0.005$, $\alpha_E = 0.0039$ and $\alpha_E = 0.3$. The results demonstrate a correlation between within-host disease processes and between-host disease transmission. In particular, the results show that higher rates of worm eggs excretion results in increased populations of infective parasites (miracidia and circariae) in the physical water environment and a noticeable increase in infected snails. Therefore, improvement in individual sanitation (which reduce environmental contamination with worm eggs) are good

for the community because they reduce the risk of human schistosomiasis transmission to the general public.

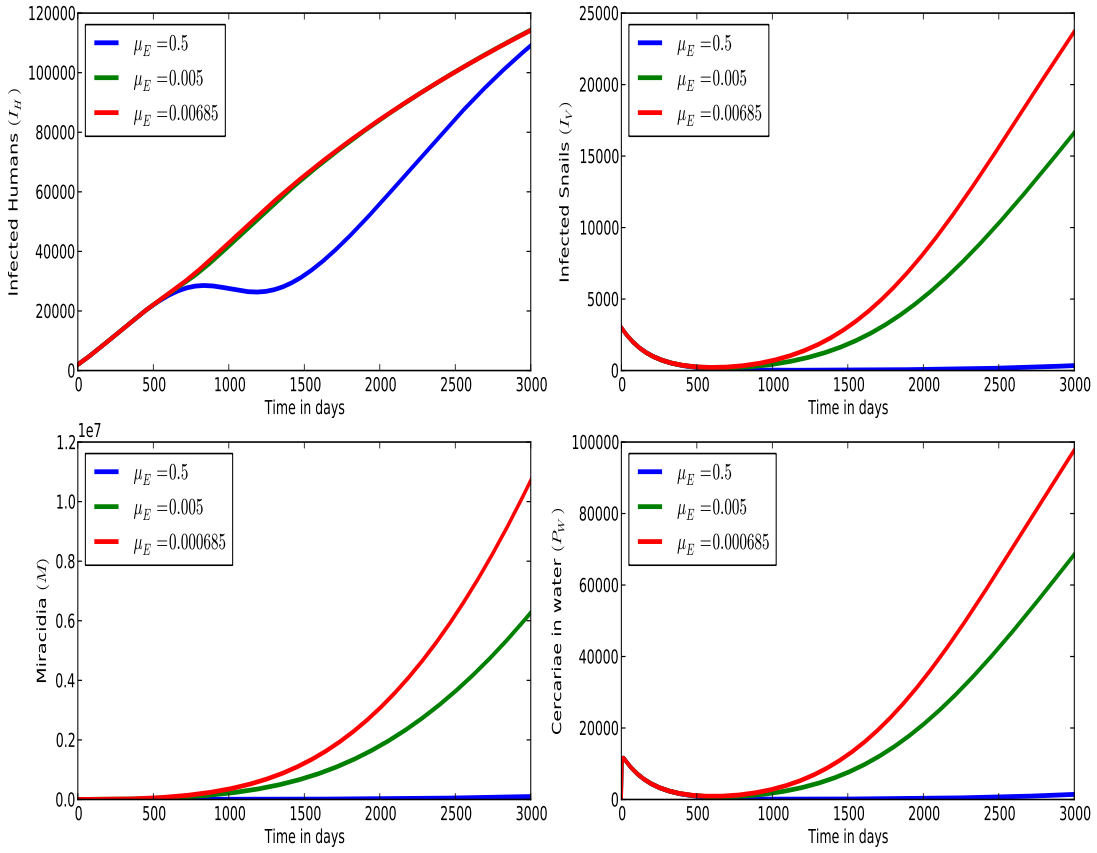

Figure 5.4: Simulations of model system (5.3.9) showing the evolution with time of (a) *top left*: infected humans, (b) *top right*: infected snails, (c) *bottom left*: miracidia in the physical water environment, and (d) *bottom right*: cercariae in the physical water environment for different values of natural death rate of worm eggs, μ_E: $\mu_E = 0.000685$, $\mu_E = 0.0025$ and $\mu_E = 0.005$.

Figure 5.4 illustrates the solution profiles of the population of (a) Top left: Infected humans (I_H), (b) Top right: Infected snails (I_V) (c) bottom left: Miracidia (M) in the physical water environment and (d): bottom right: cercariae (P_W) in the physical water environment for different values of natural death of worm eggs μ_E: $\mu_E = 0.000685$, $\mu_E = 0.0025$ and $\mu_E = 0.005$. The numerical results show that the within-host process of death of worm eggs affect transmission of the disease in the population. Increased death of worm eggs reduces transmission of the disease at population level. Therefore, immune mechanisms which enhance the killing of worm eggs within an infected individual reduce transmission risk of the disease within a community.

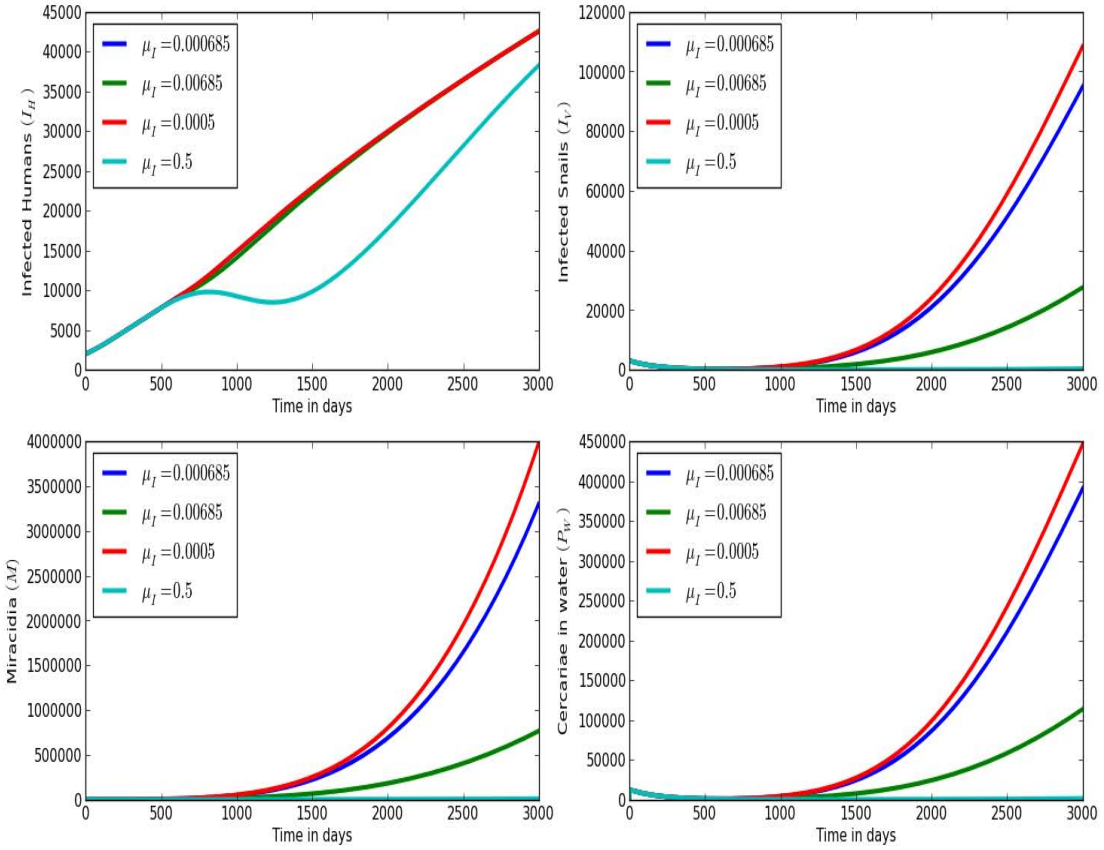

Figure 5.5: Graphs of numerical solutions showing propagation of (a) *top left*: infected humans, (b) *top right*: infected snails, (c) *bottom left*: miracidia in the physical water environment, and (d) *bottom right*: cercariae in the physical water environment for different values of natural death rate of immature worms, μ_I: $\mu_I = 0.000685$, $\mu_I = 0.0005$ and $\mu_I = 0.5$.

Figure 5.5 shows graphs of numerical solutions showing propagation of (a) Top left: Infected humans (I_H), (b) Top right: Infected snails (I_V) (c) bottom left: Miracidia in the physical water environment, and (M) in the physical water environment and (d): bottom right: cercariae (P_W) in the physical water environment for different values of natural death of immature worms μ_I: $\mu_I = 0.000685$, $\mu_I = 0.0005$ and $\mu_I = 0.5$. The results in Figure 5.5 show that an increase in the death rate of immature worms within an infected individual reduces the transmission risk of human schistosomiasis at population level. Therefore immune mechanisms which kill immature worm within an infected individual have an epidemiological influence on human schistosomiasis transmission.

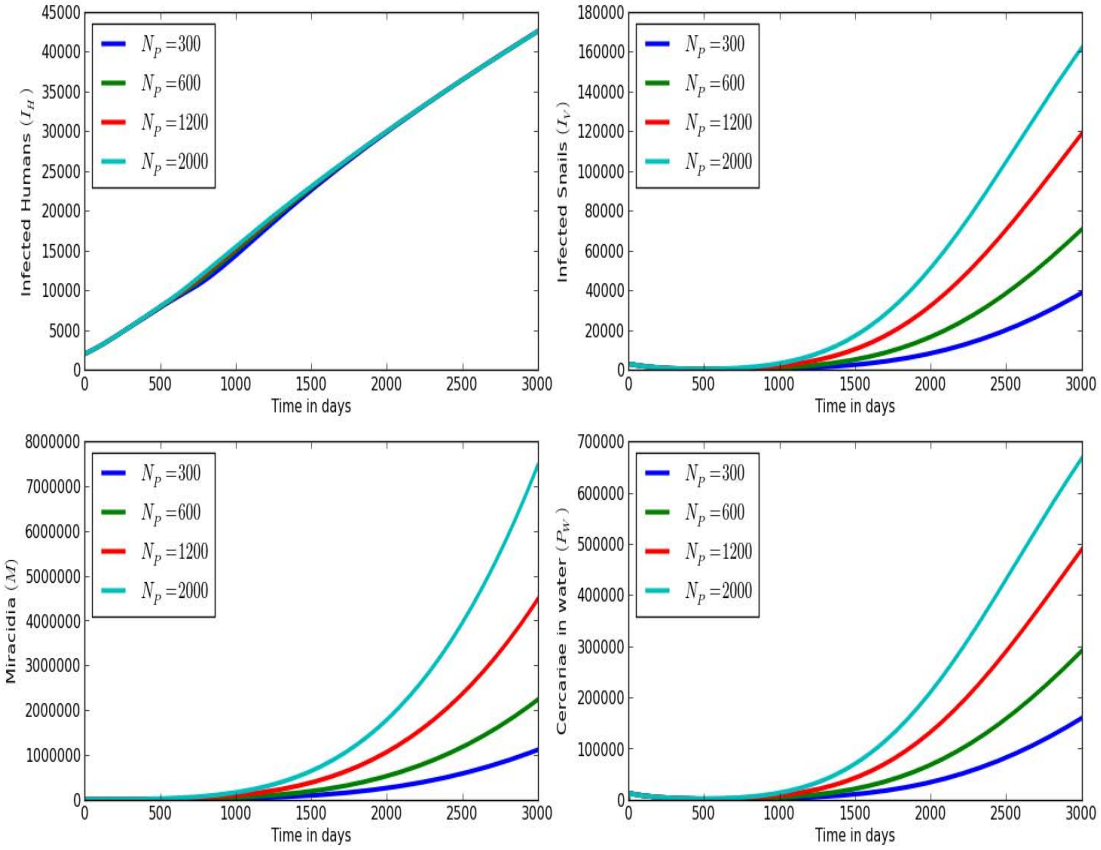

Figure 5.6: Graphs of numerical solutions showing propagation of (a) *top left*: infected humans I_H, (b) *top right*: infected snail hosts I_V, (c) *bottom left*: miracidia in the physical water environment, and (d) *bottom right*: cercariae in physical water environment for different values of the rate of mature worm fecundity within an infected human, N_P: $N_P = 300$, $N_P = 600$, $N_P = 1200$ and $N_P = 2000$.

Figure 5.6 shows graphs of the numerical solutions of (a) Top left: Infected humans (I_H), (b) Top right: Infected snails (I_V) (c) bottom left: Miracidia in the physical water environment, and (d): bottom right: cercariae (P_W) in the physical water environment for different values of mature worm fecundity N_p, within a single infected human host: $N_P = 300$, $N_P = 600$, $N_P = 1200$ and $N_P = 2000$. We observe from Figure 5.6 that an increase in production worm eggs per day by each worm pair of mature worms increases the transmission risk of human schistosomiasis. Therefore, immune mechanisms which reduce worm fecundity within an infected individual reduce the transmission risk of human schistomiasis in the community.

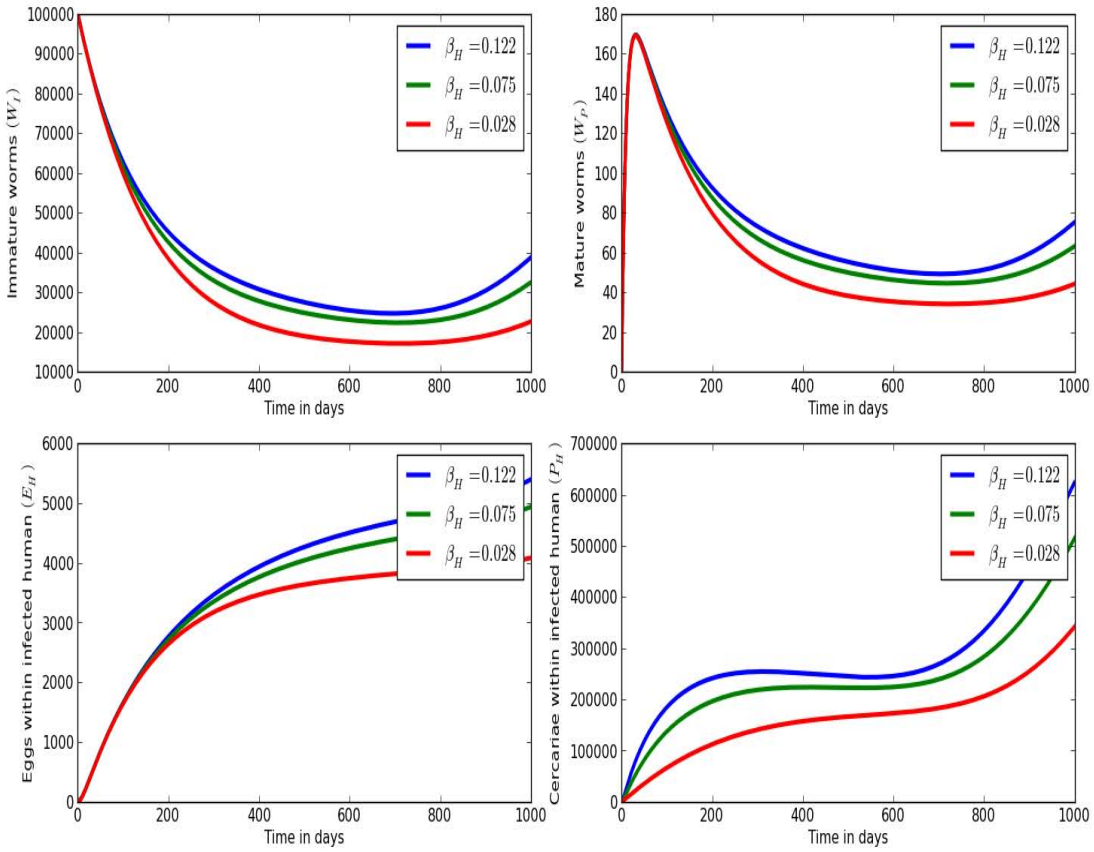

Figure 5.7: Graphs of numerical solutions showing propagation of (a) *top left*: immature worms within an infected human (W_I), (b) *top right*: mature worms within an infected human (W_P), (c) *bottom left*: worm eggs within an infected human (E_H), and (d) *bottom right*: cercariae within an infected human (P_H), for different values of the infection rate of humans by cercariae, β_H: $\beta_H = 0.028$, $\beta_H = 0.075$ and $\beta_H = 0.122$.

Figure 5.7 shows graphs of numerical solutions showing propagation of (a) *top left*: immature worms within an infected human (W_I), (b) *top right*: mature worms within an infected human (W_P), (c) *bottom left*: worm eggs within an infected human (E_H), and (d) *bottom right*: cercariae within an infected human (P_H), for different values of the infection rate of humans by cercariae, β_H: $\beta_H = 0.028$, $\beta_H = 0.075$ and $\beta_H = 0.122$. The results show qualitatively the influence of between-host disease process on within-host schistosomiasis infection intensity. In this case, as transmission rate of between-host increases, the within-host infection intensity of schistosomiasis also increases. The numerical results demonstrate that the transmission of disease at the population level influence the dynamics within an infected individual. Therefore,

human behavioural changes which reduce contact with infected water bodies reduces the infection intensity at individual level. Equally, good sanitation practices by the community which reduce contamination of water bodies reduce the intensity of infection at individual level.

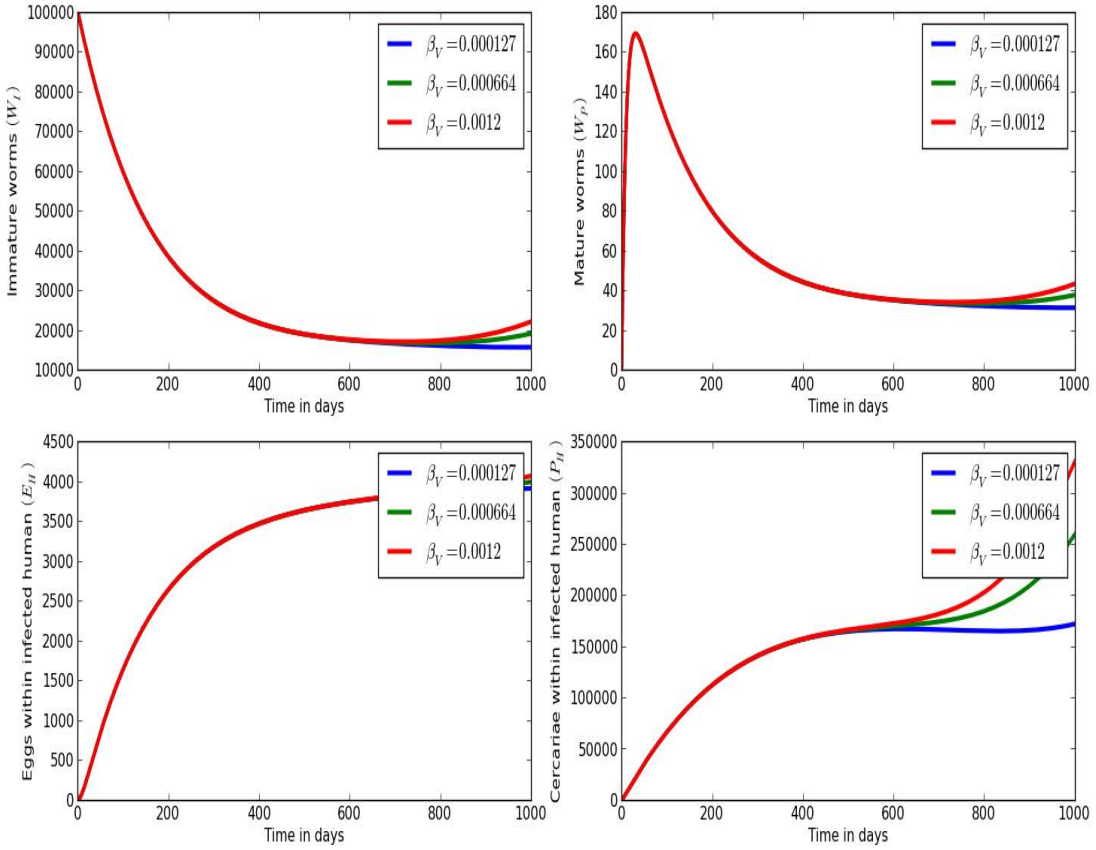

Figure 5.8: Graphs of numerical solutions showing propagation of (a) *top left*: immature worms within an infected human (W_I), (b) *top right*: mature worms within an infected human (W_P), (c) *bottom left*: worm eggs within an infected human (E_H), and (d) *bottom right*: cercariae within an infected human (P_H), for different values of the infection rate of snails by miracidia, β_V: $\beta_V = 0.000127$, $\beta_V = 0.000664$ and $\beta_V = 0.0012$.

Figure 5.8 illustrates graphs of numerical solutions showing propagation of (a) *top left*: immature worms within an infected human (W_I), (b) *top right*: mature worms within an infected human (W_P), (c) *bottom left*: worm eggs within an infected human (E_H), and (d) *bottom right*: cercariae within an infected human (P_H), for different values of the infection rate of snails by miracidia, β_V: $\beta_V = 0.000127$, $\beta_V = 0.000664$ and $\beta_V = 0.0012$.

The numerical results in 5.8 illustrate that an increase in the rate of infection of snails by miracidia increases the infection intensity at individual level for humans. This demonstrates the influence of between-host disease transmission parameters on within-host infection intensity. Therefore, public health interventions intended to reduce transmission risk of human schistosomiasis to snails also reduce the disease intensity with an infected individual. The numerical results in Figure 5.8 show direct relationship between population level transmission of the disease and the within-host infection intensity.

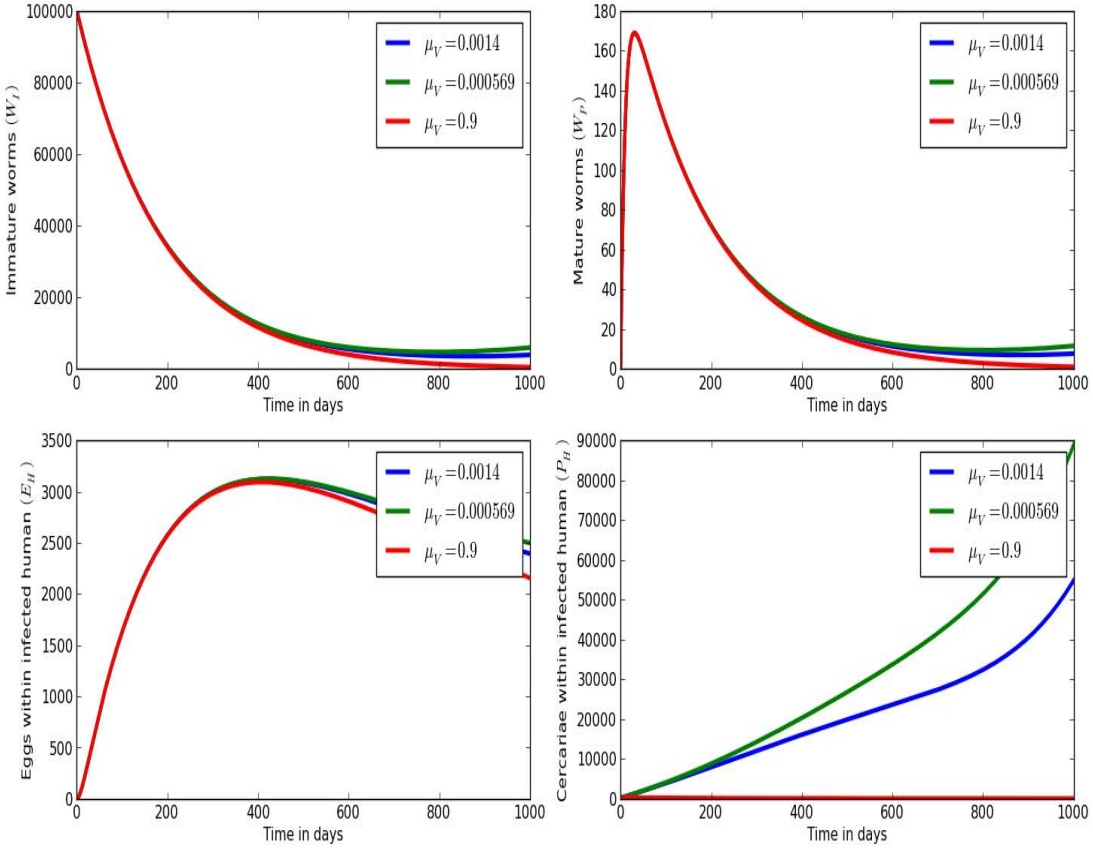

Figure 5.9: Graphs of numerical solutions showing propagation of (a) *top left*: immature worms within an infected human (W_I), (b) *top right*: mature worms within an infected human (W_P), (c) *bottom left*: worm eggs within an infected human (E_H), and (d) *bottom right*: cercariae within an infected human (P_H), for different values of natural death rate of snails, μ_V: $\mu_V = 0.000596$, $\mu_V = 0.0014$, $\mu_V = 0.8$ and $\mu_V = 0.9$.

Figure 5.9 illustrates graphs of numerical solutions showing propagation of (a) *top left*: immature worms within an infected human (W_I), (b) *top right*: mature worms within an infected

human (W_P), (c) *bottom left*: worm eggs within an infected human (E_H), and (d) *bottom right*: cercariae within an infected human (P_H), for different values of natural death rate of snails, μ_V: $\mu_V = 0.000596$, $\mu_V = 0.0014$ and $\mu_V = 0.9$. The numerical results in Figure 5.9 show direct relationship between public health interventions intended to reduce snail population and infection intensity within an infected individual. This is in agreement with analytical results which show influence of between-host disease parameters on within-host disease processes. Here the numerical results show that the death of snails μ_V, reduce the intensity of the disease with an infected individual. Therefore, public health interventions intended to kill snails have beneficial effect on an individual through reduced infection intensity.

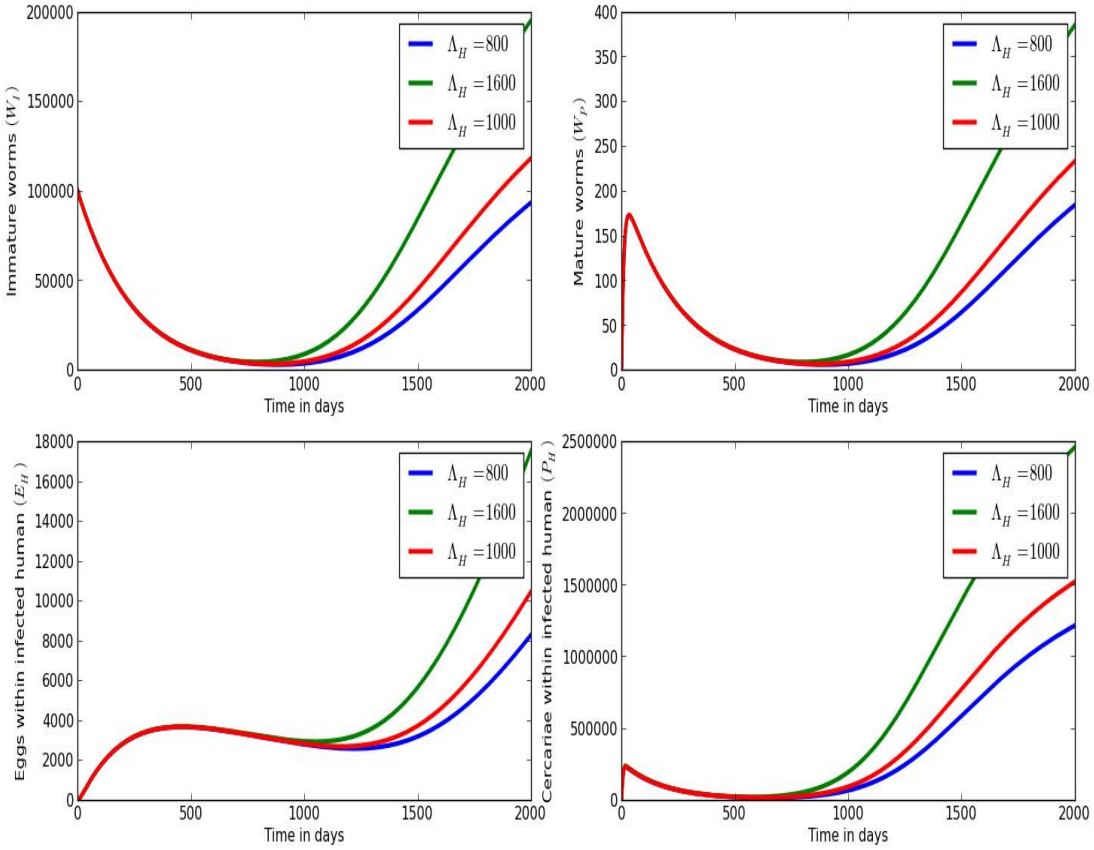

Figure 5.10: Graphs of numerical solutions showing propagation of (a) *top left*: immature worms within an infected human (W_I), (b) *top right*: mature worms within an infected human (W_P), (c) *bottom left*: worm eggs within an infected human (E_H), and (d) *bottom right*: cercariae within an infected human (P_H), within a single infected human, for different values of recruitment rate of new susceptible humans, Λ_H: $\Lambda_H = 800$, $\Lambda_H = 1000$ and $\Lambda_H = 1600$.

Figure 5.10 shows graphs of numerical solutions showing propagation of (a) *top left*: immature worms within an infected human (W_I), (b) *top right*: mature worms within an infected human (W_P), (c) *bottom left*: worm eggs within an infected human (E_H), and (d) *bottom right*: cercariae within an infected human (P_H), within a single infected human, for different values of recruitment rate of new susceptible humans, Λ_H: $\Lambda_H = 800$, $\Lambda_H = 1000$ and $\Lambda_H = 1600$.

We note from Figure 5.10 that the supply of new human susceptibles increases the intensity of infection of an infected individual. This again confirms the influence of between-host disease parameters on within-host disease processes. But overall, the numerical results presented in this section show bi-directional influence of within-host and between-host disease parameters on human schistosomiasis transmission.

5.6 Summary

In this chapter, we developed a mathematical modelling framework for linking the within-host and between-host dynamics of infections that are environmentally trasmitted. The resulting linked models are sometimes called immuno-epidemiological models. However, there is still no generalized framework for linking the within-host and between-host dynamics of infectious diseases. Furthermore, for environmentally trasmitted pathogens in the environment, there is an additional stumbling block in that there is a gap in knowledge on how environmental factors (through water, air, soil, food, formites, etc.) alter many aspects of such infections including susceptibility to infective dose, persistence of infection, pathogen shedding and severity of the disease. In this work, we link the two subsystems (within-host and between-host models) by identifying the within-host and between-host variables and parameters associated with the environmental dynamics of the pathogen and then design a feedback of the variables and parameters across the within-host and between-host models using human schistosomiasis as a case study. We studied the mathematical properties of the linked model and show that the model is epidemiologically well-posed. Using results from the analysis of the endemic equilibrium expression, the disease reproductive number R_0, and numerical simulations of the full model, we adequately account for the reciprocal influence of the linked within-host and between-host models. In particular, we illustrate that for human schistosomiasis, the outcome of infection at the individual level determines if, when and how much the individual host will further transmit the infectious agent into the environment, eventually affecting the spread of the infection in the host population. We expect the conceptual modelling framework developed here to be applicable to many infectious diseases that are environmentally trasmitted beyond the specific disease system of human schistosomiasis considered here.

Chapter 6

Conclusions and Future Research Directions

6.1 Conclusions

In this study, we developed multi-scale models based on two representative vector-borne diseases, namely; schistosomiasis which represents all environmentally transmitted vector-borne diseases and malaria which represents all directly transmitted vector-borne diseases. We established new mathematical modelling frameworks that we used to illustrate their applications in control of vector-borne diseases. Traditionally, vector-borne diseases have been modelled at a single scale level, that is, at the population level also known as between-host level. These models fail to account for a broader spectrum of vector-borne diseases systems replication and transmission dynamics (between-host and within-host levels) concurrently. As such, we followed multi-scale modelling approach that enabled us to concurrently account for between-host and within-host vector-borne disease dynamics. We started by developing single scale sub-models for the two representative vector-borne diseases and later integrated them into a single multi-scale models. The obtained multi-scale models are coupled and embedded types.

To be more specific, in Chapter 2 we developed a multi-scale model based on integrating four

sub-models which are: (i) a sub-model for the mosquito-to-human transmission of malaria parasite; (ii) a sub-model for the human-to-mosquito transmission of malaria parasite; (iii) a within-mosquito malaria parasite population dynamics sub-model and (iv) a within-human malaria parasite population dynamics sub-model. Thus, we established an uni-directionally coupled multi-scale model where the within-human and within-mosquito sub-models are uni-directionally coupled to the human-to-mosquito and mosquito-to-human sub-models, respectively. This was achieved based on the assumption that the transmission parameters of malaria in the mosquito-to-human sub-model is a function of vector population, changing in time, t and sporozoite population, changing in time, s making it possible for us to talk in terms of community level of infectiousness. Thus, by assuming that individual mosquitoes and humans are small homogeneous and unevenly distributed habitats for malaria parasites in the community we developed a multi-scale model which describes the mechanics of malaria transmission in a community in terms of the complete parasite life cycle. The result is a simple multi-scale model which describes the mechanics of malaria transmission in terms of the major components of the complete malaria parasite life-cycle. This multi-scale modelling approach may be found useful in guiding malaria or any other directly transmitted vector-borne diseases control and elimination.

In Chapter 3, we used the multi-scale model developed in Chapter 2 to compare the effectiveness of malaria treatment and preventive interventions in terms of three different viewpoints: (i) the interventions targeted at the human host using community gametocyte as the indicator of intervention effectiveness; (ii) the interventions targeted at the mosquito vector using community sporozoite as the indicator of intervention effectiveness; and (iii) the impact of interventions on overall disease dynamics using disease reproductive number as the indicator of intervention effectiveness. The results showed that of the two components of ACT (killing of merozoites effect, and killing of gametocytes effect), treatments that kill gametocytes at individual level have a higher comparative effectiveness than those that kill merozoites at population/community level. The results also showed that among the three components of LLTNs which are targeted at the mosquito vector (killing of mosquitoes effect; repelling of mosquitoes effect and protection of host from mosquito bites effect), repellency effect of LLTNs and protective effect of LLTNs have a higher comparative effectiveness than the killing of mosquito effect. This result also provided a proof-of-principle about the public health benefits of treatment as prevention (TasP) as an important preventive intervention for malaria. In general, the use of TasP as a preventive intervention measure for any infectious disease is based on the fact that the transmission of an infectious disease system can be prevented by treating infected individuals so that they become less likely to transmit the infection to others. Since the treatment of malaria operates at within-host scale while other malaria interventions such as long-lasting insecticide treated nets operate at between-host scale, mathematical models that link the within-host scale and the between-host scale can be

useful in evaluating the comparative effectiveness of malaria transmission preventive measures are done at different scale domains of the infectious disease system. Although the focus was on one of the most important vector-borne disease malaria, the framework is robust enough to be applied to many other vector-borne diseases that have a direct transmission mode.

In Chapter 4, we developed a sub-model that monitors the transmission dynamics of schistosome parasites in three different environments, namely, physical water environment, physical land environment and within infected snail and human hosts. Snail and schistosome parasite populations as well as human population are modelled mechanistically whereas parasite in human and snail biological environments are modelled phenomenologically. The model incorporated man-made and natural control measures. Man-made control mechanisms include vector-control; treatment; improved sanitation associated with construction and toilets usage; good hygienic practices and providing endemic communities with human waste disposal systems and conducting health education campaigns whereas natural control mechanisms include extreme weather changes. The sensitivity analysis results indicated that the reproductive number is most sensitive to snail mortality rate. Increasing snail mortality rate by 10% lead to a decline in the reproductive number, R_0 by 7%, implying that more effort has to focus on killing infected snails. It is also noted that increasing the natural death rates and parasites saturations, lead to a decline in R_0, though increasing either of these rates is neither practical nor ethical. Such natural control mechanisms can be the option in this case though their occurrence cannot be predicted. Other sensitive parameters include all that are associated with the disease transmission, recruitment rates, eggs on the land and in the water environments and parasites within infected hosts. Increasing either of theses rates by 10% leads to an increase in the R_0 by 5%. Since there is a direct relationship between R_0 and these rates, it implies that also decreasing either of the rates by 10% will eventually lead to a decrease in the R_0 by 5%. In this case, man-made control mechanisms can be applied in reducing the transmission of schistosome parasites. These results were confirmed numerically and that if man-made control mechanisms are simultaneously implemented, in particular, vector-control, treating infected individuals, conducting health education campaigns and improving sanitation. The same implies when health education campaigns and improved sanitation associated with construction and toilets usage are implemented. The sub-model can be useful in evaluating the comparative effectiveness of schistosomiasis interventions at the between-host/population level only.

Finally, in Chapter 5 we extended the sub-model in Chapter 4 without schistosomiasis interventions by linking the within-host and between-host sub-models after identifying the within-host and between-host variables and parameters associated with the environmental dynamics of

the pathogen and then designing a feedback of the variables and parameters across the within-host and between-host models. The resulting linked models are sometimes called immuno-epidemiological models. However, there is still no generalized framework for linking the within-host and between-host dynamics of infectious diseases. Furthermore, for infections that are environmentally trasmitted, there is an additional stumbling block in that there is a gap in knowledge on how environmental factors (through water, air, soil, food, formites, etc.) alter many aspects of such infections including susceptibility to infective dose, persistence of infection, pathogen shedding and severity of the disease. We linked the two subsystems (within-host and between-host models) by identifying the within-host and between-host variables and parameters associated with the environmental dynamics of the pathogen and then designed a feedback of the variables and parameters across the within-host and between-host sub-models using human schistosomiasis as a representative for environmentally transmitted vector-borne diseases. We studied the mathematical properties of the multi-scale model and showed that the model is epidemiologically well-posed. Using results from the analysis of the endemic equilibrium state, the disease reproductive number R_0, and numerical simulations of the full model, we adequately accounted for the reciprocal influence of the linked within-host and between-host models. In particular, we illustrated that for human schistosomiasis, the outcome of infection at the individual level determines if, when and how much the individual host will further transmit the infectious agent into the environment, eventually affecting the spread of the infection in the host population. We expect the conceptual modelling framework to be applicable to many infectious diseases that are environmentally trasmitted beyond the specific disease system of human schistosomiasis considered here.

The major innovations of this study are as follows: (i) The establishment of an infectious disease modelling science base for directly transmitted vector-borne diseases which is comparable to an existing modelling science base for environmentally transmitted vector-borne diseases where pathogen load in the environment is explicitly incorporated into the multi-scale model; (ii) the establishment of comparative effectiveness of malaria treatment and preventive interventions technique in terms of a number of viewpoints and (iii) The adoption of a linked modelling framework of the within-host and between-host dynamics of infectious diseases while the building blocks are specific to human schistosomiasis, the framework approach is general and is in principle reproducible with other infectious diseases that are environmentally transmitted.

6.2 Future Research Directions

Since the work in this study is a basis for future work, there are a variety of vector-borne disease systems aspects that are not considered. As such, future research directions can take into account the following aspects:

- The multi-scale model for environmentally transmitted vector-borne diseases can be extended by explicitly incorporating pathogen load in the physical land and within-human concurrently. The model can further be extended by incorporating interventions that target both the within-host and between-host disease dynamics. This will results into immuno-epidemiological multi-scale model.
- The main risk of vector-borne diseases include climate variations, certain human activities as well as movements of animals, people and goods. This is because human life depends on the earth's climate system. That is, the interactions of the oceans, atmosphere, terrestrial and marine bioshperes, chrospheres and land surface determine the earth's surface climate change [12]. Therefore the two multi-scale models developed in this study can be extended by incorporating climate change aspects though their occurrence is unpredictable.
- The two multi-scale models can be extended by incorporating pathogens life cycles. This will assist in identifying whether to implement the interventions either during the disease replication phase or during the disease transmission phase.
- It is also imperative to take cost effectiveness into consideration when designing and implementing vector-borne diseases interventions. The two models may be extended by incorporating cost effectiveness focusing on a specific endemic area.
- It is also possible that there can be a series of hosts being infected by one pathogen or the other way round. This is another aspect that can be incorporated in our multi-scale models.

Bibliography

[1] Wikipedia contributors. (2018, July 4). Artemisinin. In Wikipedia, The Free Encyclopedia. Retrieved 19:37, August 22, 2018, from https://en.wikipedia.org/w/index.php?title=Artemisini ldid=848869102

[2] Holford, T. R., Hardy, R. J. 1976. A stochastic model for the analysis of age- specific prevalence curves in schis- tosomiasis. J. Chronic Dis. 29:445-58

[3] R. Ross, The Prevention of Malaria, second ed., Murray, London, 1911.

[4] G. Macdonald, The analysis of equilibrium in malaria, Trop. Dis. Bull. 49 (1952) 813-828.

[5] L. Esteva, C. Vargas, A model for dengue disease with variable human population, J. Math. Biol. 38 (1999) 220-240.

[6] J. Tumwiine, J.Y.T. Mugisha, L.S. Luboobi, A host-vector model for malaria with infective immigrants, J. Math. Anal. Appl. 361 (2010) 139-149.

[7] Lozano R et al. (2012). Global and regional mortality from 235 causes of death for 20 age groups in 1990 and 2010: a systematic analysis for global burden of disease study 2010. Lancet 380, 2095-2128.

[8] http://www.vdh.state.va.us/epidemiology/DEE/Vectorborne, Vector-borne disease Control.

[9] http://www.enotes.com/vector-borne-diseases-reference/vector-borne-disease, Vector-borne diseases.

[10] Wayne M. Getz, Host-Vector-Parasite Models, University of Califonia, Berkeley, 2003.

[11] http://www.mosquitozone.com, Vector-borne disease, primary examples.

[12] Andrew K. Githeko, Steve W. Lindsay, Ulisses E. Confalonieri and Jonathan A. Patz. Climate change and vector-borne diseases: a regional analysis, World Health Organization, 2000.

[13] Lisa Gardiner, Climate change and vector-borne disease, 2011.

[14] http://www.who.int/heli/risks/vectors/vector, WHO, World Health Report.

[15] http://www.sabin.org/vaccine-development, Schistosomiasis vaccine initiative.

[16] Management of water-related microbial diseases, DWAF, 2003.

[17] http://www.who.int/mediacentre/factsheets, WHO, World Health Report, Fact-sheet No.115.

[18] G. Macdonald, The dynamics of helminth infections, with special reference to schistosomes. Transactions of the Royal Society of Tropical Medicine and Hygiene, 59, 489-506, 1965.

[19] Brian J Coburn, Bradley G Wagner, and Sally Blower. Review: Modelling influenza epidemics and pandemics: insights into the future of swine flu h1n1. 2009.

[20] R.M. Anderson, R.M. May, Regulation and stability of host-parasite population interactions, I. Regulatory processes, J. Anim. Ecol. 47, 219, 1978.

[21] R.M. May, R.M. Anderson, Population biology of infectious diseases II, Nature 280, 455, 1979.

[22] R.M Anderson and R.M. May, Prevalence of schistosome infections within molluscan populations: observed patterns and theoretical predictions, Parasitology 79, 63, 1979.

[23] M.S. Chan, R.M. Anderson, G.F. Medley1, D.A.P. Bundy, Dynamic aspects of morbidity and acquired immunity in schistosomiasis control, Acta Tropica, Volume 62, Issue 2, 105–117, 1996.

[24] http://en.wikipedia.org/wiki/Schistosomiasis/Snails.

[25] Juan Zhang and Zhien Ma, Global dynamics of an seir epidemic model with saturating contact rate, Mathematical Biosciences Journal 185, 15–32, 2003.

[26] W. Garira and Edward T. Chiyaka, Mathematical analysis of the transmission dynamics of schistosomiasis in the human-snail hosts, Journal of Biological systems Volume 17, No.3, 397-423, 2009.

[27] W. Garira, (2013). The Dynamical Behaviours of Diseases in Africa, in: Handbook of Systems and Complexity in Health Sturmberg, Joachim P and Martin, Carmel M. (Eds.). ISBN 978-1-4614-4997-3, Springer.

[28] Chiyaka, C., Garira, W., and Dube, S. (2007). Mathematical modelling of the impact of vaccination on malaria epidemiology. Theor. Diff. Equat. Anal, 1(1), 28-58.a

[29] Chiyaka, C., Tchuenche, J. M., Garira, W., and Dube, S. (2008). A Mathematical analysis of the effects of control strategies on the transmission dynamics of Malaria. Applied Mathematics and Computation, 195(2), 641-662.

[30] Mukandavire, Z., Bowa, K. and Garira, W. (2007). Modelling circumcision and condom use as HIV/AIDS preventive control strategies. Mathematical and Computer Modelling, 46(11), 1353-1372. disease parameters. Mathematical Biosciences and engineering, 2(4), 811-832.

[31] Mukandavire, Z., and Garira, W. (2007). Effects of public health educational campaigns and the role of sex workers on the spread of HIV/AIDS among heterosexuals. Theoretical population biology, 72(3), 346-365.

[32] Mukandavire, Z., and Garira, W. (2007). Sex-structured HIV/AIDS model to analyse the effects of condom use with application to Zimbabwe. Journal of mathematical biology, 54(5), 669-699.

[33] Z. Mukandavire and W. Garira, (2007). Age and sex structured model for assessing the demographic impact of mother-to-child transmission of HIV/AIDS. Bulletin of Mathematical Biology, 69(6): 2061-2092 .

[34] Bhunu C.P. ,Mukandavire Z., Garira W. and Zimba, M. (2008). Tuberculosis transmission model with chemoprophylaxis and treatment. Bulletin of Mathematical Biology , 70(4), 1163-1191.

[35] Bhunu C.P. and Garira W. (2009). Modelling the transmission of multidrug-resistant and extensively drug-resistant TB, in:, Advances in Disease Epidemiology. J. M. Tchuenche and Z. Mukandavire (eds.), ISBN: 160741452X, Nova Science Publishers, pp. 195-220.

[36] Keeling, M. J., and Rohani, P. (2008). Modeling infectious diseases in humans and animals. Princeton University Press.

[37] Brauer, F., and Castillo-Chavez, C. (2011). Mathematical models in population biology and epidemiology. Springer.

[38] Diekmann, O., and Heesterbeek, J. A. P. (2000). Mathematical epidemiology of infectious diseases (Vol. 146). Wiley, Chichester.

[39] Magombedze, G., Garira, W. and Mwenje, E. (2006). Modelling the human immune response mechanisms to Mycobacterium tuberculosis infection in the lungs. Mathematical Biosciences and engineering, 3(4), 661-682.

[40] Magombedze, G., Garira, W., and Mwenje, E. (2008). In-vivo mathematical study of co-infection dynamics of HIV-1 and Mycobacterium tuberculosis. Journal of Biological Systems, 16(03), 357-394.

[41] Chiyaka, C., Garira, W., and Dube, S. (2008). Modelling immune response and drug therapy in human malaria infection. Computational and Mathematical Methods in Medicine, 9(2), 143-163.

[42] Shiri, T., Garira, W. and Musekwa, S. D. (2005). A two-strain HIV-1 mathematical model to assess the effects of chemotherapy on

[43] Magombedze G., Garira W. and and Mwenje E. (2008). Modelling the immunopathogenesis of HIV-1 infection and the effect of multidrug therapy: the role of fusion inhibitors in HAART. Journal of Mathematical Biosciences and Engineering. 5(3): 485-504.

[44] W. Garira, S. D. Musekwa and T. Shiri, (2005). Optimal control of combined therapy in a single strain HIV-1 model. Electronic Journal of Differential Equations, 2005(52): 1-22.

[45] Chiyaka, E.T, Magombedze, G., Mutimbu, L., (2010). Modelling within host parasite dynamics of schistosomiasis. Computational and mathematical methods in medicine, 11(5), 255-280.

[46] Nowak, M., and May, R. M. (2000). Virus Dynamics: Mathematical Principles of Immunology and Virology: Mathematical Principles of Immunology and Virology. Oxford university press.

[47] Bundy, D.A. et al. (1991). Immunoepidemiology of lymphatic filariasis: the relationship between infection and disease. Immunolology Today, 12, A71-A75.

[48] Bundy, D.A.P. and Medley, G.F. (1992). Immunoepidemiology of human geohelminthiasis: ecological and immunological determinants of worm burden. Parasitology, 104 (Suppl.), S105-S119.

[49] Woolhouse, M.E.J. (1992). A theoretical framework for the immunoepidemiology of helminth infection. Parasite Immunol., 14, 563-578.

[50] Gupta, S. and Day, K.P. (1994). A theoretical framework for the immunoepidemiology of Plasmodium falciparum malaria. Parasite Immunology, 16, 361-370.

[51] Hellriegel B (2001). Immunoepidemiology - bridging the gap between immunology and epidemiology. Trends Parasitology, 17(2), 102-106.

[52] Roberts, M. G. (999). The immuno-epidemiology of nematode parasites of farmed animals: a mathematical approach. Parasitology Today, 15(6), 246-251.

[53] Gilchrist, M. A. and Sasaki, A. (2002). Modeling host-parasite co-evolution: a nested approach based on mechanistic models. Journal of Theoretical Biology, 218, 289-308.

[54] Esposito N, Rossi C. (2004). A nested-epidemic model for the spread of hepatitis C among injecting drug users. Mathematical Biosciences. 188(117, 2917.

[55] Coombs, D., Gilchrist, M. A., and Ball, C. L. (2007). Evaluating the importance of within- and between-host selection pressures on the evolution of chronic pathogens. Theoretical population biology, 72(4), 576-591.

[56] Dushoff J. (1996). Incorporating immunological ideas in epidemiological models. Journal of Theoretical Biology, 180(3), 181-187.

[57] Grenfell, B. T., Pybus, O. G., Gog, J. R., Wood, J. L., Daly, J. M., Mumford, J. A. and Holmes, E. C. (2004). Unifying the epidemiological and evolutionary dynamics of pathogens. Science, 303(5656), 327-332.

[58] Mideo, N., Alizon, S. and Day, T. (2008). Linking within- and between-host dynamics in the evolutionary epidemiology of infectious diseases. Trends in ecology and evolution, 23(9), 511-517.

[59] Milner F.A and Sega, L. M. (2009). Integrating immunological and epidemiological models. 18th World IMACS/MODSIM Congress, Cairns, Australia, 13-17 July. 685-690. http://mssanz.org.au/modsim09.

[60] Martcheva, M. (2011). An Immuno-epidemiological Model of Paratuberculosis. In AIP Conference Proceedings. International conference; 3rd, Application of mathematics in technical and natural science. 1404(1),176-183.

[61] Vickers, D.M. and Osgood, N.D (2007). A unified framework of immunological and epidemiological dynamics for the spread of viral infections in a simple network-based population. Theoretical Biology and Medical Modelling, 4(49), 1-13.

[62] Feng, Z., Velasco-Hernandez, J., Tapia-Santos,B. and Leite, M.C.a. (2012). A model for coupling within-host and between-host dynamics in an infectious disease. Nonlinear Dynamics, 68, 401-411.

[63] Tuckwell H, Toubiana L, Vibert J. (1998). Spatial epidemic network models with viral dynamics. Physical Review E, 57, 2163-2169.

[64] Rujeni N, Nausch N, Bourke CD, Midzi N, Mduluza T, Taylor D.W, Mutapi F. (2012). Atopy is inversely related to schistosome infection intensity: A Comparative Study in Zimbabwean Villages with Distinct Levels of Schistosoma haematobium Infection. International Archives of Allergy and Immunology,158(3), 288-298.

[65] Lama, J. and Planelles, V. (2007). Host factors influencing susceptibility to HIV infection and AIDS progression. Retrovirology, 4(1), 52.

[66] Chiyaka, C., Garira, W. and Dube, S. (2007). Transmission model of endemic human malaria in a partially immune population. Mathematical and computer modelling, 46(5), 806-822.

[67] Yang, H. M. (2000). Yang, H. M. (2000). Malaria transmission model for different levels of acquired immunity and temperature-dependent parameters (vector). Revista de Sade Pblica, 34(3), 223-231.

[68] Tumwiine, J., Mugisha, J. Y. T. and Luboobi, L. S. (2007). A mathematical model for the dynamics of malaria in a human host and mosquito vector with temporary immunity. Applied Mathematics and Computation, 189(2), 1953-1965.

[69] Ghani, A. C., Sutherland, C. J., Riley, E. M., Drakeley, C. J., Griffin, J. T., Gosling, R. D. and Filipe, J. A. (2009). Loss of population levels of immunity to malaria as a result of exposure-reducing interventions: consequences for interpretation of disease trends. PLoS One, 4(2), e4383.

[70] Martcheva, M., and Pilyugin, S. S. (2006). An epidemic model structured by host immunity. Journal of Biological Systems, 14(02), 185-203.

[71] Kostova, T, (2007). Persistence of viral infections on the population level explained by an immuno-epidemiological model. Mathematical Biosciences, 206(2), 309-319.

[72] Feng Z, Velasco-Hernandez J, Tapia-Santos B. (2013). A mathematical model for coupling within-host and between-host dynamics in an environmentally-driven infectious disease. Mathematical Biosciences. 241(1), 4917.

[73] Pruss-Ustum A. and Corvalan C. (2006). Preventing disease through healthy environments: Towards an estimate of the environmental burden of disease. [http://www.who.int/quantifying_ehimpacts/publications/preventingdisease.pdf]. Geneva: World Health Organization

[74] Pruss-Ustum A. and Corvalan C. (2007). How much disease burden can be prevented by environmental interventions? Epidemiology, 18(1), 167-178.

[75] Smith K.R, Smith K.R, Corvalan F.C, Kjellstrom T. (1999). How much global ill health is attributable to environmental factors? Epidemiology, 10(5):573-584.

[76] World Health Organization: Environmental Burden of Disease Series. Geneva. (2007). [http://www.who.int/quantifying_ehimpacts/national].

[77] Bani-Yaghoub, M., Gautam, R., Döpfer, D., Kaspar, C. W. and Ivanek, R. (2012). Effectiveness of environmental decontamination as an infection control measure. Epidemiology and infection, 140(3), 542.

[78] Gilligan, C. A. (2002). An epidemiological framework for disease management. Advances in botanical research, 38, 1-64.

[79] World Health Organization: World Health Report. Reducing risks, promoting healthy life. Geneva (2002). [http://www.who.int/whr/2002].

[80] Caraco, T., and Wang, I. N. (2008). Free-living pathogens: life-history constraints and strain competition. Journal of theoretical biology, 250(3), 569-579.

[81] Boots, M. (1999). A general host-pathogen model with free-living infective stages and differing rates of uptake of the infective stages by infected and susceptible hosts Researches on Population Ecology, 41(2), 189-194.

[82] Mangal, T. D., Paterson, S., and Fenton, A. (2008). Predicting the impact of long-term temperature changes on the epidemiology and control of schistosomiasis: a mechanistic model. PLoS One, 3(1), e1438.

[83] Wu, J., Dhingra, R., Gambhir, M., and Remais, J. V. (2013). Sensitivity analysis of infectious disease models: methods, advances and their application. Journal of The Royal Society Interface, 10(86), 20121018.

[84] Chiyaka, E. T., and Garira, W. (2009). Mathematical analysis of the transmission dynamics of schistosomiasis in the human-snail hosts. Journal of Biological Systems, 17(03), 397-423.

[85] Riley, S., Carabin, H., Marshall, C., Olveda, R., Willingham, A. L., and McGARVEY, S. T. (2005). Estimating and modeling the dynamics of the intensity of infection with Schistosoma japonicum in villagers of Leyte, Philippines. Part II: Intensity-specific transmission of

S. japonicum. The schistosomiasis transmission and ecology project. The American journal of tropical medicine and hygiene, 72(6), 754-761.

[86] Coon, D. R. (2005). Schistosomiasis: Overview of the history, biology, clinicopathology, and laboratory diagnosis. Clinical Microbiology Newsletter,27(21), 163-168.

[87] Liang, S., Maszle, D., and Spear, R. C. (2002). A quantitative framework for a multi-group model of *Schistosomiasis japonicum* transmission dynamics and control in Sichuan, China. Acta tropica, 82(2), 263-277.

[88] Feng, Z., Eppert, A., Milner, F. A., and Minchella, D. J. (2004). Estimation of parameters governing the transmission dynamics of schistosomes. Applied Mathematics Letters, 17(10), 1105-1112.

[89] Gryseels, B., Polman, K., Clerinx, J., and Kestens, L. (2006). Human schistosomiasis. The Lancet, 368(9541), 1106-1118.

[90] Hussein, A. N. A., Hassan, I. M., and Khalifa, R. (2010). Development and hatching mechanism of Fasciola eggs, light and scanning electron microscopic studies. Saudi journal of biological sciences, 17(3), 247-251.

[91] Spear, R. C., Hubbard, A., Liang, S., and Seto, E. (2002). Disease transmission models for public health decision making: Toward an approach for designing intervention strategies for Schistosomiasis japonica. Environmental health perspectives, 110(9), 907.

[92] Jordan, P., Webbe, G. and Sturrock, R. (1993). Human Schistosomiasis. CAB International, Wallingford.

[93] Milner, F. A., and Zhao, R. (2008). A deterministic model of schistosomiasis with spatial structure. Mathematical biosciences and engineering, 5(3), 505-522.

[94] Chu, K. Y., and Dawood, I. K. (1970). Cercarial production from Biomphalaria alexandrina infected with Schistosoma mansoni. Bulletin of the World Health Organization, 42(4), 569.

[95] Bani-Yaghoub, M., Gautam, R., Shuai, Z., van den Driessche, P. and Ivanek, R. [2012]. Reproduction numbers for infections with free-living pathogens growing in the environment. Journal of Biological Dynamics, 6(2), 923-940.

[96] Smith, D. L., McKenzie, F. E., Snow, R. W. and Hay, S. I. (2007). Revisiting the basic reproductive number for malaria and its implications for malaria control. PLoS biology, 5(3), e42.

[97] Van den Driessche, P. and Watmough, J. (2002). Reproduction numbers and sub-threshold endemic equilibria for compartmental models of disease transmission. Mathematical biosciences, 180(1), 29-48.

[98] Diekmann, O., Heesterbeek, J. A. P., and Metz, J. A. J. (1990). On the definition and the computation of the basic reproduction ratio R_0 in models for infectious diseases in heterogeneous populations. Journal of mathematical biology, 28(4), 365-382.

[99] Hyman, J. M., and Li, J. (2000). An intuitive formulation for the reproductive number for the spread of diseases in heterogeneous populations. Mathematical biosciences, 167(1), 65-86.

[100] Castillo-Chavez, C., Feng, Z. and Huang, W. (2002). On the computation of R_0 and its role in global stability. In Mathematical Approaches for Emerging and Re-emerging Infectious Diseases Part 1: An Introduction to Models, Methods and Theory. The IMA Volumes in Mathematics and Its Applications, Vol. 125, C. Castillo-Chavez, S. Blower, P. van den Driessche, and D. Kirschner, eds., Springer-Verlag, Berlin, 229-250.

[101] Carr J, (1981). Applications Centre Manifold Theory, Springer-Verlag, New York, 1981.

[102] Dushoff J., Huang W. and Castillo-Chavez C. (1998). Backwards bifurcations and catastrophe in simple models of fatal diseases, J. Math. Biol., 36, 227178.

[103] http://www.sabin.org/vaccine-development, schistosomiasis vaccine initiative. Date viewed: 02/07/2012.

[104] http://www.who.int/mediacentre/factsheets, WHO, World Health Report, Fact-sheet No.115. Date viewed:10/03/2012.

[105] Roy M. Anderson and Robert M.May, Regulation and stability of Host-parasite population Interactions:I. Regulatory processes. Journal of Animal Ecology. (47) (1978) pp.219-247.

[106] M.S. Chan, R.M. Anderson, G.F. Medley1, D.A.P. Bundy. Dynamic aspects of morbidity and acquired immunity in schistosomiasis control. Volume 62,(1996) Issue 2, 105117, Acta Tropica.

[107] Xiao-Nong Zhou, Guo-Jing, Kun Yang, Xian-Hong Wang, Qing-Biao Hong, Le-Ping Sun, John B.Malone, Thomas K.Kristensen, N.Robert Bergquist and Jurg Utzinger. Potential impact of climate change on schistosomiaisis transmission in China, The American Society of Tropical Medicine and Hygien, 2008.

[108] G. Macdonald, The dynamics of helminth infections, with special reference to schistosomes. Transactions of the Royal Society of Tropical Medicine and Hygiene. (59) (1965) 489-506.

[109] R.M. Anderson, R.M. May, Regulation and stability of host-parasite population interactions, I. Regulatory processes, J. Anim. Ecol. (47) (1978) 219.

[110] R.M. May, R.M. Anderson, Population biology of infectious diseases II, Nature 280, 455, 1979.

[111] R.M Anderson and R.M. May, Prevalence of schistosome infections within molluscan populations: observed patterns and theoretical predictions, Parasitology. (79) (1979), 63.

[112] Helena S.R, Teresa T. Monteriro and Delfim F.M Torres (2013), Sensitivity Analysis.

[113] N.Chitnis, J.M. Hyman, and J.M. Cusching. Determining important parameters in the spread of malaria through the sensitivity analysis of a mathematical model. Bull. Math. Biol,70 (5),(2008)1272-1296.

[114] Barron, L. and Wynn, T.A, Macrophages activation governs schistosomiasis-induced inflammation and fibrosis. Eur. J. Immuno, 41, (2011)2509-2514.

[115] Shadab H.A, MD, AAHIVS, FACP, FIDSA, Schistosomiasis: Background, Pathophysiology, Etiology. Medscape Drugs, Diseases and Procedures,(2015) 1-9, .

[116] World Health Organization. Schistosomiasis and soil-transmitted helminth infections preliminary estimates of the number of children treated with alben-dazole or mebendazole. Wkly Epidemiol Rec, 2006, 81: 145-163.

[117] http://www.who.int/mediacentre/factsheets, WHO, World Health Report, Fact-sheet No.115. Date accessed:10/03/2012.

[118] World Health Organization:available http://www.who.int/schistosomiasis/en/, on September, 2007. Date accessed:09/01/2013.

[119] Woolhouse, M. E. J. (1991). On the application of mathematical models of schistosome transmission dynamics. I. Natural transmission. Acta tropica, 49(4), 241-270.

[120] Chiyaka, E. T., Magombedze, G., & Mutimbu, L. (2010). Modelling within host parasite dynamics of schistosomiasis. Computational and mathematical methods in medicine, 11(3), 255-280.

[121] Shujing Gao, Yujiang Liu, Youquan Luo, Dehui Xie. Control problems of a mathematical model for schistosomiasis transmission dynamics, Nonlinear Dyn, 2011, 63: 503-512.

[122] Feng, Z., Curtis, J., & Minchella, D. J. (2001). The influence of drug treatment on the maintenance of schistosome genetic diversity. Journal of Mathematical Biology, 43(1), 52-68.

[123] Macdonald, G. (1965). The dynamics of helminth infections, with special reference to schistosomes. Transactions of the Royal Society of Tropical Medicine and Hygiene, 59(5), 489-506.

[124] Yang, Y., Feng, Z., Xu, D., Sandland, G. J., & Minchella, D. J. (2012). Evolution of host resistance to parasite infection in the snail–schistosome–human system. Journal of mathematical biology, 65(2), 201-236.

[125] Zhou, X. N., Yang, G. J., Yang, K., Wang, X. H., Hong, Q. B., Sun, L. P., ... & Utzinger, J. (2008). Potential impact of climate change on schistosomiasis transmission in China. The American journal of tropical medicine and hygiene, 78(2), 188-194.

[126] Anderson, R. M., & May, R. M. (1978). Regulation and stability of host-parasite population interactions: I. Regulatory processes. The Journal of Animal Ecology, 219-247.

[127] May, R. M., & Anderson, R. M. (1979). Population biology of infectious diseases: Part II. Nature, 280(5722), 455.

[128] Anderson, R. M., & May, R. M. (1979). Prevalence of schistosome infections within molluscan populations: observed patterns and theoretical predictions. Parasitology, 79(1), 63-94.

[129] Chiyaka, E. T., & GARIRA, W. (2009). Mathematical analysis of the transmission dynamics of schistosomiasis in the human-snail hosts. Journal of Biological Systems, 17(03), 397-423.

[130] Cohen, J. E. (1977). Mathematical models of schistosomiasis. Annual Review of Ecology and Systematics, 8(1), 209-233.

[131] Coon, D. R. (2005). Schistosomiasis: overview of the history, biology, clinicopathology, and laboratory diagnosis. Clinical Microbiology Newsletter, 27(21), 163-168.

[132] Dias, L. C. D. S., Marçal Jr, O., & Glasser, C. M. (1995). Control of schistosomiasis transmission. Memórias do Instituto Oswaldo Cruz, 90(2), 285-288.

[133] Fenwick, A. (1987). The Control of Schistosomiasis. World Health Organization Technical Report Series No. 728.

[134] De Wolfe Miller F. Steering Committee for Cooperative Action for the international Drinking Water Supply and Sanitation, World Health Organization (unpublished document; available on request from Community Water Supply and Sanitation, World Health Organization,1990 1211, Geneva 27, Switzerland.)

[135] McJunkin FE. Water and human health. Development Information center, Agency for International Development, Washington, DC, 1993, 134pp.

[136] McCullough, F. S., Gayral, P. H., Duncan, J., & Christie, J. D. (1980). Molluscicides in schistosomiasis control. Bulletin of the World Health Organization, 58(5), 681.

[137] Davis, A. (1986). Recent advances in schistosomiasis. QJM: An International Journal of Medicine, 58(2), 95-110.

[138] McCreesh, N., Nikulin, G., & Booth, M. (2015). Predicting the effects of climate change on Schistosoma mansoni transmission in eastern Africa. Parasites & vectors, 8(1), 4.

[139] Macdonald, G. (1965). The dynamics of helminth infections, with special reference to schistosomes. Transactions of the Royal Society of Tropical Medicine and Hygiene, 59(5), 489-506.

[140] Chitsulo, L., Engels, D., Montresor, A., & Savioli, L. (2000). The global status of schistosomiasis and its control. Acta tropica, 77(1), 41-51.

[141] Adie, H. A., Okon, O. E., Arong, G. A., Ekpo, U. F., & Braide, E. I. (2014). Environmental factors and distribution of urinary schistosomiasis in Cross River State, Nigeria. Inte J Zool Res, 10(2), 42-58.

[142] McCreesh, N., & Booth, M. (2013). Challenges in predicting the effects of climate change on Schistosoma mansoni and Schistosoma haematobium transmission potential. Trends in parasitology, 29(11), 548-555.

[143] Ferrari, M. L. A., Coelho, P. M. Z., Antunes, C. M. F., Tavares, C. A. P.,& Da Cunha, A. S. (2003). Efficacy of oxamniquine and praziquantel in the treatment of Schistosoma mansoni infection: a controlled trial. Bulletin of the World Health Organization, 81, 190-196.

[144] King, C. H., Sutherland, L. J., & Bertsch, D. (2015). Systematic review and meta-analysis of the impact of chemical-based mollusciciding for control of Schistosoma mansoni and S. haematobium transmission. PLoS neglected tropical diseases, 9(12), e0004290.

[145] Andrade, I. G., Queiroz, J. W., Cabral, A. P., Lieberman, J. A., & Jeronimo, S. M. (2009). Improved sanitation and income are associated with decreased rates of hospitalization for diarrhoea in Brazilian infants. Transactions of the Royal Society of Tropical Medicine and Hygiene, 103(5), 506-511.

[146] Boelee, E., & Laamrani, H. (2004). Environmental control of schistosomiasis through community participation in a Moroccan oasis. Tropical Medicine & International Health, 9(9), 997-1004.

[147] World Health Organization. (2015). Guidelines for the treatment of malaria. World Health Organization.

[148] World Health Organization. (2016). World malaria report 2015. World Health Organization.

[149] Garira, W. (2017). A complete categorization of multiscale models of infectious disease systems. Journal of biological dynamics, 11(1), 378-435.

[150] Legros, M., & Bonhoeffer, S. (2016). A combined within-host and between-hosts modelling framework for the evolution of resistance to antimalarial drugs. Journal of the Royal Society Interface, 13(117), 20160148.

[151] Chiyaka, C., Garira, W., & Dube, S. (2008). Modelling immune response and drug therapy in human malaria infection. Computational and Mathematical Methods in Medicine, 9(2), 143-163.

[152] Clark, I. A., Virelizier, J. L., Carswell, E. A., & Wood, P. R. (1981). Possible importance of macrophage-derived mediators in acute malaria. Infection and Immunity, 32(3), 1058-1066.

[153] Elloso, M. M., Van der Heyde, H. C., Vande Waa, J. A., Manning, D. D., & Weidanz, W. P. (1994). Inhibition of Plasmodium falciparum in vitro by human gamma delta T cells. The Journal of Immunology, 153(3), 1187-1194.

[154] Gurarie, D., Zimmerman, P. A., & King, C. H. (2006). Dynamic regulation of single- and mixed-species malaria infection: insights to specific and non-specific mechanisms of control. Journal of theoretical biology, 240(2), 185-199.

[155] Chitnis, N., Cushing, J. M., & Hyman, J. M. (2006). Bifurcation analysis of a mathematical model for malaria transmission. SIAM Journal on Applied Mathematics, 67(1), 24-45.

[156] Eckhoff, P. A. (2011). A malaria transmission-directed model of mosquito life cycle and ecology. Malaria journal, 10(1), 303.

[157] Traoré, B., Sangaré, B., & Traoré, S. (2017). A mathematical model of malaria transmission with structured vector population and seasonality. Journal of Applied Mathematics, 2017.

[158] Mikucki, M. A. (2012). Sensitivity analysis of the basic reproduction number and other quantities for infectious disease models (Doctoral dissertation, Colorado State University. Libraries).

[159] Bousema, J. T., Gouagna, L. C., Drakeley, C. J., Meutstege, A. M., Okech, B. A., Akim, I. N., ... & Sauerwein, R. W. (2004). Plasmodium falciparum gametocyte carriage in asymptomatic children in western Kenya. Malaria journal, 3(1), 18.

[160] Rodrigues, H. S., Monteiro, M. T. T., & Torres, D. F. (2013). Sensitivity analysis in a dengue epidemiological model. In Conference Papers in Science (Vol. 2013). Hindawi.

[161] Gubler, D. J. (2009). Vector-borne diseases. Revue scientifique et technique, 28(2), 583.

[162] World Health Organization. (2014). A global brief on vector-borne diseases.

[163] Reiner, R. C., Perkins, T. A., Barker, C. M., Niu, T., Chaves, L. F., Ellis, A. M., ... & Buckee, C. (2013). A systematic review of mathematical models of mosquito-borne pathogen transmission: 1970–2010. Journal of The Royal Society Interface, 10(81), 20120921.

[164] Hollingsworth, T. D., Pulliam, J. R., Funk, S., Truscott, J. E., Isham, V., & Lloyd, A. L. (2015). Seven challenges for modelling indirect transmission: vector-borne diseases, macroparasites and neglected tropical diseases. Epidemics, 10, 16-20.

[165] Lemon, S. M., Sparling, P. F., Hamburg, M. A., Relman, D. A., Choffnes, E. R., & Mack, A. (2008). Vector-borne diseases: understanding the environmental, human health, and ecological connections. Workshop summary. In Vector-borne diseases: understanding the environmental, human health, and ecological connections. Workshop summary.. National Academies Press.

[166] Martens, W. J. M., Jetten, T. H., Rotmans, J., & Niessen, L. W. (1995). Climate change and vector-borne diseases: a global modelling perspective. Global environmental change, 5(3), 195-209.

[167] Boldin, B., & Diekmann, O. (2008). Superinfections can induce evolutionarily stable coexistence of pathogens. Journal of mathematical biology, 56(5), 635-672.

[168] Feng, Z., Velasco-Hernandez, J., & Tapia-Santos, B. (2013). A mathematical model for coupling within-host and between-host dynamics in an environmentally-driven infectious disease. Mathematical biosciences, 241(1), 49-55.

[169] Gandolfi, A., Pugliese, A., & Sinisgalli, C. (2015). Epidemic dynamics and host immune response: a nested approach. Journal of mathematical biology, 70(3), 399-435.

[170] Dang, Y. X., Li, X. Z., & Martcheva, M. (2016). Competitive exclusion in a multi-strain immuno-epidemiological influenza model with environmental transmission. Journal of biological dynamics, 10(1), 416-456.

[171] Wei, H. M., Li, X. Z., & Martcheva, M. (2008). An epidemic model of a vector-borne disease with direct transmission and time delay. Journal of Mathematical Analysis and Applications, 342(2), 895-908.

[172] Martcheva, M., & Li, X. Z. (2013). Competitive exclusion in an infection-age structured model with environmental transmission. Journal of Mathematical Analysis and Applications, 408(1), 225-246.

[173] F.E. McKenzie and W.H. Bossert, An integrated model of Plasmodium falciparum dynamics, J. Theor. Biol. 232(3) (2005), pp. 411-426.

[174] Shen, M., Xiao, Y., & Rong, L. (2015). Global stability of an infection-age structured HIV-1 model linking within-host and between-host dynamics. Mathematical biosciences, 263, 37-50.

[175] Numfor, E., Bhattacharya, S., Martcheva, M., & Lenhart, S. (2015). Optimal control in multi-group coupled within-host and between-host models. Electron. J. Differential Equations.

[176] Roman Ullah, Sakhi Jan, Gul Zaman, Saleem Khan, Saeed Islam, Muhammad Altaf Khan, Hakeem Ullah (2016). Mathematical Modeling of Vector-Borne Diseases. J. Appl. Environ. Biol. Sci., 6(1)57-62.

[177] Cai, L. M., Martcheva, M., & Li, X. Z. (2013). Competitive exclusion in a vector–host epidemic model with distributed delay. Journal of biological dynamics, 7(sup1), 47-67.

[178] Dang, Y. X., Li, X. Z., & Martcheva, M. (2016). Competitive exclusion in a multi-strain immuno-epidemiological influenza model with environmental transmission. Journal of biological dynamics, 10(1), 416-456.

[179] Martcheva, M., & Li, X. Z. (2013). Linking immunological and epidemiological dynamics of HIV: the case of super-infection. Journal of biological dynamics, 7(1), 161-182.

[180] Gillespie, D. T. (2001). Approximate accelerated stochastic simulation of chemically reacting systems. The Journal of Chemical Physics, 115(4), 1716-1733.

[181] Legros, M., & Bonhoeffer, S. (2016). A combined within-host and between-hosts modelling framework for the evolution of resistance to antimalarial drugs. Journal of the Royal Society Interface, 13(117), 20160148.

[182] Martcheva, M., & Li, X. Z. (2013). Competitive exclusion in an infection-age structured model with environmental transmission. Journal of Mathematical Analysis and Applications, 408(1), 225-246.

[183] F.E. McKenzie and W.H. Bossert, An integrated model of Plasmodium falciparum dynamics, J.Theor. Biol. 232(3) (2005), pp. 411-426.

[184] Numfor, E., Bhattacharya, S., Martcheva, M., & Lenhart, S. (2015). Optimal control in multi-group coupled within-host and between-host models. Electron. J. Differential Equations.

[185] Shen, M., Xiao, Y., & Rong, L. (2015). Global stability of an infection-age structured HIV-1 model linking within-host and between-host dynamics. Mathematical biosciences, 263, 37-50.

[186] Cen, X., Feng, Z., & Zhao, Y. (2014). Emerging disease dynamics in a model coupling within-host and between-host systems. Journal of theoretical biology, 361, 141-151.

[187] Feng, Z., Velasco-Hernandez, J., Tapia-Santos, B., & Leite, M. C. A. (2012). A model for coupling within-host and between-host dynamics in an infectious disease. Nonlinear Dynamics, 68(3), 401-411.

[188] Feng, Z., Velasco-Hernandez, J., & Tapia-Santos, B. (2013). A mathematical model for coupling within-host and between-host dynamics in an environmentally-driven infectious disease. Mathematical biosciences, 241(1), 49-55.

[189] Feng, Z., Cen, X., Zhao, Y., & Velasco-Hernandez, J. X. (2015). Coupled within-host and between-host dynamics and evolution of virulence. Mathematical biosciences, 270, 204-212.

[190] Wang, X., & Wang, J. (2017). Disease dynamics in a coupled cholera model linking within-host and between-host interactions. Journal of biological dynamics, 11(sup1), 238-262.

[191] Luz, P. M., Struchiner, C. J., & Galvani, A. P. (2010). Modeling transmission dynamics and control of vector-borne neglected tropical diseases. PLoS neglected tropical diseases, 4(10), e761.

[192] Garira, W. (2017). A complete categorization of multi-scale models of infectious disease systems. Journal of Biological Dynamics, 11(1), 378-435.

[193] Daefler, S. (2013). Using Datasets for Modeling of Infectious Diseases. J Data Mining Genomics Proteomics, 4, e103.

[194] Durmus, S., Çakır, T., Özgür, A., & Guthke, R. (2015). A review on computational systems biology of pathogen–host interactions. Frontiers in microbiology, doi:10.3389fmicb.2015.00235.

[195] Schulze, S., Henkel, S. G., Driesch, D., Guthke, R., & Linde, J. (2015). Computational prediction of molecular pathogen-host interactions based on dual transcriptome data. Frontiers in Microbiology, 6.

[196] Nourani, E., Khunjush, F., & Durmuş, S. (2015). Computational approaches for prediction of pathogen-host protein-protein interactions. Frontiers in Microbiology, 6.

[197] World Health Organization. (2007). Malaria elimination: a field manual for low and moderate endemic countries. Malaria elimination: a field manual for low and moderate endemic countries.

[198] Gutierrez, J. B., Galinski, M. R., Cantrell, S., & Voit, E. O. (2015). From within host dynamics to the epidemiology of infectious disease: Scientific overview and challenges. Mathematical Biosciences, (270), 143-155.

[199] Martcheva, M., Tuncer, N., & St Mary, C. (2015). Coupling Within-Host and Between-Host Infectious Diseases Models. BIOMATH, 4(2), 1510091.

[200] Garira, W., Mathebula, D., & Netshikweta, R. (2014). A mathematical modelling framework for linked within-host and between-host dynamics for infections with free-living pathogens in the environment. Mathematical biosciences, 256, 58-78.

[201] Netshikweta, R., & Garira, W. (2017). A multi-scale Model for the World's First Par-asitic Disease Targeted for Eradication: Guinea Worm Disease. Computational and Mathematical Methods in Medicine. https://doi.org/10.1155/2017/1473287

[202] Chiyaka, C., Garira, W. and Dube, S. [2007]. Transmission model of endemic human malaria in a partially immune population. Mathematical and Computer Modelling, 46(5), 806-822.

[203] Legros, M., & Bonhoeffer, S. (2016). A combined within-host and between-hosts modelling framework for the evolution of resistance to antimalarial drugs. Journal of the Royal Society Interface, 13(117), 20160148.

[204] Cai, L., Tuncer, N., & Martcheva, M. (2017). How does within-host dynamics affect population level dynamics? Insights from an immuno-epidemiological model of malaria. Mathematical Methods in the Applied Sciences, 40(18), 6424-6450.

[205] McKenzie, F. E., & Bossert, W. H. (2005). An integrated model of Plasmodium falciparum dynamics. Journal of theoretical biology, 232(3), 411-426.

[206] Gulbudak, H., Cannataro, V. L., Tuncer, N., & Martcheva, M. (2016). Vector-borne pathogen and host evolution in a structured immuno-epidemiological system. Journal, 44(7).

[207] Teboh-Ewungkem, M. I., Podder, C. N., & Gumel, A. B. (2010). Mathematical study of the role of gametocytes and an imperfect vaccine on malaria transmission dynamics. Bulletin of mathematical biology, 72(1), 63-93.

[208] White, L. J., Maude, R. J., Pongtavornpinyo, W., Saralamba, S., Aguas, R., Van Effelterre, T., ... & White, N. J. (2009). The role of simple mathematical models in malaria elimination strategy design. Malaria Journal, 8(1), 1.

[209] World Health Organization. (2014). From malaria control to malaria elimination: a manual for elimination scenario planning. World Health Organization.

[210] Rynkiewicz, E. C., Pedersen, A. B., & Fenton, A. (2015). An ecosystem approach to understanding and managing within-host parasite community dynamics. Trends in parasitology, 31(5), 212-221.

[211] Lofgren, E. T, Egizi, A. M and Fefferman, N. H (2016). Patients as patches: Ecology and Epidemiology in Healthcare Environments. Infection control and hospital epidemiology, 1-6.

[212] Sicard, M, Dittmer, J, Greve, P., Bouchon, D. and Braqquart-Varnier, C. [2014]. A host as an ecosystem: Wolbachia coping with environmental constrains. Environmental microbiology, doi:10.1111/1462-2920.12573.

[213] Miller, W. C., Powers, K. A., Smith, M. K., & Cohen, M. S. (2013). Community viral load as a measure for assessment of HIV treatment as prevention. The Lancet infectious diseases, 13(5), 459-464.

[214] Das, M. (2014). Community Viral Load. Encyclopedia of AIDS. DOI$10.1007/978-4614-9610-6_122-1$.

[215] Castel, A. D., Befus, M., Willis, S., Griffin, A., West, T., Hader, S., & Greenberg, A. E. (2012). Use of the community viral load as a population-based biomarker of HIV burden. Aids, 26(3), 345-353.

[216] Kranzer, K., Lawn, S. D., Johnson, L. F., Bekker, L. G., & Wood, R. (2013). Community viral load and CD4 count distribution among people living with HIV in a South African township: implications for treatment as prevention. Journal of acquired immune deficiency syndromes (1999), 63(4), 498.

[217] Hansen, E., & Buckee, C. O. (2013). Modeling the human infectious reservoir for malaria control: does heterogeneity matter?. Trends in parasitology, 29(6), 270-275.

[218] Shiell, A., Hawe, P., & Gold, L. (2008). Complex interventions or complex systems? Implications for health economic evaluation. BMJ: British Medical Journal, 336(7656), 1281.

[219] Hetzel, C., & Anderson, R. M. (1996). The within-host cellular dynamics of bloodstage malaria: theoretical and experimental studies. Parasitology, 113(1), 25-38.

[220] Teboh-Ewungkem, M. I., & Yuster, T. (2010). A within-vector mathematical model of Plasmodium falciparum and implications of incomplete fertilization on optimal gametocyte sex ratio. Journal of theoretical biology, 264(2), 273-286.

[221] Clark, I. A., Virelizier, J. L., Carswell, E. A., & Wood, P. R. (1981). Possible importance of macrophage-derived mediators in acute malaria. Infection and Immunity, 32(3), 1058-1066.

[222] Elloso, M. M., Van der Heyde, H. C., Vande Waa, J. A., Manning, D. D., & Weidanz, W. P. (1994). Inhibition of Plasmodium falciparum in vitro by human gamma delta T cells. The Journal of Immunology, 153(3), 1187-1194.

[223] Gurarie, D., Zimmerman, P. A., & King, C. H. (2006). Dynamic regulation of single- and mixed-species malaria infection: insights to specific and non-specific mechanisms of control. Journal of theoretical biology, 240(2), 185-199.

[224] Chiyaka, C., Garira, W., & Dube, S. (2008). Modelling immune response and drug therapy in human malaria infection. Computational and Mathematical Methods in Medicine, 9(2), 143-163.

[225] Chitnis, N., Cushing, J. M., & Hyman, J. M. (2006). Bifurcation analysis of a mathematical model for malaria transmission. SIAM Journal on Applied Mathematics, 67(1), 24-45..

[226] Castillo-Chavez C, Song B. Dynamical models of tuberculosis and their applications. Math Biol Eng 1(2)(2004) 361-404.

[227] Griffin, J. T., Hollingsworth, T. D., Okell, L. C., Churcher, T. S., White, M., Hinsley, W., ... & Ghani, A. C. (2010). Reducing Plasmodium falciparum malaria transmission in Africa: a model-based evaluation of intervention strategies. PLoS medicine, 7(8), e1000324.

[228] Garira, W. (2013). The dynamical behaviours of diseases in Africa. In Handbook of Systems and Complexity in Health (pp. 595-623). Springer New York.

[229] Carr J, [1981]. Applications Centre Manifold Theory, Springer-Verlag, New York, 1981.

[230] Castillo-Chavez C, Song B, [2004]. Dynamical models of tuberculosis and their applications, Math Biol Eng 1(2), 361-404.

[231] Chitnis N., Hyman J.M., Cushing J.M.,[2008]. Determining important parameters in the spread of malaria through the sensitivity analysis of a mathematics model. Bulletin of Mathematical Biology, 70, 1272-1296.

[232] Beier, J. C. (1998). Malaria parasite development in mosquitoes. Annual review of entomology, 43(1), 519-543.

[233] Sinden, R. E. (1999). Plasmodium differentiation in the mosquito. Parassitologia, 41(1-3), 139-148.

[234] Churcher, T. S., Dawes, E. J., Sinden, R. E., Christophides, G. K., Koella, J. C., & Basáñez, M. G. (2010). Population biology of malaria within the mosquito: density-dependent processes and potential implications for transmission-blocking interventions. Malaria journal, 9(1), 1.

[235] Leroy, D., Campo, B., Ding, X. C., Burrows, J. N., & Cherbuin, S. (2014). Defining the biology component of the drug discovery strategy for malaria eradication. Trends in parasitology, 30(10), 478-490.

[236] Da, D. F., Churcher, T. S., Yerbanga, R. S., Yaméogo, B., Sangaré, I., Ouedraogo, J. B., ... & Cohuet, A. (2015). Experimental study of the relationship between Plasmodium gametocyte density and infection success in mosquitoes; implications for the evaluation of malaria transmission-reducing interventions. Experimental parasitology, 149, 74-83.

[237] Baton, L. A., & Ranford-Cartwright, L. C. (2005). Spreading the seeds of million-murdering death: metamorphoses of malaria in the mosquito. Trends in parasitology, 21(12), 573-580.

[238] Hillyer, J. F., Barreau, C., & Vernick, K. D. (2007). Efficiency of salivary gland invasion by malaria sporozoites is controlled by rapid sporozoite destruction in the mosquito haemocoel. International journal for parasitology, 37(6), 673-681.

[239] Bousema, J. T., Gouagna, L. C., Drakeley, C. J., Meutstege, A. M., Okech, B. A., Akim, I. N., ... & Sauerwein, R. W. (2004). Plasmodium falciparum gametocyte carriage in asymptomatic children in western Kenya. Malaria journal, 3(1), 18.

[240] Bousema, T., Okell, L., Shekalaghe, S., Griffin, J. T., Omar, S., Sawa, P., ... & Drakeley, C. (2010). Revisiting the circulation time of Plasmodium falciparum gametocytes: molecular detection methods to estimate the duration of gametocyte carriage and the effect of gametocytocidal drugs. Malaria journal, 9(1), 136.

[241] Day, K. P., Hayward, R. E., & Dyer, M. (1998). The biology of Plasmodium falciparum transmission stages. Parasitology, 116(S1), S95-S109.

[242] Eichner, M., Diebner, H. H., Molineaux, L., Collins, W. E., Jeffery, G. M., & Dietz, K. (2001). Genesis, sequestration and survival of Plasmodium falciparum gametocytes: parameter estimates from fitting a model to malariatherapy data. Transactions of the Royal Society of Tropical Medicine and Hygiene, 95(5), 497-501.

[243] Bousema, T., & Drakeley, C. (2011). Epidemiology and infectivity of Plasmodium falciparum and Plasmodium vivax gametocytes in relation to malaria control and elimination. Clinical microbiology reviews, 24(2), 377-410.

[244] Drakeley, C., Sutherland, C., Bousema, J. T., Sauerwein, R. W., & Targett, G. A. (2006). The epidemiology of Plasmodium falciparum gametocytes: weapons of mass dispersion. Trends in parasitology, 22(9), 424-430.

[245] Garcia, J. E., Puentes, A., & Patarroyo, M. E. (2006). Developmental biology of sporozoite-host interactions in Plasmodium falciparum malaria: implications for vaccine design. Clinical microbiology reviews, 19(4), 686-707.

[246] Churcher, T. S., Bousema, T., Walker, M., Drakeley, C., Schneider, P., Ouédraogo, A. L., & Basáñez, M. G. (2013). Predicting mosquito infection from Plasmodium falciparum gametocyte density and estimating the reservoir of infection. Elife, 2, e00626.

[247] Billker, O., M. K. Shaw, G. Margos, and R. E. Sinden. The roles of temperature, pH and mosquito factors as triggers of male and female gametogenesis of Plasmodium berghei in vitro. Parasitology 115, no. 01 (1997): 1-7.

[248] Zollner, G. E., Ponsa, N., Garman, G. W., Poudel, S., Bell, J. A., Sattabongkot, J., ... & Vaughan, J. A. (2006). Population dynamics of sporogony for Plasmodium vivax parasites from western Thailand developing within three species of colonized Anopheles mosquitoes. Malaria journal, 5(1), 1.

[249] Leroy, D., Campo, B., Ding, X. C., Burrows, J. N., & Cherbuin, S. (2014). Defining the biology component of the drug discovery strategy for malaria eradication. Trends in parasitology, 30(10), 478-490.